TOXIC MITOCHONDRIAL EFFECTS INDUCED BY "RED DEVIL" CHEMOTHERAPY

by

Caleigh Margaret Opperman

Thesis presented in fulfillment of the requirements for the degree of Master of Science (Physiological Sciences) at Stellenbosch University

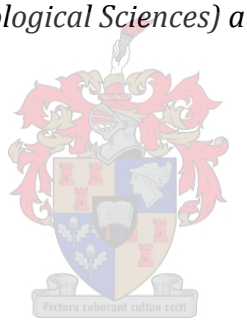

Supervisor: Dr. Balindiwe JN Sishi

Co-Supervisor: Prof. Jacques Van Rooyen

March 2015

The financial assistance of the National Research Foundation (NRF) towards this research is hereby acknowledged. Opinions expressed and conclusions arrived at, are those of the author and are not necessarily to be attributed to the NRF

Stellenbosch University https://scholar.sun.ac.za

Declaration

By submitting this thesis electronically, I declare that the entirety of the work contained therein is my own, original work, that I am the sole author thereof (save to the extent explicitly otherwise stated), that reproduction and publication thereof by Stellenbosch University will not infringe any third party rights and that I have not previously in its entirety or in part submitted it for obtaining any qualification.

March 2015

Copyright © 2015 Stellenbosch University

All rights reserved

Stellenbosch University https://scholar.sun.ac.za

Abstract

Introduction: Doxorubicin (DOX), infamously known as the "red devil," is considered the most effective antineoplastic drug utilized in oncologic practice today. However, its clinical use is hampered due to cumulative, dose-dependent cardiotoxicity, which can lead to reduced quality of life, irreversible heart failure and death. The mechanisms involved in the pathogenesis of cardiotoxicity have not been fully elucidated, but have previously been demonstrated to involve oxidative stress, calcium dysregulation and mitochondrial dysfunction. Since the mitochondria play a critical role in generation of reactive oxygen species, the maintenance of calcium homeostasis and are the most extensively damaged by DOX, they have become the main focus of novel therapeutic interventions. The morphology and function of these dynamic organelles are regulated in part by mitochondrial fission and fusion events, as well as mitochondrial quality control systems. Since mitochondrial morphology is often associated with crucial cellular functions, this study aimed to investigate the long-term effects of DOX on mitochondrial dynamics and the mitochondrial quality control systems, mitophagy and the ubiquitin-proteasome pathway (UPP). Additionally, since the mitochondria and the endoplasmic reticulum (ER) are two interconnected organelles, and both play a role in maintaining calcium homeostasis, this study further assessed the effects of chronic DOX treatment on ER function and calcium status.

Materials and Methods: In order to fully establish the effect of chronic DOX treatment *in vitro,* two cardiac cell lines were utilized in this study. H9C2 cardiomyoblasts and human-derived Girardi heart cells were cultured under standard culture conditions until ± 70-80% confluency was reached, where after treatment commenced. Cells were treated daily with 0.2 and 1.0 µM of DOX for 96 and 120 hours in order to simulate chronic, cumulative cardiotoxicity. Cell viability and apoptotic cell death were assessed with the MTT assay and Caspase Glo 3/7 assays, respectively. The expression of proteins involved in mitochondrial dynamics, mitochondrial biogenesis, the ubiquitin-proteasome pathway, mitophagy and ER stress were determined with Western blotting. Organelle morphology was visualized with fluorescence microscopy, and flow cytometry was used to assess mitochondrial and ER load. In order to determine the oxidative capacity, stress and status within the cells following treatment, the Oxygen radical absorbance capacity (ORAC), Thiobarbituric acid reactive

Stellenbosch University https://scholar.sun.ac.za

substances (TBARS) and Glutathione (GSH) assays were employed respectively. Finally, intracellular and mitochondrial calcium was assessed and quantified with superresolution structured illumination microscopy (SR-SIM) and flow cytometry respectively.

Results: DOX significantly reduced cell viability and increased apoptosis in both *in vitro* cardiac cell models. This study further demonstrated that the expression of mitochondrial fusion proteins, Mfn 1 and Mfn 2 were significantly downregulated, whilst the regulators of fission, Drp1 and hFis1, were significantly elevated, therefore shifting the balance of mitochondrial dynamics towards fission. Unopposed and elevated mitochondrial fission was clearly evident from the morphology of these organelles, which displayed short, highly fragmented mitochondria with a dispersed network following treatment. Chronic DOX also downregulated the regulator of mitochondrial biogenesis, PGC-1α, thus inhibiting the formation of new, functional mitochondria. The E3 ligases, MARCH5 and Parkin were highly upregulated following treatment, indicating activation of the UPP and mitophagy. Although chronic DOX stimulated K48 ubiquitination following treatment, it inhibited the catalytic activity of the 26S proteasome, therefore blocking proteasomal degradation. Although the antioxidant capacity (measured as ORAC) was significantly enhanced by both concentrations of DOX, an increase in oxidative stress status was shown following DOX treatment. In this regard lipid peroxidation significantly increased, while redox status of the endogenous antioxidant, glutathione, significantly decreased. Additionally chronic DOX treatment induced ER stress, which lead to an increase in cytosolic and mitochondrial calcium. In response to ER stress, the unfolded protein response (UPR) was then stimulated.

Discussion: Results from this study indicate that chronic DOX treatment disrupts the balance of mitochondrial dynamics, favouring mitochondrial fission. Mitochondrial fragmentation is mediated by the downregulation of fusion proteins regulated by the E3 ubiquitin ligase, MARCH5 as well as by the increase in mitochondrial calcium. Mitochondrial fission results in mitophagy, an adaptive response to protect the cardiac cell against damaged mitochondria. This study also indicates that during chronic DOX-induced cardiotoxicity ER stress and the UPR are induced, which is possibly responsible for the disruption in calcium homeostasis. The inhibition of mitochondrial biogenesis coupled with elevated mitophagy as observed in this chronic study, elucidates a plausible mechanism whereby DOX induces mitochondrial dysfunction. Unregulated mitochondrial fragmentation and inhibited mitochondrial biogenesis are known to regulate various cardiomyopathies,

Stellenbosch University https://scholar.sun.ac.za

therefore since both these effects are induced by chronic DOX treatment suggests a mechanism whereby cardiotoxicity, and ultimately heart failure are produced. This study provides new insight into the role of chronic DOX plays in altering mitochondrial dynamics and mitochondrial quality control systems. Further investigations targeted at limiting mitochondrial fission may reduce the cardiovascular side effects associated with DOX.

Stellenbosch University https://scholar.sun.ac.za

Uittreksel

Inleiding: Doksorubisien (DOX), ook bekend as die "rooiduiwel," word beskou as die mees effektiewe anti-neoplastiese middel wat tans in onkologie praktyke gebruik word. Die kliniese gebruik hiervan word gerem deur die kumulatiewe dosis-afhanklike kardiotoksisiteit wat tot verlaagde lewenskwaliteit, onomkeerbare hartversaking, en tot die dood kan lei. Die meganismes wat by die kardiotoksiese patogenese betrokke is, is nog onbekend, maar die meganisme het moontlik te doen met oksidatiewe stres, kalsiumwanregulering en mitochondriale wanfunksionering. Omrede die mitochondria 'n kritieke rol in die vorming van reaktiewe suurstofspesies speel, asook die handhawing van kalsiumhomeostase en die mees beskadigde organelle deur DOX, het die hooffokus na nuwe terapeutiese intervensies verskuif. Die morfologie en funskie van hierdie dinamiese organelle word gereguleer deels deur mitochondriale fragmentering en fussie, asook mitochondriale kwaliteitsbeheersisteme. Omrede mitochondriale morfologie geassosieer is met noodsaaklike sellulêre funksies, het hierdie studie gepoog om die langtermyneffkte van DOX op mitochondriale dinamika en die mitochondriale kwaliteitsbeheersisteme, mitofagie en die ubikwitien-proteosoomweg (UPW) te ondersoek. Siende dat die mitochondria en die endoplasmiese retikulum (ER) twee interverweefde organelle is, en beide 'n rol speel in die handhawing van kalsiumhomeostase, het hierdie studie verder die effekte van chroniese DOX behandeling op ER funksie en kalsiumstatus ondersoek.

Materiaal en Metodes: Om die effek van chroniese DOX behandeling *in vitro* te verstaan in hierdie studie, is twee hartsellyne gebruik. H9C2 kardiomioblaste en menslike Girardi hartselle is onder standaardtoestande tot ± 70-80% konfluensie bereik is gekweek, waarna behandeling begin is. Selle is daagliks met 0.2 en 1.0 µM DOX vir 96 en 120 uur behandel om chroniese en kumulatiewe kardiotoksisiteit n ate boots. Selvatbaarheid en apoptotiese seldood is onderskeidelik ondersoek deur middel van die MTT en Caspase Glo 3/7 toetse. Die proteïenuitdrukking betrokke by mitochondriale dinamika, mitochondriale biogenese, die ubikwitien-proteosoom weg, mitofagie en ER stres is deur middel van westerse afblatting bepaal. Organelmorfologie is deur middel van fluoresensie mikroskopie gevisualiseer, en vloeisitometrie was gebruik om die aantal mitochondria en ER lading te bepaal. Om die oksidatiewe kapasiteit, stres en status binne die selle na behandeling te bepaal, is die ORAC, TBARS en GSH toetse onderskeidelik gebruik. Laastens was die intrasellulêre en

Stellenbosch University https://scholar.sun.ac.za

mitochondriale kalsium ondersoek en gekwantifiseer met superresolussie gestruktureerde illuminasie mikroskopie (SR-SIM) en vloeisitomerie.

Resultate: DOX het selvatbaarheid betekenisvol verlaag en apoptose in beide *in vitro* kardiale selmodelle verhoog. Hierdie studie het verder aangetoon dat die uitdrukking van mitochondriale fussie proteïene, Mfn 1 en Mfn 2 betekenisvol afgereguleer is, terwyl die reguleerders van fragmentering, Drp1 en hFis1, betekenisvol verhoog is en daardeur die balans van mitochondriale dinamika na fussie verskuif. Onverhinderde en verhoogde mitochondriale fragmentering is duidelik sigbaar deur die morfologie van die organelle, wat as kort, hoogsgefragmenteerde mitochondria met ‘n verspreide netwerk na behandeling vertoon. Chroniese DOX het ook die mitochondriale biogenese reguleerder, PGC-1α, afgereguleer en daardeur die vorming van nuwe, funksionele mitochondria geinhibeer. Die E3 ligase, MARCH5 en Parkin is hoogs opgereguleer na behandeling, wat aktivering van UPW en mitofagie aantoon. Alhoewel chroniese DOX K48 ubikwitinering na behandeling gestimuleer het, het dit die katalitiese aktiwiteit van die 26S proteasoom geinhibeer en dus die proteosomale degradasie geblokkeer. Antioksidantkapasiteit en oksidatiewe status was betekenisvol na behandeling wat gevolglik tot hoë vlakke oksidatiewe skade binne die selle gelei het. Addisioneel het chroniese DOX behandeling ER stres geïnduseer wat tot ‘n toename in sitosoliese en mitochondriale kalsium gelei het. In reaksie op die ER stres is die UPW gestimuleer.

Bespreking: Resultate van hierdie studie het aangetoon dat chroniese DOX behandeling die balans van mitochondriale dinamika onderbreek en sodoende mitochondriale fragmentering bevoordeel. Mitochondriale fragmentering word gemediëer deur die afregulering van fussie proteïene wat deur die E3 ubikwitienligase, MARCH5, gereguleer word, en ook deur die toename in mitochondriale kalsium. Mitochondriale fragmentering induseer mitofagie, ‘n aanpassingsreaksie om die hartselle teen beskadigde mitochondria te beskerm. Hierdie studie toon verder ook dat gedurende chroniese DOX-geïnduseerde ER stres, word die UPW ook geïnduseer, wat moontlik dan verantwoordelik is vir die ontwrigting van kalsiumhomeostase. Die inhibering van mitochondriale biogenese gekoppel met verhoogde mitofagie soos waargeneem in hierdie studie, verklaar ‘n moontlike meganisme waardeur DOX mitochondriale wanfunksionering veroorsaak. Ongereguleerde mitochondriale fragmentering en geinhibeerde mitochondriale biogenese is bekend om verskeie kardiomiopatieë te reguleer. Omrede beide hierdie effekte geinduseer word deur chroniese DOX behandeling kan dit

Stellenbosch University https://scholar.sun.ac.za

moontlik ‘n meganisme voorstel waarby kardiotokiese en uiteindelik hartversaking ontwikkel. Hierdie studie bied nuwe insig in die rol wat chroniese DOX speel in die wysiging van mitochondriale- dinamika en kwaliteitskontrole sisteme. Verdere ondersoeke wat die mitochondriale fragmentering kan verminder mag moontlik die kardiovaskulêre newe-effekte wat met DOX behandeling geassosieer is, verlaag.

Stellenbosch University https://scholar.sun.ac.za

Acknowledgments

I would like to thank the following people, for without them I would not have been able to complete this project.

My deepest gratitude is to **my supervisor, Dr Balindiwe Sishi.** I have been so amazingly fortunate to have the unwavering support and guidance, from someone passionate and brilliant as you. Not only did you allow me the freedom to discuss my thoughts and practice my ideas, but your patience and supervision helped me overcome difficult days in the lab. Thank you for entrusting me with this project, for believing in me and for being just the best supervisor in the world.

To my **co-supervisor, Prof Jacques van Rooyen,** thank you for much for always making yourself available to listen and give advice. Thank you also for the many long and inspiring discussions over coffee. They provided me with the motivation I needed to continue with the work, when at times I thought I would never see results. Your mentorship, your kindness and your support throughout these last two years is greatly appreciated, thank you.

Toni Goldswain, without your friendship and support I would not be handing in this project. Thank you for being my "partner-in-crime". From lab duty to many, many weekends spent in tissue culture and western blotting, thank you for sticking by my side and encouraging me every step of the way.

To **Dr Ben Loos,** I cannot express enough my sincerest thanks for the all your assistance regarding my fluorescence microscopy work. Thank you for always making yourself available in the CAF lab, and for your encouragement along the way.

I am also thankful to **Dr Theo Nell**, for not only for taking the time to help me translate my abstract, but for the many discussions and laughs that always make my day.

I am extremely grateful to **Lize Engelbrecht.** Thank you so much for all your technical assistance and guidance in the CAF lab. I would also like to acknowledge **Rozaan Adams**

Stellenbosch University https://scholar.sun.ac.za

for the many hours spent at the flow cytometer. It would not have been successful, let alone as enjoyable without you.

A very BIG thank you to **Fanie Rautenbach** from the **Oxidative Stress Research Center at CPUT** for the training you provided for oxidative stress assays used in this study.

To the **DSG and CORG research groups,** thank you for the all the discussions, laughs, encouragement and enthusiasm you greeted me with everyday.

Thank you to all of the **Academic and Technical staff** of the Physiological Sciences Department for their great leadership.

Most importantly, none of this would have been possible without the love, support and patience of my family. To **My Parents and my Sister,** thank you for always providing me with a shoulder to cry on when I needed it most, for always believing in me, listening to my problems and guiding me towards the solutions. To **Tygue Theron,** thank you for your continued love and understanding, if you hadn't been there to pick me up, calm me down and wake me up on weekend lab days, I would not be where I am today. To my extended family, **the Therons,** thank you so much for your constant encouragement throughout this study.

And finally thank you to the **National Research Foundation** for your financial assistance that enabled me to continue with my studies

Stellenbosch University https://scholar.sun.ac.za

Table of Contents

Acknowledgments vii

List of Figures xii

List of Tables xvi

List of Abbreviations xvii

Units of Measurement xxii

Chapter 1 - Literature Review 1

1.1 Introduction 1

1.2 Anthracycline Induced Cardiotoxicity 2

1.2.1 Acute Cardiotoxicity 2

1.2.2 Chronic Cardiotoxicity 4

1.2.3 Delayed Cardiotoxicity 5

1.3 Doxorubicin Antitumor Activity 6

1.3.1 DNA Intercalation 6

1.3.2 Topoisomerase II Poisoning 7

1.3.3 Generation of Reactive Oxygen Species 9

1.3.4 Ceramide Overproduction 10

1.4 Mechanisms for Doxorubicin-induced Cardiotoxicity 10

1.4.1 Oxidative Stress 10

1.4.2 The Oxidative Stress Hypothesis 11

1.4.3 Apoptosis 13

1.4.4 Intracellular Calcium Dysregulation 15

1.5 Endoplasmic Reticulum Stress 18

1.5.1 Understanding the Unfolded Protein Response 19

1.5.2 Calcium Dysregulation During ER Stress 21

1.6 DOX-induced Cardiotoxicity and the Mitochondria 22

1.6.1 Mitochondrial Dynamics 23

1.6.2 Mitochondrial Quality Control 26

1.7 The Proteolytic Pathways 27

1.7.1 The Ubiquitin-Proteasome Pathway 27

1.7.2 The 26S Proteasome and its Role in DOX cardiotoxicity 29

1.7.3 Autophagy 31

Stellenbosch University https://scholar.sun.ac.za

1.7.4 Mitophagy 33
1.7.5 The Role of Autophagy in DOX Cardiotoxicity 34
1.8 Motivation for Current Study 35
1.9 Research Aims 37
Chapter 2 - Materials and Methods 38
2.1 Cell Culture 38
2.2 Pilot Study 39
2.2.1 Doxorubicin Treatment 39
2.2.2 Cell Viability 39
2.2.3 Apoptosis 40
2.3 Main Study 40
2.3.1 Flow Cytometry 41
2.3.2 Fluorescence Microscopy 42
2.3.3 Superresolution Structured Illumination Microscopy (SR-SIM) 42
2.3.4 Oxidative Stress and Antioxidant Capacity 43
2.3.5 Proteasomal Activity 45
2.3.6 Western Blot Analysis 46
2.3.7 Statistical Analysis 48
Chapter 3 –Results 49
3.1 Pilot Study: Cell Viability 49
3.2 The Effect of Chronic DOX Treatment Regimes on Mitochondrial Dynamics 52
3.2.1 Evaluation of Mitochondrial Fission 52
3.2.2 Evaluation of Mitochondrial Fusion 52
3.2.3 Evaluation of Mitochondrial Morphology 56
3.3 The Effect of Chronic DOX Treatment Regimes on the Ubiquitin Proteasome Pathway 60
3.3.1 Evaluation of E3 ligase expression 60
3.3.2 Evaluation of K48 Protein Ubiquitination 62
3.3.3 Evaluation of the 26S Proteasome 65
3.4 The Effect of Chronic DOX Treatment Regimes on Autophagy 67
3.5 The Effect of Chronic DOX Treatment Regimes on Mitochondrial Biogenesis 70
3.6 The Effect of Chronic DOX Treatment Regimes on Apoptosis 72
3.7 The Effect of Chronic DOX Treatment Regimes on Oxidative Stress 74
3.7.1 Evaluation of Antioxidant Capacity (ORAC assay) 74
3.7.2 Evaluation of Oxidative Damage (TBARS assay) 75

Stellenbosch University https://scholar.sun.ac.za

3.7.3 Evaluation of Oxidative Status (GSH assay) 76
3.8 The Effect of Chronic DOX Treatment Regimes on the Endoplasmic Reticulum 78
3.8.1 Evaluation of BiP Expression 78
3.8.2 Evaluation of ATF4 Expression 79
3.8.3 Evaluation of ER Load and DOX Localization 80
3.9 The Effect of Chronic DOX Treatment Regimes on Intracellular and Mitochondrial Calcium Levels 83
Chapter 4 – Discussion 87
References 101
APPENDIX A – Supplementary Data 142
APPENDIX B – Protocols 167
APPENDIX C – Reagent and Solution Preparation 189
APPENDIX D – List of Reagents and Materials 193

Stellenbosch University https://scholar.sun.ac.za

List of Figures

Chapter 1

Figure 1.1: The family of Anthracyclines

Figure 1.2: The effect of cumulative Doxorubicin treatment of the development of heart failure

Figure 1.3: Structure of Doxorubicin-DNA complex

Figure 1.4: The action of Topoisomerase I and II

Figure 1.5: The chemical structure of Doxorubicin

Figure 1.6: Intrinsic and extrinsin apoptotic pathways activated in the myocardium following Doxorubicin treatment

Figure 1.7: Intracellular calcium dysregulation and cell signaling induced by Doxorubicin treatment

Figure 1.8: The unfolded protein response

Figure 1.9: Mitochondrial morphology regulated by mitochondrial fusion and fission events

Figure 1.10: The ubiquitin-proteasome pathway

Figure 1.11: The 26S proteasome

Figure 1.12: The stages of autophagy

Figure 1.13: The E3 ubiquitin ligase, Parkin mediates autophagy

Chapter 3

Figure 3.1: The effect of increasing, cumulative doses of Doxorubicin on H9C2 cell viability

Stellenbosch University https://scholar.sun.ac.za

Figure 3.2: The effect of increasing, cumulative doses of Doxorubicin on Girardi cell viability

Figure 3.3: The effect of increasing, cumulative doses of Doxorubicin on H9C2 caspase 3/7 luminescence

Figure 3.4: The effect of increasing, cumulative doses of Doxorubicin on Girardi caspase 3/7 luminescence

Figure 3.5: The effect chronic Doxorubicin treatment regimes on Drp1 expression in H9C2 cardiomyoblasts

Figure 3.6: The effect chronic Doxorubicin treatment regimes on hFis1 expression in H9C2 cardiomyoblasts

Figure 3.7: The effect chronic Doxorubicin treatment regimes of Mitofusin 1 expression in H9C2 cardiomyoblasts

Figure 3.8: The effect chronic Doxorubicin treatment regimes of Mitofusin 2 expression in H9C2 cardiomyoblasts

Figure 3.9: The effect chronic Doxorubicin treatment regimes on mitochondrial morphology and DOX localization in H9C2 cardiomyoblasts

Figure 3.10: The effect chronic Doxorubicin treatment regimes on mitochondrial load in H9C2 cardiomyoblasts

Figure 3.11: Area of Doxorubicin and mitochondria colocalization

Figure 3.12: The effect chronic Doxorubicin treatment regimes on MARCH5 expression in H9C2 cardiomyoblasts

Figure 3.13: The effect chronic Doxorubicin treatment regimes on Parkin expression in H9C2 cardiomyoblasts

Figure 3.14: The effect chronic Doxorubicin treatment regimes on K4 ubiquitination in H9C2 cardiomyoblasts

Stellenbosch University https://scholar.sun.ac.za

Figure 3.15: The effect chronic Doxorubicin treatment regimes on chymotrypsin-like catalytic activity in H9C2 cardiomyoblasts

Figure 3.16: The effect chronic Doxorubicin treatment regimes on trypsin-like catalytic activity in H9C2 cardiomyoblasts

Figure 3.17: The effect chronic Doxorubicin treatment regimes on caspase-like catalytic activity in H9C2 cardiomyoblasts

Figure 3.18: The effect chronic Doxorubicin treatment regimes on LC3 expression in H9C2 cardiomyoblasts

Figure 3.19: The effect chronic Doxorubicin treatment regimes of p62 expression in H9C2 cardiomyoblasts

Figure 3.20: The effect chronic Doxorubicin treatment regimes on PGC-1α expression in H9C2 cardiomyoblasts

Figure 3.21: The effect chronic Doxorubicin treatment regimes on apoptosis in H9C2 cardiomyoblasts

Figure 3.22: The effect chronic Doxorubicin treatment regimes on antioxidant capacity in H9C2 cardiomyoblasts

Figure 3.23: The effect chronic Doxorubicin treatment regimes on lipid peroxidation in H9C2 cardiomyoblasts

Figure 3.24: The effect chronic Doxorubicin treatment regimes on the GSH:GSSG ratio in H9C2 cardiomyoblasts

Figure 3.25: The effect chronic Doxorubicin treatment regimes on BiP expression in H9C2 cardiomyoblasts

Figure 3.26: The effect chronic Doxorubicin treatment regimes on ATF4 expression in H9C2 cardiomyoblasts

Figure 3.27: The effect chronic Doxorubicin treatment regimes on ER load in H9C2 cardiomyoblasts

Stellenbosch University https://scholar.sun.ac.za

Figure 3.28: The effect chronic Doxorubicin treatment regimes on ER morphology and DOX localization in H9C2 cardiomyoblasts

Figure 3.29: Area of Doxorubicin and ER colocalization

Figure 3.30: The effect chronic Doxorubicin treatment regimes on intracellular calcium in H9C2 cardiomyoblasts

Figure 3.31: Visualization of intracellular calcium following chronic Doxorubicin treatment

Figure 3.32: The effect chronic Doxorubicin treatment regimes on mitochondrial calcium in H9C2 cardiomyoblasts

Chapter 4

Figure 4.1: A unifying image of the molecular mechanisms involved in regulating mitochondrial dysfunction associated with chronic DOX-induced cardiotoxicity.

Stellenbosch University https://scholar.sun.ac.za

List of Tables

Chapter 2

Table 1: Amount of cells seeded for each experiment

Table 2: The effect of chronic DOX treatment on GSH, GSSG and the GSH/GSSG ratio

Stellenbosch University https://scholar.sun.ac.za

List of Abbreviations

A

AA	Antibiotic-Antimycotic
Ang-1	Angiopoietin
ANT/s	Anthracycline/s
ATF	Activating transcription factor
ATP	Adenosine Triphosphate

B

Bax	Bcl-2-associated X protein
Bcl	B-cell lymphoma
Bcl-$X_{L/1}$	Bcl-extra large/Bcl associated X protein
BiP	Binding immunoglobulin protein/GRP78
BSA	Bovine serum albumin

C

C	Control
Caspase	Cysteine aspartate-specific protease
CHF	Congestive Heart Failure
CsA	Cyclosporin

D

DMEM	Dulbecco's modified Eagle's medium
DMSO	Dimethyl sulfoxide
DNA	Deoxyribonucleic acid
DNR	Daunorubicin
Drp1	Dynamin related protein 1/DNM1L
DOX	Doxorubicin

Stellenbosch University https://scholar.sun.ac.za

DXZ	Dexrazoxane/Zinecard/Cardioaxane

E

E1	Ubiquitin-activating enzyme
E2	Ubiquitin-conjugating enzyme
E3	Ubiquitin-protein ligase
ECG	electrocardiogram
elF2α	Eukaryotic initiation factor 2α
et al.	Et alii
ER	Endoplasmic reticulum
ERAD	Endoplasmic reticulum-associated protein degradation

F

FADD	Fas-associated death domain
FasL	Fas ligand
FBS	Fetal bovine serum
FIP200	200 kDa focal adhesion kinase family interaction protein

G

GAPDH	Glyceraldehyde 3-phosphate dehydrogenase
GSSG	Oxidized glutathione/glutathione disulfide
GSH	Reduced glutathione

H

HCl	Hydrogen Chloride
HPLC	High performance liquid chromatography

I

IMM	Inner mitochondrial membrane

Stellenbosch University https://scholar.sun.ac.za

IRE1α	Inositol-requiring enzyme 1α

L

LC-3	Microtubule-associated protein light chain-3

M

MAFbx	Muscle atrophy F-box
MARCH5	Mitochondrial ubiquitin ligase/MITOL
MDA	Malondialdehyde
Mdivi-1	selective cell-permeable inhibitor of mitochondrial fission
Mfn	Mitofusin
monoHER	7-mono-O-(beta-hydroxyethyl)-rutoside
mPTP	Mitochondrial permeability transition pore
mRNA	Messenger ribonucleic acid
MTT	3-(4,5-dimethythiazol-2-yl)-2, 5-diphenyle terazolium bromide
MuRF-1	Muscle RING finger-1

N

NaCl	Sodium Chloride
Na/Ca^{2+}	Sodium/Calcium
NADH	Nicotinamide adenine dinucleotide reduced
Na/K	Sodium/Potassium
NADPH	Nicotinamide adenine dinucleotide phosphate
NFAT	Nuclear factor of activated T cells

O

OMM	Outer mitochondria membrane
Opa1	Optic atrophy protein 1
ORAC	Oxygen radical absorbance capacity

Stellenbosch University https://scholar.sun.ac.za

P

P	Phosphate
p62	Sequestersome/SQSTM1
PBS	Phosphate buffered saline solution
PERK	endoplasmic reticulum kinase
PGC-1α	Peroxisome proliferator-activated receptor gamma coactivator 1-alpha
PI3	Phosphatidylinsitol 3
PINK1	PTEN-induced kinase 1
polyUb	polyubiquitin
PTEN	Phosphate and tensin homolog
PTN	Protein

Q

QC	Quality control

R

Rhod	Rhodamine
RIPA	Radio immuniorecipitation assay
ROS	Reactive oxygen species
RyR	Ryanodine calcium release

S

SDS	Sodium dodecyl sulphate
SEM	standard error of the mean
SR-SIM	Superresolution structured illumination microscopy

Stellenbosch University https://scholar.sun.ac.za

T

TBARS	Thiobarbituric acid reactive substances
TOMM20	Translocase of outer mitochondrial membrane 20 homolog
Temed	Tertramethylethylenediamine
TNF	Tumor necrosis factor
TRIS	Tri-(hydroxyl-methyl)-aminomethane

U

U1k1	Unc-51 like kinase
Ub	Ubiquitin
UPP	Ubiquitin-proteasome pathway
UPR	Unfolded protein response

V

vs.	versus

X

XBP1	transcriptional factor X-box binding protein 1

Stellenbosch University https://scholar.sun.ac.za

Units of Measurement

&	And
%	Percent/percentage
°C	degree Celsius
AU	Arbitrary units
A	ampere
g	gram
hr/s	hour/s
kDa	kilodalton
L/l	liter
M	molar
mg	milligram
mg/m^2	milligram/square meter
ml	milliliters
RFU	Relative Fluorescence units
TE/L	Trolox equivalents/liter
V	voltage
µg	microgram
µl/µL	microliter
µM	micromolar
µm	micrometer
µmol/L	micromole/liter

Stellenbosch University https://scholar.sun.ac.za

Chapter 1 - Literature Review

1.1 Introduction

Every year, approximately 14 million people are diagnosed with cancer, and in South Africa alone it has been predicted that the number of new cancer cases will increase up to 78% by the year 2030 (Bray *et al*., 2012; Globocan, 2012). Although cancer remains one of the leading causes of death worldwide, research over the last two decades has brought us no closer to discovering a cure, but has lead to significant advances in therapeutic interventions. Since their discovery in the early 1960's anthracyclines (ANTs), a class of chemotherapeutic agents, still remain amongst the most effective anti-cancer drugs utilized in oncologic practice today (Aubel-Sadron *et al*., 1984; Gharanei *et al*., 2014).

Doxorubicin (DOX, Adriamycin), infamously known as the "red devil" chemotherapy, together with its cousin daunorubicin (DNR), belong to the family of ANTs (Figure 1.1) and are considered essential antineoplastics used in the treatment of breast cancer and pediatric cancers such as childhood solid tumors, leukemia, aggressive lymphomas and soft tissue sarcomas (Minotti *et al*., 2004; Octavia *et al*., 2012). However, unlike other chemotherapeutic agents, the clinical use of DOX is limited due to its cumulative, dose-dependent cardiotoxicity, which may lead to a reduced quality of life, irreversible congestive heart failure (CHF) or worse, death (Lefrak *et al*., 1973; Swain *et al*., 2003; Minotti *et* a*l*., 2004).

Cancer is fast becoming more manageable due to early diagnosis and advances in both basic and clinical cancer research (DeVita and Chu, 2008; Gharanei *et al*., 2013), however the adverse cardiotoxic effects of DOX and other systemic anticancer agents are still a major health concern (Swain *et al*., 2003; Doyle *et al*., 2005). This highlights the importance of understanding both the cellular and molecular mechanisms involved in the pathophysiology of DOX-induced cardiomyopathy, in order to establish novel adjuvant therapies that will offer cardioprotection without affecting DOX's antineoplastic properties. Therapeutic interventions involving the use of β-blockers, antioxidants, renin-angiotensin system inhibitors and free radical scavengers have all been unsuccessful due to their negative side effects and interactions associated with DOX (Boucek, 1997a; Granger, 2006; Gharanei *et al*., 2013). Based on the unsuccessful nature of these interventions, it is clear that there is still

Stellenbosch University https://scholar.sun.ac.za

a lot that we do not know about DOX-induced toxicity. Moreover, results from these studies suggest that other mechanisms, other than those already proposed, may be involved in inducing the detrimental effects of DOX.

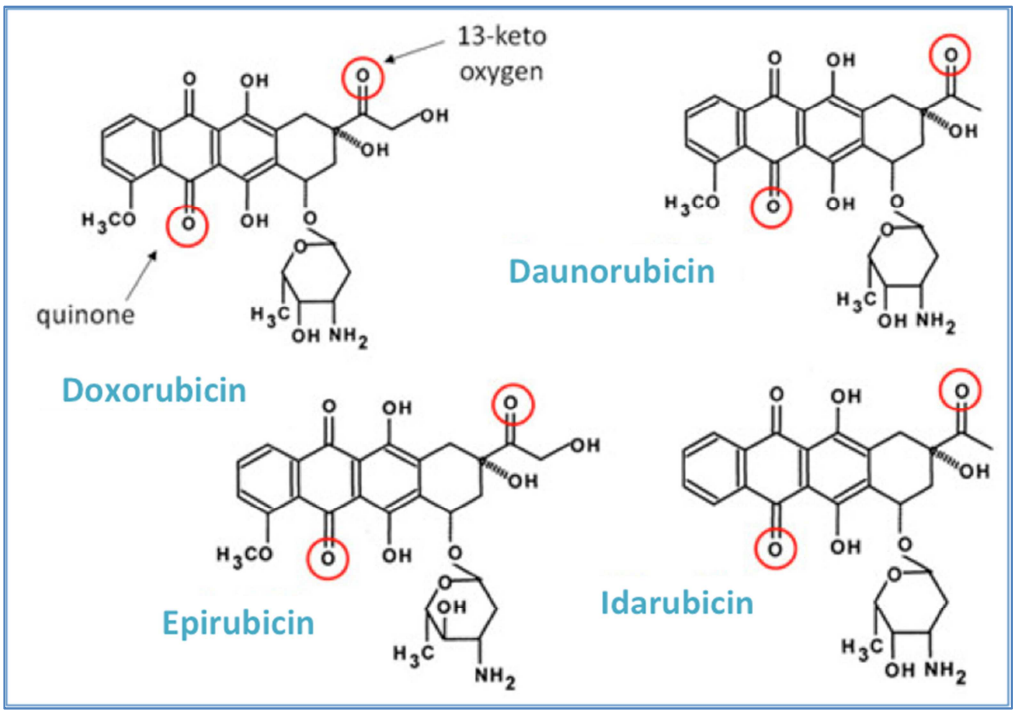

Figure 1.1: The Family of Anthracyclines. Epirubicin and Idarubicin are derived from the original anthracyclines, Doxorubicin and Daunorubicin respectively. However all anthracyclines share a common chemical backbone, with minor changes in their chemical moieties. The quinone moieties at the 5 and 13 positions are responsible for the cardiotoxic effects of anthracyclines. Image sourced from Gem Pharmaceuticals

1.2 Anthracycline Induced Cardiotoxicity

In patients undergoing DOX chemotherapy, both acute and chronic cardiovascular effects have been reported, each with distinct signs and symptoms. Researchers have thus classified the cardiotoxicity into three main categories: acute, chronic and delayed-onset cardiotoxicity.

1.2.1 Acute Cardiotoxicity

Acute cardiotoxicity begins within the first few minutes of DOX administration and lasts for approximately 24 hours (De Beer *et al.*, 2001; Octavia *et al.*, 2012). This is an extremely rare

Stellenbosch University https://scholar.sun.ac.za

condition that can occur independently of ANT-dose, and rather depends on a patient's individual susceptibility to the drug. Symptoms of acute cardiotoxicity include changes in electrocardiogram (ECG), sinus tachycardia (Singal *et al*., 1997), arrhythmias, premature supraventricular and ventricular complexes (Barrett-Lee *et al*., 2009), hypotension and myocarditis (De Beers *et al*., 2001). These effects are usually described as minor and the prognosis at this stage remains fairly optimistic, as the majority of these cardiac conditions are clinically manageable and are asymptomatic. It has been reported that these acute-side effects resolve spontaneously following completion of a treatment course (De Beers *et al*, 2001).

Due to its high sensitivity and specificity, an endomyocardial biopsy of the right ventricle is the most favoured diagnostic tool utilized in the detection of acute DOX-induced cardiotoxicity. Tissue from the biopsy will indicate typical histopathological changes associated with acute cardiotoxicity. These include cytoplasmic vacuolization and the loss of myofibrils via electron microscopy (Chatterjee *et al*., 2010). Depending on the severity of these changes, the biopsy sample can be scored between 1 – 3, where a score of 2.5 or greater is considered high risk for cardiac dysfunction, resulting in termination of DOX infusion (Bristow, 1982). However, even though obtaining a biopsy sample is considered the most effective diagnostic procedure, it is rarely used as it is considered a high-risk procedure and is extremely invasive. More favoured procedures include monitoring ECG abnormalities, assessing both adrenergic denervation and energy metabolism via radionuclide scanning, and evaluating cellular injury through the measurement of cardiac biomarkers, such as cardiac troponin-T or troponin I (Lipshultz *et al*., 1997; Sparano *et al*., 2002; Takemura and Fujiwara, 2007)

Within this class, there is also sub-acute ANT cardiotoxicity, which is an even more uncommon form of DOX–induced acute cardiotoxicity, occurring in only 1.4 - 2% of all reported cases (Buzdar *et al*., 1985). Symptoms only appear several weeks to months following the last dose of ANT therapy (Hengel *et al*., 2006). Similarly to acute cardiotoxicity, the sub-acute form occurs independently of ANT dose administrated. Succeeding treatment, sub-acute cardiotoxicity most commonly manifests itself in the form of pericarditis-myocarditis, which is defined as inflammation of the pericardium, and ultimately reduces a patient's quality of life (Hengel *et al.*, 2006). Other symptoms include left ventricular wall thickening and interstitial myocardial edema and as consequence has

Stellenbosch University https://scholar.sun.ac.za

been associated with approximately 60% mortality (Octavia *et al*., 2012; Montagaine *et al*, 2012; Barrett-Lee *et al*, 2009). This myocardial dysfunction is however described as being reversable.

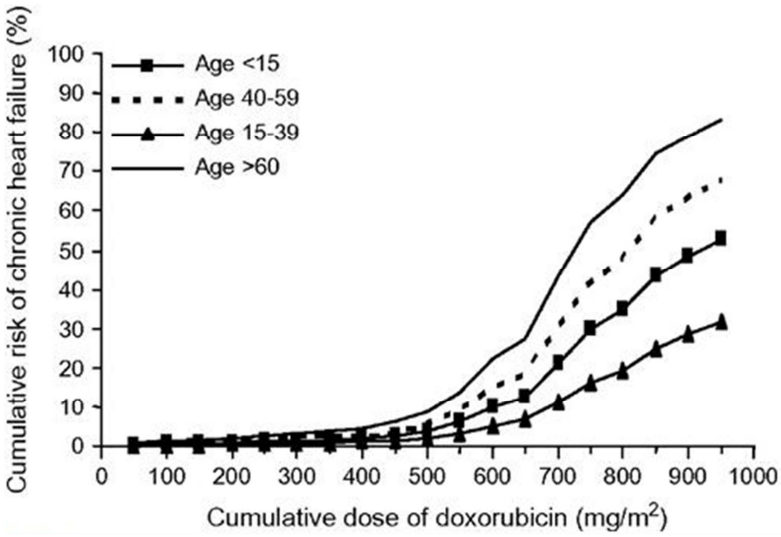

Figure 1.2: The Effect of Cumulative Doxorubicin Treatment on the Development of Chronic Heart Failure. The graph represents the cumulative risk for developing heart failure (%) vs. cumulative dose of doxorubicin treatment (mg/m^2). Reproduced from Von Hoff *et al*., 1979.

1.2.2 Chronic Cardiotoxicity

In contrast to the acute forms of ANT cardiotoxicity, the life-threatening chronic cardiotoxicity may not become apparent until a few months following the last treatment dose of DOX (De Beer *et al.*, 2001; Octavia *et al*., 2012; Takemura and Fujiwara, 2007). Chronic ANT-induced cardiotoxicity has been clinically defined as the most detrimental type of toxicity, as it leads to irreversible cardiomyopathies and CHF. Moreover, this type of chronic cardiomyopathy is dose-dependent and associated with repetitive and cumulative ANT regimes, as demonstrated in Figure 1.2 (Von Hoff *et al*., 1979). Clinical symptoms indicative of chronic cardiotoxicity include a rapid decline in blood pressure and ejection fraction, tachycardia, dilated cardiomyopathy, ventricular failure and eventually CHF (Singal *et al*., 1997; De Beer *et al*., 2001; Minotti *et al*., 2004). The ultrastructural features characterized from a patient's endomyocardial biopsy demonstrates the loss of myofibrils, sarcoplasmic

Stellenbosch University https://scholar.sun.ac.za

reticulum dilation, cytoplasmic vacuolization, mitochondrial swelling and increased lysosome formation (Minotti *et al*., 2004).

Studies have shown that life-time cumulative doses of DOX that exceed 550 mg/m^2 induce an increasing prevalence of chronic DOX-related cardiotoxicity and a 26% chance of developing heart failure (Figure 1.2) (Yeh and Bickford, 2009; Von Hoff *et al*., 1979). Therefore, in order to minimize the risk of developing cardiomyopathy while continuing treatment with a relatively "safe" dose of DOX, the maximum cumulative dose of DOX has been cautiously set to 500 - 550 mg/m^2 (Minotti *et al*., 2004; De Beer *et al*., 2001). However by setting an empirical dose limit, patients are deprived of an effective anticancer treatment regime in order to try and eliminate the incidence of cardiomyopathies. These findings highlight the importance of fully understanding and identifying the molecular mechanisms responsible for chronic DOX-induced cardiotoxicity. In this manner, researchers will be able to establish novel adjuvant therapy regimes and ensure that patients are receiving the best possible medical care in fighting cancer.

1.2.3 Delayed Cardiotoxicity

Late-onset or delayed ANT-induced cardiotoxicity usually occurs years or even decades after ANT treatment, and commonly occurs in patients who have received relatively low doses of ANT treatment for longer periods of time (Lipshultz *et al*., 2008; Bernaba *et al*., 2010). The pathogenesis of late-onset cardiotoxicity is not very well defined in the literature, but what we do know is that this form of toxicity presents itself as either dilated or restrictive cardiomyopathy or as myocardial arrhythmias (Bernaba *et al*., 2010). Studies by Leandro *et al.* (1994) and Lipshultz *et al.* (2008) further suggest that this form of ANT-induced cardiotoxicity is most likely to occur in patients who previously underwent rigorous, childhood chemotherapy. Moreover, this type of cardiotoxicity can clinically manifest over a number of years until it is triggered by various cardiovascular stressors, such as pregnancy or viral infections (Sereno *et al*., 2008; Ali *et al*., 2004). Despite on-going research, the cellular mechanisms for the delayed cardiotoxicity and explanation of its astonishing molecular so-called "dose-memory" are still poorly understood (Lebrecht *et al*., 2003; Bernaba *et al*., 2010). What is clear from the literature is that cardiotoxicity is not governed by a single mechanism, but is rather a multi-factorial process (Minotti *et al*., 2004). It is thus imperative

Stellenbosch University https://scholar.sun.ac.za

to understand and define these multi-factorial mechanisms in order to find effective therapeutic strategies that would prevent or delay the onset of chronic cardiotoxicity.

1.3 Doxorubicin Antitumor Activity

It is clear that following treatment with DOX, detrimental chronic-cardiotoxic side effects arise. Yet, the mechanisms of DOX's antitumor activity are different from those mechanisms that mediate cardiotoxicity (Chatterjee *et al*., 2010; Yang *et al*., 2014).

1.3.1 DNA Intercalation

In the late 1950's the first anthracycline antibiotic, DNR, was first isolated from *Streptomyces peucetius*, a bacterium species located in soil, which was found to have active anticancer properties (Mross *et al.*, 2006). It was only later in 1969 that DOX was successfully isolated and purified from a mutant of the original *Streptomyces* species, which was found near the Adriatic Sea (hence the DOX's alternate name, Adriamycin) (Mross *et al.*, 2006). It was around the same time, that Lerman (1961) introduced the term "intercalation" for the first time. Since this idealistic concept was introduced nearly 55 years ago, enormous progress has been made in understanding the mechanism of DNA intercalation as well as identifying ANTs, such as DOX as DNA-intercalators.

Intercalating agents are clinically used today as antibacterial, antiparasitic and antitumor drugs, since DNA intercalation inhibits DNA replication and thereby inhibits further cell growth (Berman and Young, 1981; Denny, 2002; Sasikala and Mukherjee, 2013). One of the mechanisms whereby DOX can inhibit cancer growth and promote cell death is through its intercalation into the cell's nuclear DNA. DOX and other ANTs are more likely to affect cancerous cells through DNA intercalation, as a result of the fast growth rate of these cells. Normal cells are however not spared in this process as they too are indirectly targeted by these drugs (Sasikala and Mukherjee, 2013).

Literature has described that DOX prefers to intercalate DNA at sites on the helix containing guanine-cytosine base pairs (Figure 1.3). This is most likely due to the specific hydrogen-bond formation between DOX and the Guanine residue (Chaires *et al.*, 1987; Chen *et al*.,

Stellenbosch University https://scholar.sun.ac.za

1986; Yang *et al*., 2014). This is evident from previous studies that have demonstrated that DOX-DNA adduct formation causes DNA damage and leads to cell death (Coldwell *et al.*, 2008). Despite the accumulating evidence of DOX-DNA adduct formation during DOX treatment is not thought to be the major mechanism involved in DOX's anticancer capabilities (Yang *et al*., 2014).

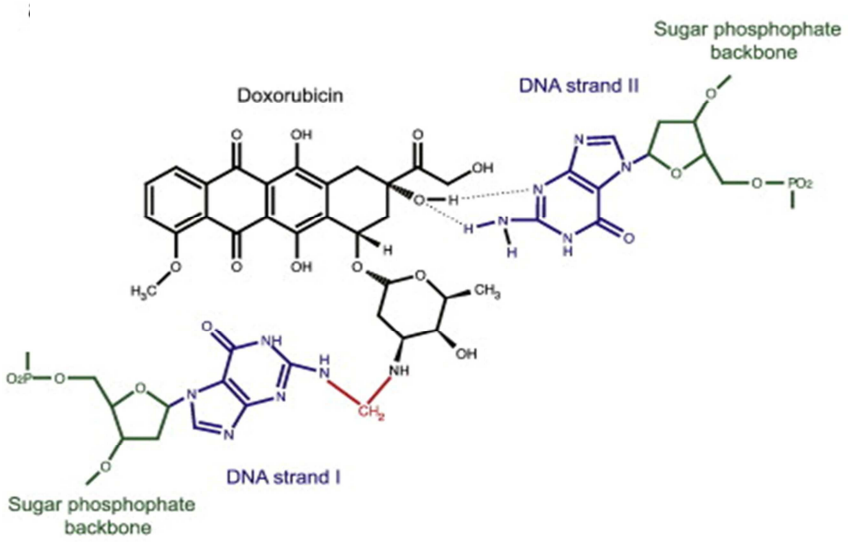

Figure 1.3: Structure of doxorubicin-DNA complex. Doxorubicin (shown in black) forms a covalent bond (shown in red) with guanine (shown in blue) on a strand of DNA. Image sourced from Yang *et al*., 2014

1.3.2 Topoisomerase II Poisoning

Topoisomerases are isomerase enzymes involved in regulating the topology of DNA and plays an important role in regulating DNA replication and transcription, as well as other nuclear processes (Pommier *et al*., 2010; Minotti *et al.*, 2004). They are able to temporarily 'cut' and 'reseal' both single-stranded (topoisomerase I) and double-stranded (topoisomerase II) DNA, in order to rearrange the twisting or winding status of the DNA double helix, ultimately preventing DNA supercoiling during DNA replication (Figure 1.4) (Minotti *et al.*, 2004).

Stellenbosch University https://scholar.sun.ac.za

Topoisomerase II is an ATP-dependent enzyme, which exists as two isoforms; topoisomerase IIα that is found in animals and rodents, and topoisomerase IIβ found in humans. This enzyme is not only essential for releasing torsional stress, which results from supercoiling of DNA during its unwinding for DNA replication, but is also involved with decatenation of DNA during mitosis (Yang *et al*., 2014). Damage to or deficiency of topoisomerase II can prevent normal cytokinesis and result in programmed cell death via apoptosis and necrosis (Minotti *et al*., 2004; Carpenter *et al*., 2004). Etoposide is a known topoisomerase II poison, which acts by trapping topoisomerase at its breakage sites and thereby inhibiting DNA resealing (Wu *et al*., 2011; Yang *et al*., 2014). Many studies have hypothesized that DOX's action on topoisomerase II is similar to that of Etoposide (Minotti *et al*., 2004; Nitiss, 2009). Furthermore, Burgess and colleagues (2008) demonstrated that the levels of topoisomerase II directly determined the effectiveness of DOX in a mouse model of lymphoma. Although there are numerous cases in support of the notion that DOX inhibits topoisomerase function, there are just as many studies indicating that DOX induces cell death independently of topoisomerase (Sorensen *et al*., 1992; Swift *et al*., 2006; Pang *et al*., 2013). Based on the above, it is clear that DOX-induced topoisomerase inhibition and the resulting cell death is still a matter of intense debate.

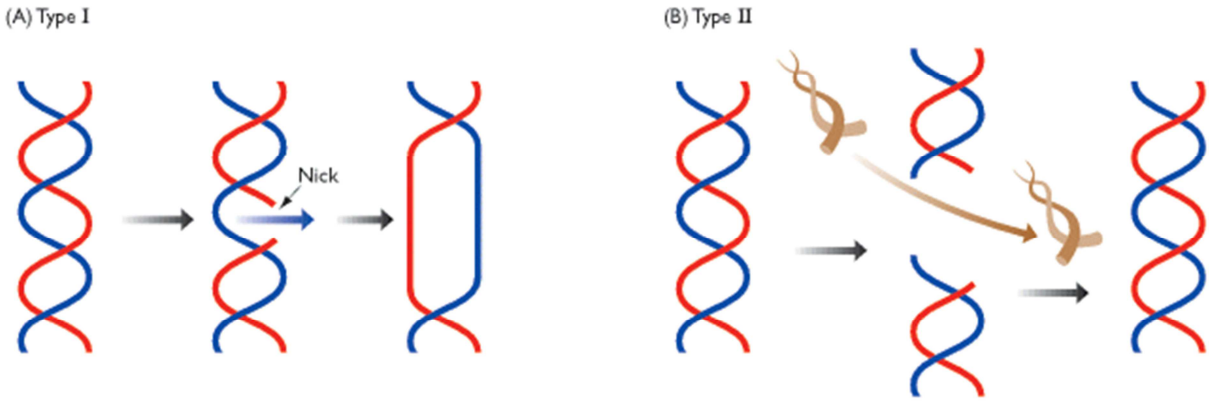

Figure 1.4: The Action of Topoisomerase I and II. Topoisomerase prevents DNA supercoiling during DNA replication and unwinding. (A) Action of Topoisomerase I: Temporarily cuts and reseals supercoiled single-stranded DNA, resulting in the uncoiling of 1 supercoil. (B) Action of Topoisomerase II: Temporarily cuts and reseals supercoiled double-stranded DNA, resulting in the uncoiling of 2 supercoils. Image sourced from Biosiva

Stellenbosch University https://scholar.sun.ac.za

1.3.3 Generation of Reactive Oxygen Species

The chemical structure of DOX consists of both aglyconic and sugar moieties (Figure 1.5). The aglyconic subunit consists of a tetracyclic ring with adjacent quinone-hydroquinone groups, whereas the sugar, daunosamine, is attached to the aglyconic subunit via a glycosidic bond (Minotti *et al*., 2004). Due to the presence of these quionone groups on the structure of DOX, it is thus prone to the generation of free radicals (Myers, 1998; Minotti *et al*., 2004). By oxidizing the quinone structure with the addition of a single electron, a semiquinone radical is formed. Furthermore, by removing a hydrogen atom (dehydrogenation) from the hydroquinone groups an additional semiquinone radical is formed. These semiquinone radicals are very unstable, and quickly react with oxygen to generate the free radicals, superoxide and hydrogen peroxide, which then induce DNA damage (Myers, 1998).

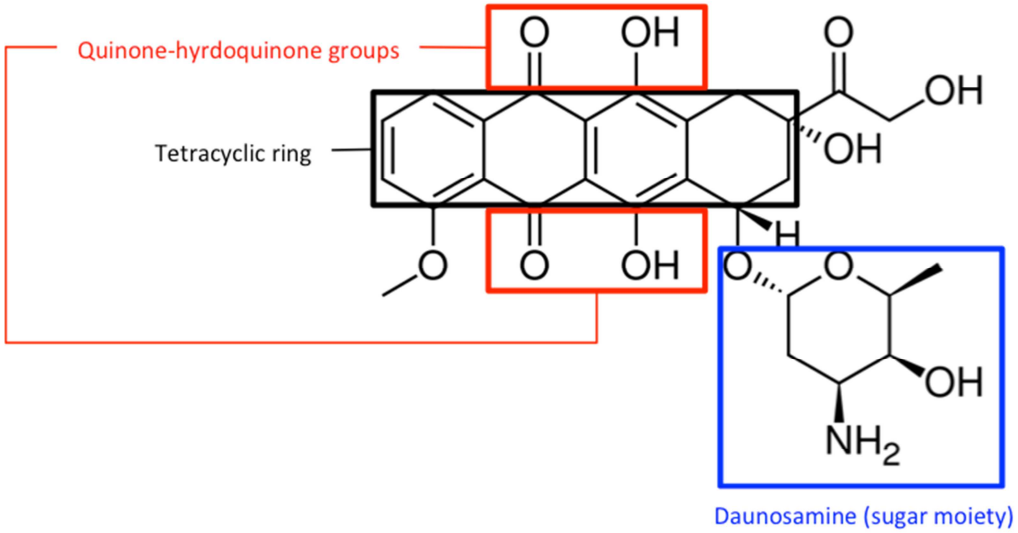

Figure 1.5: The Chemical Structure of Doxorubicin. Doxorubicin contains aglyconic and sugar moieties. Black square: Tetracyclic ring; Red square: Quinone-hydroquinone groups; Blue square: Daunosamine, the sugar moiety. Image adapted from Minotti *et al*., 2004

The semiquinone radicals formed are also able to oxidize the glyosidic bond between daunosamine and the aglyconic subunit. By detaching the sugar from the aglycone, increasing the aglycones lipid solubility, allows it to intercalate into the biologic membrane and induce reactive oxygen species (ROS) production (Gille and Nohl, 1997; Licata *et al*., 2000). This one-electron redox cycling of DOX is accompanied by the release of iron from its intracellular stores (Minotti *et al*., 2004). In patients undergoing chemotherapy for leukemia or bone marrow transplantation, the body's iron stores become disrupted as a result

Stellenbosch University https://scholar.sun.ac.za

of blood transfusions, blood loss or iron supplementation. In these situations iron overload can develop (Barton and Bertoli, 2000). Due to the high availability of iron, DOX-iron complexes form, which in turn act as catalysts and convert hydrogen peroxide to highly reactive hydroxyl radicals (Myers, 1998; Minotti *et al.*, 1999). The production and release of these free radicals from DOX causes oxidative stress within the cancer cells, resulting in DNA damage and ultimately cell death. It is in this manner that oxidative stress is considered as one of the major mechanisms of ANT antitumor activity.

1.3.4 Ceramide Overproduction

DOX treatment not only increases oxidative stress within cells, but it also increases ceramide levels (Yang *et al*., 2014). Ceramide is a naturally occurring lipid molecule also named a membrane sphingolipid (Steinbrecher *et al*., 2004). It is involved in a variety of processes, such as growth arrest and other functions, and has long been considered a pro-apoptotic mediator (Senchenkov *et al*., 2001; Steinbrecher *et al*., 2004). Literature indicates that ceramide production sensitizes the cancer cells to DOX chemotherapy, allowing DOX to have full effect within these cells by inducing cell death (Ji *et al.*, 2010). It is speculated that ceramides, which are lipid second messengers, generated as a result of DOX-induced oxidative stress trigger signaling cascades involving apoptosis (Martínez *et al*., 2009).

1.4 Mechanisms for Doxorubicin-induced Cardiotoxicity

1.4.1 Oxidative Stress

DOX-induced free radical production and associated ROS generation, is not only the major mechanism associated with the drugs antitumor capabilities, but is also thought to be the major mechanism contributing to the development of DOX-induced cardiotoxicity (Horenstein *et al*., 2000; Xu *et al*., 2001; Simůnek *et al*., 2009; Yang *et al*., 2014). As discussed previously, DOX induces ROS from a variety of sources, ranging from mitochondria to DOX-iron complexes. The problem is that the heart is vulnerable to ROS and oxidative stress irrespective of its source (Doroshow *et al*., 1980). This is because the myocardium has a relatively poor antioxidant defense system, and as such makes it prone to

Stellenbosch University https://scholar.sun.ac.za

oxidative damage (Horestein *et al*., 2000). When ROS levels rise in the myocardium causing oxidative stress, cardiomyocytes enzymatic defenses become overwhelmed. The absence of enzymatic protection allows ROS to interact with regulatory proteins and directly modify myocardial gene expression (Octavia *et al.*, 2012). It is also widely accepted in the literature that these free radicals target the cell membrane and induce lipid peroxidation, a process known to kill cardiomyocytes (Goormaghtigh *et al*., 1990; Xu *et al*., 2001). This particularly targets membrane bound G-proteins and directly affects myocardial intercellular signaling (Dhalla *et al.*, 2000; Octavia *et al*., 2012; Zhang and Mende, 2011). G-protein mediated signal transduction is essential for the regulation of cardiovascular function as it regulates heart rate and contraction, myocardial growth and vascular tone. Therefore by disrupting this signaling mechanism, pathophysiological changes such as hypertrophy, myocardial fibrosis, arrthymias and heart failure can occur (Sugamura and Keaney, 2011; Zhang and Mende, 2011).

In addition proteins are major targets for oxidative modification in cells (Chondrogianni *et al*., 2012). ROS can induce structural changes of protein tertiary structures via the oxidation of the covalent bonds (Octavia *et al*., 2012). This can result in the accumulation of misfolded or damaged proteins and thereby place strain on the myocardium's proteolytic systems. Proteins thus loose their biochemical functions, and as a consequence, can have detrimental downstream effects on intracellular signaling pathways (Chondrogianni *et al*., 2012).

1.4.2 The Oxidative Stress Hypothesis

Since free radical formation and ROS production was thought to account for the majority of DOX-mediated cell death, researchers proposed that treatment with antioxidants or free radical scavengers in conjunction with DOX would protect the heart against DOX cardiotoxicity (De Beer *et al*., 2001; Wergeland *et al*., 2011). However, very few free radical scavengers have thus far demonstrated protection in the heart against DOX-induced cardiotoxicity. They include dexrazoxane (DXZ) hydrochloride (Zinecard or Cardioaxane) and flavonoids (De Beer *et al.*, 2001). Currently DXZ is the only agent utilized in clinical studies owing to its ability to reduce toxicity associated with DOX (Imondi *et al*., 1996; Speyer *et al*., 1988; Swain *et al*., 1997). Hasinoff (1997) proposed that DXZ inhibits free radical formation through iron-chelation, and in this manner prevents the formation of DOX-

Stellenbosch University https://scholar.sun.ac.za

iron adducts. Speyer and colleagues (1992) previously demonstrated that when DXZ is administrated to woman with advanced breast cancer 15 – 30 minutes prior to treatment with DOX, that this did not hinder DOX distribution or its antitumor function. This study further indicated that the incidence of cardiotoxicity was reduced and therefore patients who received DXZ could be treated with higher, cumulative doses of DOX.

Over the last few years however there has been a reconsideration of DXZ's pharmacological and clinical cardioprotective properties. In addition to its iron-chelative effects, DXZ has been identified as an important anticancer agent itself (Hasinoff *et al*., 1997). Numerous studies have indicated that DXZ functions as an inhibitor of topoisomerase II, in a manner similar to DOX (Hasinoff *et al*., 1997; Langer *et al*., 2000). This has sparked new interest in using this agent as an antineoplastic drug, either as a single agent or in combination with DOX (Tetef *et al*., 2001). However since the mechanisms and underlying interactions between DXZ and DOX have not been clinically evaluated, some studies have expressed concern that DXZ might in fact compete against DOX within the cell and therefore reduce DOX's anticancer capabilities (Minotti *et al*., 2004).

Flavonoids are believed to also act as free radical scavengers as well as iron-chelators (Haenen *et al*., 1993; Van Acker *et al*., 1995). Quercetin is one of the most commonly studied flavonoids (Hertog *et al*., 1993; Jacobs *et al*., 2010). A semi-synthetic flavonoid, 7-mono-O-(β-hydroxyethyl)-rutoside (monoHER), which closely resembles the chemical structure of Quecetin has been shown to provide protection against chronic DOX-induced cardiotoxicity *in vivo* (Van Acker *et al*., 1995; Van Acker *et al*., 1997). However due to monoHER's negative effects on the glutathione (GSH) antioxidant defense system in the heart, researchers have been unable to replicate or reproduce these results in the clinical setting (Bruynzeel *et al*., 2007a; Bruynzeel *et al*., 2007b). The majority of free radical scavengers, like dexrazoxane and flavonoids, are utilized as protectants against DOX-induced cardiotoxicity, but many of them have failed to provide long-term protection against chronic cardiotoxicity (Yang *et al*., 2014). This suggests that alternate mechanisms, other than the production of free radicals, may be involved in the progression of cardiotoxicity.

The administration of antioxidants in conjunction with DOX treatment has been successful *in vivo* in reducing oxidative stress and cardiotoxicity (Saleem *et al*., 2014; Wergeland *et al*., 2011), but again results have been unsuccessful in clinical trials (Bjelogrlic *et al*., 2005;

Stellenbosch University https://scholar.sun.ac.za

Dresdale *et al*., 1982; Vejpongsa and Yeh, 2014). Yagmurca (2003) demonstrated that Erdosteine, an antioxidant agent, protected against chronic DOX cardiotoxicity *in vivo*, but reduced DOX's antitumor effects. Vitamin E (α-tocopherol), another important antioxidant, was found to be effective in ameliorating acute DOX toxicity *in vivo* (Mimnaugh *et al*., 1979), while offering no protection in the chronic setting (Breed *et al*., 1980; Legha *et al*., 1982; Van Vleet *et al*., 1980). Administration with other antioxidant compounds such as vitamin C (ascorbic acid) (Tavares *et al*., 1998), vitamin A (Shimpo *et al*., 1991) and coenzyme Q (Greenlee *et al*., 2012) also found to be ineffective in reducing or inhibiting chronic DOX cardiotoxicity. Evidence from the literature suggests that antioxidants may only assist in delaying the onset of DOX's toxic effects, rather than completely preventing cardiomyopathy. Although it is clear that oxidative stress plays a major role in mediating DOX-induced cardiotoxicity, the failure of antioxidants to reduce chronic toxicity implies that other cellular mechanisms are involved. DOX-activated apoptotic signaling, which has previously been linked to the formation of ROS, is another mechanism thought to contribute to DOX-mediated cardiomyopathy (Nitobe *et al.,* 2003; Wang *et al*., 2004).

1.4.3 Apoptosis

It is long been understood that ANTs induce cardiotoxicity by mechanisms other than those initiated in mediating its antineoplastic efficacy. Until a few years ago, apoptosis was overlooked as a possible mechanism for DOX-induced cardiotoxicity and CHF. Since then, it has been shown extensively in the literature that DOX mediates both intrinsic and extrinsic apoptotic pathways, as shown in Figure 1.6 (Liu *et al*., 2007; Wang *et al*., 1998; Yamaoka *et al*., 2000).

Initially it was thought that DOX initiated apoptosis indirectly via the generation of ROS only (Wang *et al*., 2002; Nitobe *et al*., 2003), but it has recently been shown that DOX can directly regulate cardiomyocyte apoptosis, bypassing ROS involvement (Papadopoulou *et al*., 1999; Liu *et al*., 2007). DOX directly induces intrinsic (mitochondrial) apoptosis by promoting the leakage of cytochrome C from the mitochondria, formation of the apoptosome complex and activation of caspase 3 (Kim *et al*., 2006; Zhang *et al*., 2012). The manner in which this occurs is possibly a result of DOX's binding to the mitochondria, which causes the collapse of the mitochondrial membrane potential. This leads to the opening of the mitochondrial permeability transition pore (mPTP), mitochondrial swelling, rupture the

Stellenbosch University https://scholar.sun.ac.za

mitochondrial outer membrane and leakage of cytochrome C (Camello-Almaraz *et al*., 2006; Deniuad *et al*., 2008). While this is happening, there is an upregulation of Bax (Bcl-2-associated X-protein, a pro-apoptotic protein) and downregulation of Bcl-X_L (an anti-apoptotic protein). In this scenario, Bcl-X_L would usually play a critical role inhibiting the effects of cytochrome C function, however due to its downregulation, apoptosis is the ultimate event (Figure 1.6) (Kim *et al*., 2006; Minotti *et al*., 2004). Indirectly, DOX-mediated intrinsic apoptosis may also be promoted not only by DOX-associated ROS production but also ceramide production (Armstrong, 2004; Parra *et al*., 2008) and p53 phosphorylation (Liu *et al*., 2008).

The Fas/Fas ligand (Fas/FasL) system is an important regulator of the extrinsic pathway of apoptosis signaling in various organisms. Fas, a member of the tumor necrosis factor (TNF)-receptor family, is a type I membrane protein, expressed in a wide variety of tissues (Nagata, 1997; Yonehara, 1989). FasL on the other hand, is a member of the TNF family, and a type II membrane protein (Suda *et al*., 1993; Nagata, 1997). The binding of Fas ligand to its receptor Fas on the target cell results in the activation of the caspase cascade.

This cascade proteolytically cleaves important proteins and cellular DNA and thereby induces cell death (Nagata, 1997; Enari *et al*., 1998). Yamaoka and colleagues (2000) confirmed this in a study and demonstrated that resting cardiomyocytes treated with DOX were sensitized to Fas/FasL induced apoptosis. Recently Ren *et al.* (2012) found that the overexpression of angiopoietin-1 (ang-1), an important growth factor protein, protected cardiomyocytes against DOX-induced apoptosis by attenuating both intrinsic and extrinsic apoptosis, which suggests that both apoptotic pathways are important in mediating DOX toxicity. Although there is no indication in the literature as to which of the two pathways is dominant or whether both pathways are stimulated concurrently, it is evident that DOX can induce apoptotic cell death.

Stellenbosch University https://scholar.sun.ac.za

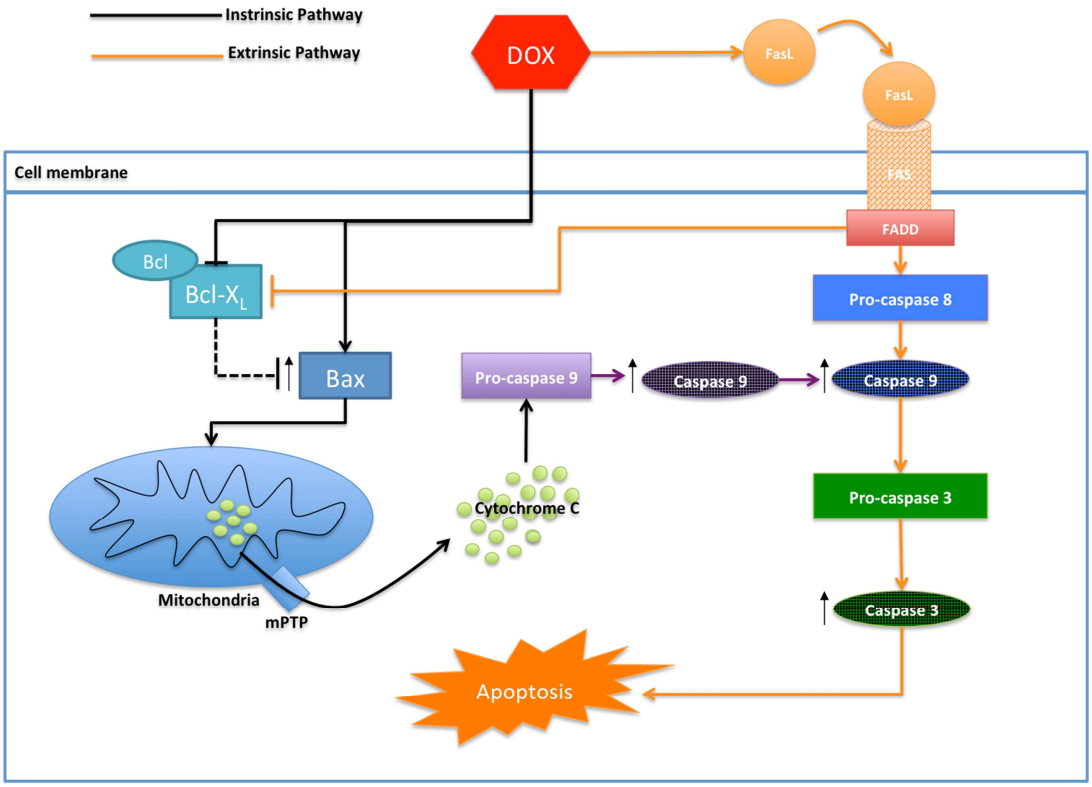

Figure 1.6: Intrinsic and extrinsic apoptotic pathways activated in the myocardium following Doxorubicin treatment. DOX induces intrinsic apoptosis (indicated with the black arrows) via the mitochondria by promoting mPTP opening and cytochrome c leakage. DOX mediates extrinsic apoptosis (indicated with the orange arrows) via activation of the Fas/FasL system. Abbreviations - Bax: apoptotic regulator, Bcl: B-cell lymphoma, Bcl-X_1: Bcl associated X protein, DOX: Doxorubicin, FADD: Fas associated protein with death domain, FasL: Fas Ligand, mPTP: mitochondrial permeability transition pore.

1.4.4 Intracellular Calcium Dysregulation

Research indicates that treatment with DOX induces an increase in intracellular calcium levels, which identifies another mechanism whereby DOX-induced cardiotoxicity may arise. Supporting this hypothesis, a study compiled in 1974 by Olson *et al.* described an incremental increase in calcium accumulation in both the ventricular myocardium and the mitochondria of rabbit hearts following DOX infusion. Other studies have shown that DOX alters the transitional sacrolemmal calcium influx, otherwise known as activator calcium (Rossini *et al.*, 1986), due to DOX's effects on the Na^+/K^+ -ATPase and Na^+/Ca^{2+}exchanger

Stellenbosch University https://scholar.sun.ac.za

pumps (Gosálves *et al*., 1979; Caroni *et al*., 1981; Boucek, 1997b). Under normal conditions, activator calcium forms an integral part of the electrical excitation within the sarcoplasmic reticulum (Rossini *et al*., 1986) and is regulated by the activity of these ion channels and exchanger pumps (Carafoli, 1985; De Beer *et al*., 2001). Activator calcium initiates the interaction between actin and myosin, ultimately determining the force of cardiac contraction (Rossini *et al*., 1986). Thus continuous disruption in the calcium flux can lead to contractile dysfunctions, and thereby contribute to the development of CHF.

The augmentation of intracellular calcium levels could be the cause or consequence of oxidative stress. DOX-induced ROS can directly disrupt sarcoplasmic reticulum function, leading to alterations in calcium homeostasis (Octavia *et al*., 2012). Studies by numerous authors show that oxidative stress, in particular hydrogen peroxide (Arai *et al*., 2000), inhibits the activity of the sarcoplasmic Ca^{2+} -ATPase pump, and causes impaired calcium handling (Boucek *et al*., 1987; Ondrias *et al*., 1990; Dodd *et al*., 1993; De Beer *et al*., 2001), in addition to indirectly activating the ryanodine calcium-release (RyR) channels (Holmberg and Williams, 1990; Boucek, 1999). Under normal conditions RyR channels represent the primary pathway responsible for calcium release during the excitation-contraction coupling process. These unique channels are found on calcium storage/release organelles, like the sarcoplasmic/endoplasmic reticulum. Regular sacrolemmal/endoplasmic calcium influx activates the RyR channels, but under DOX-induced calcium distress, these channels remain open (Boucek, 1999; Fill and Copello, 2002). It is possible that DOX binds to one of the many sites on the channel, and in this manner directly influences RyR channel opening (Saeki *et al*., 2002). Taking all this into consideration, together with other reviews (Boucek, 1999; Octavia *et al*., 2012), dysregulation in sarcolemmal calcium loading and release is a major factor in the pathogenesis of DOX-induced chronic-cardiotoxicity.

To further emphasize the damaging role of DOX-induced oxidative stress, Kalivendi *et al.* (2005) illustrated that when intracellular calcium accumulation occurs, NFAT (nuclear factor of activated T-cells) is activated and Fas/FasL apoptosis is stimulated. Calineurin, a calcium-dependent phosphatase, dephosphorylates and activates NFAT in response to a sustained elevation of intracellular calcium (Baksh and Burakoff, 2000; Hogan *et al*., 2003). Dephosphorylated NFAT in the cardiac cell then translocates to the nucleus where it initiates hypertrophic gene expression and cardiac hypertrophy (Schulz *et al*., 2004) as well as the activation FasL and extrinsic apoptosis (Latinis *et al*., 1997) (Figure 1.7). Thus, the

Stellenbosch University https://scholar.sun.ac.za

calcineurin/NFAT pathway under pathological conditions can induce both cardiac hypertrophy and cell death, contributing to DOX-induced contractile dysfunction and toxicity. Additionally DOX-induced oxidative stress can also result in calcium 'leakage' from the sarcoplasmic reticulum (Solem *et al*., 1996). Prolonged conditions of increased intracellular calcium can lead to the activation of the calcium-dependent proteolytic enzyme, Calpain (Campos *et al*., 2011; Octavia *et al*., 2012). Calpain activation can induce the cleavage of caspase 12 (usually seen under conditions of endoplasmic/sarcoplasmic reticulum stress) and activation of apoptotic pathways (Figure 1.7) (Nakagawa *et al*., 2000). In support of this theory, Jang *et al.* (2004) demonstrated that DOX-induced calpain activation is one of the mechanisms involved in progression towards cardiomyopathy and heart failure, in both male and female rats. Additionally, it is known that DOX-induced cardiotoxicity is associated with myofibrillar deterioration (Sawyer *et al*., 2002) and it is thought that calpain activation mediates this effect. Considering that myofibrillar proteins (e.g. titin) are essential components involved in maintaining myocardial contraction and cardiac integrity, uncontrolled degradation could result in detrimental consequences for the myocardium (Danialou *et al.*, 2001; Lapidos *et al*., 2004; Tidball and Wehling-Henricks, 2007).

Stellenbosch University https://scholar.sun.ac.za

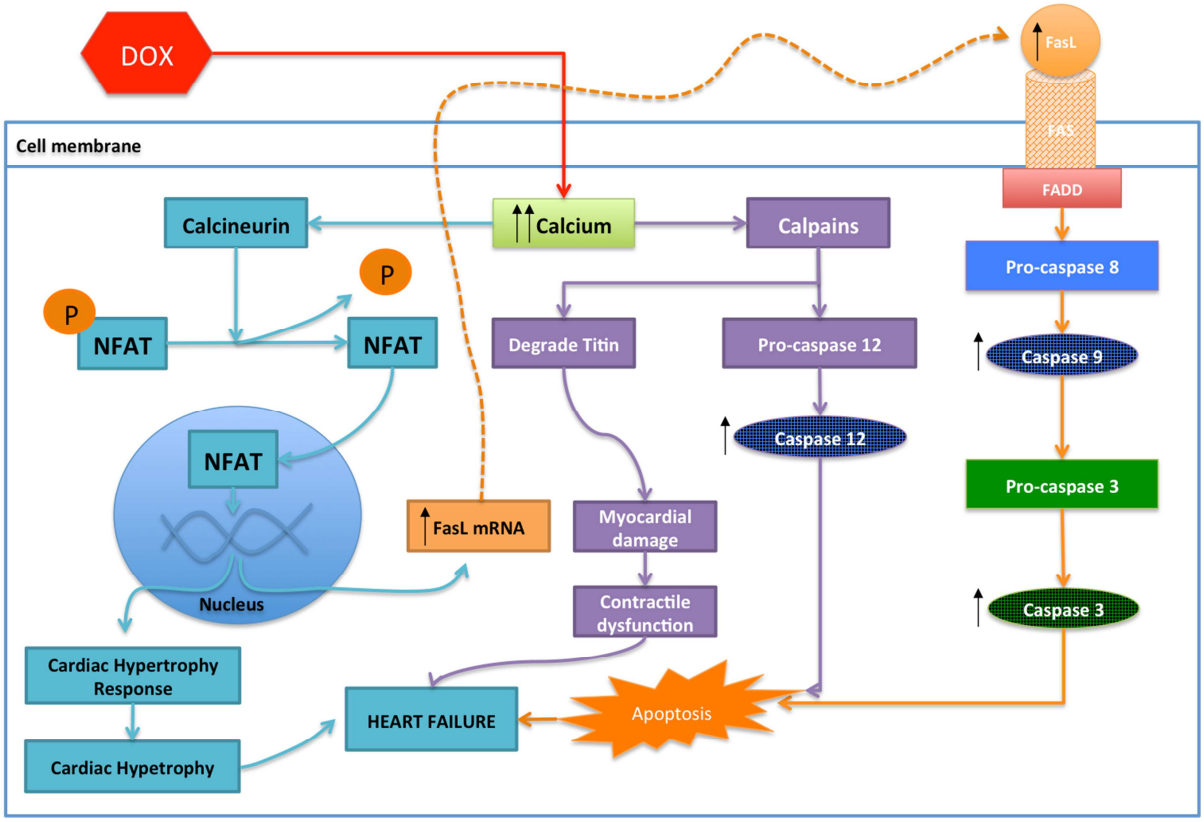

Figure 1.7: Intracellular Calcium Dysregulation and cell signaling induced by Doxorubicin treatment. DOX increases intracellular calcium levels. Calineurin dephosphorylates and activates NFAT in response to a sustained elevation of intracellular calcium and results in cardiac hypertrophy and activation of FasL (pathway indicated in blue). An increase in FasL expression activates Fas/FasL apoptosis (pathway indicated in orange). Elevated intracellular calcium results in calpain activation, which leads to contractile dysfunction and apoptosis (pathway indicated in purple). Abbreviations - DOX: Doxorubicin, FADD: Fas associated protein with death domain, FasL: Fas Ligand, NFAT: nuclear factor of activated T-lymphocytes, P: Phosphate.

1.5 Endoplasmic Reticulum Stress

The endoplasmic reticulum (ER) forms part of an extension of the nuclear envelope within a mammalian cell, and is the major organelle responsible for the synthesis, post-translational modification and folding of proteins (Xu *et al.*, 2005; Malhi and Kaufman, 2011; Grim, 2012). The ER is involved in various cellular processes, such as the maintenance of calcium homeostasis and lipid biosynthesis (Ron and Walter, 2007; Kaufman, 2002). Under conditions of oxidative stress, calcium dysregulation or a decrease in ATP levels (adenosine

Stellenbosch University https://scholar.sun.ac.za

triphosphate), the ER becomes overwhelmed and cannot function efficiently. This leads to the accumulation of misfolded proteins within the ER lumen and when this occurs, a phenomenon termed ER stress is stimulated (Stutzmann and Mattson, 2011). Special receptors or transmembrane sensors detect the build up of these proteins within the lumen and initiate the unfolded protein response (UPR) in order to try and overcome the resulting ER stress (Minamino *et al*., 2010; Wang *et al*., 2014). However, in order to elucidate the role the ER plays in the pathophysiological progression of DOX-induced cardiotoxicity, a deeper understanding of ER stress and the UPR is required.

1.5.1 Understanding the Unfolded Protein Response

The UPR is stimulated when ER transmembrane sensors detect signals of ER stress. These sensors include protein kinase RNA-like endoplasmic reticulum kinase (PERK), inositol-requiring enzymes 1α (IRE1α) and activating transcription factor 6 (ATF6) (Shamu and Walter, 1996; Haze *et al*., 1999; Harding *et al*., 2000). Under normal homeostatic conditions PERK, IRE1α and ATF6 form complexes with the ER binding immunoglobulin protein (BiP/GRP78), which inhibits their activity (Kozutsumi *et al*., 1988; Bertolotti *et al*., 2000; Hetz, 2012). When misfolded or damaged proteins accumulate in the ER lumen, they bind to BiP competitively, causing its dissociation from the BiP transmembrane receptors and thereby inducing their activation (Figure 1.8) (Bertolotti *et al*., 2000; Hampton, 2000; Hetz, 2012).

PERK is a serine-threonine kinase. These particular types of kinases are generally responsible for regulating cell proliferation, cell death signaling and cellular differentiation (Avivar-Valderas *et al*., 2011) Following the onset of ER stress and subsequent activation, PERK phosphorylates and inactivates eIF2α (eukaryotic translation initiation factor 2α). The now inactive eIF2α inhibits mRNA translation resulting in a reduction protein synthesis and ER protein load. IRE1α, also a serine-threonine kinase, has been termed the most fundamental ER stress sensor in the cell (Minamino *et al*., 2010). Upon its activation, IRE1α stimulates specific endoribonuclease cleavage of mRNA encoding for the protein XBP1 (transcriptional factor X-box binding protein 1). XBP1 activates an adaptive transcriptional response focused on inducing normal ER homeostasis. Interestingly IRE1α appears to stimulate c -dependent signaling pathways, as described by Ogata *et al*. (2006), and later by Green and colleagues (2011). This activation regulates autophagy, and thus identified a potential cross-link or

Stellenbosch University https://scholar.sun.ac.za

pairing between the UPR and autophagy, which was unknown before. It is important to note that activation of c-JUN has also been implicated with an increase in tumor invasiveness implying that the activation of IRE1α could have a potentially negative impact in the cell, rather than just trying to alleviate ER stress (Ogata *et al*., 2006; Green *et al*., 2011; Yang *et al*., 2014).

ER stress also induces the release of BiP from ATF6, thereby unmasking ATF6's Golgi-apparatus signal (Minamino *et al*., 2010). This permits ATF6 translocation from the nucleus to the Golgi- apparatus, where is it proteolytically cleaved. Cleaved ATF6 acts as a transcription factor, and induces the transcription of XPB1 and ERAD (Endoplasmic-reticulum-associated protein degradation proteins (Yoshida *et al*., 2000; Minamino *et al*., 2010; Wang *et al*., 2014). Upregulation of ERAD proteins directly increases activity through the ERAD pathway, which mediates the translocation of misfolded proteins to the 26S proteasome, a process known as retrotranslation (Kaufman, 2002; Ron and Walter, 2007). Therefore based on the above, the UPR does not work alone in the process of alleviating ER stress. It elicits the help of the cell's major degradation pathways, autophagy and the ubiquitin-proteasome pathway (UPP) in an effort to try and bring the cell back to homeostasis. However, should ER stress not be resolved, apoptosis can be induced (Benbrook and Long, 2012).

Stellenbosch University https://scholar.sun.ac.za

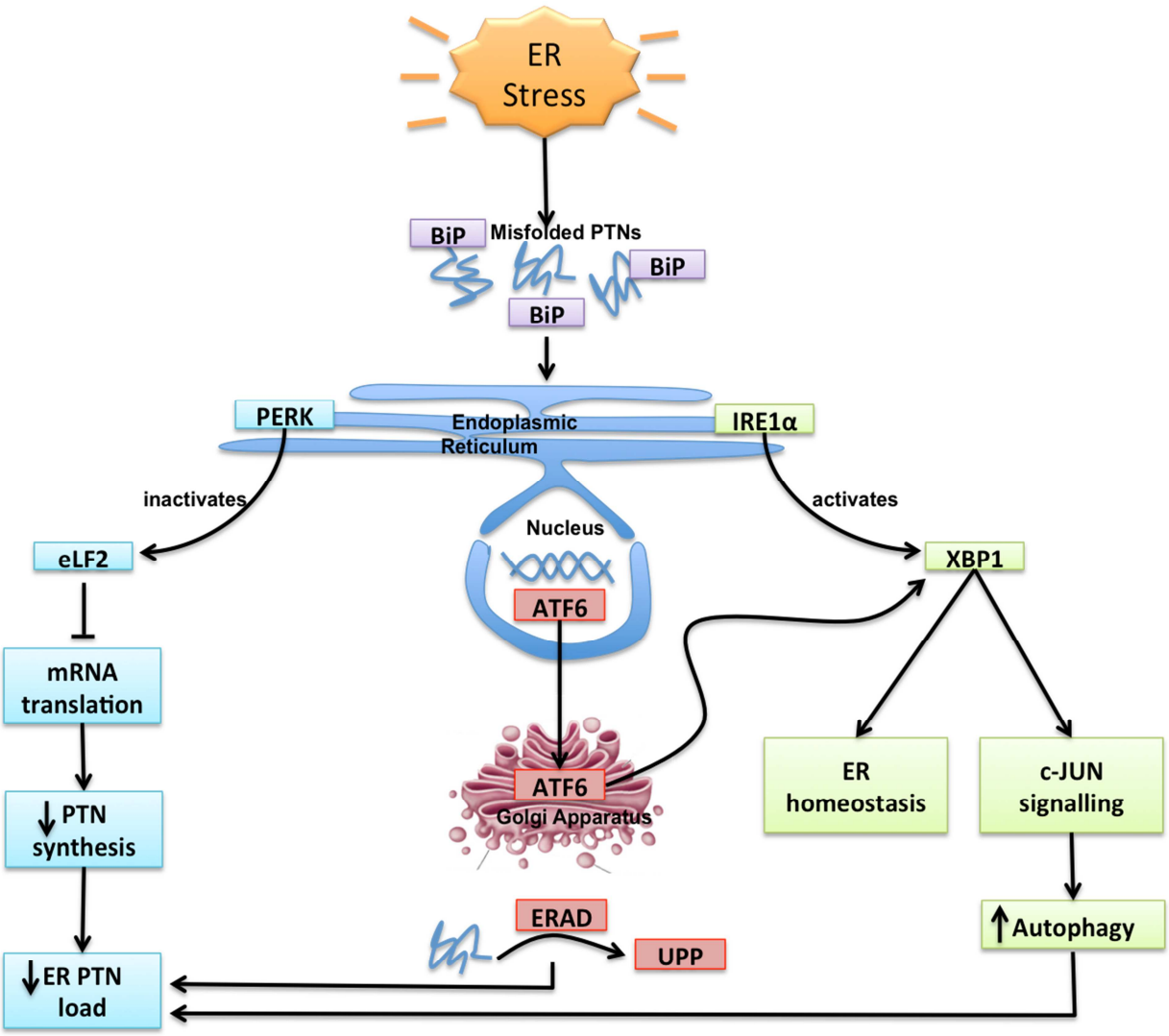

Figure 1.8: The Unfolded Protein Response. Misfolded or damaged proteins accumulate, which bind to BiP, which releases BiP inhibitory effects on the ER's transmembrane sensors PERK, ATF6 and IRE1. Through a serious of downstream activities, the UPR is initiated in order to try and decrease the ER protein load. Abbreviations - ATF6: activating transcription factor 6, BiP: ER binding immunoglobulin protein, ER: endoplasmic reticulum, ERAD: Endoplasmic reticulum associated protein degradation, IRE1: inositol-requiring enzymes 1 alpha, PERK: endoplasmic reticulum kinase, PTN: protein, UPP: the ubiquitin proteasome pathway, XBP1: transcriptional factor X-box binding protein 1.

1.5.2 Calcium Dysregulation During ER Stress

It is only natural that there be a high calcium concentration in the lumen. Since the ER is responsible for the storage and maintenance of calcium homeostasis, elevated calcium concentrations and a low oxidative environment within the lumen creates the optimal

Stellenbosch University https://scholar.sun.ac.za

environment that the ER requires for synthesizing and folding proteins into their proper conformation (Lam and Galione, 2013). When ER stress occurs, calcium from the ER is released causing an increase in free intracellular calcium (Doroudgar *et al*., 2013). Considering that the ER is in close proximity to the mitochondria, the mitochondrial will likely take up the calcium via the calcium uniporter until a certain threshold is reached (Trenker *et al*., 2007; Brookes *et al*., 2008). Once this threshold is reached, the mitochondrial membrane potential collapses, the mPTP opens, cytochrome c leaks and apoptosis is induced (Williams *et al*., 2013). DOX appears to have an affinity for the ER, as demonstrated by Sishi *et al.* (2013b), potentially demonstrating a mechanism whereby DOX can directly initiate ER stress. Considering this study made use of an acute cellular model of DOX-induced cardiotoxicity, it remains to be elucidated whether this phenomenon is also present in the chronic scenario of this condition. Not only is the ER sensitive to changes in calcium homeostasis; it is just as sensitive to condition of elevated oxidative stress. It is therefore not surprising that ER stress is detected in conditions such a cardiotoxicity and other cardiovascular diseases caused by proteasome inhibition or ERAD overload (Minamino and Kitakaze, 2010).

Many studies have shown coordinated calcium signaling between the mitochondria and ER (Chami *et al*., 2008; Pizzo and Pozzan, 2007), and in order to stimulate oxidative phosphorylation, calcium is required (Brookes *et al*., 2004; Dedkova and Blatter, 2013; Duchen, 2000). Since the ER is the major source of calcium within the cell, and the mitochondrial rely on calcium for various functions, proper communication between these two organelles is essential (Brookes *et al*., 2004). In the presence of DOX however this is not the case, as both organelles become dysfunctional and induce cell death mechanisms (Paradies *et al*., 2009; Solem *et al*., 1994).

1.6 DOX-induced Cardiotoxicity and the Mitochondria

Research indicates that the mitochondria are the most extensively and progressively damaged organelles during DOX-induced cardiotoxicity (Octavia *et al*., 2012). DOX directly affects mitochondrial respiration, induces oxidative stress and disrupts mitochondrial membrane potential, by either binding directly to the mitochondria or by other indirect mechanisms (Childs *et al*., 2002; Tokarska-Schlattner *et al*., 2007). Literature has also demonstrated the

Stellenbosch University https://scholar.sun.ac.za

involvement of the mitochondria in the activation of the cell death pathways, apoptosis and necrosis (Berthiaume and Wallace, 2007; Parra *et al*., 2008). Considering that clinical therapeutic interventions involving the use of antioxidants has been widely unsuccessful in treating the chronic side effects of DOX, novel investigations into new adjuvant therapies targeting mitochondria are focused on preventing their damage by DOX.

One of the main reasons why the mitochondria may be so extensively damaged and prone to abnormal morphological features in the presence of DOX is due to DOX's ability to form complexes with cardiolipin present in inner mitochondrial membrane (Schlame *et al*., 2000; Schlame and Hostetler, 1992). Once bound, DOX can be retained within the mitochondria and interrupt important cardiolipin-protein complexes (Goormaghtigh *et al.,* 1990; Schlame *et al*., 2000). Cardiolipin is a phospholipid bio-synthesized in the mitochondrial matrix (Daum, 1985; Schlame *et al*., 2000; Schlame and Hostetler, 1992). It plays an integral role in mitochondrial oxidative phosphorylation and in maintaining the structural integrity of the mitochondrial membranes (Zhong *et al*., 2014), thus any alterations in its activity or compositions can induce mitochondrial dysfunction (Petrosillo *et al*., 2003; Lesnefsky Hoppel, 2008; Pope *et al*., 2008). One of the critical functions of cardiolipin is that proteins of the electron-transport chain require cardiolipin binding to function effectively (Goormaghtigh *et al.,* 1990). Once this balance is disturbed by the formation of DOX-cardiolipin complexes, superoxide is instead produced (Schlame *et al*., 2000). This prevents normal mitochondria from performing critical cellular functions such as ATP production. Bearing all of the above in mind, an important aspect that needs serious consideration is mitochondrial morphology. Since mitochondrial morphology governs many biological functions including cell survival and cell death, it is important to investigate the effects of DOX on mitochondrial dynamics.

1.6.1 Mitochondrial Dynamics

The mitochondrion has long been considered as the "energy powerhouse" of the cell, which works consistently, and tirelessly to provide the energy, in the form of ATP, that is required for biological functioning (McBride *et al*., 2006). Recent studies have however demonstrated that the maintenance of the mitochondria's bioenergetic demand relies heavily on the morphological plasticity of the organelle (Galloway *et al*., 2012b). The steady state of the

Stellenbosch University https://scholar.sun.ac.za

mitochondrial morphology is regulated by the two dynamic events; mitochondrial fission and mitochondrial fusion.

Mitochondrial fusion is a mechanism whereby neighboring mitochondria fuse together creating elongated, interconnected mitochondrial tubules. Conversely, mitochondrial fission is involved in the fragmentation of the tubular interconnected mitochondria into smaller, discontinuous ones (Dimmer and Scorrano, 2006; Ong *et al*., 2010). Mitochondrial fusion involves fusion of both the outer and inner mitochondrial membranes in order to form a functional mitochondrion (Hammerling and Gustafsson, 2014). Fusion of the outer mitochondrial membranes (OMM) is regulated by the two mitochondrial fusion proteins mitofusin 1 (Mfn1) and mitofusin 2 (Mfn2), whereas inner mitochondrial membrane (IMM) fusion is dependent on the optic atrophy protein 1 (Opa1) (Chen *et al*., 2013; Chen *et al*., 2011b) (Figure 1.9a). Two proteins that mediate Mitochondrial fission are dynamin-related protein 1 (Drp1/DLP1) and mitochondrial fission protein 1 (hFis1/TTC11) (Mozdy *et al*., 2000; Yoon *et al*., 2003). Cytosolic Drp1 translocates to the OMM, through its interaction with the hFis1, and forms a ring around the mitochondrion, pinching it into two daughter mitochondria (Lee *et al*., 2007; Smirnova *et al*., 2001) (Figure 1.9b). Disruption of fine balance of mitochondrial dynamics has been linked to the cell's regulation of apoptosis, as well as many cardiac diseases, including cardiac hypertrophy, dilated cardiomyopathy and heart failure (Dorn, 2013; Zungu *et al*., 2011).

Mitochondrial fission has previously been shown to be induced by oxidative stress, a mechanism proposed by Frank *et al.* (2001). In conditions where oxidative stress levels are high, Drp1 translocates from the cytosol into the mitochondria, where mitochondrial division is initiated. Drp1 hydrolyses GTP (Guanosine-5'-triphosphate), which in turn dysregulates the fine balance between mitochondrial fission and fusion, tipping the scale towards fission (Karbowski and Youle, 2003; Chen and Chan, 2009; Ong and Hausenloy, 2010). This fission, under pathological conditions, can stimulate the release of cytochrome C from the mitochondria, activate caspases and ultimately apoptosis (Green and Reed, 1998; Frank *et al*., 2001). In the context of DOX cardiotoxicity, it is highly possible that the ER stress and calcium dysregulation that occurs triggers mitochondrial fission and contributes to the pathological consequences of DOX toxicity (Brookes *et al*., 2004; Iglewski *et al*., 2010).

Stellenbosch University https://scholar.sun.ac.za

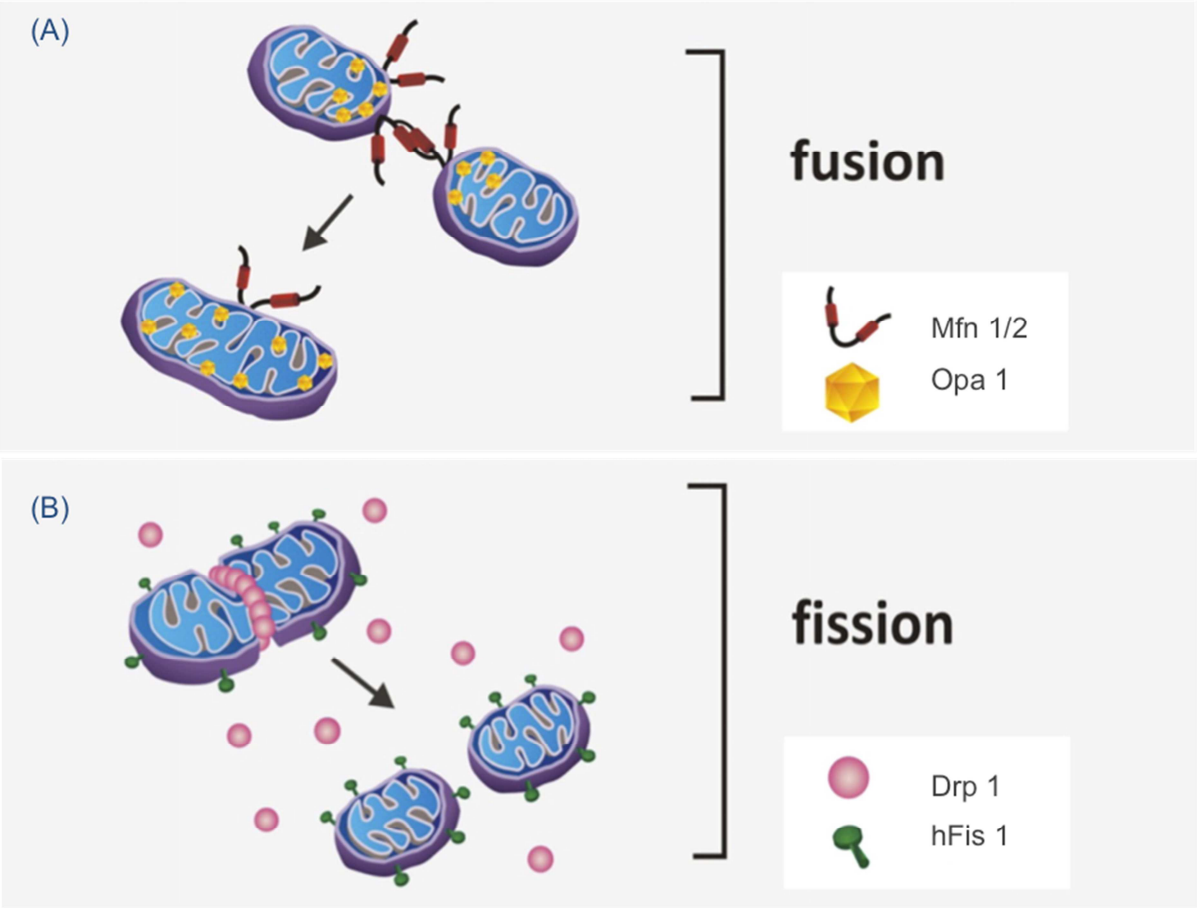

Figure 1.9: Mitochondrial morphology regulated by mitochondrial fusion and fission events. (A) Mitochondrial Fusion; OMM fusion is mediated by the mitofusin proteins Mfn1 and Mfn2, whereas IMM is controlled by Opa1. (B) Mitochondrial Fission; Fission of the mitochondria is regulated by both Drp1 and hFis. Abbreviations - Drp1: Dynamin-related protein 1, hFis1; mitochondrial fission protein 1, IMM: inner mitochondrial membrane, Mfn: mitofusin protein, OMM: outer mitochondrial membrane, Opa1: optic atrophy protein 1. Powers *et al*., 2012.

In support of the above, studies by Parra *et al.* (2008) and Ong *et al.* (2010) identified that inhibition of mitochondrial fission with mitochondrial division inhibitor 1 (mdivi-1) protected the heart against DOX-induced cardiac injury. This suggests that inhibition of mitochondrial fission could be cardioprotective. Mdivi-1 is described to provide cardioprotection through the elimination of left ventricular dysfunction and the promotion of angiogenesis (Givvimani *et al*., 2012). Co-administration of mdivi-1 with DOX treatment significantly reduced DOX-associated cardiac dysfunction *in vitro*, while mdivi-1 had no effects on DOX's antineoplastic properties (Gharanei *et al*., 2013). Interestingly, low doses of

Stellenbosch University https://scholar.sun.ac.za

cyclosporin (CsA), a known mPTP inhibitor, prevented mitochondrial fragmentation and consequently lead to a significant attenuation of DOX-induced cardiac dysfunction (Marechal *et al*., 2011). Disruption of mitochondrial dynamics, through the upregulation of mitochondrial fission in the heart may play a critical role in mediating DOX cardiotoxicity (Marechal *et al*., 2011; Galloway *et al*., 2012a). Mitochondrial dynamics are however not only responsible for maintaining mitochondrial integrity and function, but also plays an important role in regulating mitochondrial quality control (QC) (Hammerling and Gustafsson, 2014). Therefore DOX may have detrimental effects not only on fission and fusion events, but could also disrupt mechanisms involved in mitochondrial QC.

1.6.2 Mitochondrial Quality Control

Since the mitochondria proteins are prone to cumulative oxidative damage, especially in the presence of DOX, cells have developed QC mechanisms to safeguard against mitochondrial dysfunction (Lionaki and Travernarakis, 2013). Since the cardiomyocytes require a continuous supply of ATP, they have high mitochondria density compared to other tissues (Iglewski *et al*., 2010). Therefore it is essential that mitochondrial QC systems are in place in order to maintain both cardiac and mitochondrial function as well as tissue homeostasis (Seo *et al*., 2010; Youle and van der Bliek, 2012). Mitochondrial QC is regulated by the balance between the synthesis of new mitochondria and degradation of the dysfunctional ones (Ikeda *et al*., 2014; Lionaki and Travernarakis, 2013). Coordination between these two processes maintains both the quantity and quality of the mitochondria (Palikaras and Tavernarakis, 2014)

Mitochondrial biogenesis is the process whereby pre-existing mitochondria grow and divide, creating new healthy mitochondria (François and Gerald, 2010) and is controlled by the synthesis of mitochondrial proteins encoded by the nuclear genome (Baker *et al*., 2007). The coordinated transcription of both mitochondrial and nuclear genomes is directed by peroxisome proliferator-activated receptor-ϒ-coactivator-1α (PGC-1α), the main regulator of mitochondrial biogenesis (Puigserver *et al*., 1998; Ventura-Clapier *et al*., 2008). Various *in vivo* studies have demonstrated that disruption of mitochondrial biogenesis, via decreased PGC-1α expression, contributed to the development of heart failure, and subsequent reversal of which resulted in cardioprotection (Faerber *et al*., 2011; Garnier *et al*., 2003; Sebastiani *et*

Stellenbosch University https://scholar.sun.ac.za

al., 2007; Witt *et al*., 2008). Bouitbir *et al.* (2012) revealed that DOX's cardiotoxic effects was inhibited via the pharmacological induction of mitochondrial biogenesis. These results not only suggest that DOX may have inhibitory effects on mitochondrial biogenetics, but also potentially implicates PGC-1α as a therapeutic target in DOX-induced cardiotoxicity. However, considering that major controversy about the role PGC-1α in human failing heart still exists, it is not surprising that it's role in mediating DOX cardiotoxicity remains to be fully elucidated (Bayeva *et al*., 2013).

The degradation of dysfunctional and redundant mitochondria is initiated by an increase in oxidative stress and mitochondrial fission (Papanicolaou *et al*., 2012; Youle and Narendra, 2011). An important proteolytic QC system, which promotes the degradation of the damaged, misfolded or oxidized OMM proteins, is the ubiquitin-proteasome pathway (UPP) (Campello *et al*., 2014; Heo and Rutter, 2011). Autophagy, another QC pathway, is the main mechanism utilized by the cell to ensure the degradation of both the dysfunctional organelles and proteins (Levine and Yuan, 2005). The accumulation of fragmented mitochondria, the opening of the mPTP and the loss of mitochondria membrane potential results in severely damaged mitochondria, which promotes a selective form mitochondrial autophagy, termed mitophagy (Tolkovsky, 2009; Twig *et al*., 2008). Mitophagy specifically targets the dysfunctional mitochondria for lysosomal degradation in an attempt to restore homeostasis (Campello *et al*., 2014).

The degradation of the mitochondria and its proteins has been termed mitochondrial proteaostasis, and each proteolytic pathway involved in this process will be discussed in detail in the following section (Campello *et al.*, 2014).

1.7 The Proteolytic Pathways

1.7.1 The Ubiquitin-Proteasome Pathway

The UPP is one of the major proteolytic pathways responsible for selective degradation of short-lived proteins (Marques *et al*., 2009). It forms a critical component of the cell cycle and inflammatory response, but also regulates mitochondrial quality control (Wilkinson, 1999; Neutzner *et al*., 2012). Targeted proteins are tagged with the small protein, ubiquitin (Ub) via a cascade of enzymatic reactions and identified for degradation by 26S proteasome (Marques *et al*., 2009; Korolchuk *et al*., 2010). Three types of enzymes are involved in this process; an Ub-activating enzyme (E1) activates free Ub in an ATP dependent manner and carries it to

Stellenbosch University https://scholar.sun.ac.za

the second enzyme, Ub-conjugating enzyme (E2). E2 is a carrier protein and presents the activated Ub to the enzyme, Ub-protein ligase (E3). E3 ligase binds to a specific lysine residue of the targeted protein, and covalently attaches Ub to it. This process, termed the 'tagging hypothesis' (Hasselgren and Fischer, 1997), is repeated until a polyubiquitin chain has been formed and tagged to the protein (Figure 1.10). Considering that there are different types of Ub configurations, in order for these "tagged" proteins to be degraded specifically by the 26S proteasome, the polyUb chain has to be attached to the lysine-48 residue (Adams, 2003; Marques *et al*., 2009). So far only one E1 enzyme (UBE1 - human ubiquitin-activating enzyme) has been identified, ± twenty E2 enzymes and hundred's of E3 ligases have been identified (Adams, 2003). This noticeable hierarchy of available E1, E2 and E3 enzymes ensures that the UPP remains highly regulated and controlled in order to prevent excessive protein degradation and cell death (Adams, 2003). The variety of E3 ligases availability however may also indicate that the UPP is a highly inducible process.

Recently several mitochondrial E3 ubiquitin ligases have been identified (Kotiadis *et al*., 2014; Livnat-Levanon and Glickman, 2011). Mitochondrial ubiquitin ligase (MARCH5/MITOL) is localized on the cytosolic side of the OMM and is essential for the regulation of mitochondrial fission (Karbowski *et al*., 2007; Kotiadis *et al*., 2014). MARCH5 ubiqitinates hFis1, Mfn1 and Mfn2, three of the essential proteins involved in regulating mitochondrial dynamics, and tags them for proteasomal degradation (Karbowski *et al*., 2007; Park *et al*., 2010; Nakamura *et al*., 2006). Additionally, Karbowski *et al.* (2007) demonstrated that MARCH5 promoted the translocation of cytosolic Drp1 to the OMM, mediating Drp1-dependent mitochondrial fission. Another specific mitochondrial E3 ligase, named mitochondrial ubiquitin ligase activated of NF- κB (MULAN/MAPL), was also found to facilitate mitochondrial fission via the ubiquitination and degradation of Mfn2 (Livnat-Levanon and Glickman, 2011; Lokireddy *et al*., 2012). Other cytosolic E3 ligases, such as Parkin and myelin leukemia cell differentiation protein 1(Mcl-1)- ubiquitin ligase E3 (MULE/ARF-BP1) also mediate the degradation of the Mfn proteins, confirming the role of the UPP in regulating mitochondrial dynamics (Geisler *et al*., 2010; Wang *et al*., 2011). However, both Parkin and MULE are known to induce mitophagy, suggesting the UPP is also an important regulator of mitochondrial quality control (Hammerling and Gustafsson, 2014; Wang *et al*., 2011). Acute DOX treatment is known to induce activation of the UPP and upregulation of specific E3 ligase expression in the heart, and is thought to be a potential mechanism whereby UPP dysfunction contributes to DOX cardiotoxicity (da Silva *et al*.,

Stellenbosch University https://scholar.sun.ac.za

2012; Ranek and Wang, 2009; Sishi *et al*., 2013b). However, DOX's effect in the chronic setting, specifically on mitochondrial E3 ligase expression has not been reported in the literature.

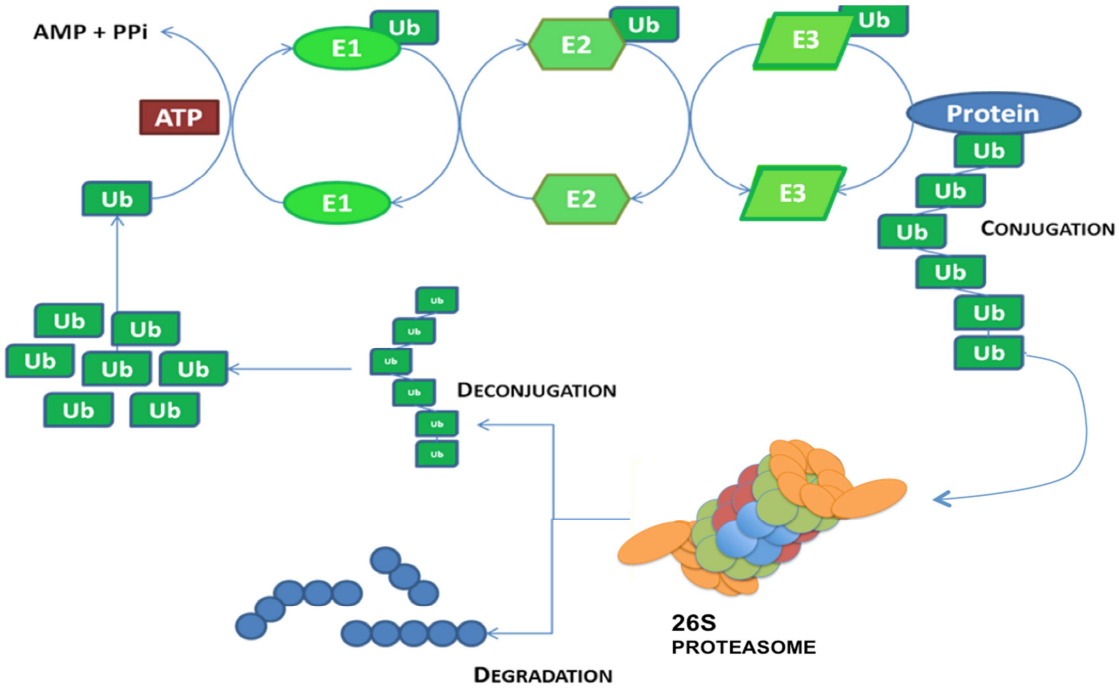

Figure 1.10: The Ubiquitin-proteasome pathway. Ubiquitin is activated by ATP and E1 and carried by E2 enzyme to the E3 ligase. The E3 ligase tags ubiquitin to the targeted protein. This process is repeated until a polyUb chain is attached to the targeted protein. This allows the protein to be recognized by the 26S proteasome and subsequently degraded. Following degradation the Ub proteins are free and can be recycled and reused to degrade other short-lived, redundant proteins. Abbreviations - E1: ubiquitin-activating enzyme, E2: ubiquitin-conjugating enzyme, E3: ubiquitin-protein ligase, polyUb: polyubiquitin Ub: ubiquitin

1.7.2 The 26S Proteasome and its Role in DOX cardiotoxicity

The main component of the UPP responsible for the degradation of poly-ubiquitinated proteins into small peptide fragments is the 26S proteasome. It is a multi-protein complex, composed of a 20S core and two 19S regulatory caps (Figure 1.11) (Adams, 2003). The 19S regulatory caps recognize the tagged poly-ubiquitinated proteins. Recognition and cleaves the

Stellenbosch University https://scholar.sun.ac.za

poly-ubiquitin chain from the protein upon binding. Once bound the protein begins to unfold and the substrate pass through the hollow core of the 19S cap to the 20S catalytic core (Adams, 2003; Kisselev *et al*., 1999).

The 20S catalytic core comprises of four rings: two outer α-rings and two inner β-rings (Adams, 2003; Kisselev *et al*., 1999). Each α-ring is composed of seven α-subunits that form a 'sandwich' around the two β-rings. The amino-terminal tails of the α-rings form a gate, which monitors the entry of the unfolded proteins into the catalytic complex of the β-rings. If a protein has not been unfolded correctly, the α-ring is able to 'close the gate' and restrict protein entry into the core thus inhibiting proteolysis. Similarly, the two inner β-rings also contain seven subunits each, however they differ from the α-rings, as they contain three specific proteolytic or 'active' sites that degrade proteins according to their residues (Figure 1.11). These catalytic sites include the caspase-like (post-glutamyl peptide hydrolase-like/PGPH), trypsin-like and chymotrypsin-like, and are named in accordance with enzymes that possess the same proteolytic activity (Adams, 2003).

It was in 1996 when Figueired-Pereira and colleagues illustrated that the ANT aclacinomycin A, inhibited proteasome activity. Since then Kiyomiya *et al.* (2001, 2002) eloquently demonstrated that DOX has a high affinity with the proteasome and that DOX uses the proteasome to gain entry into the nucleus. In doing so, proteasome activity is compromised, particularly the chymotrypsin-like site (Kiyomiya *et al*., 2002). Therefore, if the proteasome is being "hijacked" into performing functions, other than protein degradation, it is plausible to speculate that proteins meant to be degraded by this pathway are not, and either protein aggregations occurs, or these proteins are being degraded by another proteolytic pathways, such as autophagy (Dirks-Naylor, 2013).

Stellenbosch University https://scholar.sun.ac.za

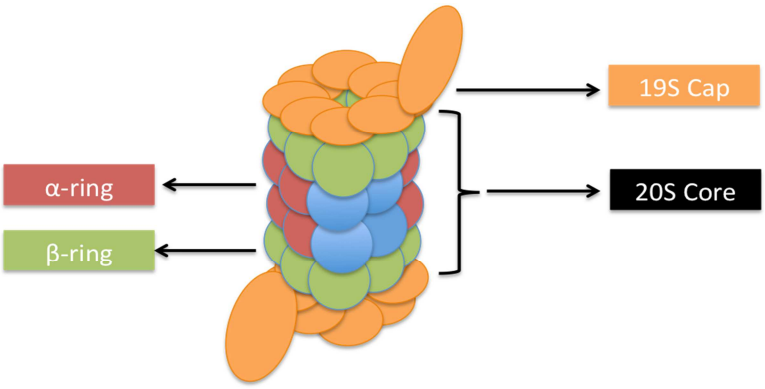

Figure 1.11: The 26S Proteasome. The proteasome is comprised of two 19S caps and a 20S core particle. The 20S core contains 4 rings: two inner alpha-rings and two out beta-rings. The alpha-rings house the catalytic site of the proteasome, responsible for degrading various types of proteins.

1.7.3 Autophagy

Autophagy is a process that degrades expired or faulty components of a cell. This form of degradation is mediated by the formation of an autophagosome, which, upon fusion with the lysosome, breaks down long-lived proteins and organelles (Loos *et al*., 2011). Autophagic flux is constant within the cell as it is a process essential for clearing cellular damage as well as maintenance of homeostasis. However, autophagic flux is dependent on cell activity and can be upregulated in situations of metabolic stress (Loos *et al*., 2011). For example, under conditions of starvation autophagy is utilized to breakdown cellular components and organelles in order to provide nutrients for the cell. Macro-autophagy (Figure 1.12), hereafter referred to as autophagy, is the major inducible pathway within the cytoplasm of all cells and will be the main focus in further discussion (Klionsky and Emr, 2000).

The process of autophagy involves various stages. Firstly autophagy is initiated by the formation of the phagophore, which requires the presence of two protein complexes; the U1k1 (Unc-51 like kinase)-Atg13-FIP200 (RB1CC1; focal adhesion kinase family interacting protein) complex and PI3 kinase (phosphatidylinositol 3)-Beclin 1-Atg14 complex (Class III PI3 complex). Next the formation of the Atg16L (autophagy-related protein 16-L) complex mediates phagophore elongation and sequestration of redundant cellular components. Once the cellular components have been selected, LC3-I is lipidated into LC3-II. LC3 lipidatation

Stellenbosch University https://scholar.sun.ac.za

is followed by membrane fusion and formation of the autophagosome (Glick *et al* 2010). Lastly the newly formed autophagosome fuses with the lysosome, which releases acidic hydrolases into the autophagosome and degrades its components (Glick *et al*., 2010; Dirks-Naylor, 2013) (Figure 1.12).

Autophagy has duel functions within the cells. Under normal conditions it is crucial in promoting normal cell function and cell survival, but in pathophysiological conditions autophagy can initially be upregulated to protect against cellular stressors, as well as contribute to cellular demise (Dirks-Naylor, 2013). It has recently been proposed that the dysregulation of autophagic activity may be an underlying mechanism contributing to the development of DOX-induced cardiotoxicity (Lu *et al*., 2009; Kawaguchi *et al*., 2012).

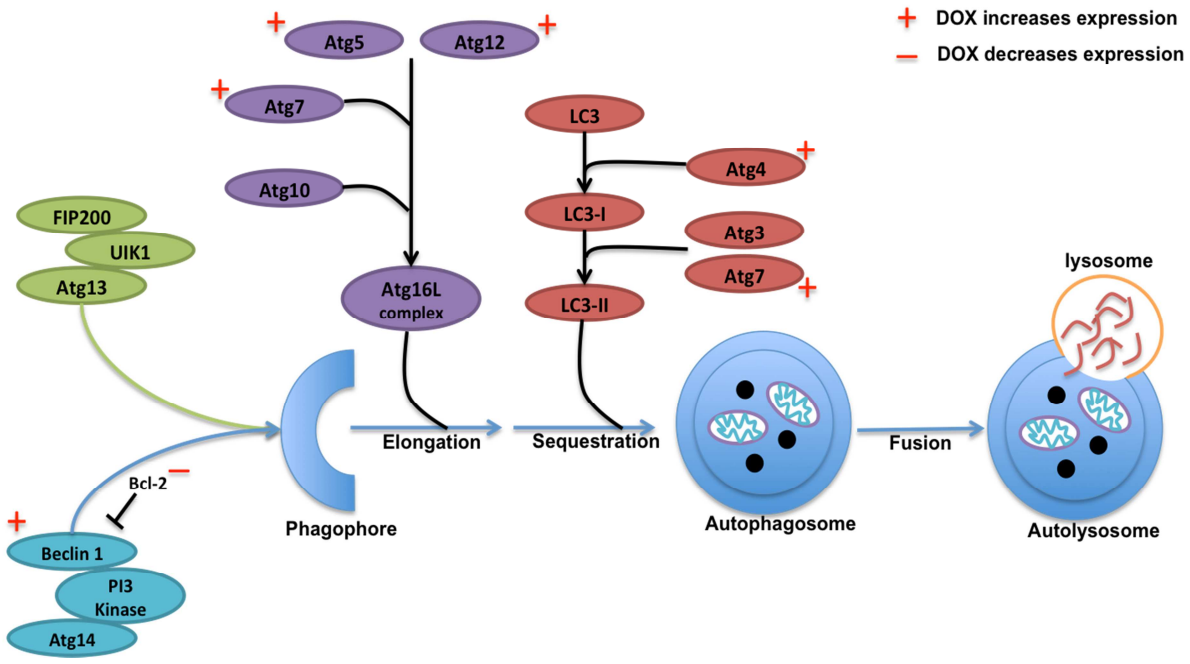

Figure 1.12: The Stages of Autophagy. The initiation of autophagy and formation of the phagomore is regulated by two important complexes; the Ulk1-Atg13-FIP200 complex and the PI3 kinase complex. Phagophore elongation and sequestration is regulated by the Atg16L complex and LC3-II lipidation. Atg7 and Atg10 are involved in the binding of Atg5 to Atg12, forming the Atg16L complex. Atg4, Atg 3 and Atg7 catalyze the two-step LC3-II lipidiation process. The autophagosome fuses with the lysosome, forming an autolysosome and redundant cytosolic material is degraded. DOX has been shown to have various regulatory (+) and inhibitory (-) effects on the autophagic pathway. Abbreviations - Atg: Autophagy-related proteins, Bcl-2: B-cell lymphoma 2, FIP200: 200 kDa focal adhesion kinase family protein, LC3: microtubule-associated protein light chain 3, Ulk1: Unc-51 like kinase. Image adapted from Dirks-Naylor, 2013.

Stellenbosch University https://scholar.sun.ac.za

1.7.4 Mitophagy

It is often thought that autophagy is a non-selective process responsible for the bulk degradation of cytosolic proteins and organelles (Svenning and Johansen, 2013). However, over the last decade it has become increasingly clear that specific autophagic substrates, such as the ER or the mitochondria, are selectively targeted for destruction rather than being randomly taken up with redundant cytoplasmic constituents (Korolchuk *et al*., 2010; Svenning and Johansen, 2013). Ubiquitination, similar to its role in the UPP, acts as a signal for triggering selective autophagy, suggesting that the E3 ligases and ubiquitin coordinate proteolysis via both the UPP and autophagy (Hammerling and Gustafsson, 2014; Korolchuk *et al*., 2010; Kraft *et al*., 2010).

In 2005 Lemasters officially proposed the term Mitophagy as a selective form mitochondrial degradation by autophagy, which is essential for the maintenance of mitochondrial function and survival. Although many studies have reported the selective degradation of the ER (Szegezdi *et al*., 2009), peroxisomes (Dunn *et al*., 2005) and ribosomes (Beau *et al*., 2008) by autophagy, mitophagy appears to be the most important (Twig and Shirihai, 2011). Since the mitochondria are the main source of ROS and the build up of dysfunctional mitochondria can result in ROS overproduction and apoptotic signaling, mitophagy is an essential process required to maintain cellular homeostasis (Crompton, 1999; Grivennikova *et al*., 2010). Mitochondrial fission and loss of mitochondrial membrane potential regulate mitophagy through the mitochondrial PTEN-induced kinase 1 (PINK1)/Parkin pathway.

PINK1 is activated on OMM in response to mitochondrial damage, and recruits the E3 ubiquitin ligase, Parkin, resulting in mitochondrial fragmentation. Parkin ubiquitinates the mitofusin proteins, Mfn1 and Mfn2, but also associates with the sequestosome 1 (p62/SQSTM1) (Geisler *et al*., 2010; Kirkin *et al*., 2009; Tanaka *et al*., 2010). P62 is an ubiquitin-binding protein that colocalizes with ubiquitinated proteins and interacts with LC3 (Bjørkøy *et al*., 2009), promoting the formation of the autophagosome and removal of the damaged mitochondria by mitophagy (Lee *et al*., 2010a; Lee *et al*., 2010b; Vives-Bauza *et al*., 2010) (Figure 1.13). Taken together, these results suggest that the UPP is not only responsible for the regulation of mitochondrial dynamics, but it is also required for Parkin-mediated mitophagy (Heo and Rutter, 2011).

Stellenbosch University https://scholar.sun.ac.za

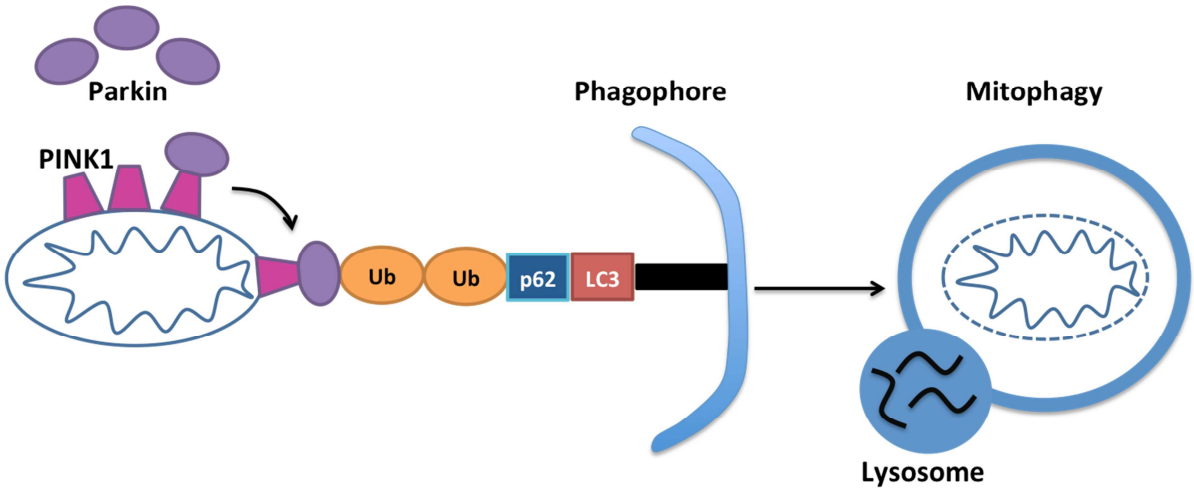

Figure 1.13: The E3 ubiquitin ligase, Parkin mediates mitophagy. Parkin is recruited to the dysfunctional mitochondria by PINK1. Once on the OMM, Parkin interacts with p62, initiating phagophore formation and mitophagy resulting in the degradation of the dysfunctional mitochondria. Image adapted from Hammerling and Gustaffson, 2014. Abbreviations - LC3: microtubule-associated protein light chain 3, PINK1: PTEN-induced kinase 1, p62: sequestersome 1, ub: ubiquitin.

1.7.5 The Role of Autophagy in DOX Cardiotoxicity

Autophagy is triggered by various pathophysiological stimuli, such as ER stress, ROS production, intracellular calcium dysregulation and apoptosis, and as such has been largely associated with various cardiomyopathies (Margariti *et al*., 2013; Muller *et al*., 2011; Xu *et al*., 2013). Considering these stimuli are known side effects associated with DOX, it has recently been suggested that autophagic dysregulation may contribute to DOX-induced cardiotoxicity (Lu *et al*., 2009; Kawaguchi *et al*., 2012). However the relationship between autophagy and DOX treatment has thus far been contradictory (Dirks-Naylor, 2013).

Kawaguchi *et al.* (2012) demonstrated that treatment with acute DOX inhibited AMPK (AMP activated protein kinase), a regulator of cellular metabolism and autophagy (Kim *et al*., 2011), and thereby suppressed autophagic activity. Similarly, Sishi *et al.* (2013a) found that acute DOX treatment induced suppression of autophagy *in vivo*. However in contrast, Kobayashi *et al.* (2010) demonstrated elevated autophagy *in vitro* in the presence of DOX.

Stellenbosch University https://scholar.sun.ac.za

This is said to occur via the inhibition of GATA4, a transcription factor highly expressed in the myocardium, which regulates Bcl-2, an inhibitor of autophagy. Xu and colleagues (2012) also found that DOX upregulated autophagy *in vitro*. Other studies have proposed that DOX-induced autophagy could be as a result of upregulation of Atg genes (ATG-4, -5, -7 and -12) and Bad (Kusama *et al*., 2009; Smuder *et al*., 2013). However one comparable finding between these studies is that inhibiting DOX's induced effect on autophagy, whatever it may be, via pharmacological manipulation of autophagic activity was found to be beneficial against DOX cardiotoxicity (Dirks-Naylor, 2013).

Until recently the effect of DOX on mitophagy had not been described in the literature, although DOX has been shown to induce both oxidative stress and mitochondrial dysfunction, physiological mediators of mitophagy. Dirks-Naylor and others (2014a) initially demonstrated that acute DOX altered mitochondrial dynamics and promoted mitophagy in the liver of treated rats. Later Dirks-Naylor *et al.* (2014b) demonstrated similar results in skeletal muscle, although DOX was found to have varying effects on mitophagy amongst the different skeletal muscle types. These are the first two studies that have investigated the effects of DOX on mitophagic activity. However the effect of DOX on mitophagy in the chronic setting and in the heart remains to be investigated.

1.8 Motivation for Current Study

DOX-induced cardiotoxicity is an important public health concern. Acute and chronic DOX treatment not only leads to irreversible heart damage but also to the development of heart failure, which may only be detected in its advanced stage and thus makes DOX-induced cardiotoxicity a life-long burden. This review highlights the numerous detrimental effects of DOX in the heart and proposes new mechanisms by which DOX mediates cardiotoxicity *in vitro*. The prevention of DOX-induced cardiotoxicity will allow for both high dose and effective treatment of advanced stage malignancies, as well as controlling the onset of CHF.

DOX treatment is known to induce cardiotoxicity via the production of ROS. Since the 1980's researchers have made use of free radical scavengers and antioxidants to reduce the oxidative stress associated with DOX and therefore also cardiotoxicity (Davies and Doroshow, 1986; Minotti *et al.*, 2004; Granger, 2006). Although results appeared promising

Stellenbosch University https://scholar.sun.ac.za

at first, researchers have been unable to reproduce positive results in the clinical setting. This observation suggests that oxidative stress is not the only mechanism involved in the pathogenesis DOX-induced cardiotoxicity, but rather a secondary downstream consequence of DOX-induced cellular damage (Simůnek *et al*., 2009). Therefore, it is worth exploring the effects of DOX on ROS-producing organelles such as the mitochondria, rather than the oxidative stress hypothesis itself.

Oxidative stress, apoptosis, ER stress and calcium dysregulation may contribute to DOX-induced cardiotoxicity by inducing mitochondrial damage. Under normal conditions, mitochondrial dynamics and mitochondrial QC systems help to maintain a healthy mitochondrial population and cellular homeostasis in response cellular stresses (Brookes *et al*., 2004; Iglewski *et al*., 2010). Since the mitochondria are so extensively damaged by DOX, it is thought that DOX-induced cardiotoxicity may be facilitated by an imbalance between mitochondrial fission and fusion as well as the impairment of mitochondrial QC (Gharanei *et al*., 2013).

Previous studies that investigated the effects of DOX in the liver, skeletal muscle and the heart demonstrated an increase in mitochondrial fragmentation (Dirks-Naylor *et al*., 2014a; Gharanei *et al*., 2013; Givvimani *et al*., 2012). Although these studies have been performed both *in vitro* (Gharanei *et al*., 2013; Givvimani *et al*., 2012; Parra *et al*., 2008) and *in vivo* (Dirks-Naylor *et al*., 2014a; Dirks-Naylor *et al*., 2014b), only acute models of cardiotoxicity or non-cardiac models have been used. Considering that the molecular mechanisms involved in the pathogenesis of chronic DOX-induced cardiotoxicity are still controversial, it is important to investigate the effects of DOX on mitochondrial dynamics in the chronic setting. Furthermore, since mitochondrial fission precedes mitophagy, it is likely that DOX treatment may indirectly trigger mitophagic activity and thereby disrupt mitochondrial QC.

The mitochondrial E3 ubiquitin ligases, MARCH5 and Parkin, play an important role in regulating mitochondrial dynamics and mitophagy through the ubiquitination and subsequent proteasomal degradation of the mitochondrial fusion proteins, Mfn1 and Mfn2. This suggests that even though mitochondrial fission is required for mitophagy, so is the activation of the UPP. DOX is known to up-regulate cardiac E3 ligases, MuRF-1 and MAFbx, however its effect on mitochondrial E3 ligase expression remains to be elucidated. It is therefore important to establish the role of the UPP during chronic DOX-induced cardiotoxicity.

Stellenbosch University https://scholar.sun.ac.za

DOX-induced cardiotoxicity is indeed an extremely complex condition that is associated with high mortality rates, yet DOX still remains one of the most effective and widely used ANTs utilized in the fight against cancer today. It is clear that at this stage the problem does not lie with identifying new chemotherapeutic regimes, but rather with identifying ways to diminish the chronic side effects associated with DOX. Unveiling the mechanisms involved in DOX-induced mitochondrial damage will help us better understand the pathogenesis involved in the development of cardiotoxicity. This study therefore investigated the effects of cumulative, chronic DOX treatment in two *in vitro* cardiac cell models. In light of this it was hypothesized that chronic DOX treatment will disrupt mitochondrial dynamics, favoring mitochondrial fission, resulting in increased mitophagy and unopposed cell death. Mitochondrial fragmentation and disruption of mitochondrial quality control will therefore ultimately contribute to the pathogenesis of DOX-induced cardiotoxicity and heart failure.

1.9 Research Aims

This study therefore aims to investigate the effects of chronic DOX treatment on:

(i) Mitochondrial fission and fusion events
(ii) E3 ligase expression and the activity of the UPP
(iii) Mitophagy
(iv) Mitochondrial biogenesis
(v) ER stress and calcium homeostasis

Stellenbosch University https://scholar.sun.ac.za

Chapter 2 - Materials and Methods

2.1 Cell Culture

H9C2 rat cardiomyoblasts (European Collection of Cell Cultures), which is an *in vitro* cell model commonly used to assess DOX-induced cardiotoxicity (Branco *et al*., 2012; Kaiserová *et al*., 2007; Sardão *et al*., 2009), and human-derived Girardi heart cells (kindly donated by Tazneem Adams - UCT), another widely used cardiac cell line (Carroll and Yellon, 2000; Dutta, 1981; Minners *et al*., 2001), were cultured for this study. Both cell lines were initially seeded and cultured in Dulbecco's Modified Eagle's Medium (DMEM) (41965-062, Invitrogen Gibco) containing glucose supplemented with 10% heat-inactivated Fetal Bovine Serum (FBS) (BC/50615-HI, Biochrom) and 1% Antibiotic-Antimycotic (15240-062, Invitrogen Gibco). Cells were incubated at 37 ˚C in a humidified atmosphere of 5% CO_2 and 95% O_2, and cell growth was monitored daily using an inverted phase contrast microscope (Olympus CKX4SF; Tokyo, Japan). Growth medium was refreshed every 48 hours (hrs.) after washing the monolayer of cells with warm, sterile Phosphate Buffered Saline (PBS) solution. Once the desired confluency was established (70 – 80%), cells were again rinsed with PBS, trypsinized (25050, Invitrogen Gibco), and re-seeded at the desired density for each experiment according to Table 1. Refer to Appendix B, protocol 1 – 2 (pg. 167-170) for a detailed protocol of the H9C2 and Girardi cell culture.

Table 1: Amount of Cells Seeded for Each Experiment

Experiment	Flask/plate	Density
MTT assay	24 well plate	±250 000
Caspase-Glo Assay	96 well plate	±30 000
Flow Cytometry	25cm^2 flask	±350 000
Fluorescence Microscopy	8-chamber slide	±20 000
Superresolution Structured Illumination Microscopy	8-chamber slide	±20 000
ORAC/TBARS/GSH assay	6 well plate	±250 000
Proteasome-Glo Assay	96 well plate	±30 000
Western Blotting	6 well plate	±250 000

Stellenbosch University https://scholar.sun.ac.za

Abbreviations – MTT: 3-(4,5-dimethythiazol-2-yl)-2, 5-diphenyle terazolium bromide, ORAC: Oxygen radical absorbance capacity, TBARS: Thiobarbituric acid reactive substances, GSH: Glutathione.

2.2 Pilot Study

Since this study aimed to establish a chronic, cumulative cell model of DOX-induced cardiotoxicity, a dose and time response study was done in order to determine a suitable, but clinically relevant DOX concentration and treatment duration for the main study.

2.2.1 Doxorubicin Treatment

A 3.4 mM stock solution of DOX (D1515, Sigma-Aldrich) was prepared using growth medium as the solvent (Refer to Appendix B, protocol 3, pg. 165). DOX was diluted in growth medium to a final concentration of 0.2, 0.4, 0.6, 0.8 and 1.0 µM. Once cells had reached desired confluency they were treated daily with DOX with the above concentrations for 72, 96 and 120 hrs.

2.2.2 Cell Viability

Following treatment H9C2 and Girardi cell viability was determined by the MTT (3-(4,5-dimethythiazol-2-yl)-2, 5-diphenyle terazolium bromide) assay. The MTT viability assay (M2003, Sigma-Aldrich) is a common technique used to determine the percentage of metabolically viable cells present in a population. The principle of the MTT assay is based on the ability of the cells' mitochondrial enzymes to reduce the water-soluble yellowish MTT (tetrazolium dye) to purple/blue formazan pigments (Berridge *et al.*, 2005). The absorbance of the formazan crystals can be detected spectrophotometrically and the amount of crystals formed is directly proportional to the number of metabolically viable cells present. This study used the MTT assay to determine H9C2 and Girardi viability following incubation with various concentrations of DOX. Cell viability was analyzed directly post-treatment.

H9C2 cardiomyoblasts and Girardi's were randomly divided into experimental groups and seeded into 24-well plates at a density in accordance to table 1. Following the experimental

Stellenbosch University https://scholar.sun.ac.za

procedure, the medium was decanted and 1% MTT (0.01 g/ml) solution was gently added to each well. Thereafter culture plates were maintained in the dark and incubated for 2 hours at 37 ˚C in a humidified 5% CO_2 atmosphere. Following incubation, the supernatant was discarded and a 50:1 solution of 1% Isopropanol (1% HCl in Isopropanol): 0.1% Triton (0.1 ml Triton-X-100 in 100 ml distilled water) was added to each well and the plates were covered with foil and placed on a "Belly Dancer" for 5 minutes to ensure that the formazan crystals were completely dissolved. Optical density was determined using a microtiter plate reader measuring at an absorbency of 540 nm and acidified isopropanol: triton-x mixture represented the blank. The values obtained are expressed as percentages of the control values. Refer to Appendix B, Protocol 4 (pg. 171) for the full experimental protocol.

2.2.3 Apoptosis

In order to evaluate apoptosis, caspase-3/7 activity was measured in both cell lines utilizing the Caspase-Glo® 3/7 assay (G8091, Promega). This is a luminescent cell based assay where following caspase-cleavage, a substrate for luciferase is released which results in the luciferase reaction and subsequent production of light. H9C2s and Girardi's were cultured and treated as previously described in 96-well illuminometer plates. Following treatment, the Caspase-Glo® 3/7 reagent was prepared according to the manufacturer's instructions and 100 µl was added to each well, and left to incubate for 30 minutes at room temperature. Luminescence was measured in a luminometer (GloMax® 96 microplate Illuminometer - E6510, Promega). The data obtained is expressed as a percentage of the control values. Refer to Appendix B, protocol 5 (pg. 172) for the full experimental protocol.

2.3 Main Study

Based on the above assay, treatment of cells with 0.2 and 1 µM DOX for 96 and 120 hrs were deemed appropriate for the duration of this study. This is because this study aimed to investigate the cumulative and chronic changes associated with DOX cardiotoxicity relevant to the clinical setting. Refer to Appendix B, protocol 6 (pg. 172) for detailed treatment procedure.

Stellenbosch University https://scholar.sun.ac.za

2.3.1 Flow Cytometry

2.3.1.1 Mitochondrial and Endoplasmic Reticulum Load

Flow cytometry with the MitoTracker® Green dye (M7514, Molecular Probes) is used to determine mitochondrial load, which is used as an indicator of mitochondrial number. This is a cell-permeant, fluorescence probe that contains a mildly thio-reactive chloromethyl moiety, which is specific for detecting mitochondria. The ER-Tracker™ Blue-White DPX dye (E12353, Molecular Probes) is used to determine ER load, a marker of ER mass. ER-Tracker™ is a photostable, fluorescence probe that is highly selective for labeling the ER. For this technique both H9C2s and Girardi cells were grown and treated as previously described in T25 cm^2 flasks. Following treatment, cells were briefly washed with sterile PBS, trypsinized, and resuspended in 500 µl warm PBS. 25 nM MitoTracker® Green and 100 nM ER-Tracker™ blue were added directly to the cells and incubated for 15 minutes. Thereafter minimum of 10 000 cells were immediately analyzed on the flow cytometer (BD FACSAria I) utilizing the 488 nm and 407 nm Coherent Sapphire solid-state laser (13 – 20 mW) and the 430 nm and 640 nm emission filters. Fluorescence intensity signal was measured using the geometric mean on the intensity histogram. It is important to note that DOX naturally emits its own intrinsic fluorescence (excitation; 480 nm, emission; 580 nm). Therefore the fluorescence intensity of DOX was also measured. Refer to Appendix B, protocol 7 (pg. 173-174) for the full experimental protocol.

2.3.1.2 Intracellular Calcium Measurements

The Calcium Green™ -5N AM (C-3739, Molecular Probes) fluorescence probe is used as an indicator for intracellular calcium. Upon binding to calcium, Calcium Green™ exhibits an increase in fluorescence emission intensity, which directly correlates to the amount of intracellular calcium present in the cell. Following treatment cells were prepared as previously described, and 5 µM Calcium Green™ was directly added to the cells and left to incubate for 20 minutes at room temperature. Analysis followed on the flow cytometer and a minimum on 10 000 cells were collected using the 488 nm laser (13 – 20 mW) and the 530 emission filter. Mean fluorescence intensity was measured using the geometric mean on the

Stellenbosch University https://scholar.sun.ac.za

intensity histogram. Refer to Appendix B, protocol 8 (pg. 174) for the full experimental protocol.

2.3.2 Fluorescence Microscopy

Girardi and H9C2 cells were grown and treated as previously stated in Nunc™ Lab-Tek™ 8-chamber slides (154534, Thermo Scientific). Following treatment cells were washed with warm PBS and incubated with MitoTracker Green™ and ER-Tracker for 15 minutes at room temperature. Using an Olympus PlanApo N60x/1.4 oil objective, with a 60X magnification, structural alterations of mitochondrial and ER morphology could then be determined. Since DOX is autofluorescent, this study additionally wanted to determine DOX localization within the cells as well as whether DOX binds to the mitochondria and/or the ER. This was done by co-localization analysis using specific settings on the Olympus Cell^R system. Images were acquired through multi-colour z-stacks with the DAPI, FITC and PE-TexasRed emission filters, performed with an Olympus Cell^R System attached to an IX 81 inverted fluorescence microscope equipped with a F-view-II cooled CCD camera (Soft Imaging Systems) using Xenon-Arc burner (Olympus Biosystems GMBH) as a light source. The top and bottom focus position parameters for the z-stacks were selected, indicating the upper and lower dimensions of the sample to be acquired after single-frame imaging. Images were processed and sharpened with the Cell^R software, and presented as the maximum intensity projection. Refer to Appendix B, protocol 9 (pg. 175) for the full experimental protocol.

2.3.3 Superresolution Structured Illumination Microscopy (SR-SIM)

Cells were grown and treated as previously described in Nunc™ Lab-Tek™ 8-chamber slides. Following treatment cells were loaded with 4 μM Rhod-2 AM (R-1244, Molecular Probes) and 5 μM Calcium Green dye respectively, in order to visualize calcium distribution with the cells. Rhod-2 is a rhodamine-based fluorescence probe used to detect mitochondrial calcium. After 20 minutes of incubation, cells were imaged at room temperature on the Carl Zeiss Laser Scanning Microscope (LSM 780) using the Plan-Apochromat 63X/1.3 Oil DICM27 objective. Mitochondrial specific calcium was detected with the 561 nm laser, and fluorescence was emitted between the 575 nm – 635 nm, while free cytosolic calcium was determined using the excitation of the 488 nm laser and measured fluorescence emitted between 534 nm – 569 nm. Images were processed using Zen 2011 Software (Zeiss). While

Stellenbosch University https://scholar.sun.ac.za

intracellular calcium could be quantified with flow cytometry, mitochondrial calcium could not. Since Rhod-2 and DOX fluoresce on the same emission spectrum, and the flow cytometer is not equipped with the correct lasers, these two fluorescence probes could not be detected simultaneously. Therefore mitochondrial calcium fluorescence was quantified in relative fluorescence units (RFU) using the Zen 2011 Software. Refer to Appendix B, protocol 10 and 11 (pg. 175-176) for the full experimental protocol.

2.3.4 Oxidative Stress and Antioxidant Capacity

The following experiments were conducted at the Oxidative Stress Research Center of Cape Peninsula University of Technology (CPUT).

2.3.4.1 ORAC Assay

Using trolox, a water-soluble analog of vitamin E, as a reference antioxidant, the antioxidant capacity of both cell lines following treatment was determined with the ORAC (Oxygen Radical Antioxidant Capacity) assay. This assay is based on the oxidation of the fluorescence probe by peroxyl radicals. If antioxidants are present, they will inhibit oxidation and peroxyl radicals will destroy the probe. Therefore antioxidant capacity directly correlates to fluorescence decay (Ou *et al*., 2001). After treatment the cells were washed with ice cold PBS, detached from plate surface with a cell scraper and transferred into corresponding, chilled eppendorf tubes. Cells were then sonnicated and centrifuged at 10 000 g for 10 minutes at 4 °C. Supernatant was allocated into new eppendorf tubes and kept on ice. The fluorescence probe, fluorescein (F6377, Sigma-Aldrich) and the peroxyl radical, AAPH (2,2'-azobis(2-amidino-propane) dihydrochloride) (440914, Sigma-Aldrich) were used to determine the ORAC value as per the method described by the Oxidative Stress Research Center (CPUT). Fluorescence was immediately measured using the Fluoroskan Ascent plate reader (Thermo Electron Corporation, USA) at excitation/emission of 485 nm/530 nm. Each sample was read in increments of 5 minutes for a total for 2 hrs. Fluorescence decay is represented as the area under the curve (AUC), which was thereby used to quantify the total antioxidant capacity. These results are then compared to the antioxidant standard curve of Trolox™ (238813, Sigma-Aldrich). Results from the assay are expressed as μmol Trolox™ equivalents (TE) per L of sample. Refer to Appendix B, protocol 12 (pg. 177) for the full experimental protocol.

Stellenbosch University https://scholar.sun.ac.za

2.3.4.2 TBARS Assay

Lipid peroxidation is a well-defined mechanism whereby lipids are oxidatively degraded thereby resulting in cellular damage. Malondialdehyde (MDA), which is a natural by-product of lipid peroxidation, is used as a marker for oxidative stress. The Thiobarbituric Acid Reactive Substances (TBARS) assay is utilized in screening and monitoring lipid peroxidation. MDA reacts with thiobarbituric acid (TBA) to form a single MDA-TBA adduct, which can measured colorimetrically or fluorometrically, thereby allowing for direct quantitative measurement of the oxidative stress by-products (Devasagayum *et al*., 2003). Samples were prepared as previously described, and 4 mM Butylated hydroxytroluene (BHT) (B1378, Sigma-Aldrich) was added to each sample, to prevent any further oxidation and immediately sonnicated. No centrifuge or allocation was required as whole cell homogenate is utilized in the assay. Reagent preparation was performed in accordance with the Oxidative Stress Research Center's (CPUT) protocol. A volume of 50 µl supernatant was added to 6.25 µl TBA reagent and incubated at 90 °C for 45 minutes. Absorbance was measured 532 nm in a 96-well flat bottom plate with the Multiskan Spectrum (Thermo Electron Corporation, USA). The concentration of TBARs per sample was determined using the MDA (820756, Merck) equivalence standard and expressed as µmol of MDA. Absorbance is directly proportional to amount of oxidative stress by-products present in the cells. Refer to Appendix B, protocol 13 (pg. 179) for the full experimental protocol.

2.3.4.3 GSH Redox Assay

Reduced glutathione (GSH) is an important antioxidant present in high levels in all living cells. It has numerous cellular functions, but most importantly it plays a role in protecting the cells against oxidative damage. To protect against oxidative stress, GSH is converted to its oxidized form, oxidized glutathione (GSSG). Therefore the ratio of GSH to GSSG within the cells can be used as a good indicator for oxidative stress (Asensi *et al*., 1999; Zitka *et al*., 2012). A decrease in this ratio can be indicative of significantly decreased GSH levels or of high amounts of GSSG present in the cells. The total glutathione (tGSH) and GSSG concentrations were measured using the method described by Asensi *et al.* (1999). The concentration of GSH was calculated according to the equation indicated below:

Stellenbosch University https://scholar.sun.ac.za

$$GSH = tGSH - 2GSSG,$$

where after the ratio of GSH to GSSG (GSH/GSSG) was determined. Following treatment, samples were prepared as previously described. 50 µl 0.3 mM DTNB (5 5'-dithiobis(2-nitrobenzoic acid)) (D8130, Sigma-Aldrich), 16 µl glutathione reductase (G3664, Sigma-Aldrich) and 50 µl of sample for GSH, or 50 µl sample with 50 µl 30 mM M2VP (1-methyl-2-vinylpyridinium) (69701, Sigma-Aldrich) for GSSG were added into clear 96-well flat bottomed plates and incubated for 5 minutes at 25 °C in a preheated BioTek plate reader. Following incubation, 50 µl 1 mM NADPH (β-nictinamide adenine dinucleotide phosphate reduced tetrasodium salt) (N7505, Sigma-Aldrich) was quickly added to each well. Absorbance was measured at 412 nm every 30 seconds for 3 minutes, and the concentration of total glutathione, GSH and GSSG were determined with GSH as standard. Refer to Appendix B, protocol 14 (pg. 180) for the full experimental protocol.

2.3.5 Proteasomal Activity

The Proteasome-Glo™ Assay (G8531, Promega) contains three separate bioluminescent assays that detect the different protease activities of the 20S proteasome catalytic sites. The luminogenic substrates: Suc-LLVY-aminoluciferin, Z-LRR-aminoluciferin and Z-LPnLD-aminoluciferin, were used to detect chymotrypsin-like, trypsin-like and caspase-like catalytic activities within the proteasome respectively. The luminescent signal produced is directly proportional to the amount of proteasomal activity present within the cells. Both cell lines were cultured and treated as previously described. After the treatment protocol the Proteasome-Glo™ assay was carried out according to the specifications and standards of the protocol supplied by manufacturer. Luminescence of the individual protease activities were detected with the GloMax® 96-well Microplate Luminometer (E6501, Promega). Refer to Appendix B, protocol 15 (pg. 182) for the full experimental protocol.

Stellenbosch University https://scholar.sun.ac.za

2.3.6 Western Blot Analysis

2.3.6.2 Protein Extraction

After treatment with DOX, cell were then rinsed with PBS where after 30 µl of lysis buffer, pH 7.4, containing: Benzamidine 1 mM, dithiothreitol 1mM, EDTA (Ethylenediaminetetra-acetic acid) 1 mM, 10 mg/ml of leupeptin, 0.5% Na-Deoxychlorate, NaF (Sodium Fluoride) 50 mM, 1%, NP40, PMSF (phenylmethylsulfonyle fluoride) 0.1 mM, 4 mg/ml of SBTI (soybean trypsin inhibitor), 0.1% SDS (Sodium dodecyle sulphate) and Tris (tri-(hydroxyl-methyl)-aminomethane)-HCl 2.5 mM, was added to each well and kept on ice for 5 minutes. Cells were scraped lose from the bottom of the wells using a sterile cell scraper and transferred into chilled eppendorf tubes. Cardiomyoblasts were sonnicated at 15% amplitude for 10 seconds with the Misonic Ultrasonic Liquid Processor (Qsonica, USA) to ensure the breakdown of the cell membranes and release of cellular proteins. Cell lysates were then centrifuged at -4 ˚C for 10 minutes at 8000 rpm and the supernatant was transferred into new, chilled eppendorf tubes. Protein content was then determined by the Bradford technique described below. Refer to Appendix B, protocol 16 (pg. 184) for the full experimental protocol.

2.3.6.3 Bradford Protein Determination and Sample Preparation

Protein content was quantified using the Bradford protein determination method. In order to determine how much protein is contained in each sample a standard curve was established; where a sequence of protein dilutions were set up in eppendorf tubes. 10 µl, 20 µl, 40 µl, 60 µl, 80 µl and 100 µl of 1 mg/ml BSA (albumin bovine serum dissolved in PBS) was added to distilled water (dH_2O). 900 µl of the Bradford Reagent was thereafter added to each eppendorf, contributing to a final volume of 1000 µl. Sample protein concentrations were subsequently determined by pipetting 5 µl of protein sample into 900 µl Bradford Reagent and 95-µl dH_2O. All eppendorf tubes were vortexed and absorbance was measured at 595 nm against the reagent blank with a spectrophotometer (Cecil 2000, type CE 2021 UV/VIS). The weight of protein in µg/ml was determined and subsequent protein concentrations (50 µg/ml) were made up using Laemmli sample buffer. Prepared samples were boiled at 95.5˚C for 5

Stellenbosch University https://scholar.sun.ac.za

minutes and stored at −80˚C until required. Refer to Appendix B, protocol 16 (pg. 184) for the full experimental protocol.

2.3.6.4 Sodium-dodecyl-sulfate-polyacrylamide Gel Electrophoresis (SDS-PAGE) and Electrotransfer

Proteins weighing between 30 – 90 kDA were separated with a 12% polyacrylamide gel, whereas lower molecular weight proteins (≤ 30 kDA) a 15% polyacrylamide gel was used. Previously prepared protein samples were thawed and boiled at a temperature of 95.5˚C for 5 minutes before being briefly centrifuged. Equal protein concentrations (50 µg/ml) were loaded into each gel. In order to determine protein molecular weight and gel orientation, BLUeye pre-stained protein ladder (PM007-0500, GeneDirex) was loaded into the first left well of each gel. Proteins separated by SDS-PAGE (Mini-PROTEAN® Tetra cell, Biorad) at a constant voltage of 100 V and current of 400 mA (Biorad Power Pac 1000) for 10 minutes, and thereafter at constant voltage of 200 V for 50 minutes. The separated proteins were transferred to PVDF (polyvinylidine fluoride) membranes (Trans-Turbo® mini transfer pack, 170-4156, Bio-Rad) using Trans-Blot Turbo System (170-4155, Bio-Rad) at a voltage of 12V and constant current of 12A for 12 minutes. Membranes were routinely stained with Ponceau Red to ensure protein transfer and equal loading. Refer to Appendix B, protocol 16 (pg. 185) for the full experimental protocol.

2.3.6.5 Immuno-dectection

Non-specific binding sites on membranes were blocked for 2 hours in 5% fat-free powered milk in TBS-T (TRIS-buffered saline-Tween Solution), after which membranes were incubated overnight at 4 °C in specific primary antibody solutions. The protein of interest was detected using manufacturers recommended dilutions of the following primary antibodies; ATF-4 (11815, Cell Signaling), BiP (3177, Cell Signaling), Cleaved Caspase 3 (9661, Cell Signaling), Drp1 (ab56788, Abcam), hFis1 (ab71498, Abcam), GAPDH (2118, Cell Signaling), K48-Ubiquitin (8081, Cell Signaling), LC3-II (2775, Cell Signaling), MARCH5 (Ab77585, Abcam), Mitofusion 1 (ab129154, Abcam), Mitofusion 2 (ab124773, Abcam), p62 (5114, Cell Signaling), Parkin (2132, Cell Signaling), PGC-1α (2178, Cell Signaling) and Tomm20 (ab56783, Abcam). Following overnight incubation, membranes were washed three times with 1X TBS-T solution where after they were incubated with their

Stellenbosch University https://scholar.sun.ac.za

corresponding secondary antibodies at room temperature for 1 hour. The secondary antibodies; HRP-linked anti-Rabbit secondary antibody (7074, Cell Signaling), Goat anti-Rabbit IgG H&L (HRP) secondary antibody (ab97069, Abcam) and Goat anti-Mouse IgG H&L (HRP) secondary antibody (ab97040, Abcam) were utilized. To eliminate background, all goat secondary antibodies were made up in 5% w/v milk blocking solution. After washing membranes with TBS-T, they were incubated with Clarity™ Western ECL Substrate (170-5061, Bio-rad) and exposed with the ChemiDoc™ XRS+ System. Lane profile analysis was performed with the Image Lab™ Software (Bio-Rad). Refer to Appendix B, protocol 16 (pg. 181) for the full experimental protocol.

2.3.7 Statistical Analysis

Data from at least three independent experiments, of which each was conducted in triplicate, were analyzed. All values are presented as a percentage of the control (100%). Comparison between the groups was achieved using one-way analysis variance (ANOVA) followed by Bonferroni's post-hoc test. All data are presented as the means $\pm$ SEM. A p-value < 0.05 was considered statistically significant. All statistical analysis was carried out on the computer program, GraphPad Prism (GraphPad Inc., version 5.0).

Stellenbosch University https://scholar.sun.ac.za

Chapter 3 –Results

3.1 Pilot Study: Cell Viability

In order to determine an appropriate DOX treatment regime over a long period of time, the MTT bio-reductive assay was employed to establish a dose- and time-response graph. Cell viability of the H9C2 cells became significantly reduced as the treatment concentration increased compared to the control group (Figure 3.1). This occurred across all times points analyzed where cell viability was at its lowest after 96 hours. Although no statistical significance was observed, there was a modest improvement in cell viability following 120 hours versus 96 hours at all DOX concentrations except 0.6 µM. Similarly the Girardi's cell viability was significantly reduced over time as the concentration of DOX was increased (Figure 3.2). Interestingly the Girardi's behaved very differently to the H9C2 cells at the 0.2 µM concentration group, where a statistical increase in viability occurred following 72 and 96 hours.

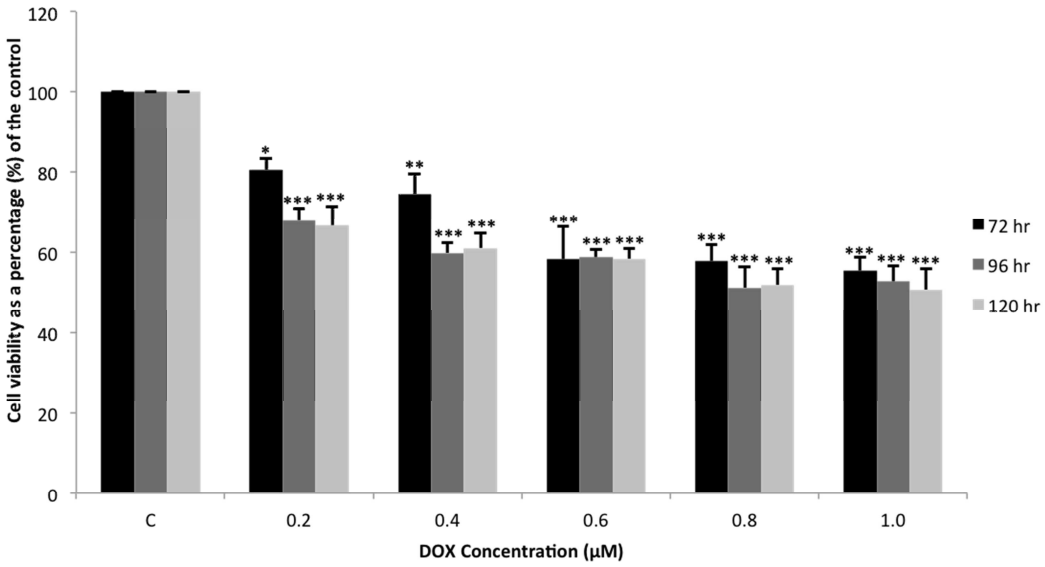

Figure 3.1: The effect of increasing, cumulative doses of doxorubicin on H9C2 cell viability. H9C2 cardiomyoblasts were incubated with 0.2, 0.4, 0.6, 0.8 and 1.0 µM of DOX for 72, 96 and 120 hours. Values are expressed as a percentage of the control (100%). Results presented as mean ± SEM (n=4). *P < 0.05, **P < 0.01 and ***P < 0.001 vs. Control. Abbreviations – C: control, DOX: doxorubicin, hr: hour, vs: versus.

Stellenbosch University https://scholar.sun.ac.za

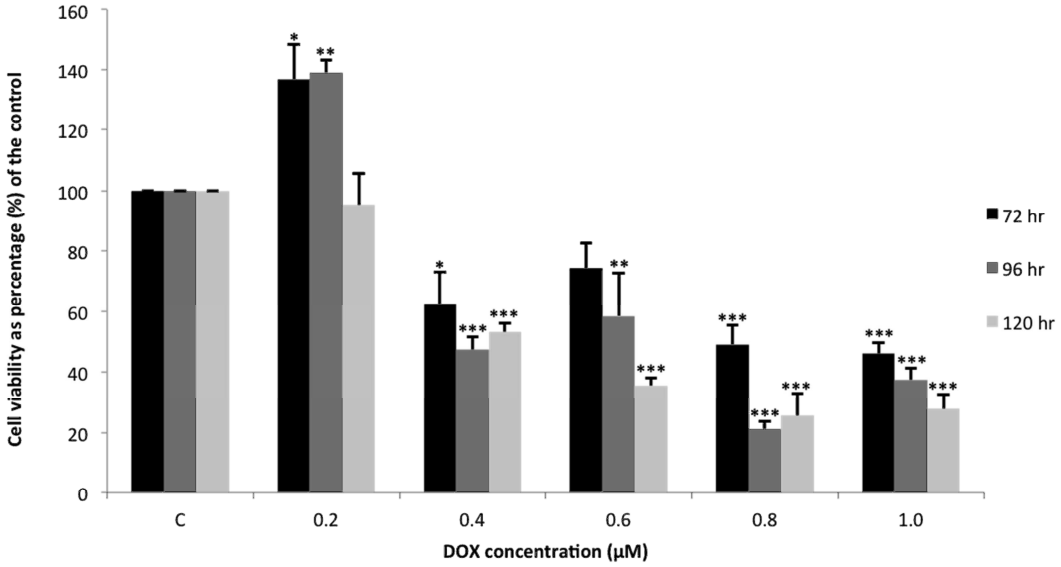

Figure 3.2: The effect of increasing, cumulative doses of doxorubicin on Girardi cell viability. Girardi cells were incubated with 0.2, 0.4, 0.6, 0.8 and 1.0 µM of DOX for 72, 96 and 120 hours. Values are expressed as a percentage of the control (100%). Results presented as mean ± SEM (n=4). *P < 0.05, **P < 0.01 and ***P < 0.001 vs. Control. Abbreviations: - C: control, DOX: doxorubicin, hr: hour, vs = versus.

This study also wanted to assess the activities of caspase 3 and 7 under these conditions. As shown in Figure 3.3, H9C2's apoptotic activity was significantly elevated when compared to the control. Interestingly after 120 hours of DOX treatment, apoptotic activity declines despite remaining above baseline values. Treatment with the highest concentration of DOX (1 µM) for 96 and 120 hours resulted in a decrease in apoptosis compared to the 72 hour group. Analysis of Girardi cell apoptosis demonstrated a significant increase in apoptotic activity at most of the concentration groups, however similar to the H9C2 cells, a decrease in activity was observed at the 1.0 µM group following 96 and 120 hours of treatment (Figure 3.4).

As this study aimed to investigate the cumulative and chronic changes associated with DOX cardiotoxicity relevant to the clinical setting, the remainder of the data will be presented with the 0.2 µM and 1.0 µM DOX treatment over 96 and 120 hours only. Since the Girardi cells appeared more sensitive to DOX compared to the H9C2 cells, the following results will only represent experiments performed on the H9C2 cell line. Please refer to Appendix A for the Girardi cell's results.

Stellenbosch University https://scholar.sun.ac.za

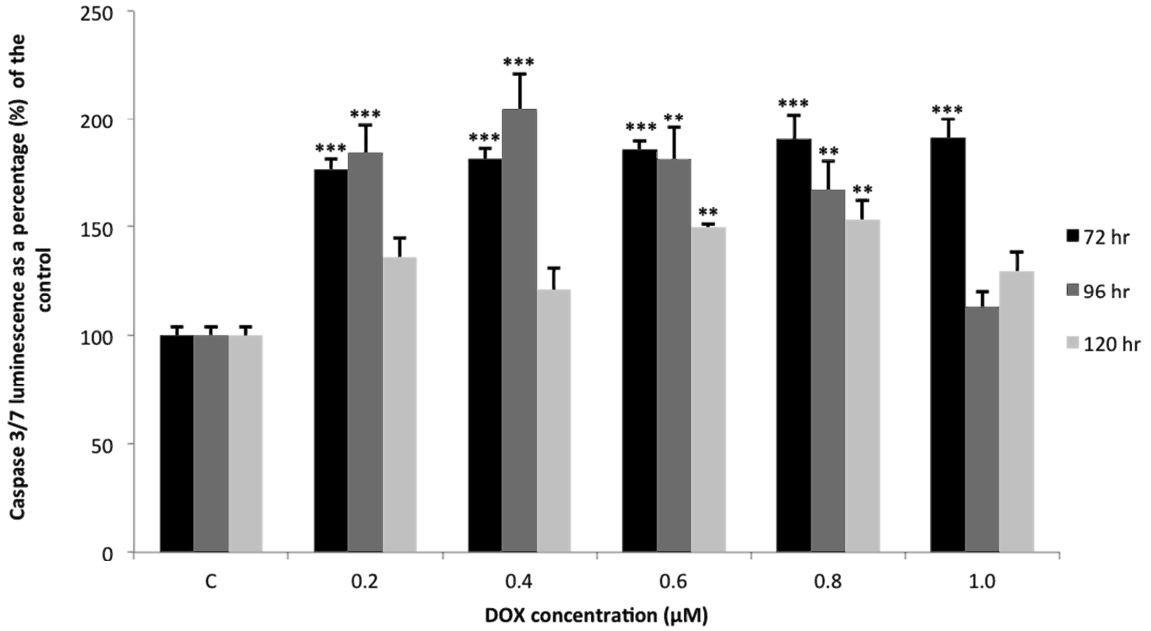

Figure 3.3: The effect of increasing, cumulative doses of doxorubicin on H9C2 caspase 3/7 luminescence. H9C2 cells were incubated with 0.2, 0.4, 0.6, 0.8 and 1.0 µM of DOX for 72, 96 and 120 hours. Values are expressed as a percentage of the control (100%). Results presented as mean ± SEM (n=3). **P < 0.01 and ***P < 0.001 vs. Control. Abbreviations – C: control, DOX: doxorubicin, hr: hour, vs: versus.

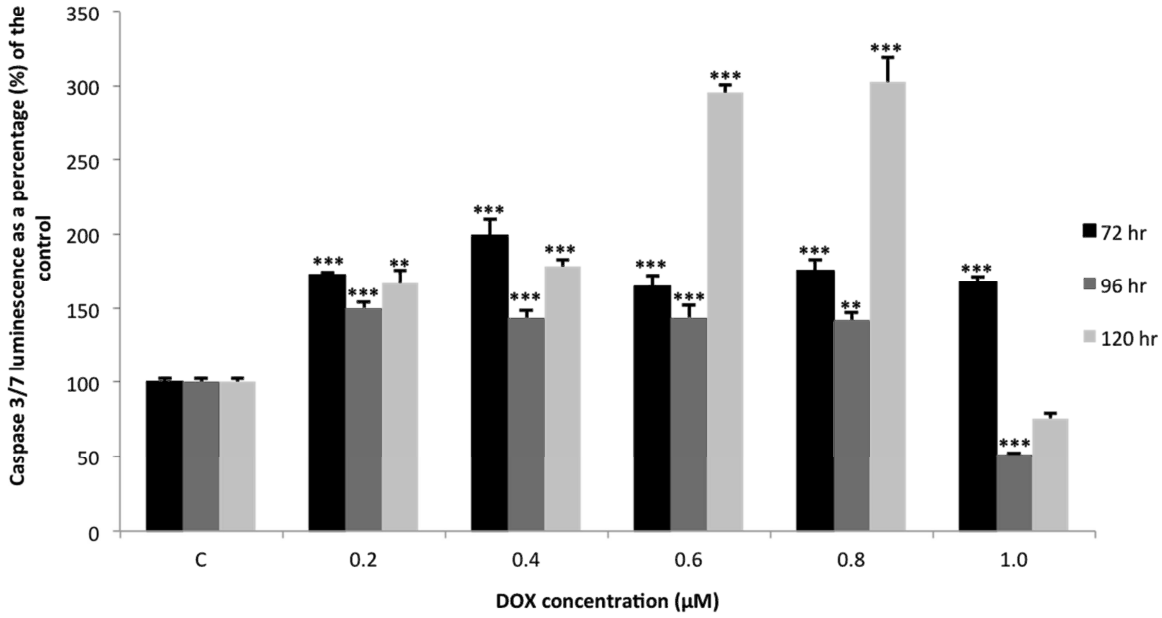

Figure 3.4: The effect of increasing, cumulative doses of doxorubicin on Girardi caspase 3/7 luminescence. Girardi cells were incubated with 0.2, 0.4, 0.6, 0.8 and 1.0 µM

Stellenbosch University https://scholar.sun.ac.za

of DOX for 72, 96 and 120 hours. Values are expressed as a percentage of the control (100%). Results presented as mean ± SEM (n=3). **P < 0.01 and ***P < 0.001 vs. Control. Abbreviations – C: control, DOX: doxorubicin, hr: hour, vs: versus.

3.2 The Effect of Chronic DOX Treatment Regimes on Mitochondrial Dynamics

Mitochondria are the "heart" of the cell as they are responsible for energy production. These organelles have previously been shown to be extensively damaged during DOX cardiotoxicity (Octavia, 2012), but the extent of the damage is relatively unknown. As the mitochondria are constantly undergoing regulated fission and fusion events, this study aimed to determine whether the balance of mitochondrial dynamic would be disturbed following chronic treatment with DOX.

3.2.1 Evaluation of Mitochondrial Fission

Drp1 and hFis1 are two essential promoters of mitochondrial fragmentation. In order to establish the effect of chronic DOX treatment regimes on mitochondrial fission, western blotting assessed the expression of both these proteins. Drp1 expression was modestly unregulated after 96 hours of treatment and significance was obtained with the higher concentration of DOX [116.70 ± 2.86%, ($p < 0.01$)] when compared to the control (100%) (Figure 3.5). Following 120 hours of exposure, DOX induced an even greater increase in Drp1 expression across both treatment groups relative to the control. Hfis1, a recruiter of Drp1, elicited a similar response although not in the same magnitude (Figure 3.6). Both the low [122.60 ± 0.33%, ($p < 0.01$)] and high [117.70 ± 4.97%, ($p < 0.05$)] concentrations of DOX significantly elevated hFis1 expression following 120 hours of treatment. Given the crucial role that both these proteins play in regulation of mitochondrial fragmentation, these results demonstrate that chronic DOX treatment increases mitochondrial fission in a time- and dose-dependent manner.

3.2.2 Evaluation of Mitochondrial Fusion

In order to fully understand the impact of chronic DOX treatment on mitochondrial dynamics in these cardiomyocytes, mitochondrial fusion proteins (Mfn1 and Mfn2) were also assessed. In contrast to the elevated Drp1 and hFis1 expression, Mfn1 was significantly reduced in response to 96 hours [0.2 μM: 73.74 ± 6.24%, ($p < 0.05$) and 1.0 μM: 22.07 ± 3.61%, ($p <$

Stellenbosch University https://scholar.sun.ac.za

0.001)] and 120 hours [0.2 µM: 52.52 ± 4.75%, ($p < 0.001$) and 1.0 µM: 29.33 ± 4.93%, ($p < 0.001$)] of chronic DOX treatment relative to the control (100%) (Figure 3.7). What was interesting to note in these results was the substantial difference within the group and between groups, suggesting that repeated administration as well as cumulative DOX concentration negatively affects expression of Mfn1. Analysis of Mfn2 results also indicated significantly reduced protein expression in a dose and time dependent manner when compared to the control (Figure 3.8). Therefore, the overall reduction in mitochondrial fusion proteins and the concomitant rise in fission factors throughout the treatment duration highlights the imbalance between mitochondrial dynamics. These results further substantiate the occurrence of mitochondrial fragmentation in DOX treated cardiomyoblasts.

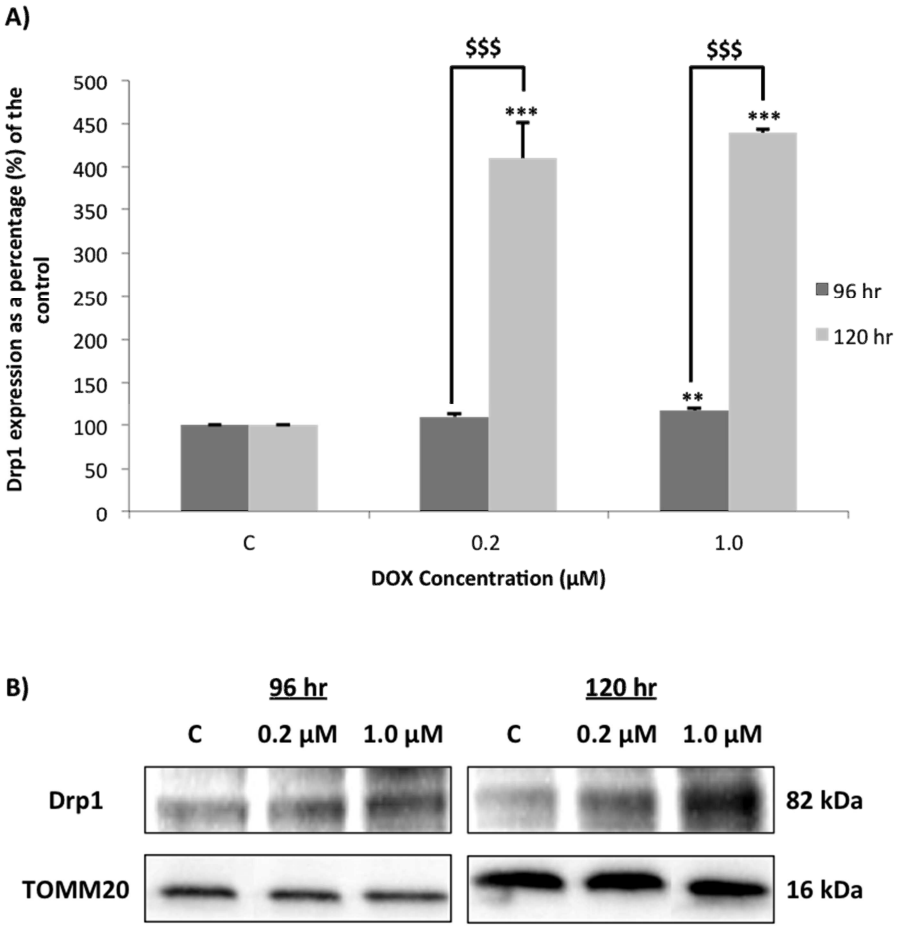

Figure 3.5: The effect of chronic doxorubicin treatment regimes on Drp1 expression in H9C2 cardiomyoblasts. (A) Lane profile analysis of Drp1. (B) Representative immunoblot of Drp1. TOMM20 served as the loading control. H9C2 cardiomyoblasts were treated daily with 0.2 and 1.0 µM DOX for 96 and 120 hours. Results are presented as mean ± SEM

Stellenbosch University https://scholar.sun.ac.za

(n=3). **P < 0.01 and ***P< 0.001 vs. Control. $^{\$\$\$}$P < 0.001 96 hr vs. 120 hr. Abbreviations – C: control, DOX: doxorubicin, Drp1: dynamin-related protein 1, hr: hour, vs: versus.

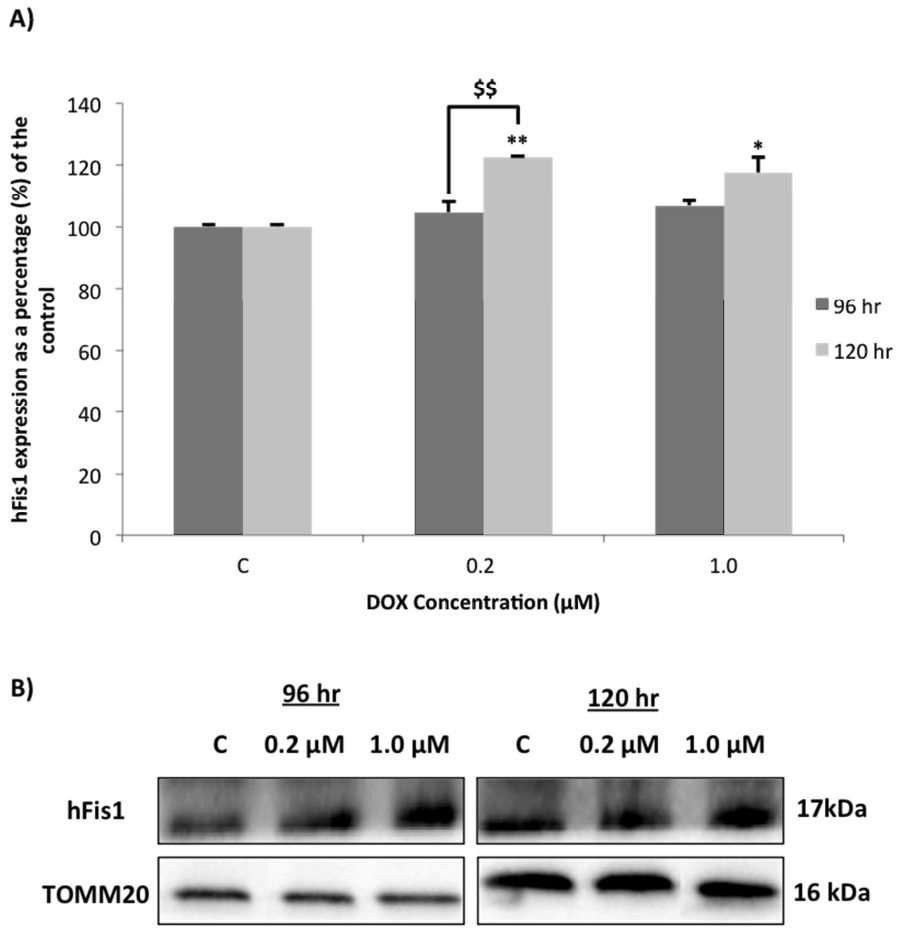

Figure 3.6: The effect of chronic doxorubicin treatment regimes on hFis1 expression in H9C2 cardiomyoblasts. (A) Lane profile analysis of hFis1. (B) Representative immunoblot of hFis1. TOMM20 served as the loading control. H9C2 cardiomyoblasts were treated daily with 0.2 and 1.0 µM DOX for 96 and 120 hours. Results are presented as mean ± SEM (n=3). *P < 0.05 and **P < 0.01 vs. Control. $^{\$\$}$P < 0.01 96 hr vs. 120 hr. Abbreviations – C: control, DOX: doxorubicin, hFis1: mitochondrial fission factor 1, hr: hour, vs: versus

Stellenbosch University https://scholar.sun.ac.za

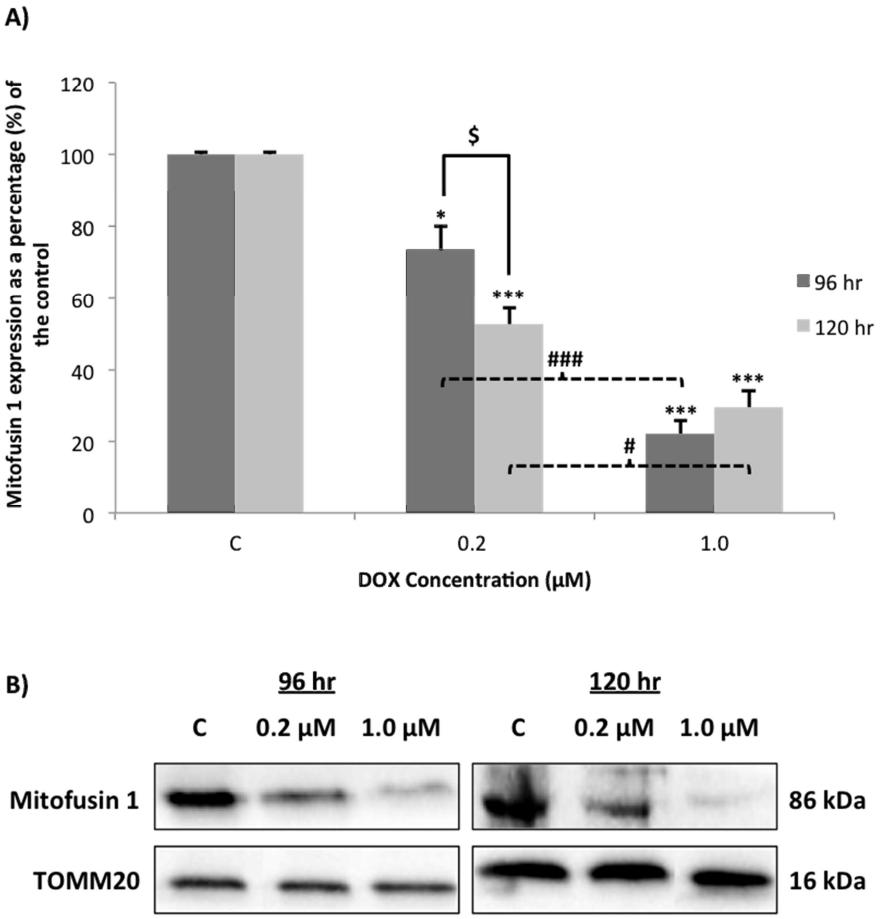

Figure 3.7: The effect of chronic doxorubicin treatment regimes on Mitofusin 1 expression in H9C2 cardiomyoblasts. (A) Lane profile analysis of Mitofusin 1. (B) Representative immunoblot of Mitofusin 1 TOMM20 served as the loading control. H9C2 cardiomyoblasts were treated daily with 0.2 and 1.0 µM DOX for 96 and 120 hours. Results are presented as mean ± SEM (n=3). *P < 0.05 and ***P< 0.001 vs. Control. $^{\$}$P < 0.05 96 hr vs. 120 hr. $^{\#}$P < 0.05 and $^{\#\#\#}$P < 0.001 0.2 µM vs. 1.0 µM. Abbreviations – C: control, DOX: doxorubicin, hr: hour, vs: versus.

Stellenbosch University https://scholar.sun.ac.za

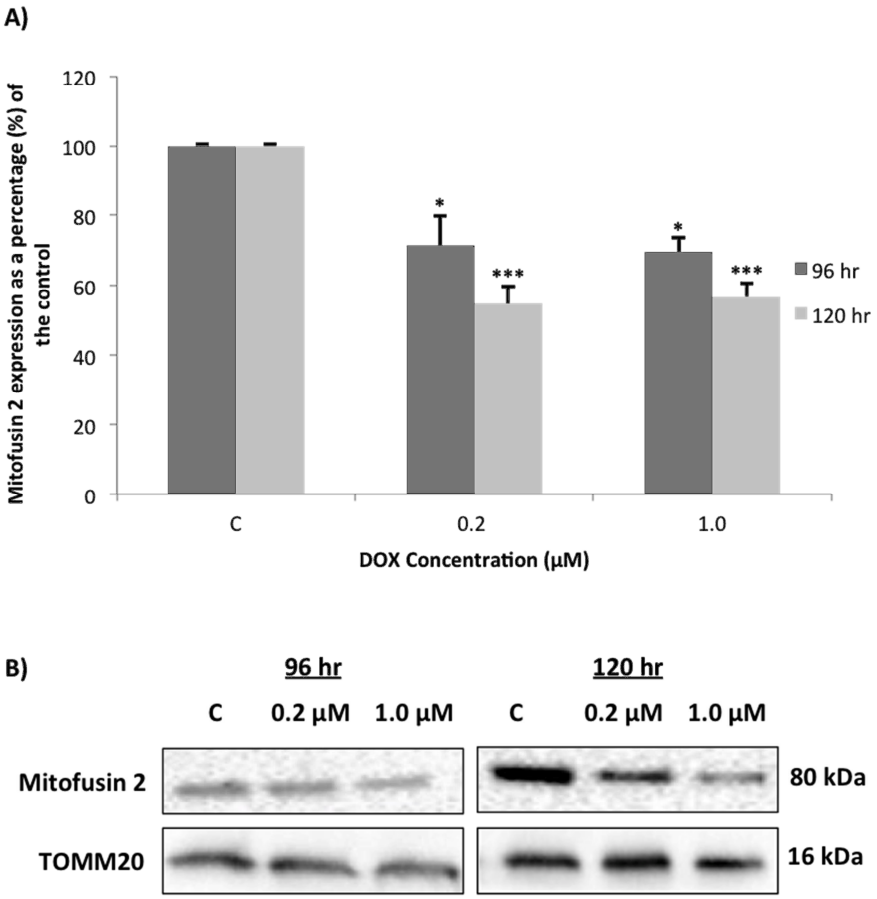

Figure 3.8: The effect of chronic doxorubicin treatment regimes on Mitofusin 2 expression in H9C2 cardiomyoblasts. (A) Lane profile analysis of Mitofusin 2. (B) Representative immunoblot of Mitofusin 2. TOMM20 served as the loading control. H9C2 cardiomyoblasts were treated daily with 0.2 µM and 1.0 µM DOX for 96 and 120 hours. Results are presented as mean ± SEM (n=3). *P < 0.05 and ***P< 0.001 vs. Control. Abbreviations – C: control, DOX: doxorubicin, hr: hour, vs: versus.

3.2.3 Evaluation of Mitochondrial Morphology

Mitochondrial morphology has been defined as the balance between fission and fusion (Rolland, 2014). Therefore, in order to establish whether chronic DOX treatment induced any changes in mitochondrial morphology, cells where stained with MitoTracker green and visualized with fluorescence microscopy (Figure 3.9). This data indicates that the control group displays a dense, interconnected mitochondrial network, with elongated and tubular

Stellenbosch University https://scholar.sun.ac.za

mitochondria. Then as the concentration of DOX increased over time, the mitochondrial network progressively appeared to dissociate and separate, as the mitochondria themselves displayed a shorter and fragmented morphology. Mitochondrial load, which is used to quantify the number of mitochondria present in the cells, was also determined in the context of chronic DOX-induced cardiotoxicity (Figure 3.10). Cells were again stained with MitoTracker green and analyzed by flow cytometry. Only treatment with 1.0 μM DOX resulted in a significant increase in fluorescence at the 96 hour [145.50 ± 14.74%, ($p < 0.05$)] and 120 hour [162.30 ± 4.88%, ($p < 0.001$)] time points in comparison to the control (100%). Therefore as the mitochondria become more fragmented, mitochondrial load increases.

Additionally, the intercellular localization of DOX was assessed following treatment. It is difficult to visualize the location of DOX, since the low concentration did not exhibit a high fluorescence. However we can determine that following 120 hours of treatment, DOX appears to be dispersed throughout the cell in the 0.2 μM DOX group, showing strong, significant localization with the mitochondria. This was confirmed by colocalization analysis (Figure 3.11). As can be seen in the images, treatment with the high dose of DOX, also resulted in a significant increase in area of colocalization following 96 hours [13.06 ± 0.47%, ($p < 0.001$)] and 120 hours [5.10 ± 0.50%, ($p < 0.001$)] compared to the 0.2 μM DOX group respectively.

Stellenbosch University https://scholar.sun.ac.za

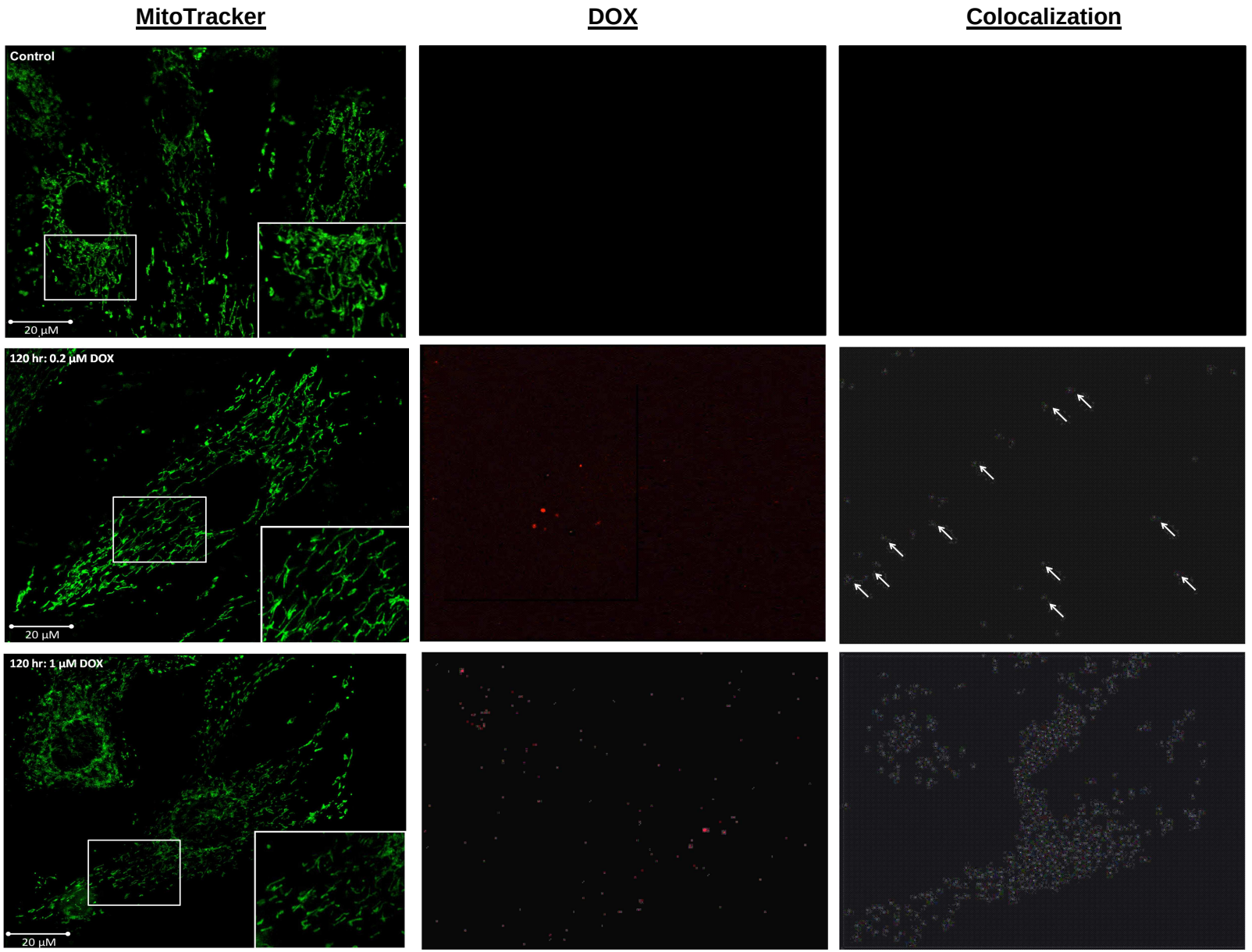

Figure 3.9: The effect of chronic doxorubicin treatment regimes on mitochondrial morphology and DOX localization in H9C2 cardiomyoblasts. Cells were treated daily with 0.2 and 1.0 µM DOX for 96 and 120 hours. Only 120 hour represented in image. Following treatment cells were stained MitoTracker Green (green) and visualized using fluorescence microscopy (n=3). Red indicates DOX and grey indicates area of colocalization Abbreviations – DOX: doxorubicin, hr: hour. Magnification = 60X. Scale Bar = 20 µm. Selected regions where magnified two-fold, and displayed in corresponding insets.

Stellenbosch University https://scholar.sun.ac.za

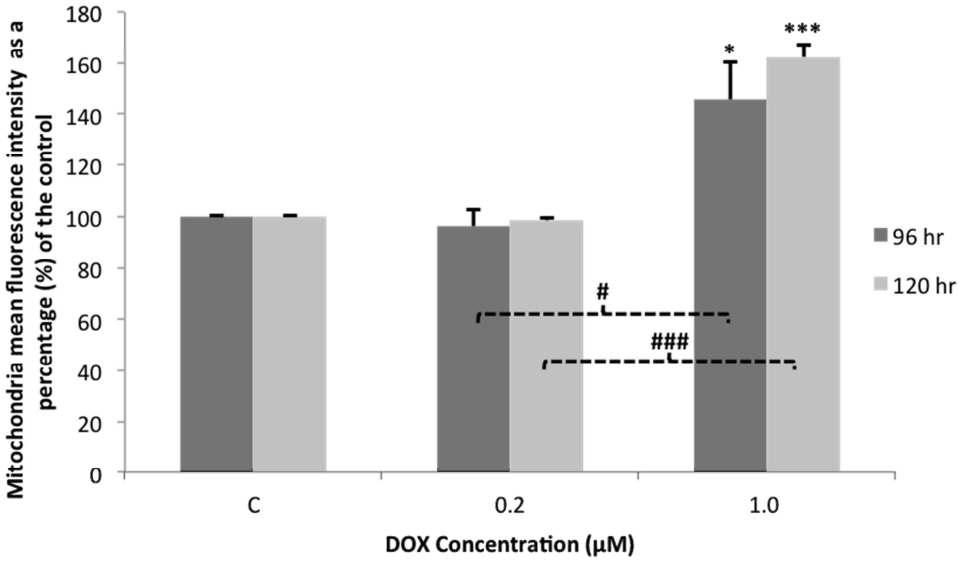

Figure 3.10: The effect of chronic doxorubicin treatment regimes on mitochondrial load in H9C2 cardiomyoblasts. H9C2 cells were treated daily with 0.2 and 1.0 µM DOX for 96 and 120 hours, followed by staining with MitoTracker Green and assessed using flow cytometry (n=3). *P < 0.05 and ***P< 0.001 vs. Control. $^{\#}$P < 0.05 and $^{\#\#\#}$P < 0.001 0.2 µM vs. 1.0 µM. Abbreviations – C: control, DOX: doxorubicin, hr: hour., vs: versus.

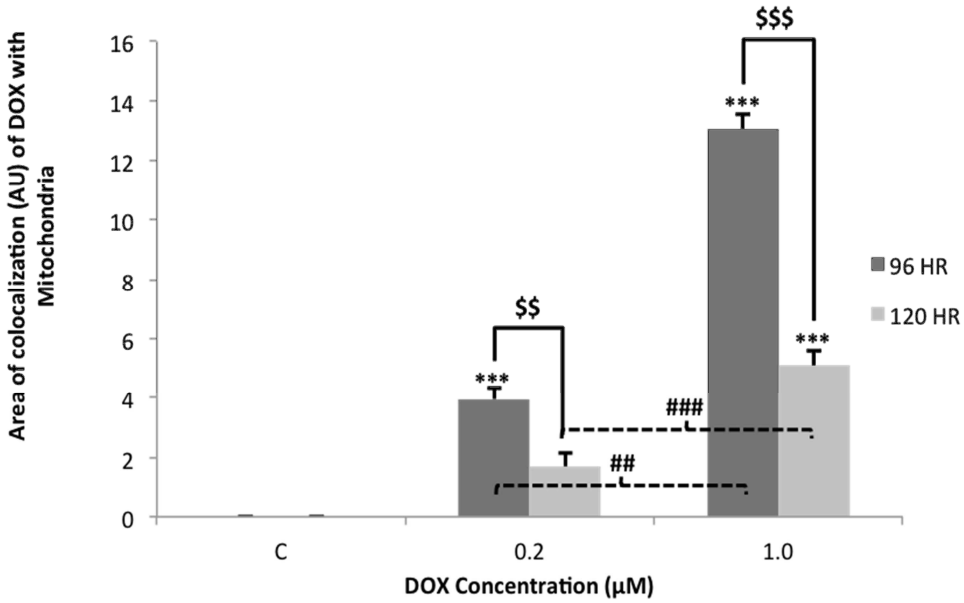

Figure 3.11: Area of doxorubicin and mitochondria colocalization. H9C2 cardiomyoblasts were treated daily with 0.2 and 1.0 µM DOX for 96 and 120 hours, followed by staining with MitoTracker Green (green) and DOX (Red) and visualized with fluorescence microscopy (n=3). Area of colocalization was determined using the Cell^R analysis software. ***P< 0.001 vs. Control. $^{\$\$}$P < 0.01 and $^{\$\$\$}$P < 0.001 96 hr vs. 120 hr. $^{\#\#}$P < 0.01 and $^{\#\#\#}$P <

Stellenbosch University https://scholar.sun.ac.za

0.001 0.2 µM vs. 1.0 µM. Abbreviations – AU: arbitrary units, C: control, DOX: doxorubicin, hr: hour., vs: versus.

3.3 The Effect of Chronic DOX Treatment Regimes on the Ubiquitin Proteasome Pathway

The UPP is a lysosomal-independent proteolytic system responsible for proteasomal degradation of misfolded, aggregated and oxidized proteins (Powell, 2006). It can be activated under cellular stress, and is highly associated with regulating mitochondrial QC as well as the UPR. In order to establish the effects of chronic DOX-induced cardiotoxicity on the UPP, some of the components involved in this pathway were assessed.

3.3.1 Evaluation of E3 ligase expression

Membrane-associated RING finger 5 (MARCH5/MARCH-V/MITOL) is an E3 ubiquitin ligase, which plays an essential role in controlling mitochondrial dynamics and morphology by regulating mitochondrial fission (Karbowski *et al*., 2007; Sugiura *et al*., 2011). This study used western blotting to examine MARCH5 expression in cardiomyoblasts following chronic DOX treatment (Figure 3.12). No significant change in MARCH5 activity was observed in the 0.2 µM DOX group after 96 hours of treatment [128.00 ± 3.3%] compared to control (100%). However, following 120 hours with 0.2 µM of DOX [148.70 ± 4.18%, ($p < 0.001$)], results showed that expression was increased significantly in relation to the control. MARCH5 expression remained considerably elevated at 96 hour [238.80 ± 11.32, ($p < 0.001$)] and 120 hour [154.60 ± 5.67%, ($p < 0.001$)] time points when treated with 1.0 µM DOX in comparison to the control.

The accumulation of fragmented mitochondrial in the cell triggers mitophagy, a select form of autophagy, to remove the damaged mitochondria. Since mitochondrial fission was elevated, this study investigated whether mitophagy was initiated under conditions of chronic DOX-induced cardiotoxicity. The expression of the E3 ubiquitin ligase, Parkin, which mediates mitophagy, was assessed with western blotting (Park *et al*., 2014a) (Figure 3.13). Results showed that treatment with 0.2 µM of DOX caused a significant increase in Parkin expression following 96 hours [141.10 ± 3.19%, ($p < 0.001$)] and 120 hours [137.60 ± 5.37%,

Stellenbosch University https://scholar.sun.ac.za

(p < 0.001)] when compared to the control (100%). Parkin remained elevated significantly after 96 hours of treatment with 1.0 µM of DOX [153.5 ± 1.95%, (p < 0.001 vs. Control)]. However following 120 hours the 1.0 µM DOX group returned to baseline values.

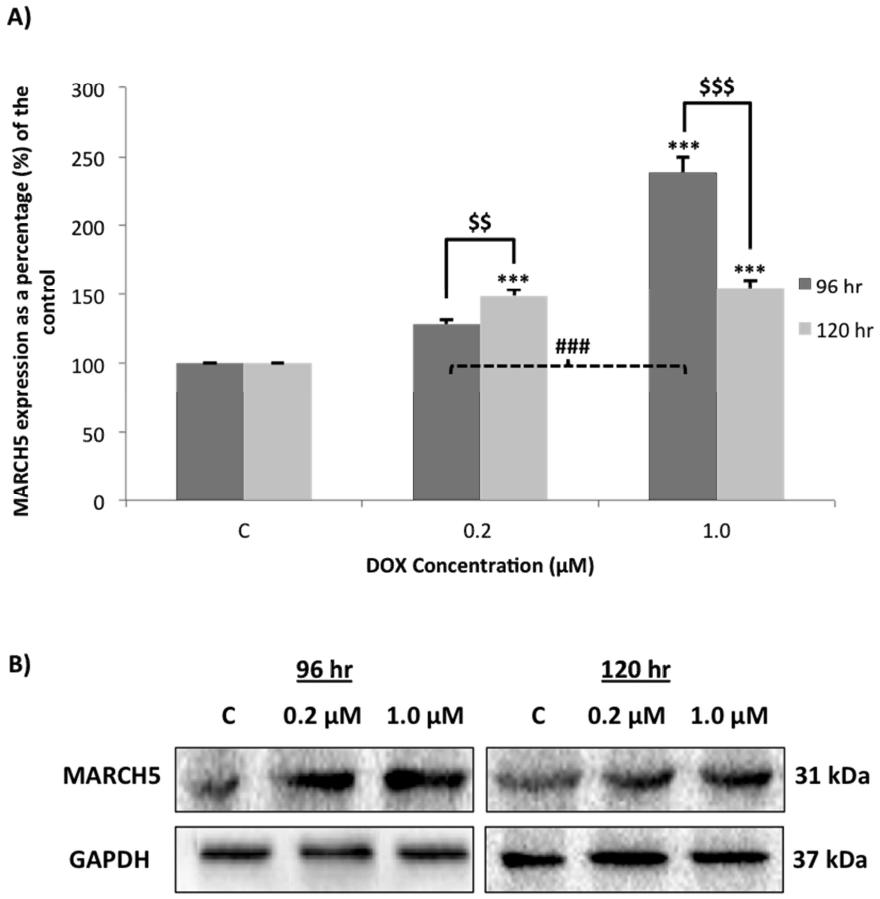

Figure 3.12: The effect of chronic doxorubicin treatment regimes on MARCH5 expression in H9C2 cardiomyoblasts. (A) Lane profile analysis of MARCH5. (B) Representative immunoblot of MARCH5. GAPDH served as the loading control. H9C2 cardiomyoblasts were treated daily with 0.2 µM and 1.0 µM DOX for 96 and 120 hours. Results are presented as mean ± SEM (n=3). ***P< 0.001 vs Control. $^{\$\$}$P < 0.01 and $^{\$\$\$}$P < 0.001 96 hr vs 120 hr. $^{\#\#\#}$P < 0.001 0.2 µM vs 1.0 µM. Abbreviations – C: control, DOX: Doxorubicin, hr: hour, MARCH5: membrane-associated RING finger 5, vs: versus.

Stellenbosch University https://scholar.sun.ac.za

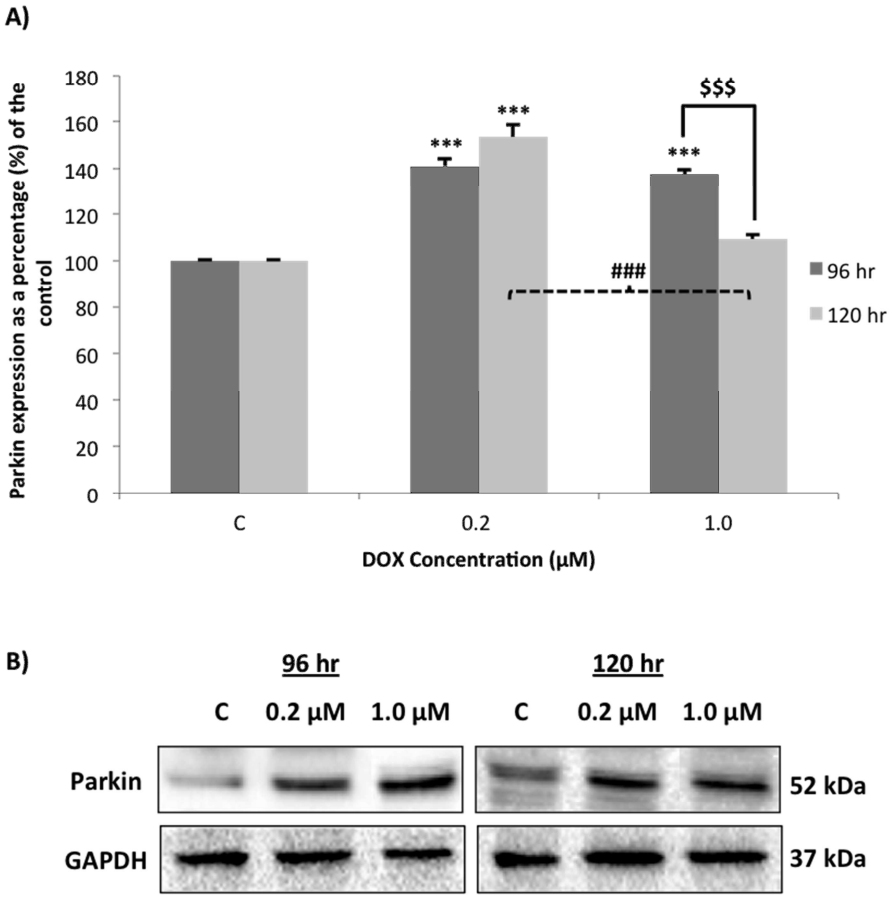

Figure 3.13: The effect of chronic doxorubicin treatment regimes on Parkin expression in H9C2 cardiomyoblasts. (A) Lane profile analysis of Parkin. (B) Representative immunoblot of Parkin. GAPDH served as the loading control. H9C2 cardiomyoblasts were treated daily with 0.2 µM and 1.0 µM DOX for 96 and 120 hours. Results are presented as mean ± SEM (n=3). ***P< 0.001 vs Control. $^{\$\$\$}$P < 0.001 96 hr vs 120 hr. $^{\#\#\#}$P < 0.001 0.2 µM vs 1.0 µM. Abbreviations – C: control, DOX: Doxorubicin, hr: hour, vs: versus.

3.3.2 Evaluation of K48 Protein Ubiquitination

The K48 ubiquitin antibody detects polyubiquitin chains formed directly by the Lys48 residue of ubiquitin. These polyubiquitin chains are commonly tagged by E3 ligases to proteins targeted for protein degradation specifically by the 26S proteasome (Komander, 2009). K48 ubiquitination was significantly augmented at the 0.2 µM concentration group following 120 hours of treatment [357.10 ± 3.73%, ($p < 0.001$)] versus the control group (100%) (Figure 3.14). No significance was observed following 96 hours of treatment with this low dose of DOX. However, treatment with 1.0 µM of DOX resulted in elevated

Stellenbosch University https://scholar.sun.ac.za

ubiquitination after 96 hours [163.20 ± 10.13%, ($p < 0.001$)] and 120 hours [439.10 ± 4.32%, ($p < 0.001$)] in comparison to the control. Additionally, as seen in the representative immunoblot image (Figure 3.14b), a difference in protein tagging was observed across the two concentration groups. Low concentrations of DOX resulted intense tagging of proteins with a molecular weight range of 50 – 85 kDa. Whereas treatment with the higher concentration of DOX resulted in ubiquitination of proteins with a relatively higher molecular weight range, suggestive of myofibrillar protein targeting.

Stellenbosch University https://scholar.sun.ac.za

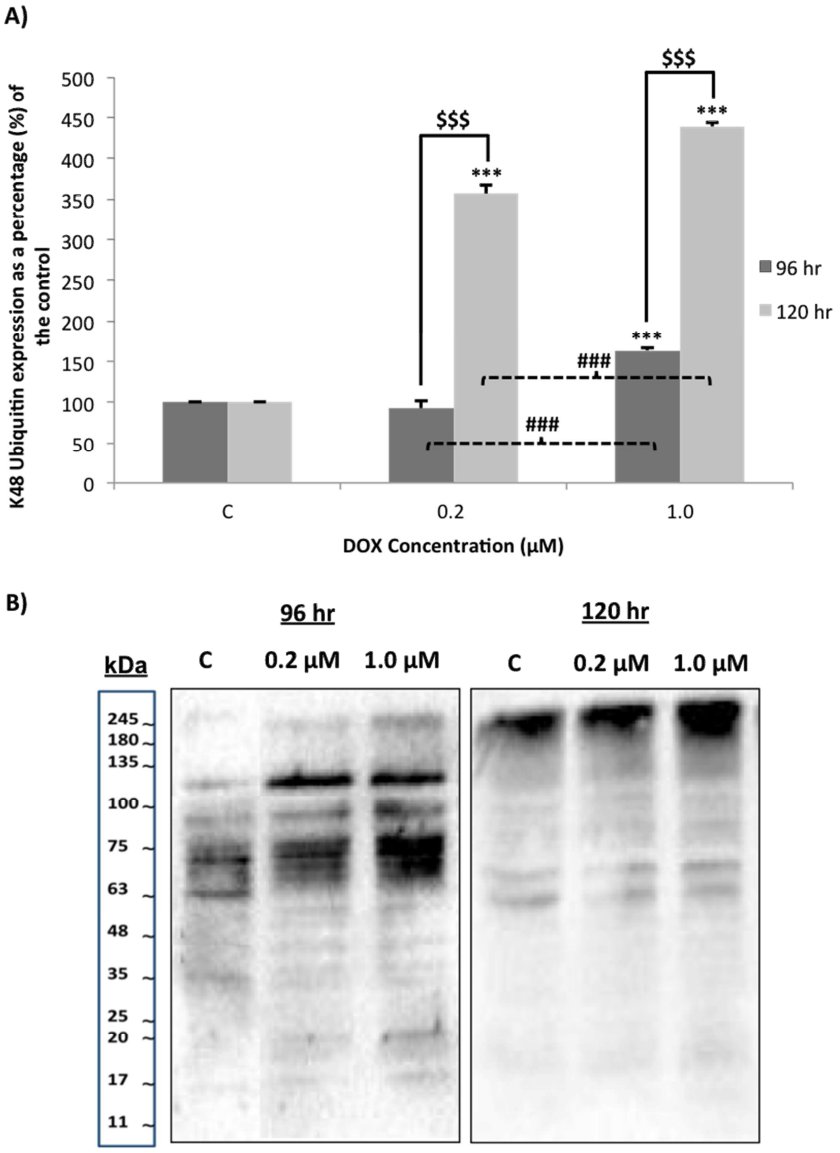

Figure 3.14: The effect of chronic doxorubicin treatment regimes on K48 ubiquitination in H9C2 cardiomyoblasts. (A) Lane profile analysis of K48 Ubiquitin. (B) Representative immunoblot of K48 ubiquitination. GAPDH served as the loading control. H9C2 cardiomyoblasts were treated daily with 0.2 µM and 1.0 µM DOX for 96 and 120 hours. Results are presented as mean ± SEM (n=3). ***P< 0.001 vs Control. $^{\$\$\$}$P < 0.001 96 hr vs 120 hr. $^{\#\#\#}$P < 0.001 0.2 µM vs 1.0 µM Abbreviations – C: control, DOX: doxorubicin, hr: hour, vs: versus.

Stellenbosch University https://scholar.sun.ac.za

3.3.3 Evaluation of the 26S Proteasome

The 26S proteasome is a multi-protein complex, which contains two 19S caps and a 20S core particle. The 20S core contains three different catalytic sites, the chymotrypsin-like, trypsin-like and caspase-like sites, which are responsible for degrading proteins into small peptide fragments. In order to fully elucidate the effect of chronic DOX treatment on the entire 20S core particle, all three catalytic moieties were evaluated.

Findings from this study demonstrate that both the chymotrypsin-like (Figure 3.15) and trypsin-like (Figure 3.16) catalytic activity was significantly and progressively reduced over time as the concentration of DOX increased relative to their controls (100%). However chymotrypsin-like activity was more sensitive to the 1.0 μM DOX treatment [96 hour: 31.45 ± 0.88%, ($p < 0.001$) and 120 hour: 21.25 ± 0.83%, ($p < 0.001$)] compared to trypsin-like activity in the same concentration group [96 hour: 64 ± 3.63%, ($p < 0.001$) and 120 hour: 54.47 ± 3.02%, ($p < 0.001$)]. On the other hand, treatment with 0.2 μM DOX resulted in no significant reduction in chymotrypsin-like activity following 96 hours, whereas a significant decrease in the activity of the trypsin-like site was observed [80.01 ± 4.17%, ($p < 0.05$)]. Both sites however, elicited a similar ±30% reduction in activity following 120 hours of treatment with the low dose of DOX.

The activity of the catalytic-site, displayed a decreasing trend, comparable to that of its counterparts (Figure 3.17). Yet, treatment with the lower dose of DOX resulted in an increase in activity, with significance attained only following 96 hours [137.40 ± 6.15%, ($p < 0.01$ vs. Control)]. Although a significant reduction in catalysis was observed after 120 hours, at the 1.0 μM concentration group [45.54 ± 7.46%, ($p < 0.01$)] compared to the control.

Stellenbosch University https://scholar.sun.ac.za

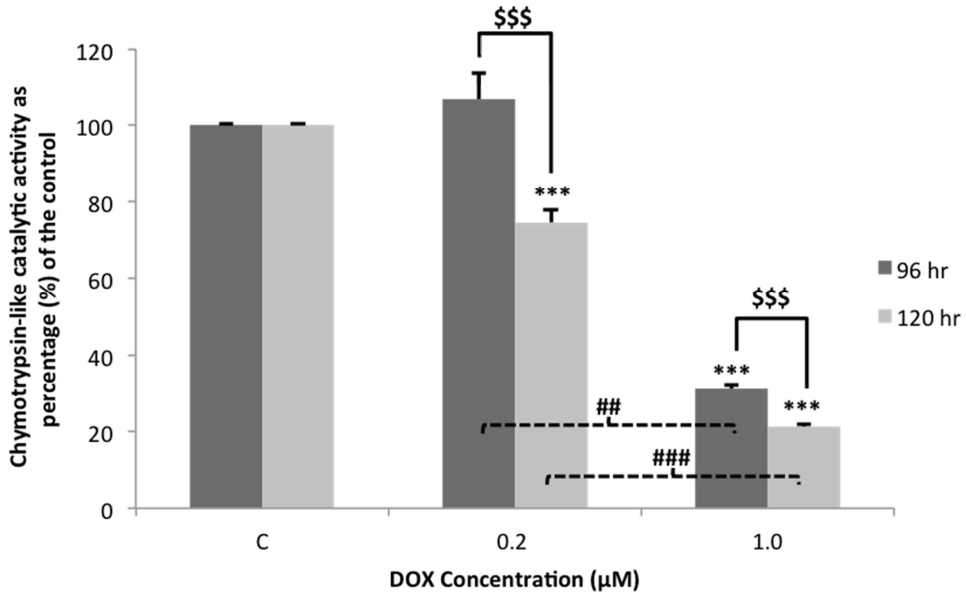

Figure 3.15: The effect of chronic doxorubicin treatment regimes on chymotrypsin-like catalytic activity in H9C2 cardiomyoblasts. Cells were treated daily with 0.2 µM and 1.0 µM DOX for 96 and 120 hours. Results are presented as mean ± SEM (n=3). ***P< 0.001 vs Control. $^{\$\$\$}$P < 0.001 96 hr vs 120 hr. $^{\#\#}$P < 0.01 and $^{\#\#\#}$P < 0.001 0.2 µM vs 1.0 µM. Abbreviations – C: control, DOX: doxorubicin, hr: hour, vs: versus.

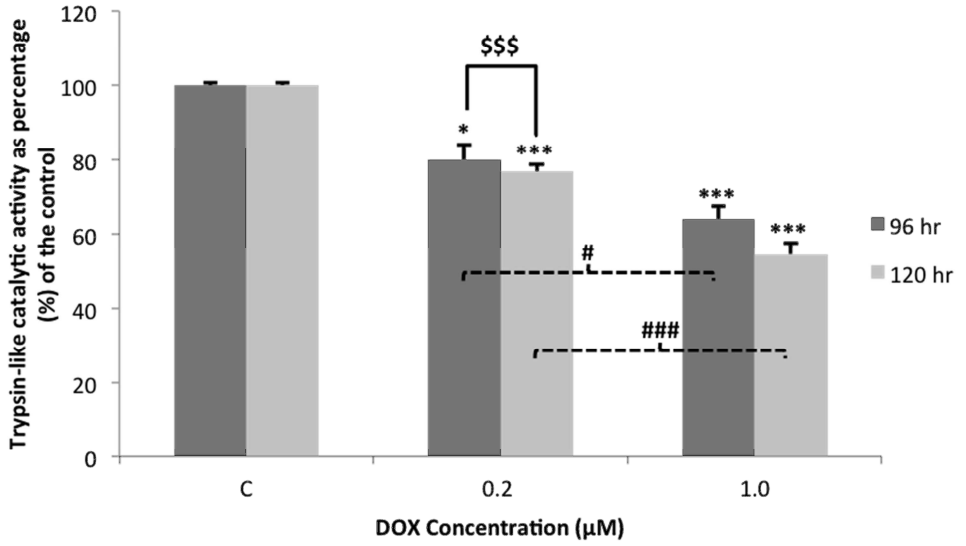

Figure 3.16: The effect of chronic doxorubicin treatment regimes on trypsin-like catalytic activity in H9C2 cardiomyoblasts. Cells were treated daily with 0.2 µM and 1.0 µM DOX for 96 and 120 hours. Results are presented as mean ± SEM (n=3). *P < 0.05 and ***P< 0.001 vs Control. $^{\$\$\$}$P < 0.001 96 hr vs 120 hr. $^{\#\#}$P < 0.01 and $^{\#\#\#}$P < 0.001 0.2 µM vs 1.0 µM. Abbreviations: C: control, DOX: doxorubicin, hr: hour., vs.: versus.

Stellenbosch University https://scholar.sun.ac.za

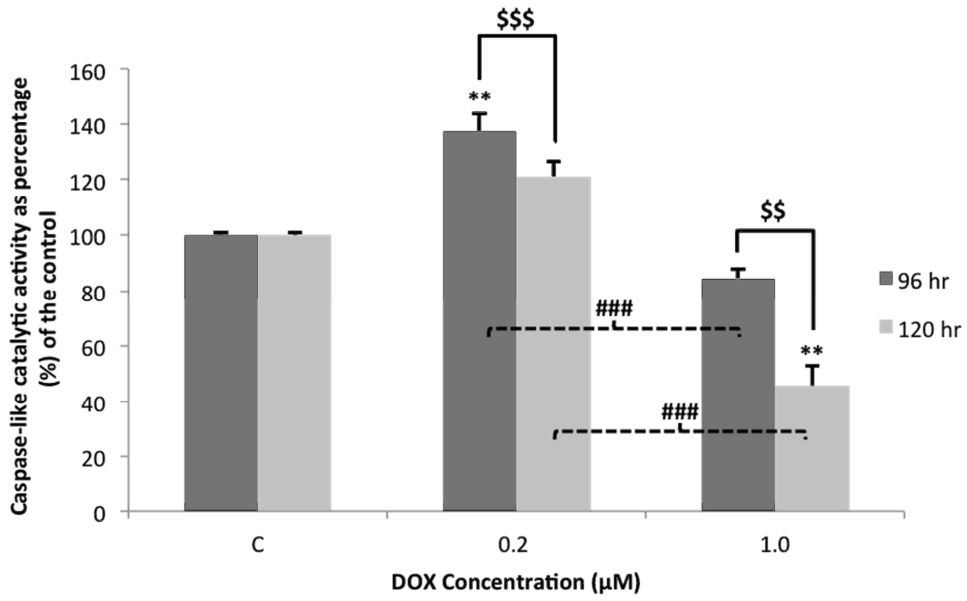

Figure 3.17: The effect of chronic doxorubicin treatment regimes on caspase-like catalytic activity in H9C2 cardiomyoblasts. Cells were treated daily with 0.2 µM and 1.0 µM DOX for 96 and 120 hours. Results are presented as mean ± SEM (n=3). **P < 0.01 vs Control. $^{\$\$}$P < 0.01 and $^{\$\$\$}$P < 0.001 96 hr vs 120 hr. $^{\#\#\#}$P < 0.001 0.2 µM vs 1.0 µM. Abbreviations – C: control, DOX: doxorubicin, hr: hour, vs: versus.

3.4 The Effect of Chronic DOX Treatment Regimes on Autophagy

Autophagy, a lysosomal-dependent proteolytic pathway, is upregulated under various conditions such as oxidative or ER stress. It is responsible for degradation of protein aggregates and redundant organelles, like the mitochondria, and is therefore an important process associated with mitochondrial QC (Marchi *et al.*, 2014). In order to effectively evaluate autophagic activity following chronic DOX treatment, two specific biomarkers for the autophagic pathway, LC-3 and p62/SQSTM1, were assessed by western blotting.

The lipidation of the cytosolic form of the microtubule-associated protein light chain (LC3-I) to its autophagosome-associated form (LC3-II) is used to assess the autophagic activity and formation of autophagosomes (Kadowaki *et al.*, 2009). There are many accepted methods in which LC3 expression can be interpreted. This study chose to analyze the LC3-II/LC3-I ratio since it is an accurate determinant for autophagic activity (Kabeya *et al.*, 2000) (Figure 3.18). These results demonstrate that at both the lowest and the highest dose of DOX, autophagic

Stellenbosch University https://scholar.sun.ac.za

activity was significantly increased following 96 hours [0.2 μM: 144.60 ± 4.56% and 1.0 μM: 159.10 ± 1.34%, ($p < 0.001$)] and 120 hours (0.2 μM: 165.00 ± 5.46% and 1 μM: 193.90 ± 8.43%, ($p < 0.001$)] of treatment in comparison to the control (100%). Additionally, statistical differences were also obtained between concentration groups ($p < 0.001$), suggesting that increases in autophagic activity are not only dependent on the duration of treatment, but also on the concentration. However, the analysis of LC3-II/LC3-I ratio does not represent autophagic flux, since the accumulation of LC3-II, as indicated in the immunoblot image (Figure 3.18b), only correlates to the extent of autophagosome formation and not to its degradation (Kabeya *et al.*, 2000).

Sequestosome, or p62 (SQSTM1) has been identified as an ubiquitin-binding protein (Vadlamudi *et al*., 1996). In the mediation of autophagy and mitophagy, p62 promotes the formation of protein aggregates, and directs them to the autophagosome through its interactions with LC3. P62, along with the targeted and defective cargo are engulfed and subsequently degraded by the autophagolysosome (Ichimura *et al.*, 2008). DOX treatment resulted in a significant reduction in p62 expression at both concentrations following 96 hours [0.2 μM: 51.39 ± 5.14% and 1.0 μM: 42.11 ± 1.98%, ($p < 0.001$)] and 120 hours [0.2 μM: 59.29± 3.02% and 1.0 μM: 61.4 ± 0.95%, ($p < 0.001$)] compared to their respective controls (Figure 3.19). Therefore, since p62 is selectively degraded by autophagy, our results demonstrate that autophagic flux increases in response to both the duration and the concentration of DOX treatment.

Stellenbosch University https://scholar.sun.ac.za

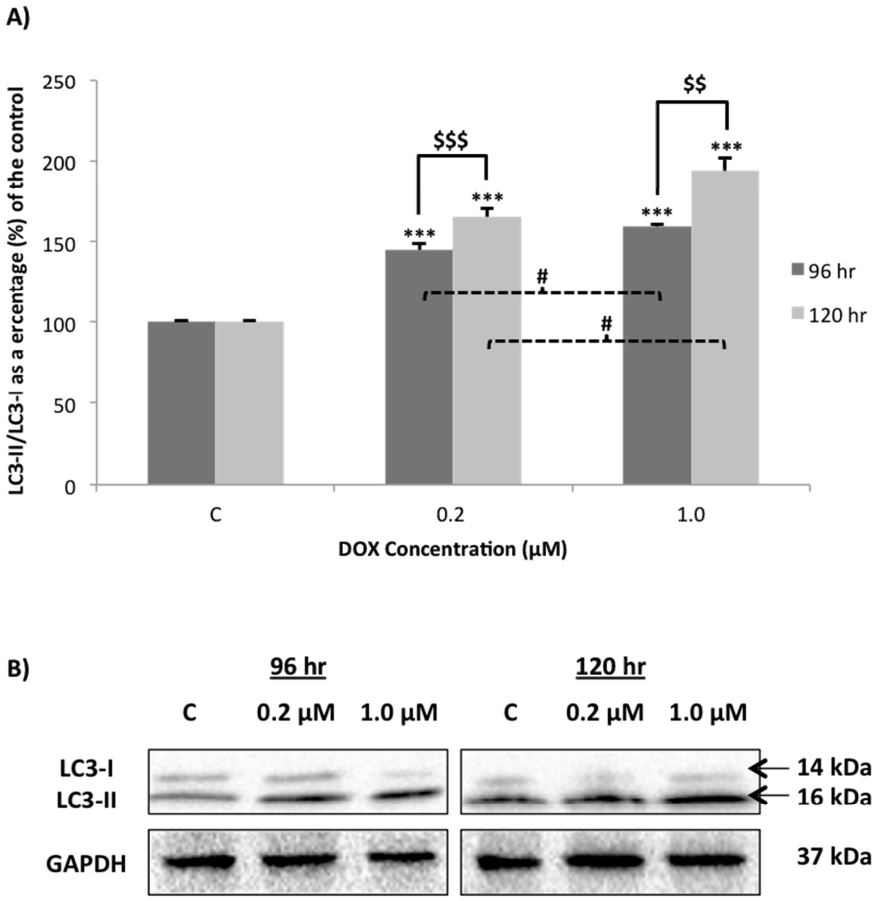

Figure 3.18: The effect of chronic doxorubicin treatment regimes on LC3 expression in H9C2 cardiomyoblasts. (A) Lane profile analysis of LC3-II/LC3-Ratio. (B) Representative immunoblot of LC3-I and LC3-II. GAPDH served as the loading control. H9C2 cardiomyoblasts were treated daily with 0.2 µM and 1.0 µM DOX for 96 and 120 hours. Results are presented as mean ± SEM (n=3). ***P < 0.01 vs Control. $^{\$\$}$P < 0.01 and $^{\$\$\$}$P < 0.001 96 hr vs 120 hr. $^{\#}$P < 0.05 0.2 µM vs 1.0 µM. Abbreviations – C: control, DOX: doxorubicin, hr: hour, LC3: microtubule –associated protein light chain 3, vs.: versus.

Stellenbosch University https://scholar.sun.ac.za

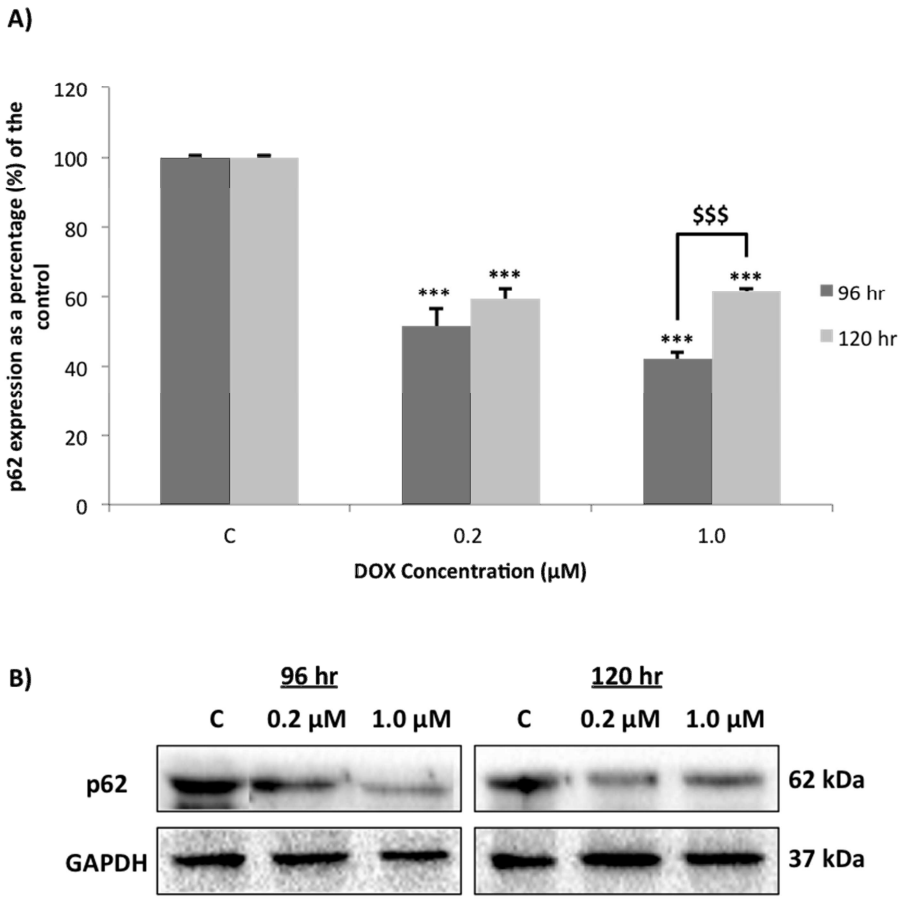

Figure 3.19: The effect of chronic doxorubicin treatment regimes on p62 expression in H9C2 cardiomyoblasts. (A) Lane profile analysis of p62. (B) Representative immunoblot of p62. GAPDH served as the loading control. H9C2 cardiomyoblasts were treated daily with 0.2 µM and 1.0 µM DOX for 96 and 120 hours. Results are presented as mean ± SEM (n=3). ***P < 0.001 vs Control. $^{\$\$\$}$P < 0.001 96 hr vs 120 hr. Abbreviations – C: control, DOX: doxorubicin, hr: hour, vs.: versus.

3.5 The Effect of Chronic DOX Treatment Regimes on Mitochondrial Biogenesis

Since the coordination and cross-talk between the proteolytic systems, specifically mitophagy, and mitochondrial biogenesis is essential for maintaining mitochondrial homeostasis (Palikaras and Tavernarakis, 2014), this study wanted to assess whether these H9C2 cells have the ability to "make new" mitochondria, considering the amount of fission observed. Western blotting was used to assess the transcription factor, PGC-1α (peroxisome proliferator-activated receptor gammer co-activator 1-alpha), an important protein involved

Stellenbosch University https://scholar.sun.ac.za

in regulating mitochondrial biogenesis. PGC-1α controls the synthesis of new mitochondrial by coordinating the transcription of both the mitochondrial and nuclear genomes (Baker *et al*., 2007; Puigserver *et al*., 1998). Compared to the control group (100%), these results demonstrated that PGC-1α levels were significantly attenuated over time following treatment with 0.2 µM DOX [96 hours: 78.68 ± 4.02% and 120 hours: 66.45 ± 5.12%, ($p < 0.01$)] and 1.0 µM DOX [96 hours: 50.56 ± 2.62% and 120 hours: 43.63 ± 6.16%, ($p < 0.001$)] (Figure 3.20).

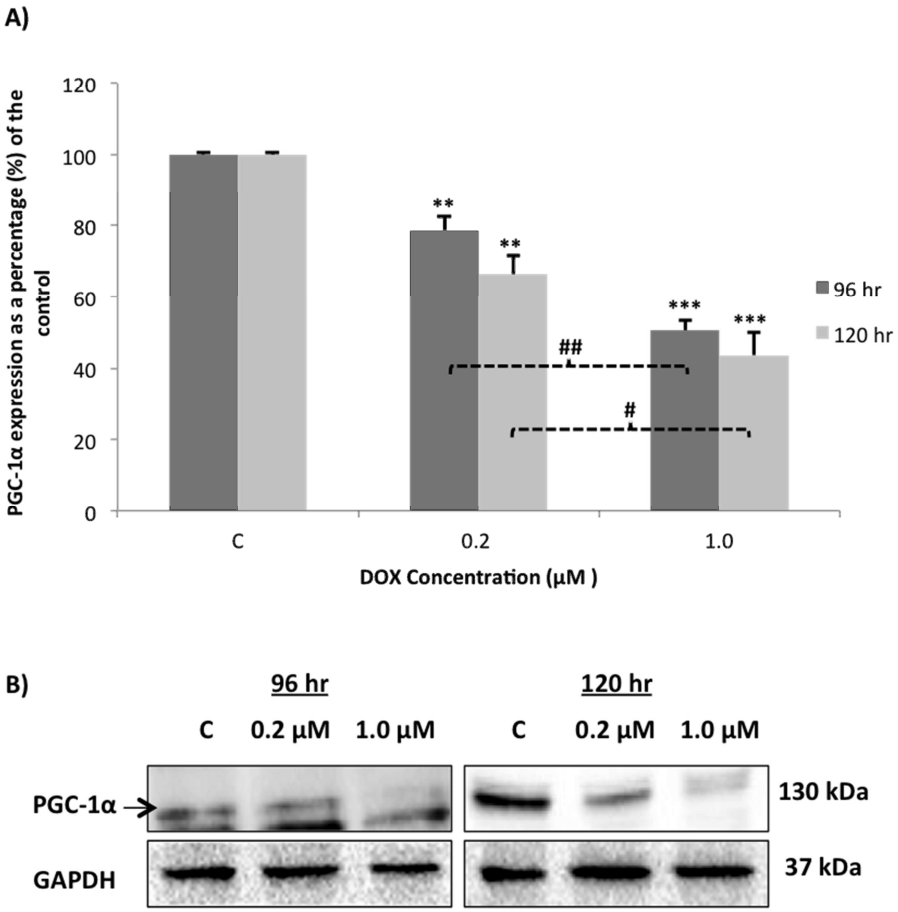

Figure 3.20: The effect of chronic doxorubicin treatment regimes on PGC-1α expression in H9C2 cardiomyoblasts. (A) Lane profile analysis of PGC-1α. (B) Representative immunoblot of PGC-1α. GAPDH served as the loading control. H9C2 cardiomyoblasts were treated daily with 0.2 µM and 1.0 µM DOX for 96 and 120 hours. Results are presented as mean ± SEM (n=3). **P < 0.01 ***P < 0.001 vs Control. $^{\#}$P < 0.05 and $^{\#\#}$P < 0.01 0.2 µM vs 1.0 µM. Abbreviations – C: control, DOX: Doxorubicin, hr: hour, PGC-1α: peroxisome proliferator-activated receptor gamma co-activator 1-alpha, vs: versus.

Stellenbosch University https://scholar.sun.ac.za

3.6 The Effect of Chronic DOX Treatment Regimes on Apoptosis

In order to further validate the results obtained from the Caspase-Glo 3/7 Assay, the expression of cleaved-caspase 3 was analyzed with immunoblotting. As seen in the Caspase-Glo assay, caspase 3 cleavage was significantly higher in both the 0.2 μM [261.60 ± 18.38%, ($p < 0.001$)] and 1.0 μM [204.60 ± 9.94%, ($p < 0.01$)] DOX concentration groups following 96 hours of treatment compared to the control (100%). Expression of cleaved-caspase after 120 hours of treatment further corresponded to results obtained from the Caspase-Glo assay. Comparison between groups revealed that although treatment with 0.2 μM DOX significantly increased caspase cleavage compared to the control, a significant reduction a cleavage was observed over time [133.50 ± 6.00%, ($p < 0.01$ 0.2 μM vs. 1.0 μM)]. Similarly, apoptosis was significantly downregulated at the higher concentration of DOX accumulated over 120 hours [65.44 ± 4.06%, ($p < 0.001$ 0.2 μM vs. 1.0 μM)]. These results demonstrate that apoptosis is downregulated in both a time- and dose-dependent manner by chronic DOX treatment regimes.

Stellenbosch University https://scholar.sun.ac.za

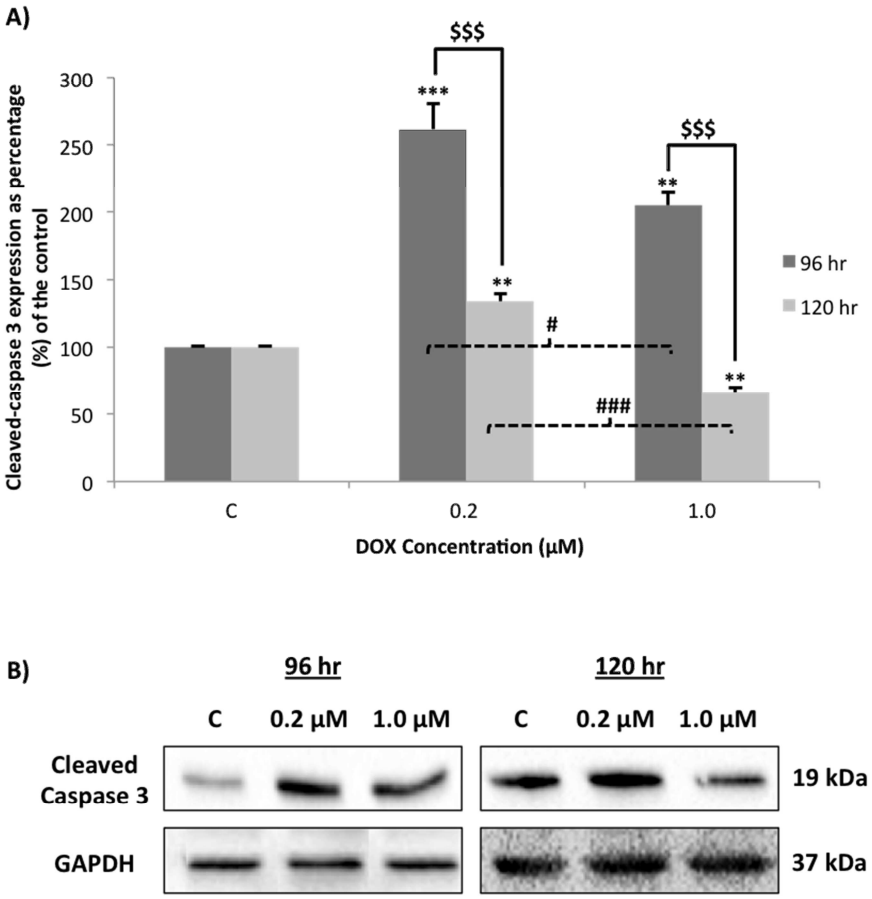

Figure 3.21: The effect of chronic doxorubicin treatment regimes on apoptosis in H9C2 cardiomyoblasts. Cells were treated daily with 0.2 µM and 1.0 µM DOX for 96 and 120 hours. Results are presented as mean ± SEM (n=3). **P < 0.01 and ***P < 0.001 vs. Control. $^{\$\$\$}$P < 0.001 96 hr vs 120 hr. P < 0.05 and $^{\#\#\#}$P < 0.001 0.2 µM vs 1.0 µM.Abbreviations: C = control, DOX = doxorubicin, hr = hour.

Stellenbosch University https://scholar.sun.ac.za

3.7 The Effect of Chronic DOX Treatment Regimes on Oxidative Stress

It has been shown extensively in the literature that dyregulation of the mitochondrial dynamics can result in the overproduction of ROS, and induce oxidative stress within the cells (Frank *et al.*, 2012; Yu *et al*., 2006). Furthermore, oxidative stress is a well-known consequence of DOX-induced cardiotoxicity. With this in mind this study employed the ORAC, TBARS and GSH assay to assess the antioxidant capacity, oxidative damage and the redox status respectively following chronic DOX treatment.

3.7.1 Evaluation of Antioxidant Capacity (ORAC assay)

Results from the ORAC assay indicated that the antioxidant capacity significantly increased following 0.2 μM DOX treatment for 96 hours [550.0 ± 5.52 μmol TE/L, ($p < 0.001$)] and 120 hours [553.40 ± 1.87 μmol TE/L, ($p < 0.001$)] compared to the control [465.30 ± 11.47 μmol TE/L] respectively (Figure 3.22). Antioxidant capacity remained significantly increased in the 1.0 μM DOX group, at both the 96 hour [543.7 ± 2.41 μmol TE/L, ($p < 0.001$)] and 120 hour [500.80 ± 8.42 μmol TE/L] time points versus the control. Interestingly, a significant ($p < 0.01$) reduction in H9C2 antioxidant capacity occurred in the highest concentration group (1.0 μM DOX) after 120 hours of treatment compared to the same concentration group after 96 hours of exposure. These results indicate that the cells initially try to survive under these harsh environmental conditions, however as the concentration of DOX increases over time the antioxidant capacity is reduced. This suggests that cumulative and chronic doses of DOX impair the cells ability to cope under conditions of oxidative stress.

Stellenbosch University https://scholar.sun.ac.za

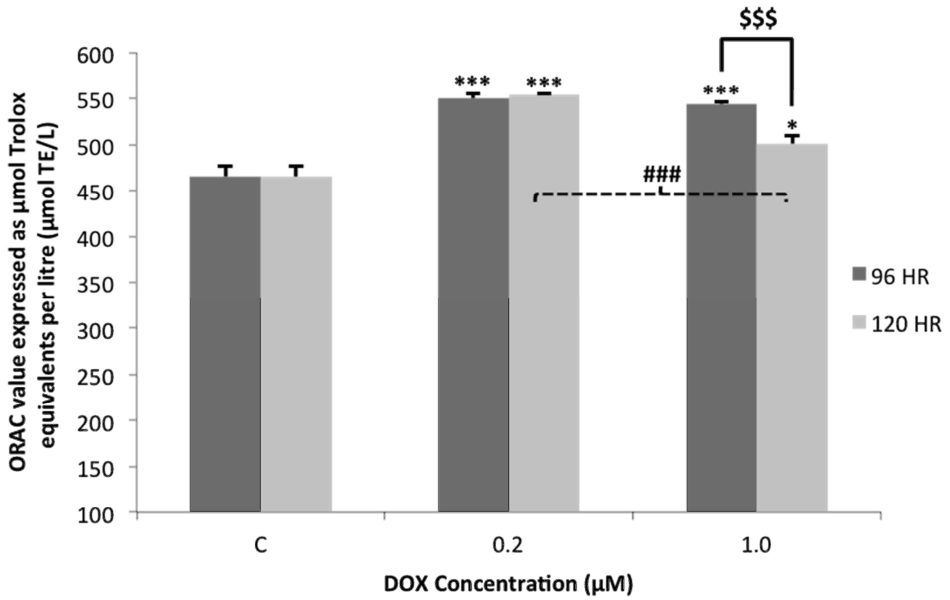

Figure 3.22: The effect of chronic doxorubicin treatment regimes on antioxidant capacity in H9C2 cardiomyoblasts. Cells were treated daily with 0.2 µM and 1.0 µM DOX for 96 and 120 hours. Following treatment the oxygen radical absorbance capacity (ORAC) of each treatment group was determined with a fluorometric assay (n=3). *P < 0.05 ***P < 0.001 vs Control. $^{\$\$\$}$P < 0.001 96 hr vs 120 hr. $^{\#\#\#}$P < 0.001 0.2 µM vs 1.0 µM. Abbreviations – C: control, DOX: doxorubicin, hr: hour, TE/L: Trolox equivalent per litre, vs: versus.

3.7.2 Evaluation of Oxidative Damage (TBARS assay)

MDA (Malondialdehyde) is a natural by-product of lipid peroxidation, and is used as an indicator for oxidative damage. Daily treatment with lower dose of DOX for 96 hours [0.20 ± 0.014 µmol/L, ($p < 0.001$)] and 120 hours [0.30 ± 0.015 µmol /L, ($p < 0.001$)] significantly elevated lipid peroxidation compared to the control [0.12 ± 0.030 µmol/L] (Figure 3.23). Similarly, treatment with the high DOX also induced a significant increase in lipid peroxidation at both time points [96 hours: 0.19 ± 0.03 µmol/L, ($p < 0.001$) and 120 hour: 0.13 ± 0.02 µmol/L, ($p < 0.01$)] compared to the control group. These results suggest that high cumulative dose and chronic treatment induce incremental lipid oxidative damage in a time and dose dependent manner.

Stellenbosch University https://scholar.sun.ac.za

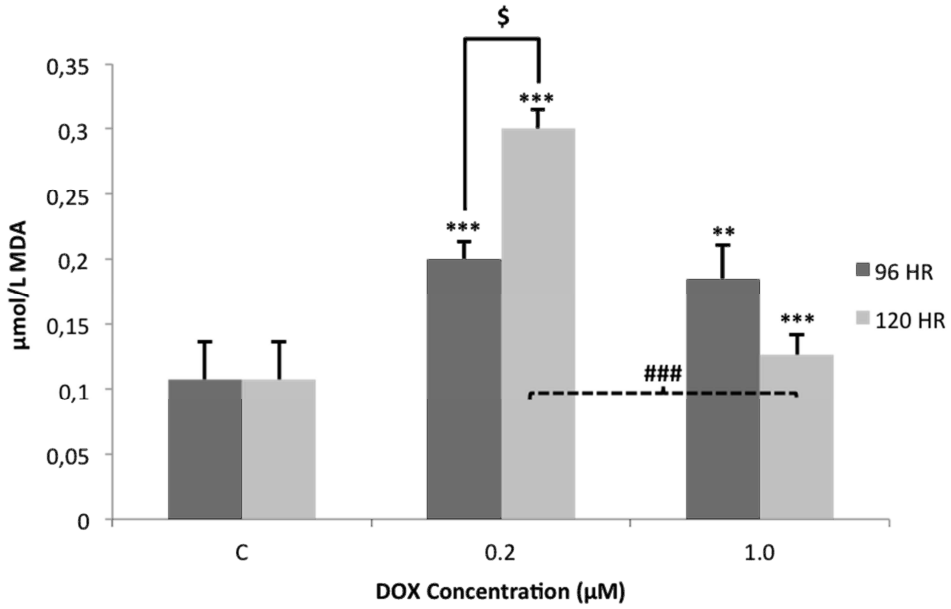

Figure 3.23: The effect of chronic doxorubicin treatment regimes on lipid peroxidation in H9C2 cardiomyoblasts. Cells were treated daily with 0.2 µM and 1.0 µM DOX for 96 and 120 hours. Following treatment the concentration of thiobarbituric acid reacting substance (TBARS) per sample was determined (n=3). ***P < 0.001 vs Control. $^{\$}$P < 0.05 96 hr vs 120 hr. $^{\#\#\#}$P < 0.001 0.2 µM vs 1.0 µM Abbreviations – C: control, DOX: doxorubicin, hr: hour, MDA: Malondialdehyde, vs.: versus.

3.7.3 Evaluation of Oxidative Status (GSH assay)

Determination of reduced glutathione (GSH) to oxidized glutathione (GSSG) was assessed using the GSH:GSSG ratio. GSH is an important antioxidant that helps maintain the redox state within the cells. As indicated in Table 2, as the concentration of DOX increased over time [96 hour: ($p < 0.001$), 120 hour: ($p < 0.05$)], GSH levels were significantly decreased versus the control group [6.73 ± 0.35]. However the concentration of GSSG was statistically elevated following 96 hours [$p < 0.001$, 0.2 µM vs. 1.0] and 120 hours [$p < 0.001$, 0.2 µM vs. 1.0 µM] of treatment as the dose increased, but no change in GSSG was observed at either time point following 1.0 µM of treatment versus the GSSG control group (Table 2). No changes in the GSH:GSSG ratio was observed following 96 hours of treatment with 0.2 µM [52.59 ± 1.14], whereas after 120 hours the ratio was significantly decreased at the 0.2 uM group [44.35 ± 1.78, ($p < 0.01$)] compared to the control [52.59 ± 1.14] (Figure 3.24). Given that GSH levels were reduced and no significant difference in GSSG occurred at either of the

Stellenbosch University https://scholar.sun.ac.za

1.0 µM treatment groups, the ratio was substantially reduced following 96 hours [41.81 ± 2.02, ($p < 0.01$)] and 120 hours [39.99 ± 0.94, ($p < 0.001$)] of treatment with 1.0 µM DOX compared to the control. Overall, GSH:GSSH ratio progressively declined indicating an elevation in oxidative stress occurs in both a time- and dose- dependent manner following chronic treatment with DOX.

Table 2: The effect of chronic DOX treatment on GSH, GSSG and the GSH/GSSG ratio

Groups	GSH (µmol/L)	GSSG (µmol/L)	GSH/GSSG Ratio
Control	6.72 ± 0.35	0.13 ± 0.01	53.68 ± 2.31
96 hr: 0.2 µM DOX	5.43 ± 0.12	0.10 ± 0.02	52.59 ± 1.14
96 hr: 1.0 µM DOX	5.31 ± 0.16	0.13 ± 0.02	41.81 ± 2.02
120 hr: 0.2 µM DOX	5.52 ± 0.26	0.11 ± 0.01	44.35 ± 1.78
120 hr: 1.0 µM DOX	5.52 ± 0.19	0.14 ± 0.03	39.99 ± 0.94

Abbreviations – DOX: Doxorubicin, GSH: reduced glutathione, GSSG: oxidized glutathione.

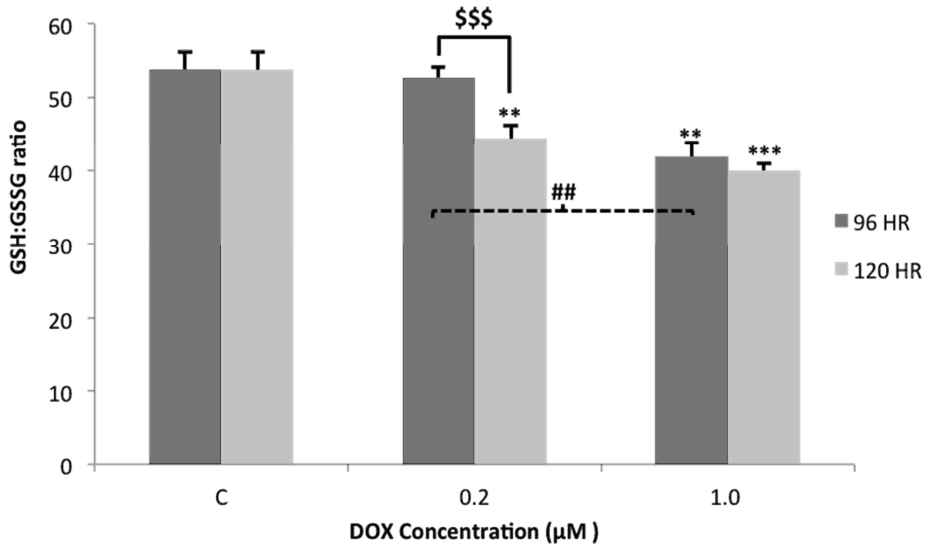

Figure 3.24: The effect of chronic doxorubicin treatment regimes on GSH:GSSG ratio in H9C2 cardiomyoblasts. Cells were treated daily with 0.2 µM and 1.0 µM DOX for 96 and 120 hours. Following treatment the GSH and GSSG content was determined, and the GSH:GSSG ratio was calculated (n=3). **P < 0.01 and ***P < 0.001 vs Control. $^{\#\#}$P < 0.01 0.2 µM vs 1.0 µM. $^{\$\$\$}$P < 0.001 96 hr vs 120 hr. Abbreviations – C: control, DOX: doxorubicin, GSH: reduced glutathione, GSSG: oxidized glutathione, hr: hour, vs: versus

Stellenbosch University https://scholar.sun.ac.za

3.8 The Effect of Chronic DOX Treatment Regimes on the Endoplasmic Reticulum

It has been established that altered mitochondrial function as well as oxidative injury, disrupts ER homeostasis and results in ER stress and activation of the UPR (Verfaillie *et al*., 2013). Given the role that DOX plays in mediating both mitochondrial dysfunction and oxidative stress, it is thought that chronic DOX treatment may also induce ER stress and UPR activation.

3.8.1 Evaluation of BiP Expression

BiP (GRP78/Gp78), an ER-associated E3 ubiquitin ligase, is activated under conditions of ER Stress and regulates UPR signaling (Minamino *et al*., 2010). The effect of chronic DOX treatment on BiP expression was evaluated with western blotting (Figure 3.25). Following 0.2 μM DOX treatment, a significant increase in BiP activity was only observed following 120 hours [151.60 ± 6.50%, ($p < 0.01$)] of exposure when compared to the control (100%). However analysis of the 1.0 μM DOX group showed a substantial elevation in BiP expression following 96 hours [177.80 ± 11.32%, ($p < 0.01$)] and 120 hours [277.20 ± 8.34%, ($p < 0.001$)] of treatment in comparison to the control. This data demonstrates that BiP expression significantly increased in both a time- and dose-dependent manner.

Stellenbosch University https://scholar.sun.ac.za

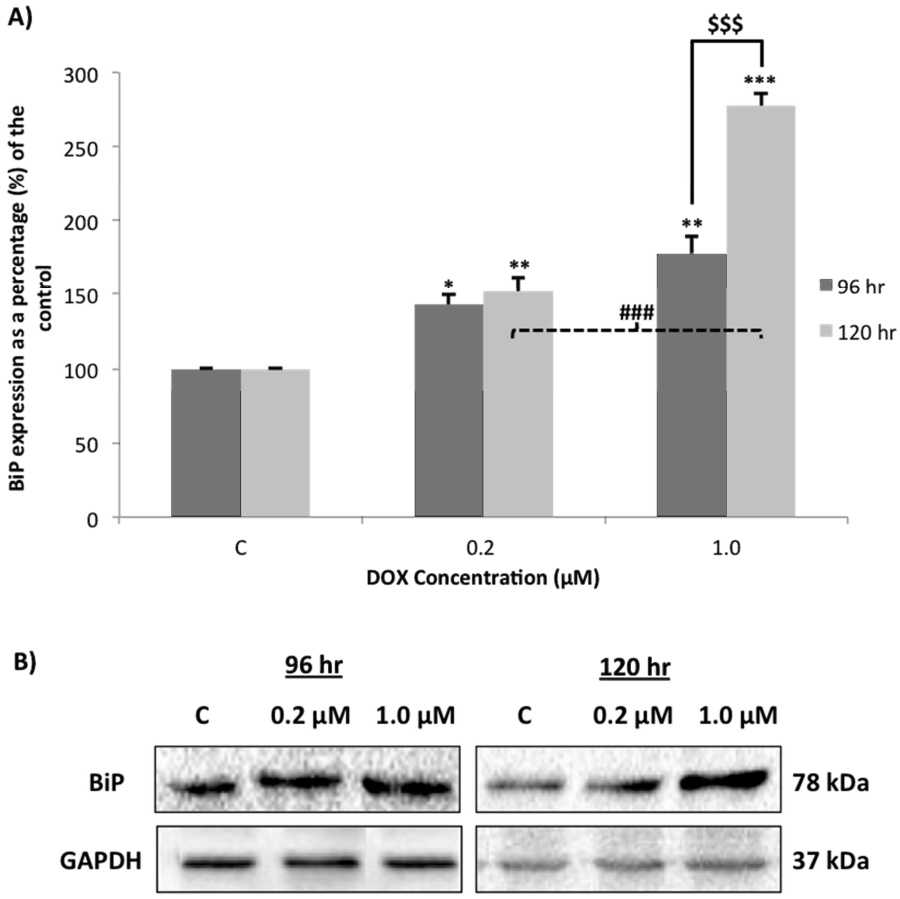

Figure 3.25: The effect of chronic doxorubicin treatment regimes on BiP expression in H9C2 cardiomyoblasts. (A) Lane profile analysis of BiP. (B) Representative immunoblot of BiP. GAPDH served as the loading control. Cells were treated daily with 0.2 µM and 1.0 µM DOX for 96 and 120 hours (n=3). *P < 0.05, **P < 0.01 and ***P < 0.001 vs Control. $^{###}$P < 0.001 0.2 µM vs 1.0 µM. $^{\$\$\$}$P < 0.001 96 hr vs 120 hr. Abbreviations – BiP: binding immunoglobulin protein, C: control, DOX: doxorubicin, hr: hour, vs: versus.

3.8.2 Evaluation of ATF4 Expression

ATF4 is a UPR protein translated under conditions of mild ER Stress (Verfaillie *et al*., 2013). To examine whether chronic DOX-induced cardiotoxicity influenced ATF4 expression by ER stress, western blotting analysis was performed (Figure 3.26). Compared to the control (100%), ATF4 expression was significantly downregulated after 96 hours at both 0.2 µM DOX [50.82 ± 3.64%, ($p < 0.001$)] and 1.0 µM DOX [43.45 ± 4.77%, ($p < 0.001$)] concentration groups. Treatment for 120 hours produced no change in ATF4 expression at

Stellenbosch University https://scholar.sun.ac.za

the 0.2 µM DOX group, yet at the 1.0 µM group [76.81 ± 2.72%, ($p < 0.01$)] a significant reduction in ATF4 occurred compared to the control group.

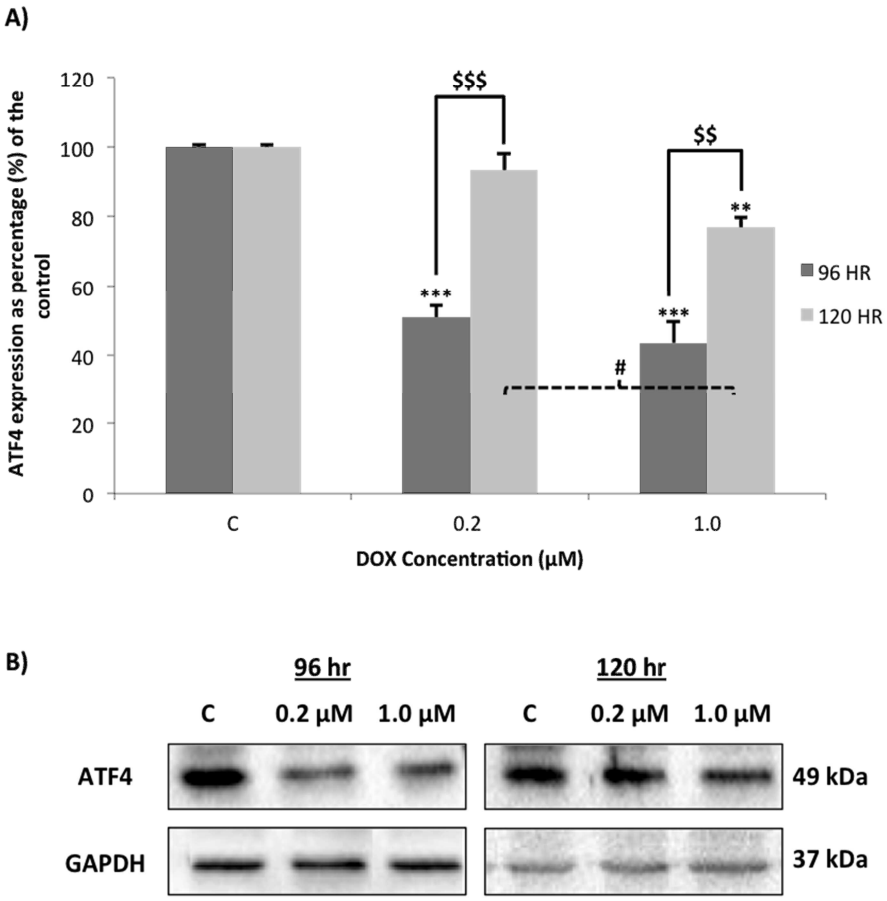

Figure 3.26: The effect of chronic doxorubicin treatment regimes on ATF4 expression in H9C2 cardiomyoblasts. (A) Lane profile analysis of ATF4. (B) Representative immunoblot of ATF4. GAPDH served as the loading control. Cells were treated daily with 0.2 µM and 1.0 µM DOX for 96 and 120 hours (n=3). **P < 0.01 and ***P < 0.001 vs Control. $^{\#}$P < 0.05 0.2 µM vs 1.0 µM. $^{\$\$}$P < 0.01 and $^{\$\$\$}$P < 0.001 96 hr vs 120 hr. Abbreviations – ATF4: activating transcription factor 4, C: control, DOX: doxorubicin, hr: hour, vs: versus.

3.8.3 Evaluation of ER Load and DOX Localization

It has previously been shown that the under conditions of ER stress and UPR activated that the ER expands (Minotti *et al*., 2004; Wang and Kaufman, 2014). Therefore ER load, an indicator for ER expansion, was used as an additional marker to evaluate ER stress. Results from flow cytometry analysis demonstrate that ER load was significantly increased after 96 hours of treatment with 0.2 µM DOX [159.30 ± 16.53%, ($p < 0.05$)] and 1.0 µM DOX

Stellenbosch University https://scholar.sun.ac.za

[216.70 ± 6.74%, (p <0.001)] when compared to the control (100%) (Figure 3.27). Treatment with both the low dose [149.00 ± 2.81%, (p < 0.001)] and high dose [212.4 ± 7.52, (p < 0.001)] of DOX for 120 hours also significantly increased ER load. Fluorescence imaging of the ER also indicates an increase in ER fluorescence in a time and dose dependent manner. An increase in ER mass and distribution were visualized in following DOX treatment compared to the normal ER observed in the control (Figure 3.28). Additionally, analysis of ER and DOX colocalization demonstrated that DOX is highly localized to the ER (Figure 3.28), and area of localization continued to significantly increase over time, as the concentration of DOX increased (Figure 3.28 and Figure 3.29).

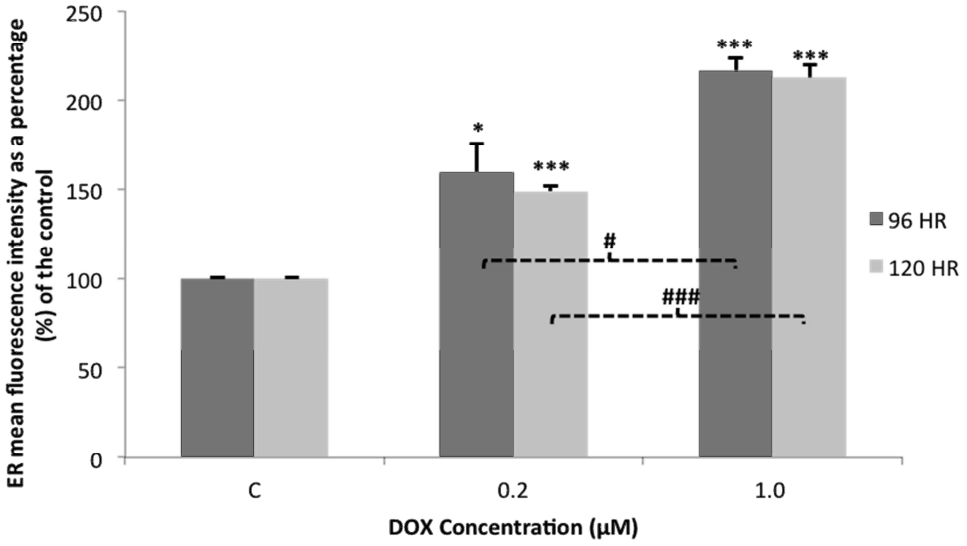

Figure 3.27: The effect of chronic doxorubicin treatment regimes on ER load H9C2 cardiomyoblasts. Cells were treated daily with 0.2 µM and 1.0 µM DOX for 96 and 120 hours. Following treatment cell were stained with ER-tracker and mean fluorescence intensity was measured by flow cytometry (n=3). *P < 0.05 and ***P < 0.001 vs Control. $^{\#}$P < 0.05 and $^{\#\#\#}$P < 0.001 0.2 µM vs 1.0 µM. Abbreviations – C: control, DOX: doxorubicin, ER: endoplasmic reticulum, hr: hour, vs: versus

Stellenbosch University https://scholar.sun.ac.za

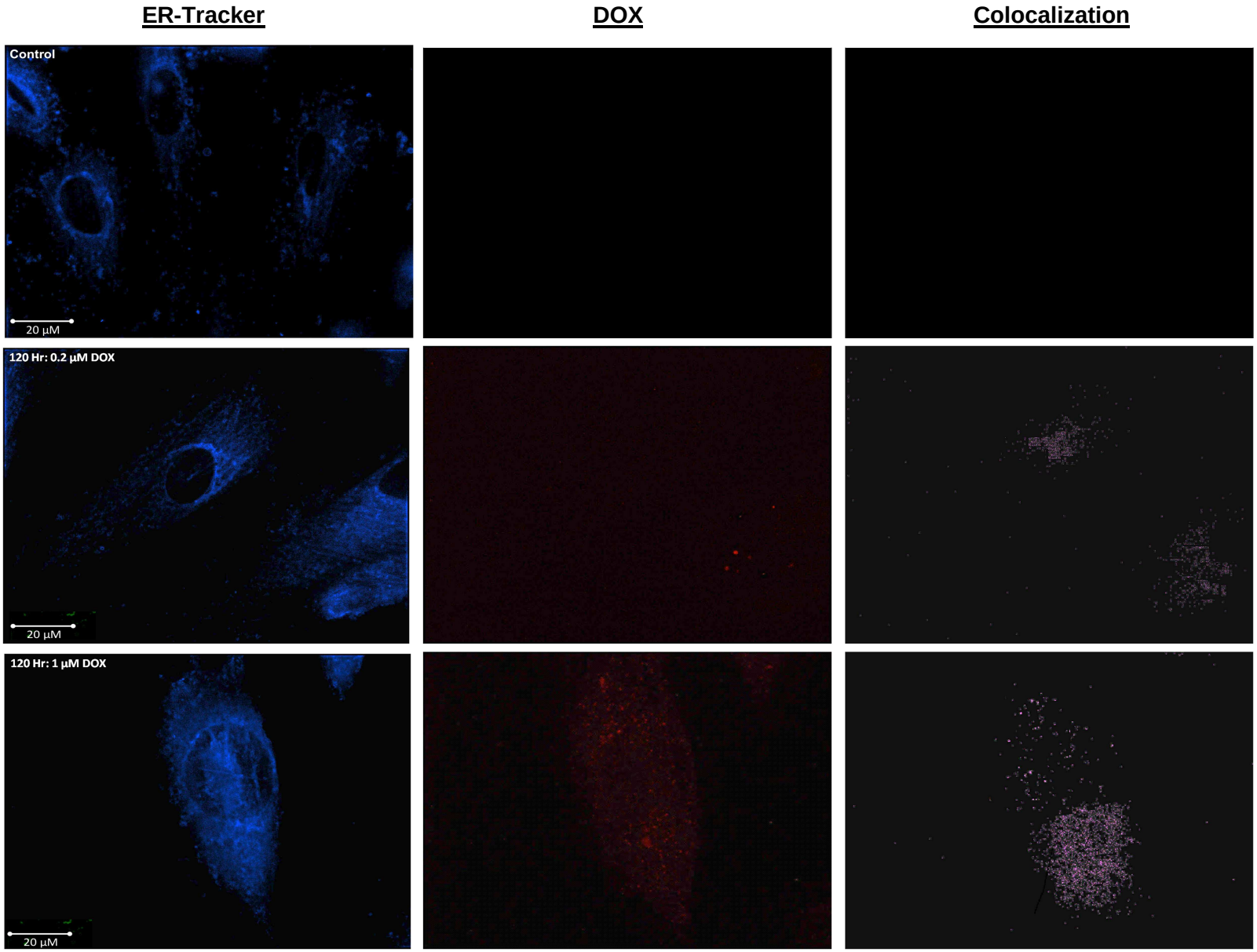

Figure 3.28: The effect of chronic doxorubicin treatment regimes on ER morphology and DOX localization in H9C2 cardiomyoblasts. Cells were treated daily with 0.2 and 1.0 µM DOX for 96 and 120 hours. Only 120 hour represented in image. Following treatment cells were stained ER-tracker blue and visualized using fluorescence microscopy (n=3). Red indicates DOX and purple indicates area of colocalization Abbreviations – DOX; doxorubicin, hr; hour. Magnification = 60X. Scale Bar = 20 µm.

Stellenbosch University https://scholar.sun.ac.za

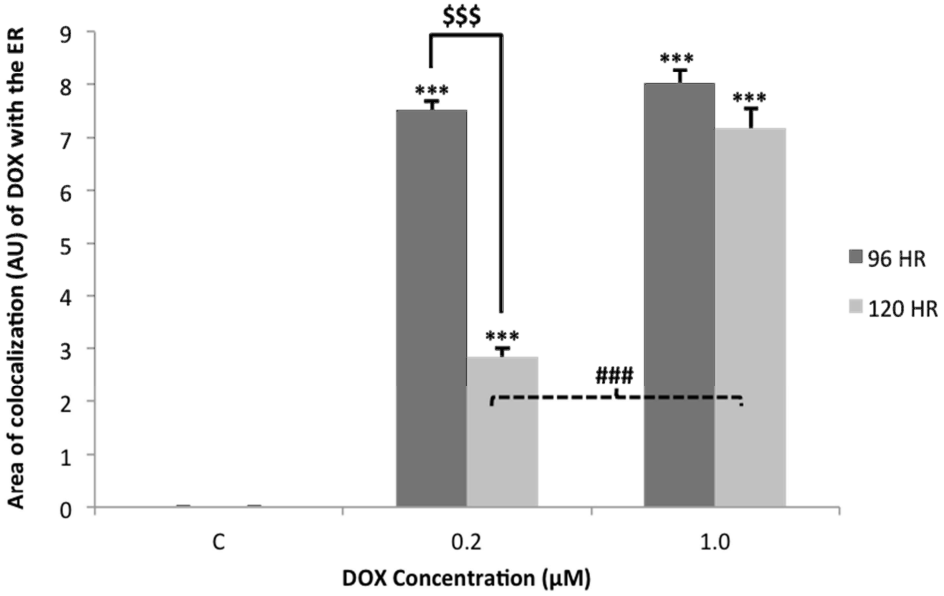

Figure 3.29: Area of Doxorubicin and ER colocalization. H9C2 cardiomyoblasts were treated daily with 0.2 and 1.0 µM DOX for 96 and 120 hours, followed by staining with ER-tracker (blue) and DOX (Red) and visualized with fluorescence microscopy (n=3). Area of colocalization was determined using the Cell^R analysis software. ***P< 0.001 vs. Control. $^{\$\$\$}$P < 0.001 96 hr vs. 120 hr. $^{\#\#\#}$P < 0.001 0.2 µM vs. 1.0 µM. Abbreviations – AU: arbitrary units, C: control, DOX: doxorubicin, hr: hour., vs: versus.

3.9 The Effect of Chronic DOX Treatment Regimes on Intracellular and Mitochondrial Calcium Levels

It has been known for decades that mitochondria and the ER are tightly associated with one another, and both play an important role in maintaining calcium homeostasis (Marchi *et al*., 2014; Grimm, 2012). Calcium is an essential component of the excitation-contraction coupling process, and a disruption of intracellular calcium levels has previously been associated with contractile dysfunction and the pathogenesis of heart failure (Rossini *et al*., 1986). Given the role ER stress, oxidative stress and mitochondrial dysfunction play in disrupting calcium homeostasis this study chose to investigate the effects of chronic DOX cardiotoxicity on calcium activity within the cells.

First, this study established the effects of DOX treatment on intracellular calcium levels located in the cytosol using flow cytometry (Figure 3.30). Results showed that after 96 and

Stellenbosch University https://scholar.sun.ac.za

120 hours, calcium levels were significantly upregulated in both the low [96 hour: 151.50 ± 2.00%, ($p < 0.001$) and 120 hour: 197.70 ± 1.43%, ($p < 0.001$)] and high [96 hour: 197.70 ± 0.50%, ($p<0.001$) and 120 hour: 212 ± 6.20%, ($p < 0.001$)] concentration groups compared to the control group (100%). These results were confirmed with SR-SIM, where little calcium was observed in the control group and an increase in intracellular calcium was visualized in the DOX treated groups (Figure 3.31). Furthermore, significant differences between concentration groups were also observed, indicating that elevated cytosolic calcium is not only highly dependent on duration of DOX treatment, but also on the concentration of DOX administrated.

Since the mitochondria take up calcium when intracellular calcium levels rise in an effort to maintain homeostasis (Hom *et al*., 2007), this study next stained cells with Rhod-2 and assessed mitochondrial-specific calcium with SR-SIM in response to chronic DOX treatment (Figure 3.32). The mitochondrial calcium profile was similar to that of cytosolic, showing a significant increase in calcium levels over time, after treatment with 0.2 μM [96 hour: 34.69 ± 1.44 RFU, ($p < 0.001$) and 120 hour: 49.16 ± 3.10 RFU, ($p < 0.001$)] and 1.0 μM [96 hour: 50.90 ± 7.84 RFU, ($p < 0.001$) and 120 hour: 96.56 ± 6.04 RFU, ($p < 0.001$)] concentrations of DOX compared to the control [11.50 ± 0.49 RFU]. Additional evaluation showed a statistical difference between the treatment groups, suggesting an increase in mitochondrial calcium occurs also in a time- and dose-dependent manner.

Stellenbosch University https://scholar.sun.ac.za

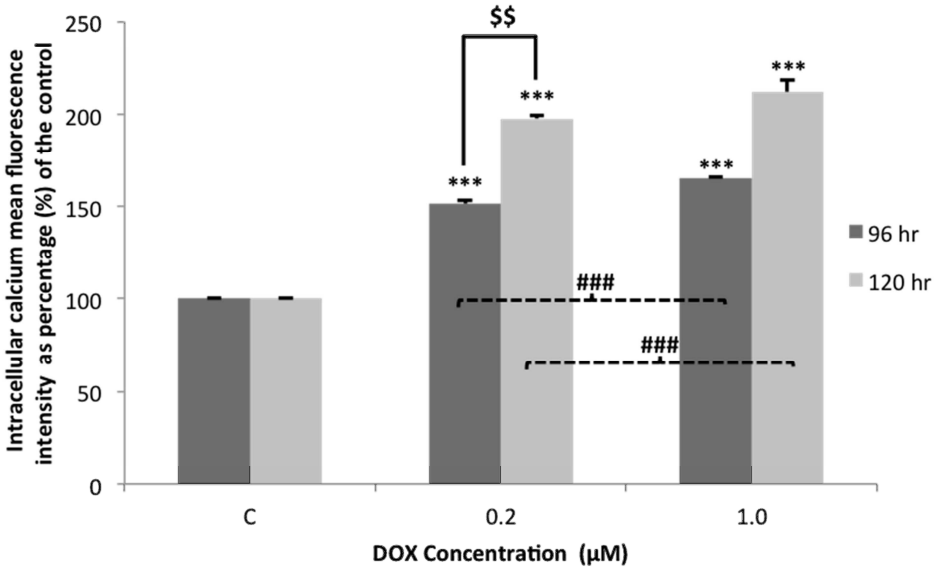

Figure 3.30: The effect of chronic doxorubicin treatment regimes on intracellular calcium in H9C2 cardiomyoblasts. Cells were treated daily with 0.2 µM and 1.0 µM DOX for 96 and 120 hours. Following treatment H9C2 cardiomyoblasts were stained with the specific intracellular calcium dye, Calcium Green and mean fluorescence intensity was measured using flow cytometry (n=3). ***P < 0.001 vs Control. $^{\$\$}$P < 0.01 96 hr vs 120 hr. $^{\#\#\#}$P < 0.001 0.2 µM vs 1.0 µM. Abbreviations – C: control, DOX: doxorubicin, hr: hour.

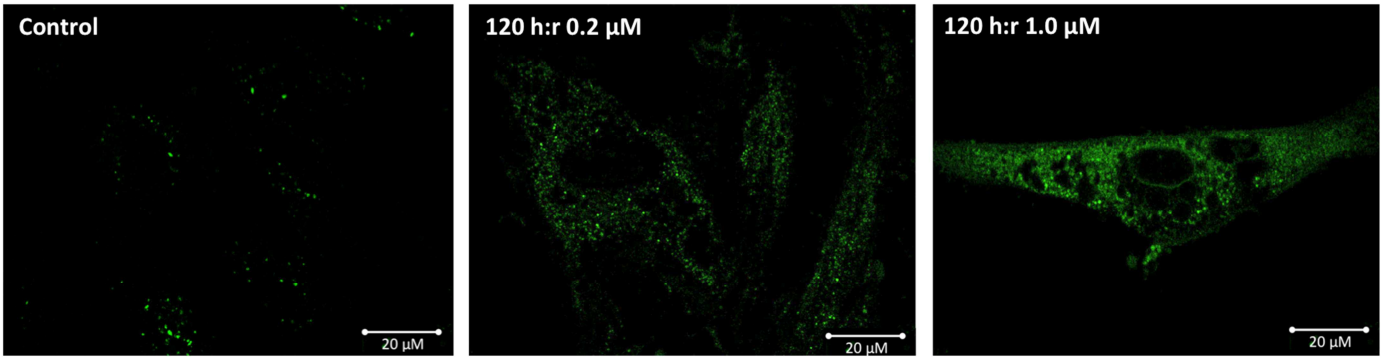

Figure 3.31: Visualization of intracellular calcium following chronic DOX treatment. Cells were treated daily with 0.2 µM and 1.0 µM DOX for 96 and 120 hours. Following treatment H9C2 cardiomyoblasts were stained with the specific intracellular calcium dye, Calcium green and visualized with SR-SIM (n=3). Abbreviations – DOX: Doxorubicin, hr: hour, SR-SIM: Superresolution structured illumination microscopy, vs: versus. Magnification = 60X. Scale bar = 20 µm.

Stellenbosch University https://scholar.sun.ac.za

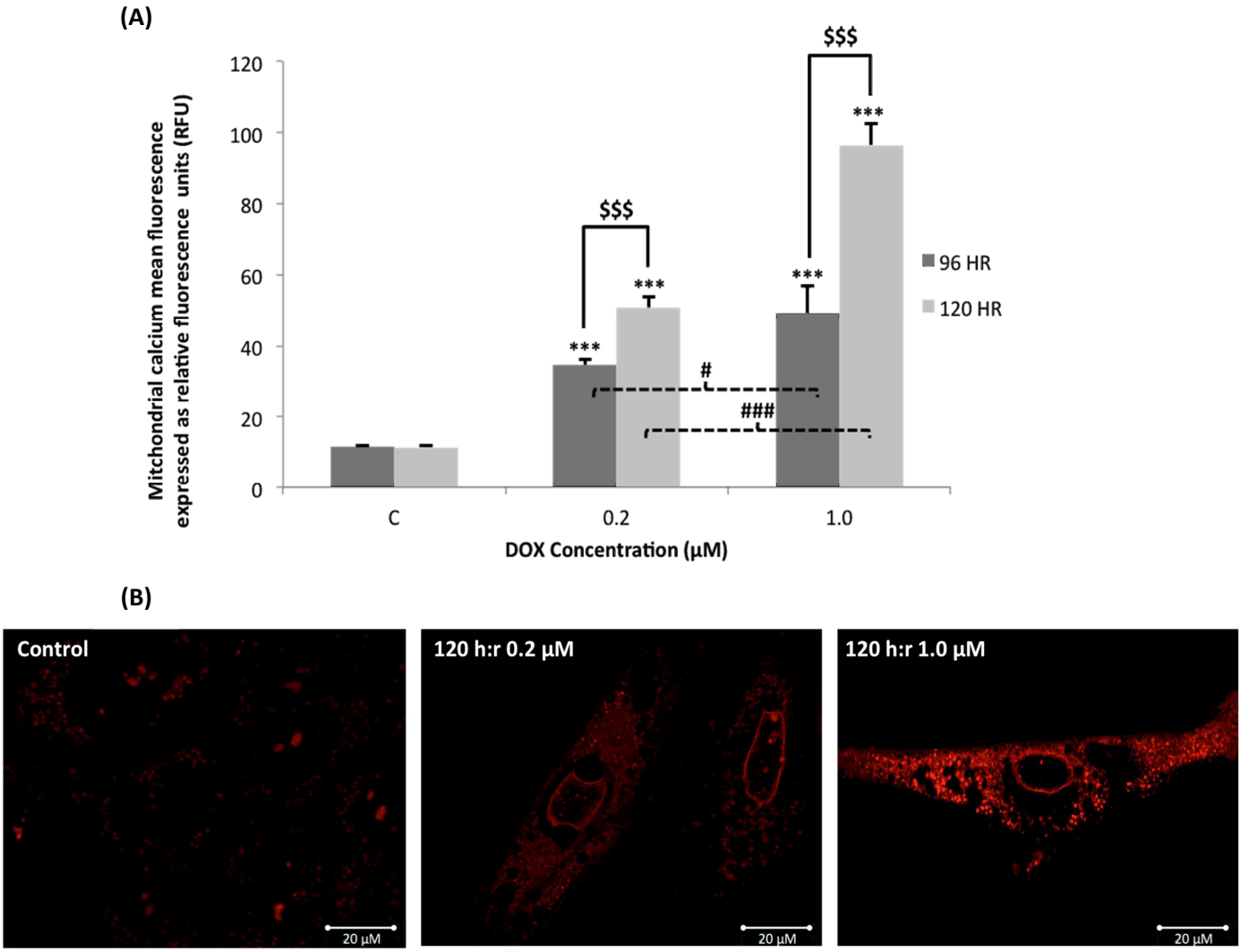

Figure 3.32: The effect of chronic doxorubicin treatment regimes on mitochondrial calcium in H9C2 cardiomyoblasts. Cells were treated daily with 0.2 µM and 1.0 µM DOX for 96 and 120 hours. Following treatment H9C2 cardiomyoblasts were stained with the specific mitochondrial calcium dye, Rhod-2AM and (A) Quantified and (B) Visualized using SR-SIM (n=3). . ***P < 0.001 vs Control. $^{\$\$\$}$P < 0.001 96 hr vs 120 hr. $^{\#}$P < 0.05 and $^{\#\#}$P < 0.01 0.2 µM vs 1.0 µM. Abbreviations - C: control, DOX: Doxorubicin, hr: hour, SR-SIM: Superresolution structured illumination microscopy, vs: versus. Magnification = 60X. Scale bar = 0.2 µm.

Stellenbosch University https://scholar.sun.ac.za

Chapter 4 – Discussion

It has been well established that the clinical utility of DOX is compromised by its induced, cumulative and dose-dependent cardiotoxicity. However, given the fact that DOX remains one of the most effective antineoplastic agents used in oncologic practice today, the search for effective cardioprotective therapies is becoming increasingly relevant. Considering that the mitochondria are the most extensively damaged organelles under conditions of DOX-mediated cardiomyopathy, they have become the main focus of novel therapeutic interventions (Doroshow, 1983; Gharanei *et al*., 2013; Gilliam *et al*., 2013). Although DOX is known to activate the mitochondrial death pathways by initiating apoptosis and necrosis (Berthiaume and Wallace, 2007; Parra *et al*., 2008), it is not understood why the heart's response to progressive mitochondrial dysfunction is limited. Bearing in mind that the myocardium normally has highly effective mitochondrial quality control systems in place regulating mitochondrial turnover (Fischer *et al*., 2012), it is thought that DOX may interfere with the efficiency of these systems (Gharanei *et al*., 2013; Suliman *et al*., 2007). It is in light of these speculations that the aim of this study was to analyze the effects of chronic DOX-induced cardiotoxicity on mitochondrial quality control, with special focus on mitochondrial dynamics and mitochondrial biogenesis. Additionally, since the mitochondria and ER are two interconnected organelles, and both play a role in maintaining calcium homeostasis, this study also assessed the effects of chronic DOX treatment on ER function and calcium status.

Chronic DOX treatment mediates mitochondrial fragmentation through the downregulation of fusion proteins

The tight regulation of mitochondrial dynamics through fission and fusion processes facilitates the maintenance of mitochondrial function, and thus are essential components of mitochondria quality control (Fischer *et al*., 2012; Westermann, 2010). Many studies have demonstrated that changes in mitochondrial morphology, due to an imbalance between the fission and fusion events within the myocardium, mediates the pathophysiology of heart failure (Chen and Chang, 2009; Kuzmicic *et al*., 2011; Marín-García *et al*., 2013; Papanicolaou *et al*., 2012). In addition, literature has indicated that elevated ROS production and oxidative stress, a known side effect of DOX treatment, regulates fission of mitochondria (Dagda *et al*., 2009; Frank *et al*., 2012; Minotti *et al*., 2004). These findings lead to the

Stellenbosch University https://scholar.sun.ac.za

hypothesis that dysregulation of mitochondrial dynamics is associated with DOX-induced cardiotoxicity. This study demonstrated that chronic DOX treatment induces a significant upregulation of DRP1 and hFis1 expression, mediators of mitochondrial fission, in a time- and dose-dependent manner. These results have also been observed in acute studies which may suggest that mitochondrial fission occurs irrespective of the treatment duration, but rather as a recurring effect in response to DOX treatment (Gharanei *et al.*, 2013; Parra *et al*., 2008). Furthermore the upregulation of mitochondrial fission described is consistent with the abnormal mitochondrial morphology observed in this study.

Changes in mitochondrial morphology are regulated by fission and fusion events. Under normal homeostatic conditions, when the balance between mitochondrial dynamics is maintained, the mitochondria display a highly dense and interconnected mitochondrial network. However, dysregulated and unopposed mitochondrial fission results in shortened mitochondria and a dispersed mitochondrial network (Ong *et al*., 2010), which was observed in the DOX-treated groups of this study. The relative increase in fragmented mitochondria observed correlates with the significant elevation of mitochondrial load. Taken together, these findings are in line with previous studies showing that elevated DRP1 and hFis1 activity induces similar morphological changes and fragmentation of mitochondria (Frank *et al.*, 2001). However to further validate the effect of DOX on mitochondrial dynamics, this study additionally investigated the effects of chronic DOX treatment on fusion protein expression.

Outer mitochondrial membrane (OMM) fusion is regulated by two mitofusin proteins, Mfn 1 and Mfn 2. Many studies conducted on Mfn1/2 knockout models have highlighted the importance of these two proteins in maintaining normal mitochondrial morphology and function. Papanicolaou and others (2012) showed that specific double knockout out of both mitofusins in mice resulted in the accumulation of abnormal mitochondria in the myocytes. While Chen and colleagues (2011b) demonstrated that cardiac specific deletion of either Mfn 1 or Mft 2 lead to mitochondrial dysfunction and lethal dilated cardiomyopathy. Therefore, from the above it can be deduced that inhibition of either of these fusion proteins can have detrimental consequences in the myocardium. This study demonstrated a significant downregulation of both Mft 1 and Mft 2, which was observed throughout the duration of treatment with both the low (0.2 μM) and high (1.0 μM) concentration of DOX, thus indicating that chronic DOX treatment inhibits mitochondrial fusion *in vitro*. These results

Stellenbosch University https://scholar.sun.ac.za

suggest that chronic treatment with DOX disrupts the balance between fission and fusion events, resulting in unopposed mitochondrial fragmentation. However, the exact mechanisms involved in DOX-induced mitochondrial fission remains to be fully elucidated. It is thought that DOX may regulate nuclear transcription of pro-fission mediators, such as MARCH5.

Chronic DOX treatment promotes mitochondrial fragmentation and mitophagy via the upregulation of mitochondrial E3 ligases

MARCH5, a mitochondrial E3 ubiquitin ligase, is an important OMM protein required for the maintenance of mitochondrial dynamics (Nagashima *et al*., 2014; Yonashiro *et al*., 2006). Numerous studies have demonstrated MARCH5's role in the regulation of mitochondrial morphology through its ubiquitination of hFis1, Mft 1 and Mft 2 (Karbowski *et al*., 2007; Park *et al*., 2010; Park *et al*., 2014b; Nakamura *et al*., 2006). Additionally, MARCH5 also interacts with DRP1 and is an essential component required for DRP1-mediated mitochondrial fragmentation (Karbowski *et al*., 2007). A recent study by Park and colleagues (2014b) demonstrated that mitochondrial stress induced MARCH5-dependent Mft ubiquitination and degradation, and thereby inhibited mitochondrial fusion in an attempt to maintain homeostasis. Given that the mitochondria are so extensively damaged by DOX, it is thought that MARCH5 may be involved in mediating mitochondrial fission, as indicated in this study. The significant decrease in both Mft1 and Mft2 expression following DOX treatment appears to directly correlate to the significant increase in MARCH5 expression observed in the same treatment groups. This is most likely due to MARCH5's ability to directly bind to the mitofusins and reduce their expression levels through intensive ubiquitination (Park *et al*., 2014b). Furthermore, considering that MARCH5 also tags hFis1 with ubiquitin moieties specific for proteasomal degradation, it is not surprising that no significant increase in hFis1 expression occurred following 96 hours of treatment with 1.0 μM DOX, when MARCH5 was most prevalent. Similar to results observed by Karbowski *et al.* (2006), MARCH5 expression also appeared to correlate to the elevated DRP1 expression. These findings suggest that DOX not only mediates DRP1-dependent fission through upregulation of MARCH5, but also regulates MARCH5-dependent degradation of the mitofusin proteins.

Stellenbosch University https://scholar.sun.ac.za

At the organelle level, the regulation of mitochondrial dynamics is only the first line of defense activated to minimize mitochondrial dysfunction. Additionally, terminally damaged and impaired mitochondria can be selectively degraded by a specific quality control pathway, termed mitophagy (Frank *et al*., 2012; Fischer *et al*., 2012). Parkin is an E3 ubiquitin ligase, which upon translocation from the cytosol to the OMM, initiates mitophagy. There is mounting evidence highlighting a functional link between the regulation of both mitochondrial dynamics and mitophagy (Tanaka *et al*., 2010; Westermann, 2010). This was confirmed by Gegg and colleagues (2011), who recently described that PINK/Parkin-dependent mitophagy regulates mitochondrial dynamics by rapid ubiquitination of Mfn 1 and Mfn 2, which was also indicated in this study. It has been hypothesized that the ubiquitination of the mitofusins helps promote fragmentation of damaged mitochondria for Parkin-mediated mitophagy (Gegg *et al*., 2011; Fischer *et al*., 2012), as does the overexpression of the pro-fission proteins, DRP1 and hFis1 (Gomes and Scorrano, 2008; Kanki *et al.*, 2009). Similarly in this study, elevated expression of DRP1 and hFis1 significantly upregulated Parkin expression following chronic DOX treatment with the lowest concentration of DOX. These levels remained elevated following 96 hours of treatment with 1.0 μM of DOX, however after 120 hours of treatment with the highest concentration of DOX elicited no changes in Parkin activity. This may be brought on by the significant cell death that occurred following the most chronic treatment with DOX, resulting in little or no cells left to degrade. However, a very recent study by Morán and colleagues (2014) observed that under conditions of severe mitochondrial damage and oxidative stress, bulk macroautophagy was upregulated, rather than Parkin-mediated mitophagy, which is also consistent with the findings in this study. Nonetheless, mitophagy is initially upregulated in response to mitochondrial fission in order to assist with the removal of the damaged mitochondria induced by chronic DOX treatment.

Chronic DOX treatment induces protein ubiquitination, but inhibits proteasome function

The UPP is an important proteolytic pathway responsible for the degradation of misfolded protein aggregates, and as such is critical for protein turnover. A recent review by Day (2013) showed that dysfunction of the UPP is fast becoming associated with the pathogenesis of cardiac diseases, including CHF. DOX has previously been shown to disrupt normal UPP activity through the overactivation or inhibition of various components involved in this

Stellenbosch University https://scholar.sun.ac.za

pathway. However, considering that contradictory evidence exists in the literature, the effect of chronic DOX treatment on UPP activity remains to be fully elucidated (Ito *et al*., 2007; Kiyomiya *et al*., 2002; Lui *et al*., 2008). Other than the elevated activity of the two ubiquitin E3 ligases already discussed, K48 ubiquitination was also significantly increased following chronic DOX administration, in a time- and dose- dependent manner. These results are in agreement with other studies who have also reported significant increases in DOX-mediated protein ubiquitination following treatment with the same clinically relevant doses utilized in this study, although different cellular models of DOX-induced cardiotoxicity were employed (Chen *et al*., 2013; Dimitrakis *et al*., 2012; Liu *et al*., 2008; Sishi *et al*., 2013b). Therefore this study confirmed that chronic DOX treatment induces an increase in polyubiquitination and UPP activity.

Results from this study further indicate that over time different types of proteins have been marked for proteasomal degradation. 96 hours of treatment with DOX resulted in proteins with a molecular weight range of ± 50 – 130 kDa being tagged with ubiquitin molecules for proteasomal degradation. After 120 hours however, proteins with a relatively higher molecular weight range (± 100 – 245 kDa) were targeted. Given that the molecular weight of both mitofusin proteins (Mfn 1 and Mfn 2) and the regulator of mitochondrial biogenesis, PGC-1α range between 80 – 130 kDA, and MARCH5 is upregulated, which specifically tags these proteins, it possible that DOX induces K48 ubiquitination and subsequent degradation of these proteins following treatment. However, after 120 hours the ubiquitination of these proteins is decreased, which is most likely due to the significant reduction in their expression at this same time point as well as DOX's inhibition of protein synthesis (Momparler *et al*., 1976). In addition, since the molecular weights of some cardiac myofibrillar proteins, such as myosin and cardiac myosin binding protein-C (cMyBP-C), are known to have very high molecular weight (Fritz *et al*., 1989), the observations discussed above further imply that these proteins are specifically targeted for degradation during chronic treatment with DOX. Although this current study did not investigate the expression of MAFbx (Muscle Atrophy F-box/Antrogin-1) and MuRF1 (Muscle RING Finger-1), the E3 ligases responsible for tagging myofibrillar proteins for degradation, it has been well established in the literature that DOX upregulates the expression of both these proteins (da Silva *et al*., 2012; Ranek and Wang, 2009; Sishi *et al*., 2013b; Yamamoto *et al*., 2008). Ultimately the destruction of these myofibrillar proteins suggests that DOX mediates the development of myocardial remodeling

Stellenbosch University https://scholar.sun.ac.za

and cardiac dysfunction associated with chronic DOX-induced cardiotoxicity by upregulating the components of the UPP.

Evaluation of the 26S proteasome revealed that chronic DOX treatment inhibits the activity of all three catalytic sites throughout duration of the study, with potent inhibition occurring following 1.0 μM DOX treatment. It has previously been shown that DOX binds directly to the proteasome in order to gain access into the nucleus, and as such high concentrations of DOX inhibit proteasomal activity (Kiyomiya *et al*., 1998; Sishi *et al.*, 2013b). Although Liu and others (2008) found that clinically relevant concentrations of DOX (0.1 – 2.5 μM) administrated over shorter, acute time periods elevated 20S core's catalytic activity, this was not the case following this study's longer, chronic treatment times. Therefore clinically relevant concentrations DOX administrated chronically, strongly inhibits proteasomal protein degradation, blocking the flow through the UPP. Although inhibition of the proteasome blocks proteasomal degradation via the UPP, it does not necessarily imply that protein degradation is completely inhibited within the cell. Instead it suggests that the proteins marked for UPP degradation may be degraded by another proteolytic pathway, such as autophagy.

Chronic DOX treatment upregulates autophagy

Autophagy is another proteolytic pathway that is functionally linked to the UPP (Ding *et al*., 2007). Under normal conditions the two pathways are responsible for degrading different types of proteins, however under conditions of cellular stress and UPP inhibition, autophagy has been shown to assist with the clearance and degradation of polyubiquitinated protein aggregates (Wang and Wang, 2014). Additionally, several studies have demonstrated that autophagy is activated as consequence to induced proteasome inhibition and thus aims to compensate for the reduced proteasomal activity (Ding *et al*., 2007; Dong *et al*., 2013; Keller *et al*., 2004; Zheng *et al*., 2011). Recently Kyrychenko and others (2014) showed that inhibition of the caspase-like catalytic activity paired together with an elevation of ER stress, as seen in this study, induced autophagy. Dirks-Naylor (2013) recently reviewed the effect of DOX treatment on regulating autophagy, and showed that DOX has been implicated in increasing and decreasing autophagic activity, depending on the cell model and concentration of DOX used. However it appears that autophagy upregulation is dependent on the

Stellenbosch University https://scholar.sun.ac.za

cumulative concentration of DOX used, rather than the duration of treatment. For example, results from *in vitro* and *in vivo* studies demonstrated that DOX elicited the same effect on autophagy after administration with a single high dose for 24 hours and multiple low doses over two weeks (Smuder *et al*., 2013; Lu *et al*., 2009). This study showed that chronic treatment with DOX induced LC3 lipidation and p62 degradation resulting in a significant increase autophagic activity over time. These results are similar to initial findings by Lu *et al.* (2009), who together with other researchers (Chen *et al*., 2011; Kobayashi *et al.*, 2010; Xu *et al*., 2012), reported that DOX stimulated autophagy both *in vitro* and *in vivo.* Therefore this study confirmed that autophagy is indeed upregulated *in vitro* by chronic DOX administration.

Chronic DOX treatment inhibits mitochondrial biogenesis by downregulating PGC-1α expression

Under conditions of oxidative stress and nutrient deprivation, mitochondrial bioenergetic mechanisms are important for generating new mitochondria and preserving mitochondrial function. Mitochondrial biogenesis is tightly associated with mitophagy since these two processes work together in regulating cellular adaption to stress and maintaining mitochondrial homeostasis. The balanced interplay between these two processes is essential for ensuring the production of healthy mitochondria (Palikaras and Tavernarakis, 2014). Excessive mitophagy, as shown in this study, together with inhibited mitochondrial biogenesis, has previously been shown to impair mitochondrial function and contribute to unsolicited cell death via the activation of apoptosis (Dagda *et al*., 2009; Yan *et al.*, 2012; Zhu *et al*., 2012). Since PGC-1α is a transcriptional co-activator that is essential in orchestrating the activity of various transcription factors associated with mitochondrial proliferation (Dominy *et al*., 2010), it is described as the “master regulator” of mitochondrial biogenesis (Palikaras and Tavernarakis, 2014). It is important to note that the downregulation of PGC-1α is not only associated with the progression of heart failure (Arany *et al*., 2008) but has also previously been shown to be exacerbated by mitochondrial dysfunction (Patten and Arany, 2012), oxidative stress and the loss of mitochondrial membrane potential (Sihag *et al.*, 2009). Since each of these characteristics are mediated by chronic DOX treatment, it is thought that DOX may inhibit PGC-1α expression and mitochondrial biogenesis. This study

Stellenbosch University https://scholar.sun.ac.za

showed that chronic DOX treatment progressively decreased PGC-1α expression throughout the duration of treatment in this *in vitro* model. In light of these results, and also considering that mitophagy and autophagy were significantly upregulated in this study, inhibition of mitochondrial biogenesis is most likely involved in the pathogenesis of chronic DOX-induced cardiotoxicity.

Chronic DOX treatment induces apoptotic toxicity in cardiomyoblasts

Apoptosis of cardiac cells has been defined an essential process in the pathogensis of DOX-induced cardiotoxicity (Lai *et al*., 2010). Similar to findings by Ueno and colleagues (2006), results from this study show that DOX administration induces a significant upregulation in cleaved caspase-3 expression, a popular marker for apoptotic cell death. However, a moderate decline in cleaved caspase-3 was observed following treatment with 1.0 μM of DOX for 120 hours. Considering that at this same time point and concentration cell viability remains significantly reduced compared to the control groups, could suggest that although caspase activity is donwregulated, caspase-independent apoptosis may be involved. p53 is a transcription factor that can activate apoptosis independently of the caspase cascade, via the activation of the pro-apoptotic factors, Bax and endonuclease G (endo G) (Amaral *et al*., 2010; Li *et al*., 2001). Although this study did not investigate p53 activity, it has previously been shown that DOX induces mitochondrial apoptosis in the heart via p53 upregulation (Lai *et al*., 2010; Wang *et al*., 2004). It has been generally accepted that DOX-induced oxidative stress activates apoptotic signaling resulting in consequential cardiomyocyte apoptosis (Nitobe *et al*., 2003; Octavia *et al*., 2012).

Chronic DOX treatment induces oxidative stress

The generation of superoxide from redox cycling of DOX's quinone moiety is known to initiate a series of oxidative chain reactions in the myocardium, which mediates acute and chronic DOX cardiotoxicity (Luo *et al*., 1999; Minotti *et al*., 2004; Xiong *et al*., 2006). DOX-induced ROS production disturbs the myocardiums already low, antioxidant defenses

Stellenbosch University https://scholar.sun.ac.za

resulting in increased lipid peroxidation and compromised enzymatic defenses (Dalloz *et al*., 1999; Kasapović *et al*., 2010; Nowak *et al*., 1995).

DOX also induces the formation of hydrogen peroxide, which can subsequently lead to the formation of hydroxyl radicals. These ROS have been shown to react with lipid, protein and nucleic acids resulting in oxidative damage to the cardiac mitochondria (Minotti *et al*., 1999; Singal *et al*., 2000). Results from this study indicate that chronic DOX treatment induces significant lipid peroxidation, as indicated by elevated MDA levels, corresponding to results reported by Lai *et al* (2010) and Luo *et al* (1999), *in vivo.* It is important to note that while lipid peroxidation is a complex process with a range of products formed in various amounts, the current TBARS method used has been critizied in the literature for its low specificity. Although it is still widely used because of the ease in performing the assay, it is recommended that for future studies high performance liquid chormatography (HPLC) is used to validate the specific MDA-TBA chromagin that is formed using the TBARS technique.

The mitochondria have adaptive responses in place to deal with the increase in ROS production, although these are not sufficient as demonstrated in this study. The ORAC assay utilized in this study demonstrates a significant increase in H9C2's antioxidant capacity, which could be a compensatory mechanism in place to protect the myoblasts against oxidative stress. However, despite this compensatory increase in antioxidant capacity, the GSH assay showed that DOX significantly reduces GSH levels, as represented by the decreased GSH:GSSG ratio. Significantly diminished GSH levels have also been observed in the brains of DOX-treated mice (Cardoso *et al*., 2008; Valko *et al*., 2007). Given that GSH is a crucial intracellular antioxidant and plays an important role in maintaining the redox state of the cells (Cardoso *et al*., 2008), a decrease in GSH can dyregulate GSH turnover and increase oxidative stress (Brechbuhl *et al*., 2012; Estrela *et al*., 2006; Jordan *et al*., 1987). This study confirms the effect of DOX on the generation of oxidative stress in the heart, as shown by the increased MDA levels, lipid peroxidation and inhibition of the important antioxidant, GSH. Oxidative stress not only alters mitochondrial function, but also disrupts ER homeostasis, which can have detrimental effects with the cells (Malhotra and Kaufman, 2007).

Stellenbosch University https://scholar.sun.ac.za

Chronic DOX treatment induces ER stress and activation of the UPR

The ER is responsible for the synthesis and major folding of proteins. However, ER function is highly sensitive to stressors that disrupt calcium homeostasis and alter intracellular oxidative status (Minamino *et al*., 2010), both of which are associated with DOX cardiotoxicity (Octavia *et al*., 2012). Perturbations in ER function result in ER stress, diminished protein folding capacity and subsequent accumulation of misfolded proteins. The UPR is thus activated in response to ER stress in order to clear unfolded/misfolded proteins in an attempt to restore ER homeostasis (Sano and Reed, 2013). Marked increases in BiP expression has been observed in patients with heart failure, suggesting that unresolved ER stress is most likely involved in the pathophysiology of this cardiomyopathy (Dally *et al*., 2009; Minamino *et al*., 2010; Okada *et al*., 2004). Previously research by Lai *et al.* (2010) found that chronic DOX induces an increase in two ER-stress proteins, BiP and CHOP *in vivo*. In relation to these results, this study demonstrated that chronic DOX induces a progressive increase in BiP expression in both a time- and dose-dependent manner, suggesting that DOX induces ER stress and thus possibly contributes to the development cardiotoxicity. BiP is also defined as an ER E3 ubiquitin ligase, which is important in mediating ER-associated degradation (ERAD) of misfolded proteins via the UPP. However, Fu *et al.* (2013) recently demonstrated that upon translocation to the mitochondrial membrane, BiP also plays a role in mediating Parkin-independent mitophagy. BiP promotes mitochondrial fragmentation by targeting the mitofusins for degradation. Therefore, DOX not only appears to mediate mitochondrial fragmentation directly, but its effect on ER could promote fission via a BiP second-messenger system.

The accumulation of unfolded proteins in the ER lumen ruptures BiP's association with the ER stress sensors; PERK, IRE1 and ATF6. Once activated, these three transmembrane proteins initiate a series of downstream signaling cascades that mediate the UPR. The PERK-elF2α-ATF4 axis regulates the transcription of proteins involved in maintaining ER homeostasis. These results show that DOX treatment significantly reduces ATF4 expression in the cardiomyoblasts. Similarly, Kim and co-workers (2005) demonstrated that DOX administration directly downregulated ATF4 transcription in MCF7 human breast carcinoma cells, interfering with the UPR. DOX has previously been shown to directly inhibit specific gene expression in heart cells (Ito *et al*., 1990), and these results confirm that DOX inhibits ATF4 expression. Although this study did not investigate other UPR proteins, there is

Stellenbosch University https://scholar.sun.ac.za

evidence in the literature to suggest that during chronic DOX cardiotoxicity that gene transcription is inhibited

One of the ultrastructural features of DOX-induced chronic cardiotoxicity is sacro/endoplasmic reticulum dilation (Minotti *et al*., 2004). Pronounced ER dilation, also represented as ER load, is another marker for ER stress (Schönthal, 2012). Mammalian and yeast cells have shown to expand their ER volume up to 5-fold under conditions of ER stress and UPR activation (Bernales *et al.,* 2006; Hartley *et al*., 2010; Welihinda *et al*., 1999). Upon visualization, drastic expansion of the ER was noted in the DOX treated groups, which was confirmed with flow cytometry analysis of ER load. These results together with the elevated BiP levels, confirm that chronic DOX induces ER stress and activation of the UPR.

Chronic DOX treatment impairs ER and mitochondrial calcium handling, disrupting calcium homeostasis

It has been well established in the literature that the cross talk between the mitochondria and ER are involved in maintaining calcium homeostasis (Dorn and Maack, 2013; Marchi *et al*., 2014). Considering that the ER is the main source of intracellular calcium, and the mitochondria require calcium in order to modulate various physiological responses, it is essential that the ER-mitochondrial interface be maintained (Brookes *et al*., 2004; Marchi *et al*., 2014). However, under conditions of DOX-induced cardiotoxicity, calcium homeostasis is disrupted (Octavia *et al*., 2012; Saeki *et al*., 2002). In this current study, chronic DOX administration resulted in progressive elevation in both intracellular and mitochondrial calcium over time. Chronic DOX treatment has been known to elicit similar effects on calcium levels in the heart before, however these results were demonstrated *in vivo* (Lebrecht *et al.,* 2010; Saeki *et al.*, 2002). Furthermore, colocalization analysis from this study revealed that DOX has a high affinity with the ER, compared to that of the mitochondria. This is most likely due to DOX interactions with the cardiac ER RyR channels. DOX binds to and prevents closing of the RyR channels and as result, calcium leaks uncontrollably from the ER lumen into the cytosol causing elevated intracellular calcium and ER stress (Pessah *et al*., 1990; Saeki *et al*., 2002). As consequence the mitochondria increase their calcium uptake in an attempt to restore homeostasis, overwhelming the mitochondrial matrix. Excessive calcium within the mitochondria is followed by mitochondrial fragmentation, ROS

Stellenbosch University https://scholar.sun.ac.za

production and apoptosis (Marchi *et al*., 2014; Dorn, 2013; Hom *et al*., 2010). Disruption of calcium signaling within the myocardium can also have serious implications on cardiac contraction considering calcium is a vital component of excitation-contraction coupling (ECC) (Dedkova and Blatter, 2013).

Conclusion

The results from the present study demonstrate that chronic DOX treatment disrupts the balance of mitochondrial dynamics, resulting in unopposed mitochondrial fission and fragmented mitochondrial networks. Since unregulated mitochondrial fission is a hallmark associated with heart failure, these results suggest that DOX mediates mitochondrial dysfunction and cardiotoxicity by stimulating fission. Furthermore this study identified that the observed degradation of the mitochondrial fusion proteins, Mfn 1 and Mfn 2, was mediated by the activation of the mitochondrial E3 ligases, MARCH5 and Parkin. These results, together with the elevated K48-specific ubiquitination, suggest that chronic DOX treatment mediates mitochondrial fission through the UPP. However, DOX inhibited 26S proteasomal activity, proposing that ubiquitin-tagged proteins targeted for proteasomal degradation were redirected and degraded by autophagy, which was significantly upregulated following chronic DOX treatment.

Mitophagy is a select form of mitochondrial autophagy and regulated by Parkin. Therefore the UPP not only plays a role in regulating mitochondrial fission following DOX treatment, but also mitophagy. Mitophagy activation helps maintain a healthy mitochondrial population and as such, is an important component required for mitochondrial QC. However, excessive mitophagy in the absence of mitochondrial biogenesis, which was evident following chronic DOX administration, is known to contribute to mitochondrial dysfunction and cell death, and has also been implicated in the pathogenesis of many cardiovascular diseases (Kubli and Gustafsson, 2012; Marechal *et al*., 2011; Palikaras and Tavernarakis, 2014). Therefore chronic DOX treatment not only mediates mitochondrial fission and mitophagy, it also inhibits mitochondrial biogenesis.

Results from this study further indicate that chronic DOX induces oxidative stress and this condition may have played a critical role in the augmentation of intracellular calcium levels.

Stellenbosch University https://scholar.sun.ac.za

It has been well-established in the literature that the ER is extremely sensitive to changes in redox status and cytosolic calcium dysregulation, and it is therefore not surprising that during chronic DOX treatment ER stress is induced and as a consequence to this, the UPR is activated. Moreover, the elevated cytosolic calcium levels appear to prompt the mitochondria, which are in close proximity to the ER, to take up the excess calcium in an attempt to restore calcium homeostasis. This resulted in a significant increase in mitochondrial calcium, which was observed following treatment. However it has been previously shown that excessive uptake of calcium by mitochondrial disrupts the mitochondrial membrane potential, which triggers mitochondrial fission and apoptosis (Otera and Mikara; 2012; Pletjushkina *et al*., 2006), both of which were increased following treatment.

Although DOX is known to induce oxidative damage within the cells, treatment with antioxidant agents in an attempt to reduce ROS production have been unsuccessful in the clinical setting. This suggests that intervention therapies should focus instead on the molecular and cellular mechanisms which mediate DOX-induced ROS production and mitochondrial damage. For the first time, results from this study demonstrate that the chronic administration of DOX mediates mitochondria fission via the activation of the mitochondrial E3 ligases (MARCH5 and Parkin), and therefore provides fundamental insight into the molecular mechanisms involved in regulating the mitochondrial dysfunction associated with chronic DOX-induced cardiotoxicity. A unifying image of this study's findings is provided in Figure 4.1. Therapeutic agents directed towards inhibiting mitochondrial fission, through the regulation of mitochondrial E3 ligases activity, and restoration to ER function and calcium homeostasis, in an attempt to restore mitochondrial dynamics may provide cardioprotection against chronic DOX-induced cardiotoxicity. These findings warrant further investigations in the relevant animal models before specific intervention therapies can be explored.

Stellenbosch University https://scholar.sun.ac.za

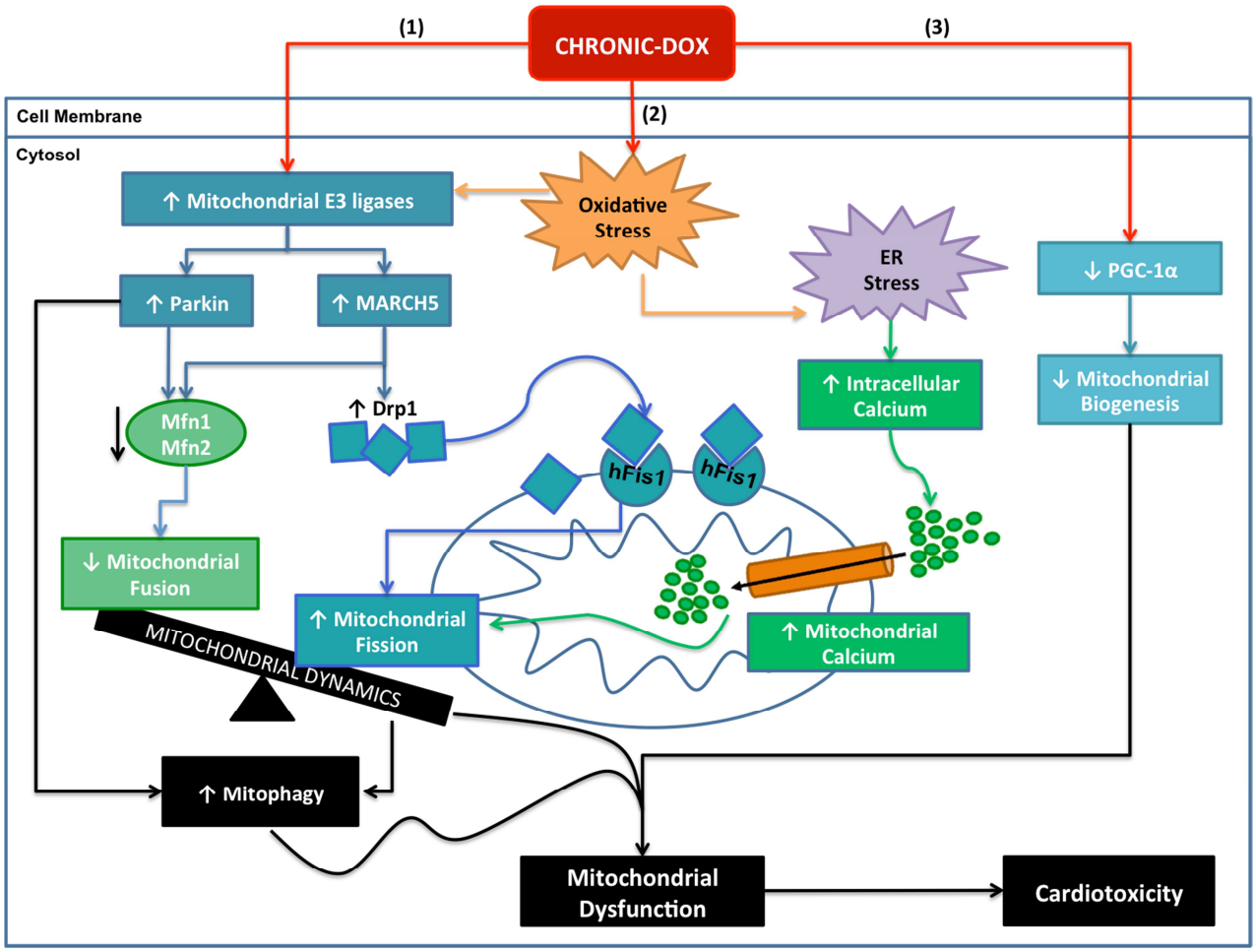

Figure 4.1: A unifying image of the molecular mechanisms involved in regulating mitochondrial dysfunction associated with chronic DOX-induced cardiotoxicity. (1) DOX activates the E3 ligases, Parkin & MARCH5, ultimately disrupting the balance of mitochondrial dynamics, resulting in unopposed mitochondrial fission & mitophagy. (2) DOX-induced oxidative stress triggering ER stress & increases intracellular calcium. Calcium is taken up by the mitochondria, further contributing mitochondrial fission. (3) DOX inhibits PGC-1α expression thereby impairing mitochondrial biogenesis. All these effects cumulate resulting in mitochondrial dysfunction which contributes to the progression of cardiotoxicity. Abbreviations – ↑: Increase, ↓: decrease, DOX: doxorubicin, Drp1: dynamin-related protein 1, E3: ubiquitin ligase protein, ER: endoplasmic reticulum; hFis1: mitochondrial fission protein 1, MARCH5: mitochondrial ubiquitin ligase, Mfn 1/2: mitofusin 1/2 protein, PGC-1α: peroxisome proliferator-activated receptor gamma coactivator 1-alpha

Stellenbosch University https://scholar.sun.ac.za

References

Adams, J. 2003. The proteasome: structure, function, and role in the cell. *Cancer Treatment Reviews*. 29: 3–9.

Ali, M. K., Ewer, M. S., Gibbs, H. R., Swafford, J., & Graff, K. L. 1994. Late doxorubicin-associated cardiotoxicity in children. *Cancer*. 74(1): 182–188.

Amaral, J. D., Zavier, J. M., Steer, C. J., & Rodriques, C. M. 2010. The role of p53 in Apoptosis. *Discovery Medicine.* 9(45): 145-152.

Arai, M., Yoguchi, A., Takizawa, T., Yokoyama, T., Kanda, T., Kurabayashi, M., & Nagai, R. 2000. Mechanism of Doxorubicin-Induced Inhibition of Sarcoplasmic Reticulum Ca2+-ATPase Gene Transcription. *Circulation Research*. 86(1): 8–14.

Arany, Z. 2008. PGC-1 coactivators and skeletal muscle adaptions in health and disease. *Current Opinion in Genetics & Developments.* 8(5): 426-434.

Armstrong, S. C. 2004. Anti-oxidants and apoptosis: attenuation of doxorubicin induced cardiomyopathy by carvedilol. *Journal of Molecular and Cellular Cardiology*. 37(4): 817–821.

Aubel-Sadron, G., & Londos-Gagliardi, D. 1984. Daunorubicin and doxorubicin, anthracycline antibiotics, a physicochemical and biological review. *Biochimie*. 66(5): 333–352.

Asensi, M., Sastre, J., Pallardo, F. V., Lloret, A., Lehner, M., Garcia-de-la Asuncion, J., & Viña, J. 1999. *Oxidants and Antioxidants Part A. Methods in Enzymology*. 299: 267–276.

Avivar-Valderas, A., Salas, E., Bobrovnikova-Marjon, E., Diehl, J. A., Nagi, C., Debnath, J., & Aguirre-Ghiso, J. A. 2011. PERK integrates autophagy and oxidative stress responses to promote survival during extracellular matrix detachment. *Molecular and Cellular Biology*. 31(17): 3616–3629.

Stellenbosch University https://scholar.sun.ac.za

Baker, M. J., Frazier, A. E., Gulbis, J. M., & Ryan, M. T. 2007. Mitochondrial protein-import machinery: correlating structure with function. *Trends in Cell Biology*. 17(9): 456–464.

Baksh, S., & Burakoff, S. J. 2000. The role of calcineurin in lymphocyte activation. *Seminars in Immunology*. 12(4): 405–415.

Barton, J. C., & Bertoli, L. F. 2000. Transfusion iron overload in adults with acute leukemia: manifestations and therapy. *The American Journal of the Medical Sciences*. 319(2): 73–78.

Barrett-Lee, P. J., Dixon, J. M., Farrell, C., Jones, A., Murray, N., Palmieri, C., Pluer, C. J., Stanley, A., & Verrill, M. W. 2009. Expert opinion on the use of anthracyclines in patients with advanced breast cancer at cardiac risk. *Annals of Oncology*. 20: 816-827.

Bayeva, M., Gheorghiade, M., & Ardehali, H. 2013. Mitochondria as a therapeutic target in heart failure. *Journal of the American College of Cardiology*. 61(6): 599–610.

Beau, I., Esclatine, A., & Codogno, P. 2008. Lost to translation: when autophagy targets mature ribosomes. *Trends in Cell Biology*. 18(7): 311–314.

Benbrook, D. M., & Long, A. 2012. Integration of autophagy, proteasomal degradation, unfolded protein response and apoptosis. *Experimental Oncology*. 34(3): 286–297.

Berman, H. M., & Young, P. R. 1981. The interaction of intercalating drugs with nucleic acids.

Bernaba, B. N., Chan, J. B., Lai, C. K., & Fishbein, M. C. 2010. Pathology of late-onset anthracycline cardiomyopathy. *Cardiovascular Pathology : The Official Journal of the Society for Cardiovascular Pathology*. 19(5): 308–311.

Bernales, S., McDonald, K. L., & Walter, P. 2006. Autophagy counterbalances endoplasmic reticulum expansion during the unfolded protein response. *PLoS Biology*. 4(12): e423.

Berridge, M. V, Herst, P. M., & Tan, A. S. 2005. Tetrazolium dyes as tools in cell biology: new insights into their cellular reduction. *Biotechnology Annual Review*. 11(5): 127–152.

Stellenbosch University https://scholar.sun.ac.za

Berthiaume, J. M., & Wallace, K. B. 2007. Adriamycin-induced oxidative mitochondrial cardiotoxicity. *Cell Biology and Toxicology*. 23(1): 15–25.

Bertolotti, A., Zhang, Y., Hendershot, L. M., Harding, H. P., & Ron, D. 2000. Dynamic interaction of BiP and ER stress transducers in the unfolded-protein response. *Nature Cell Biology*. 2(6): 326–332.

Biosiva. 2014. *Topoisomerase I and II.* Available from: <http://biosiva.50webs.org/rep2.24.gif>. [June 2014].

Bjelogrlic, S. K., Radic, J., Jovic, V., & Radulovic, S. 2005. Activity of d,l-alpha-tocopherol (vitamin E) against cardiotoxicity induced by doxorubicin and doxorubicin with cyclophosphamide in mice. *Basic & Clinical Pharmacology & Toxicology*. 97(5): 311–319.

Bjørkøy, G., Lamark, T., Pankiv, S., Øvervatn, A., Brech, A., & Johansen, T. 2009. Monitoring autophagic degradation of p62/SQSTM1. *Methods in Enzymology*. 452: 181–197.

Boucek R. J. 1997a. Contractile Failure in Chronic Doxorubicin-induced Cardiomyopathy. *Journal of Molecular and Cellular Cardiology*. 29(10): 2631–2640.

Boucek, R. J. 1997b. Mechanisms for anthracycline-induced cardiomyopathy: clinical and laboratory correlations. *Progress in Pediatric Cardiology*. 8(2): 59–70.

Boucek, R. J., Miracle, A., Anderson, M., Engelman, R., Atkinson, J., & Dodd, D. A. 1999. Persistent effects of doxorubicin on cardiac gene expression. *Journal of Molecular and Cellular Cardiology*. 31(8): 1435–46.

Boucek, R. J., Olson, R. D., Brenner, D. E., Ogunbunmi, E. M., Inui, M., & Fleischer, S. 1987. The major metabolite of doxorubicin is a potent inhibitor of membrane-associated ion pumps. A correlative study of cardiac muscle with isolated membrane fractions. *The Journal of Biological Chemistry*. 262(33): 15851–15856.

Bouitbir, J., Charles, A.-L., Echaniz-Laguna, A., Kindo, M., Daussin, F., Auwerx, J., Piquard, F., Geny, B., & Zoll, J. 2012. Opposite effects of statins on mitochondria of

Stellenbosch University https://scholar.sun.ac.za

cardiac and skeletal muscles: a “mitohormesis” mechanism involving reactive oxygen species and PGC-1. *European Heart Journal*. 33(11): 1397–407.

Bray, F., Jemal, A., Grey, N., Ferlay, J., & Forman, D. 2012. Global cancer transitions according to the Human Development Index (2008-2030): a population-based study. *The Lancet Oncology*. 13(8): 790–801.

Brechbuhl, H. M., Kachadourian, R., Min, E., Chan, D., & Day, B. J. 2012. Chrysin enhances doxorubicin-induced cytotoxicity in human lung epithelial cancer cell lines: the role of glutathione. *Toxicology and Applied Pharmacology*. 258(1): 1–9.

Breed, J. G., Zimmerman, A. N., Dormans, J. A., & Pinedo, H. M. 1980. Failure of the antioxidant vitamin E to protect against adriamycin-induced cardiotoxicity in the rabbit. *Cancer Research*. 40(6): 2033–2038.

Bristow, M. R. 1982. Toxic cardiomyopathy due to doxorubicin. *Hospital Practice (Office Ed.)*. 17(12): 101–108, 110–111.

Brookes, P. S., Parker, N., Buckingham, J. A., Vidal-Puig, A., Halestrap, A. P., Gunter, T. E., Nicholls, D. G., Bernardi, P., Lemasters, J. J., & Brand, M. D. 2008. UCPs--unlikely calcium porters. *Nature Cell Biology*. 10(11): 1235–1237.

Brookes, P. S., Yoon, Y., Robotham, J. L., Anders, M. W., & Sheu, S.-S. 2004. Calcium, ATP, and ROS: a mitochondrial love-hate triangle. *American Journal of Physiology. Cell Physiology*. 287(4): C817–C833.

Bruynzeel, A. M. E. 2007a. *Clinical and pre-clinical aspects of monoHER in combination with Doxorubicin*. Published PhD Thesis. VU University of Amsterdam.

Bruynzeel, A. M. E., Niessen, H. W. M., Bronzwaer, J. G. F., van der Hoeven, J. J. M., Berkhof, J., Bast, A., van der Vijgh, W. J., & van Groeningen, C. J. 2007b. The effect of monohydroxyethylrutoside on doxorubicin-induced cardiotoxicity in patients treated for metastatic cancer in a phase II study. *British Journal of Cancer*. 97(8): 1084–1089.

Burgess, D. J., Doles, J., Zender, L., Xue, W., Ma, B., McCombie, W. R., Hannon, G. J., Lowe, S. W., & Hemann, M. T. 2008. Topoisomerase levels determine chemotherapy

Stellenbosch University https://scholar.sun.ac.za

response in vitro and in vivo. *Proceedings of the National Academy of Sciences of the United States of America*. 105(26): 9053–9058.

Buss, J. L., & Hasinoff, B. B. 1995. Ferrous ion strongly promotes the ring opening of the hydrolysis intermediates of the antioxidant cardioprotective agent dexrazoxane (ICRF-187). *Archives of Biochemistry and Biophysics*. 317(1): 121–127.

Buzdar, A A., Marcus, C., Smith, T. L., & Biumenschein, G. R. 1985. Early and delayed clinical cardiotoxicity of doxorubicin. *Cancer*. 55(12): 2761-2765

Camello-Almaraz, C., Gomez-Pinilla, P. J., Pozo, M. J., & Camello, P. J. 2006. Mitochondrial reactive oxygen species and Ca2+ signaling. *American Journal of Physiology. Cell Physiology*. 291(5): C1082–C1088.

Campello, S., Strappazzon, F., & Cecconi, F. 2014. Mitochondrial dismissal in mammals, from protein degradation to mitophagy. *Biochimica et Biophysica Acta*. 1837(4): 451–460.

Campos, E. C., O'Connell, J. L., Malvestio, L. M., Romano, M. M. D., Ramos, S. G., Celes, M. R. N., Prado, C. M., Simões, M. V., & Rossi, M. A. 2011. Calpain-mediated dystrophin disruption may be a potential structural culprit behind chronic doxorubicin-induced cardiomyopathy. *European Journal of Pharmacology*. 670(2-3): 541–53.

Carafoli, E. 1985. The homeostasis of calcium in heart cells. *Journal of Molecular and Cellular Cardiology*. 17(3): 203–212.

Cardoso, S., Santos, R. X., Carvalho, C., Correia, S., Pereira, G. C., Pereira, S. S., Oliveira, P. J., Santos, M.S., Proença, T., Moreira, P. I. 2008. Doxorubicin increases the susceptibility of brain mitochondria to Ca(2+)-induced permeability transition and oxidative damage. *Free Radical Biology & Medicine*. 45(10): 1395–1402.

Caroni, P., Villani, F., & Carafoli, E. 1981. The cardiotoxic antibiotic doxorubicin inhibits the Na+/Ca2+ exchange of dog heart sarcolemmal vesicles. *FEBS Letters*. 130(2): 184–186.

Stellenbosch University https://scholar.sun.ac.za

Carpenter, A. J., & Porter, A. C. G. 2004. Construction, characterization, and complementation of a conditional-lethal DNA topoisomerase IIalpha mutant human cell line. *Molecular Biology of the Cell*. 15(12): 5700–5711.

Carroll, R., & Yellon, D. M. 2000. Delayed cardioprotection in a human cardiomyocyte-derived cell line: the role of adenosine, p38MAP kinase and mitochondrial KATP. *Basic Research in Cardiology*. 95(3): 243–249.

Chaires, J. B., Fox, K. R., Herrera, J. E., Britt, M., & Waring, M. J. 1987. Site and sequence specificity of the daunomycin-DNA interaction. *Biochemistry*. 26(25): 8227–8236.

Chami, M., Oulès, B., Szabadkai, G., Tacine, R., Rizzuto, R., & Paterlini-Bréchot, P. 2008. Role of SERCA1 truncated isoform in the proapoptotic calcium transfer from ER to mitochondria during ER stress. *Molecular Cell*. 32(5): 641–51.

Chatterjee, K., Zhang, J., Honbo, N., & Karliner, J. S. 2010. Doxorubicin cardiomyopathy. *Cardiology*. 115(2): 155–62.

Chen, H., & Chang, D. C. 2009. Mitochondrial dynamics-fusion, fission, movement, and mitophagy-in neurodegenerative disease. *Human Molecular Genetics.* 18(R2): R169-R176.

Chen, H., Detmer, S. A., Ewald, A. J., Griffin, E. E., Fraser, S. E., & Chan, D. C. 2003. Mitofusins Mfn1 and Mfn2 coordinately regulate mitochondrial fusion and are essential for embryonic development. *The Journal of Cell Biology*. 160(2):189–200.

Chen, K. S., Gresh, N., & Pullman, B. 1986. A theoretical investigation on the sequence selective binding of adriamycin to double-stranded polynucleotides. *Nucleic Acids Research*. 14(5): 2251–2267.

Chen, K., Xu, X., Kobayashi, S., Timm, D., Jepperson, T., & Liang, Q. 2011a. Caloric restriction mimetic 2-deoxyglucose antagonizes doxorubicin-induced cardiomyocyte death by multiple mechanisms. *The Journal of Biological Chemistry*. 286(25): 21993–2006.

Stellenbosch University https://scholar.sun.ac.za

Chen, Y., Liu, Y., & Dorn, G. W. 2011b. Mitochondrial fusion is essential for organelle function and cardiac homeostasis. *Circulation Research*. 109(12): 1327–31.

Chen, Z., Zhong, Y., Wang, Y., Xu, S., Liu, Z., Baskakov, I. V., Monteiro, M. J, Karbowski, M., Shen, Y., & Fang, S. 2013. Ubiquitination-induced fluorescence complementation (UiFC) for detection of K48 ubiquitin chains in vitro and in live cells. *PloS One*. 8(9): e73482.

Childs, A. C., Phaneuf, S. L., Dirks, A. J., Phillips, T., & Leeuwenburgh, C. 2002. Doxorubicin Treatment in Vivo Causes Cytochrome c Release and Cardiomyocyte Apoptosis, As Well As Increased Mitochondrial Efficiency, Superoxide Dismutase Activity, and Bcl-2:Bax Ratio. *Cancer Research*. 62(16): 4592–4598.

Chondrogianni, N., Petropoulos, I., Grimm, S., Georgila, K., Catalgol, B., Friguet, B., Grune, T., & Gonos, E. S. 2012. Protein damage, repair and proteolysis. *Molecular aspects of Medicine*. 35: 1-71.

Coldwell, K. E., Cutts, S. M., Ognibene, T. J., Henderson, P. T., & Phillips, D. R. 2008. Detection of Adriamycin-DNA adducts by accelerator mass spectrometry at clinically relevant Adriamycin concentrations. *Nucleic Acids Research*. 36(16): e100.

Crompton, M. 1999. The mitochondrial permeability transition pore and its role in cell death. *The Biochemical Journal*. 341: 233–249.

Dagda, R. K., Cherra, S., Kulich, S. M., Tandon, A., Park, D., & Chu, C. T. 2009. Loss of PINK1 function promotes mitophagy through effects on oxidative stress and mitochondrial fission. *The Journal of Biological Chemistry*. 284(20): 13843-13855.

Da Silva, M. G., Mattos, E., Camacho-Pereira, J., Domitrovic, T., Galina, A., Costa, M. W., & Kurtenbach, E. 2012. Cardiac systolic dysfunction in doxorubicin-challenged rats is associated with upregulation of MuRF2 and MuRF3 E3 ligases. *Experimental and Clinical Cardiology*, 17(3): 101–109.

Dalloz, F., Maingon, P., Cottin, Y., Briot, F., Horiot, J.-C., & Rochette, L. 1999. Effects of combined irradiation and doxorubicin treatment on cardiac function and antioxidant defenses in the rat. *Free Radical Biology and Medicine*. 26(7-8): 785–800.

Stellenbosch University https://scholar.sun.ac.za

Dally, S., Monceau, V., Corvazier, E., Bredoux, R., Raies, A., Bobe, R., de Monte, F., & Enouf, J. 2009. Compartmentalized expression of three novel sarco/endoplasmic reticulum Ca2+ATPase 3 isoforms including the switch to ER stress, SERCA3f, in non-failing and failing human heart. *Cell Calcium*. 45(2): 144–154.

Danialou, G., Comtois, A. S., Dudley, R., Karpati, G., Vincent, G., Des Rosiers, C., & Petrof, B. J. 2001. Dystrophin-deficient cardiomyocytes are abnormally vulnerable to mechanical stress-induced contractile failure and injury. *FASEB Journal : Official Publication of the Federation of American Societies for Experimental Biology*. 15(9): 1655–1657.

Daum, G. 1985. Lipids of mitochondria. *Biochimica et Biophysica Acta*. 822(1): 1–42.

Davies, K. J., & Doroshow, J. H. 1986. Redox cycline of anthracyclines by cardiac mitochondrial I. Anthracycline radical formation b NADH dehydrogenase. *The Journal of Biological Chemistry*. 261(7): 3060-3067.

Day, S. M. 2013. The ubiquitin proteasome system in human cardiomyopathies and heart failure. *American Journal of Physiology Heart and Circulatory Physiology*. 304(10): H1283-H1293.

De Beer, E. L., Bottone, A. E., & Voest, E. E. 2001. Doxorubicin and mechanical performance of cardiac trabecular after acute and chronic treatment: a review. *European Journal of Pharmacology*. 415(1): 1–11.

Dedkova, E. N., & Blatter, L. A. 2013. Calcium signaling in cardiac mitochondria. *Journal of Molecular and Cellular Cardiology*, *58*, 125–33. doi:10.1016/j.yjmcc.2012.12.021

Deniaud, A., Sharaf el dein, O., Maillier, E., Poncet, D., Kroemer, G., Lemaire, C., & Brenner, C. 2008. Endoplasmic reticulum stress induces calcium-dependent permeability transition, mitochondrial outer membrane permeabilization and apoptosis. *Oncogene*. 27(3): 285–299.

Denny, W. A. 2002. Acridine derivatives as chemotherapeutic agents. *Current Medicinal Chemistry*. 9(18): 1655–1665.

Stellenbosch University https://scholar.sun.ac.za

Devasagayam, T. P. A., Boloor, K. K., & Ramasarma, T. 2003. Methods for estimating lipid peroxidation : An analysis of merits and demerits. 40: 300–308.

DeVita, V. T., & Chu, E. 2008. A history of cancer chemotherapy. *Cancer Research*. 68(21): 8643–8653.

Dhalla, N. S., Temsah, R. M., & Netticadan, T. 2000. Role of oxidative stress in cardiovascular diseases. *Journal of Hypertension*. 18(6): 655–673.

Dimmer, K. S., & Scorrano, L. 2006. (De)constructing mitochondria: what for? *Physiology*. 4: 233–421.

Dirks-Naylor, A. J. 2013. The role of autophagy in doxorubicin-induced cardiotoxicity. *Life Sciences*. 93(24): 913-916.

Dirks-Naylor, A. J., Kouzi, S. A., Bero, J. D., Phan, D. T., Taylor, H. N., Whitt, S. D., & Mabolo, R. 2014a. Doxorubicin alters the mitochondrial dynamics machinery and mitophagy in the liver of treated animals. *Fundamental & Clinical Pharmacology*.

Dirks-Naylor, A., Yang, S., & Kouzi, S. 2014b. The effects of doxorubicin on the mitochondrial dynamics and mitophagy machinery in varying types of skeletal muscles (1164.1). *The Journal of the Federation of American Societies for Experimental Biology*.

Dodd, D. A., Atkinson, J. B., Olson, R. D., Buck, S., Cusack, B. J., Fleischer, S., & Boucek, R. J. 1993. Doxorubicin cardiomyopathy is associated with a decrease in calcium release channel of the sarcoplasmic reticulum in a chronic rabbit model. *The Journal of Clinical Investigation*. 91(4): 1697–1705.

Dominy, J. E., Lee, Y., Gerhart-Hines, Z., & Puigserver, P. 2010. Nutrient-dependents regulation of PGC-1alpha's acetylation and metabolic function through the enzymatic activities of Sirt1/GCN5. *Biochemica et Biophysica acta*. 1804(8): 1676-1683.

Dong, S., Jia, C., Fan, G., Li, Y., Shan, P., Sun, L., Xiao, W., Li, L., Wei, H., Hu, C., Zhang, W., Chin, Y. E., Zhai, Q., Li, Q., Jia, F., Mo, Q., Edwards, D. P., Huang, S., Chan, L.,

Stellenbosch University https://scholar.sun.ac.za

O'Malley, B. W., Li, X., & Wang, C. 2012. The REGγ proteasome regulation hepatic lipid metabolism through the inhibition of autophagy. *Cell Metabolism.* 8(12): 380-391.

Dorn, G. W. 2013. Mitochondrial dynamics in heart disease. *Biochimica et Biophysica Acta*, 1833(1): 233–241.

Dorn, G. W., & Maack, C. 2013. SR and mitochondria: calcium cross talk between kissing cousins. *Journal of Molecular and Cellular Cardiology*

Doroshow, J. H. 1983. Effect of anthracycline antibiotics on oxygen radical formation in rat heart. *Cancer Research*. 43(2): 460–472.

Doroshow, J. H., Locker, G. Y., & Myers, C. E. 1980. Enzymatic defenses of the mouse heart against reactive oxygen metabolites: alterations produced by doxorubicin. *The Journal of Clinical Investigation*. 65(1): 128–135.

Doroudgar, S., & Glembotski, C. C. 2013. New concepts of endoplasmic reticulum function in the heart: programmed to conserve. *Journal of Molecular and Cellular Cardiology*. 55: 85–91.

Doyle, J. J., Neugut, A. I., Jacobson, J. S., Grann, V. R., & Hershman, D. L. 2005. Chemotherapy and cardiotoxicity in older breast cancer patients: a population-based study. *Journal of Clinical Oncology : Official Journal of the American Society of Clinical Oncology*. 23(34): 8597–8605.

Dresdale, A. R., Barr, L. H., Bonow, R. O., Mathisen, D. J., Myers, C. E., Schwartz, D. E., d'Angelo, T., & Rosenberg, S. A. 1982. Prospective randomized study of the role of N-acetyl cysteine in reversing doxorubicin-induced cardiomyopathy. *American Journal of Clinical Oncology*. 5(6): 657–663.

Duchen, M. R. 2000. Mitochondria and calcium: from cell signaling to cell death. *The Journal of Physiology*. 529(1): 57–68.

Dunn, W. A., Cregg, J. M., Kiel, J. A. K. W., van der Klei, I. J., Oku, M., Sakai, Y., Sibirny, A. A., Stasyk, O.K., Veenhuis, M. 2005. Pexophagy: the selective autophagy of peroxisomes. *Autophagy*. 1(2): 75–83.

Stellenbosch University https://scholar.sun.ac.za

Dutta, S. 1981. Cardiac Uptake and Binding of Cardiac Glycosides. In K. Greeff (Ed.). *Cardiac Glycosides SE,* Springer Berlin Heidelberg. pp. 141-168.

Enari, M., Sakahira, H., Yokoyama, H., Okawa, K., Iwamatsu, A., & Nagata, S. 1998. A caspase-activated DNase that degrades DNA during apoptosis, and its inhibitor ICAD. *Nature*. 391(6662): 43–50.

Estrela, J. M., Ortega, A., & Obrador, E. 2006. Glutathione in cancer biology and therapy. *Critical Reviews in Clinical Laboratory Sciences*. 43(2): 143–81.

Faerber, G., Barreto-Perreia, F., Schoepe, M., Gilsbach, R., Schrepper, A., Schwarzer, M., Mohr, F. W., Hein, L., & Doenst, T. 2011. Induction of heart failure by minimally invasive aortic constriction in mice: reduced peroxisome proliferator-activated receptor γ coactivator levels and mitochondrial dysfunction. *The Journal of Thoracic and Cardiovascular Surgery*. 141(2): 492–500.

Fill, M., & Copello, J. A. 2002. Ryanodine receptor calcium release channels. *Physiological Reviews*. 82(4): 893–922.

Fischer, F., Hamann, A., & Osiewacz, H. D. 2012. Mitochondrial quality control: an integrated network of pathways. *Trends in Biochemical Sciences*. 37(7): 284–292.

François, R. J., & Gerald, I. S. 2010. Regulation of mitochondrial biogenesis. *Essays in Biochemistry*. 47: 69-84.

Frank, M., Duvezin-Caubet, S., Koob, S., Occhipinti, A., Jagasia, R., Petcherski, A., Ruanala, O. M., Priault, M., Salin, B., & Reichert, A. S. 2012. Mitophagy is triggered by mild oxidative stress in a mitochondrial fission dependent manner. *Biochimica et Biophysica Acta*. 1823(12): 2297–310.

Frank, S., Gaume, B., Bergmann_Leitner, E. S., Leitner, W. W., Robert, E. G., Catez, F., Smith, C. L., & Youle, R. 2001. The role of dynamin-related protein 1, a mediator of mitochondrial fission, in apoptosis. *Developmental Cell*. 1(4): 515-525.

Stellenbosch University https://scholar.sun.ac.za

Fritz, J. D., Swartz, D. R., & Greaser, M. L. 1989. Factors affecting polyacrylamide gel electrophoresis and electroblotting of high-molecular-weight myofibrillar proteins. *Analytical Biochemistry*. 180(2): 205–210.

Fu, M., St-Pierre, P., Shankar, J., Wang, P. T. C., Joshi, B., & Nabi, I. R. 2013. Regulation of mitophagy my the Gp78 E3 ubiquitin ligase. *Molecular Biology of the Cell.* 24(8): 1153-1162.

Galloway, C. A., Lee, H., Nejjar, S., Jhun, B. S., Yu, T., Hsu, W., & Yoon, Y. 2012a. Transgenic control of mitochondrial fission induces mitochondrial uncoupling and relieves diabetic oxidative stress. *Diabetes*. 61(8): 2093–2104.

Galloway, C. A., Lee, H., & Yoon, Y. 2012b. Mitochondrial morphology-emerging role in bioenergetics. *Free Radical Biology & Medicine*. 53(12): 2218–2228.

Garnier, A., Fortin, D., Deloménie, C., Momken, I., Veksler, V., & Ventura-Clapier, R. 2003. Depressed mitochondrial transcription factors and oxidative capacity in rat failing cardiac and skeletal muscles. *The Journal of Physiology*. 551: 491–501.

Gegg, M. E., & Schapira, A. H. V. 2011. PINK1-parkin-dependent mitophagy involves ubiquitination of mitofusins 1 and 2: Implications for Parkinson disease pathogenesis. *Autophagy*. 7(2): 243–245.

Geisler, S., Holmström, K. M., Skujat, D., Fiesel, F. C., Rothfuss, O. C., Kahle, P. J., & Springer, W. 2010. PINK1/Parkin-mediated mitophagy is dependent on VDAC1 and p62/SQSTM1. *Nature Cell Biology*. 12(2): 119–31.

Gem Pharmaceuticals. 2014. *Proprietary technology platform.* Available from: <http://www.gempharmaceuticals.com/proprietary-technology-platform.shtml>. [June 2014].

Gharanei, M., Hussain, A., Janneh, O., & Maddock, H. 2013. Attenuation of doxorubicin-induced cardiotoxicity by mdivi-1: a mitochondrial division/mitophagy inhibitor. *PloS One*. 8(10): e77713.

Stellenbosch University https://scholar.sun.ac.za

Gharanei, M., Hussain, A., Janneh, O., & Maddock, H. L. 2014. 15 Mitochondrial Division Inhibitor-1 Protects against Doxorubicin-Induced Cardiotoxicity. *Heart*. 100: A6–A6.

Gille, L., & Nohl, H. 1997. Analyses of the Molecular Mechanism of Adriamycin-Induced Cardiotoxicity. *Free Radical Biology and Medicine*. 23(5): 775–782.

Gilliam, L. A. A., Fisher-Wellman, K. H., Lin, C.-T., Maples, J. M., Cathey, B. L., & Neufer, P. D. 2013. The anticancer agent doxorubicin disrupts mitochondrial energy metabolism and redox balance in skeletal muscle. *Free Radical Biology & Medicine*. 65: 988–96.

Givvimani, S., Munjal, C., Tyagi, N., Sen, U., Metreveli, N., & Tyagi, S. C. 2012. Mitochondrial division/mitophagy inhibitor (Mdivi) ameliorates pressure overload induced heart failure. *PloS One*. 7(3): e32388.

Glick, D., Barth, S., & Macleod, K. F. 2010. Autophagy: cellular and molecular mechanisms. *The Journal of Pathology*. 221(1): 3–12.

Globocan. 2012. *Estimated Cancer Incidence Mortality and Prevalence Worldwide in 2012*. Available from: <http://globocan.iarc.fr/Pages/fact_sheets_cancer.aspx>. [01 July 2014].

Gomes, L. C., & Scorrano, L. 2008. High levels of Fis1, a pro-fission mitochondrial protein, trigger autophagy. *Biochimica et Biophysica Acta*, *1777*(7-8): 860–6.

Goormaghtigh, E., Huart, P., Praet, M., Brasseur, R., & Ruysschaert, J. M. 1990. Structure of the adriamycin-cardiolipin complex. Role in mitochondrial toxicity. *Biophysical Chemistry*. 35(2-3): 247–57.

Gosálvez, M., van Rossum, G. D., & Blanco, M. F. 1979. Inhibition of sodium-potassium-activated adenosine 5'-triphosphatase and ion transport by adriamycin. *Cancer Research*. 39(1): 257–261.

Granger, C. B. 2006. Prediction and prevention of chemotherapy-induced cardiomyopathy: can it be done? *Circulation*. 114(23): 2432–3.

Green, D. R., Galluzzi, L., & Kroemer, G. 2011. Mitochondria and the autophagy-inflammation-cell death axis in organismal aging. *Science*. 333(6046): 1109–1112.

Stellenbosch University https://scholar.sun.ac.za

Green, D. R., & Reed, J. C. 1998. Mitochondria and apoptosis. *Science.* 281:1309-1312.

Greenlee, H., Shaw, J., Lau, Y.-K. I., Naini, A., & Maurer, M. 2012. Lack of effect of coenzyme q10 on doxorubicin cytotoxicity in breast cancer cell cultures. *Integrative Cancer Therapies*. 11(3): 243–250.

Grimm, S. 2012. The ER-mitochondria interface: the social network of cell death. *Biochimica et Biophysica Acta*. 1823(2): 327–334

Grivennikova, V. G., Kareyeva, A. V, & Vinogradov, A. D. 2010. What are the sources of hydrogen peroxide production by heart mitochondria? *Biochimica et Biophysica Acta*. 1797(6-7): 939–944.

Haenen, G. R. M. M., Jansen, F. P., & Bast, A. 1993. Antioxidant properties of five-O-9fl-Hydroxyethyl)-rutosides of the flavonoid mixture Venoruton. *Phenology*. 1: 10-17.

Hammerling, B. C., & Gustafsson, Å. B. 2014. Mitochondrial Quality Control in the Myocardium: Cooperation between Protein Degradation and Mitophagy. *Journal of Molecular and Cellular Cardiology*. 75C: 122–130.

Hampton, R. Y. 2000. ER stress response: Getting the UPR hand on misfolded proteins. *Current Biology*. 10(14): R518–R521.

Harding, H. P., Zhang, Y., Bertolotti, A., Zeng, H., & Ron, D. 2000. Perk is essential for translational regulation and cell survival during the unfolded protein response. *Molecular Cell*. 5(5): 897–904.

Hartley, T., Siva, M., Lai, E., Teodoro, T., Zhang, L., & Volchuk, A. 2010. Endoplasmic reticulum stress response in an INS-1 pancreatic beta-cell line with inducible expression of a folding-deficient proinsulin. *BMC Cell Biology*. 11: 59.

Hasinoff, B. B., Kuschak, T. I., Creighton, A. M., Fattman, C. L., Allan, W. P., Thampatty, P., & Yalowich, J. C. 1997. Characterization of a Chinese hamster ovary cell line with acquired resistance to the bisdioxopiperazine dexrazoxane (ICRF-187) catalytic inhibitor of topoisomerase II. *Biochemical Pharmacology*. 53(12): 1843–1853.

Stellenbosch University https://scholar.sun.ac.za

Hasselgren, P., & Fischer, J. E. 1997. The ubiquitin-proteasome pathway: Review of a novel intracellular mechanism of muscle protein breakdown during sepsis and other catabolic conditions. *Annals of Surgery*. 225(3): 307-316.

Haze, K., Yoshida, H., Yanagi, H., Yura, T., & Mori, K. 1999. Mammalian transcription factor ATF6 is synthesized as a transmembrane protein and activated by proteolysis in response to endoplasmic reticulum stress. *Molecular Biology of the Cell*. 10(11): 3787–3799.

Heo, J.-M., & Rutter, J. 2011. Ubiquitin-dependent mitochondrial protein degradation. *The International Journal of Biochemistry & Cell Biology*. 43(10): 1422–1426.

Hertog, M. G., Hollman, P. C., Katan, M. B., & Kromhout, D. 1993. Intake of potentially anticarcinogenic flavonoids and their determinants in adults in The Netherlands. *Nutrition and Cancer*. 20(1): 21–29.

Hetz, C. 2012. The unfolded protein response: controlling cell fate decisions under ER stress and beyond. *Nature Reviews. Molecular Cell Biology*. 13(2): 89–102.

Hogan, P. G., Chen, L., Nardone, J., & Rao, A. 2003. Transcriptional regulation by calcium, calcineurin, and NFAT. *Genes & Development*, *17*(18): 2205–32.

Holmberg, S.R., & Williams, A. J. 1990. The cardiac sarcoplasmic reticulum calcium-release channel: modulation of ryanodine binding and single-channel activity. *Biochemica et Biophysica Acta.* 1022(2): 187-193.

Hom, J. R., Gewandter, J. S., Michael, L., Sheu, S.-S., & Yoon, Y. 2007. Thapsigargin induces biphasic fragmentation of mitochondria through calcium-mediated mitochondrial fission and apoptosis. *Journal of Cellular Physiology*. 212(2): 498–508.

Hom, J., Yu, T., Yoon, Y., Porter, G., & Sheu, S.-S. 2010. Regulation of mitochondrial fission by intracellular Ca2+ in rat ventricular myocytes. *Biochimica et Biophysica Acta*. 1797(6-7): 913

Stellenbosch University https://scholar.sun.ac.za

Horenstein, M. S., Vander Heide, R. S., & L'Ecuyer, T. J. 2000. Molecular basis of anthracycline-induced cardiotoxicity and its prevention. *Molecular Genetics and Metabolism*. 71(1-2): 436–444.

Ichimura, Y., Kumanomidou, T., Sou, Y., Mizushima, T., Ezaki, J., Ueno, T., Kominami, E., Yamane, T., Tanaka, K., & Komatsu, M. 2008. Structural basis for sorting mechanism of p62 in selective autophagy. *The Journal of Biological Chemistry*. 283(33): 22847–57.

Iglewski, M., Hill, J. A., Lavandero, S., & Rothermel, B. A. 2010. Mitochondrial fission and autophagy in the normal and diseased heart. *Current Hypertension Reports*. 12(6): 418–25.

Ikeda, Y., Sciarretta, S., Nagarajan, N., Rubattu, S., Volpe, M., Frati, G., & Sadoshima, J. 2014. New insights into the role of mitochondrial dynamics and autophagy during oxidative stress and aging in the heart. *Oxidative Medicine and Cellular Longevity*. 210934.

Imondi, A. R., Torre, P. Della, Mazué, G., Mazuã, G., Sullivan, M., Robbins, L., Hagerman, L. M., Podestà, A., & Pinciroli, G. 1996. Dose-Response Relationship of Dexrazoxane for Prevention of Doxorubicin-induced Cardiotoxicity in Mice , Rats , and Dogs. *Cancer Research*. 56(18): 4200–4204.

Ito, H., Miller, S. C., Billingham, M. E., Akimoto, H., Torti, S. V, Wade, R., Gahlmann, R., Lyones, G., Kedes, L., & Torti, F. M. 1990. Doxorubicin selectively inhibits muscle gene expression in cardiac muscle cells in vivo and in vitro. *Proceedings of the National Academy of Sciences of the United States of America*. 87(11): 4275–9477.

Ito, T., Fujio, Y., Takahashi, K., & Azuma, J. 2007. Degradation of NFAT5, a transcriptional regulator of osmotic stress-related genes, is a critical event for doxorubicin-induced cytotoxicity in cardiac myocytes. *The Journal of Biological Chemistry*. 282(2): 1152–1160.

Jacobs, H., Moalin, M., Bast, A., van der Vijgh, W. J. F., & Haenen, G. R. M. M. 2010. An essential difference between the flavonoids monoHER and quercetin in their interplay with the endogenous antioxidant network. *PloS One*. 5(11): e13880.

Stellenbosch University https://scholar.sun.ac.za

Jang, Y. M., Kendaiah, S., Drew, B., Phillips, T., Selman, C., Julian, D., & Leeuwenburgh, C. 2004. Doxorubicin treatment *in vivo* activates caspase-12 mediated cardiac apoptosis in both male and female rats. *FEBS Letters.* 577(3): 483-490.

Ji, C., Yang, B., Yang, Y.-L., He, S.-H., Miao, D.-S., He, L., & Bi, Z.-G. 2010. Exogenous cell-permeable C6 ceramide sensitizes multiple cancer cell lines to Doxorubicin-induced apoptosis by promoting AMPK activation and mTORC1 inhibition. *Oncogene*. 29(50): 6557–6658.

Jordan, J., d'Arcy Doherty, M., & Cohen, G. M. 1987. Effects of glutathione depletion on the cytotoxicity of agents toward a human colonic tumour cell line. *British Journal of Cancer*. *55(*6): 627–631.

Kabeya, Y., Mizushima, N., Ueno, T., Yamamoto, A., Kirisako, T., Noda, T., Kominami, E., Yoshinori, O., & Yoshimori, T. 2000. LC3, a mammalian homologue of yeast Apg8p, is localized in autophagosome membranes after processing. *The EMBO Journal*. 19(21): 5720–5728.

Kadowaki, M., & Karim, M. R. 2009. Cytosolic LC3 ratio as a quantitative index of macroautophagy. *Methods in Enzymology*. *452*: 199–213.

Kaiserová, H., Simůnek, T., van der Vijgh, W. J. F., Bast, A., & Kvasnicková, E. 2007. Flavonoids as protectors against doxorubicin cardiotoxicity: role of iron chelation, antioxidant activity and inhibition of carbonyl reductase. *Biochimica et Biophysica Acta*. 1772(9): 1065–1074.

Kalivendi, S. V, Konorev, E. A., Cunningham, S., Vanamala, S. K., Kaji, E. H., Joseph, J., & Kalyanaraman, B. 2005. Doxorubicin activates nuclear factor of activated T-lymphocytes and Fas ligand transcription: role of mitochondrial reactive oxygen species and calcium. *The Biochemical Journal*. 389(2): 527–539.

Kanki, T., Wang, K., & Klionsky, D. J. 2010. A genomic screen for yeast mutants defective in mitophagy. *Autophagy*. 6(2): 278–280.

Stellenbosch University https://scholar.sun.ac.za

Karbowski, M., Neutzner, A., & Youle, R. J. 2007. The mitochondrial E3 ubiquitin ligase MARCH5 is required for Drp1 dependent mitochondrial division. *The Journal of Cell Biology*. *178* (1): 71–84.

Karbowski, M. & Youle, R. J. 2003. Dynamics of mitochondrial morphology in healthy cells and during apoptosis. *Cell Death and Differentiation.* 10: 870-880.

Kasapović, J., Pejić, S., Stojiljković, V., Todorović, A., Radošević-Jelić, L., Saičić, Z. S., & Pajović, S. B. 2010. Antioxidant status and lipid peroxidation in the blood of breast cancer patients of different ages after chemotherapy with 5-fluorouracil, doxorubicin and cyclophosphamide. *Clinical Biochemistry*. *43*(16-17): 1287–93.

Kaufman, R. J., Scheuner, D., Schröder, M., Shen, X., Lee, K., Liu, C. Y., & Arnold, S. M. 2002. The unfolded protein response in nutrient sensing and differentiation. *Nature Reviews. Molecular Cell Biology*. *3*(6): 411–421.

Kawaguchi, T., Takemura, G., Kanamori, H., Takeyama, T., Watanabe, T., Morishita, K.,Ogino, A., Goto, K., Marugama, R., Kawasaki, M., Mikami, A., Fujiwara, T., Fujiwara, H., & Minatoguchi, S. 2012. Prior starvation mitigates acute doxorubicin cardiotoxicity through restoration of autophagy in affected cardiomyocytes. *Cardiovascular Research*. *96*(3): 456–65.

Keller, J. N., Dimayuga, E., Chen, Q., Thorpe, J., Gee, J., & Ding, Q. 2004. Autophagy, proteasomes, lipofuscin, and oxidative stress. *Cell Biology.* 36(12): 2376-2391.

Klionsky, D. J., & Emr, S. D. 2000. Autophagy as regulated pathways of cellular degradation. *Science.* 290(5497): 1712-1721.

Kim, J., Kundu, M., Viollet, B., & Guan, K.-L. 2011. AMPK and mTOR regulate autophagy through direct phosphorylation of Ulk1. *Nature Cell Biology*. *13*(2): 132–141.

Kim, S.-Y., Kim, S.-J., Kim, B.-J., Rah, S.-Y., Chung, S. M., Im, M.-J., & Kim, U.-H. 2006. Doxorubicin-induced reactive oxygen species generation and intracellular Ca2+ increase are reciprocally modulated in rat cardiomyocytes. *Experimental & Molecular Medicine*. *38*(5): 535–545.

Stellenbosch University https://scholar.sun.ac.za

Kim, S. J., Park, K. M., Kim, N., & Yeom, Y. I. 2005. Doxorubicin prevents endoplasmic reticulum stress-induced apoptosis. *Biochemical and Biophysical Research Communications.* 339(2): 463-468.

Kirkin, V., McEwan, D. G., Novak, I., & Dikic, I. 2009. A role for ubiquitin in selective autophagy. *Molecular Cell*. *34*(3): 259–269.

Kisselev, A. F., Akopian, T. N., Castillo, V., & Goldberg, A. L. 1999. Proteasome Active Sites Allosterically Regulate Each Other, Suggesting a Cyclical Bite-Chew Mechanism for Protein Breakdown. *Molecular Cell*. *4*(3): 395–402.

Kiyomiya, K., Matsuo, S., & Kurebe, M. 1998. Proteasome is a carrier to translocate doxorubicin from cytoplasm into nucleus. *Life Sciences*. *62*(20): 1853–1860.

Kiyomiya. K.. Matsuo. S.. & Kurebe. M. 2001. Mechanism of specific nuclear transport of adriamycin: the mode of nuclear translocation of adriamycin-proteasome complex. *Cancer Research*, *61*(6): 2467–2471.

Kiyomiya. K.. Satoh. J.. Horie. H.. Kurebe. M.. Nakagawa. H.. & Matsuo. S. 2002. Correlation between nuclear action of anthracycline anticancer agents and their binding affinity to the proteasome. *International Journal of Oncology*. 21(5): 1081–105.

Kubli, D. A., & Gustafsson, Á. B. 2012. Mitochondrial and mitophagy: the ying and yang of cell death. *Circulation Research.* 111(9): 1208-1212.

Kusama, Y., Sato, K., Kimura, N., Mitamura, J., Ohdaira, H., & Yoshida, K. 2009. Comprehensive analysis of expression pattern and promoter regulation of human autophagy related genes. *Apoptosis.* 14(10): 1165-1175.

Kobayashi. S.. Volden. P.. Timm. D.. Mao. K.. Xu. X.. & Liang. Q. 2010. Transcription factor GATA4 inhibits doxorubicin-induced autophagy and cardiomyocyte death. *The Journal of Biological Chemistry*. 285(1): 793–804.

Korolchuk, V. I., Menzies, F. M., & Rubinsztein, D. C. 2010. Mechanisms of cross-talk between the ubiquitin-proteasome and autophagy-lysosome systems. *FEBS Letters*. 584(7): 1393–1398.

Stellenbosch University https://scholar.sun.ac.za

Kotiadis, V. N., Duchen, M. R., & Osellame, L. D. 2014. Mitochondrial quality control and communications with the nucleus are important in maintaining mitochondrial function and cell health. *Biochimica et Biophysica Acta*. 1840(4): 1254–1265.

Kozutsumi, Y., Segal, M., Normington, K., Gething, M. J., & Sambrook, J. 1988. The presence of malfolded proteins in the endoplasmic reticulum signals the induction of glucose-regulated proteins. *Nature*. 332(6163): 462–464.

Kraft, C., Peter, M., & Hofmann, K. 2010. Selective autophagy: ubiquitin-mediated recognition and beyond. *Nature Cell Biology*. 12(9): 836–841.

Kuzmicic, J., Del Campo, A., López-Crisosto, C., Morales, P. E., Pennanen, C., Bravo-Sagua, R., Hechenleitner, J., Zepeda, R., Castro, P. F., Verdejo, H. E., Parra, V., Chlong, M., & Lavandero, S. (2011). Mitochondrial dynamics: a potential new therapeutic target for heart failure. *Revista Española de Cardiología.* 64(10): 916–923.

Kyrychenko, V. O., Nagibin, V. S., Tumanovska, L. V, Pashevin, D. O., Gurianova, V. L., Moibenko, A. A., Dosenko, V. E., & Klionsky, D. J. 2014. Knockdown of PSMB7 induces autophagy in cardiomyocyte cultures: possible role in endoplasmic reticulum stress. *Pathobiology : Journal of Immunopathology, Molecular and Cellular Biology*. 81(1): 8–14.

Lai, H.-C., Yeh, Y.-C., Ting, C.-T., Lee, W.-L., Lee, H.-W., Wang, L.-C., Lai, H. C., Wu, A., & Liu, T.-J. 2010. Doxycycline suppresses doxorubicin-induced oxidative stress and cellular apoptosis in mouse hearts. *European Journal of Pharmacology*. 644(1-3): 176–187.

Lam, A. K. M., & Galione, A. 2013. The endoplasmic reticulum and junctional membrane communication during calcium signaling. *Biochimica et Biophysica Acta*. 1833(11): 2542–2559.

Langer, S. ., Sehested, M., & Jensen, P. 2000. The catalytic topoisomerase II inhibitor dexrazoxane inhibits anthracycline-induced necrosis in mice: A new treatment of accidental extravasation of anthracyclines. *Lung Cancer*. 29(1): 10.

Stellenbosch University https://scholar.sun.ac.za

Lapidos, K. A., Kakkar, R., & McNally, E. M. 2004. The dystrophin glycoprotein complex: signaling strength and integrity for the sarcolemma. *Circulation Research*. 94(8): 1023–1031.

Latinis, K. M., Norian, L. A., Eliason, S. L., & Koretzky, G. A. 1997. Two NFAT transcription factor binding sites participate in the regulation of CD95 (Fas) ligand expression in activated human T cells. *The Journal of Biological Chemistry*. 272(50): 31427–31434.

Leandro, J., Dyck, J., Poppe, D., Shore, R., Airhart, C., Greenberg, M., Gilday, D., Smallhorn, J., & Benson, L. 1994. Cardiac dysfunction late after cardiotoxic therapy for childhood cancer. *The American Journal of Cardiology*. 74(11): 1152–1156.

Lebrecht, D., Kirschner, J., Geist, A., Haberstroh, J., & Walker, U. A. 2010. Respiratory chain deficiency precedes the disrupted calcium homeostasis in chronic doxorubicin cardiomyopathy. *Cardiovascular Pathology*. 19(5): e167–174.

Lebrecht, D., Setzer, B., Ketelsen, U.-P., Haberstroh, J., & Walker, U. A. 2003. Time-dependent and tissue-specific accumulation of mtDNA and respiratory chain defects in chronic doxorubicin cardiomyopathy. *Circulation*. 108(19): 2423–2429.

Lee, J., Koga, H., Kawaguchi, Y., Tang, W., Wong, E., Gao, Y., Pandey, U. B., Kaushik, S., Tresse, E., Lu, J., Taylor, J. P., Cuervo, A. M., & Yao, T. 2010a. HDAC6 controls autophagosome maturation essential for ubiquitin selective quality-control autophagy. *The EMBO Journal*. 29(5): 969-980.

Lee, S., Jeong, S.-Y., Lim, W.-C., Kim, S., Park, Y.-Y., Sun, X., Youle, R. J., & Cho, H. 2007. Mitochondrial fission and fusion mediators, hFis1 and OPA1, modulate cellular senescence. *The Journal of Biological Chemistry*. 282(31): 22977–82293.

Lee, J., Nagano, Y., Taylor, J. P., Lim, K. L., & Yoa, T. 2010b. Disease-causing mutations in parkin impair mitochondrial ubiquitination, aggregation and HDAC6-dependent mitophagy. *The Journal of Cell Biology*. 189(4): 671-679.

Lefrak, E. A., Pitha, J., Rosenheim, S., & Gottlieb, J. A. 1973. A clinicopathologic analysis of adriamycin cardiotoxicity. *Cancer*. 32(2): 302–14.

Stellenbosch University https://scholar.sun.ac.za

Legha, S. S., Wang, Y. M., Mackay, B., Ewer, M., Hortobagyi, G. N., Benjamin, R. S., & Ali, M. K. 1982. Clinical and pharmacologic investigation of the effects of alpha-tocopherol on adriamycin cardiotoxicity. *Annals of the New York Academy of Sciences*. 393: 411–418.

Lemasters, J. J. 2005. Selective mitochondrial autophagy, or mitophagy, as a targeted defense against oxidative stress, mitochondrial dysfunction, and aging. *Rejuvenation Research*. 8(1): 3–5.

Lerman, L.S. 1961. Structural considerations in the interaction of DNA and acridines. *Journal of Molecular Biology*. 3(1): 18-30

Lesnefsky, E. J., & Hoppel, C. L. 2008. Cardiolipin as an oxidative target in cardiac mitochondria in the aged rat. *Biochimica et Biophysica Acta*. 1777(7-8): 1020–1027.

Levine, B., & Yuan, J. 2005. Autophagy in cell death: an innocent convict? *The Journal of Clinical Investigation*. 115(10): 2679–2688.

Li, L. Y., Luo, X., & Wang, X. 2001. Endonuclease G is an apoptotic DNase when released from mitochondria. *Nature*. 412(6842): 95–99.

Liang Walter F., H. W. 2006. PGC-1α: a key regulator of energy metabolism. *Advances in Physiology Education*. 30(4): 145–151.

Licata, S., Saponiero, A., Mordente, A., & Minotti, G. 2000. Doxorubicin metabolism and toxicity in human myocardium: role of cytoplasmic deglycosidation and carbonyl reduction. *Chemical Research in Toxicology*. 13(5): 414–420.

Lionaki, E., & Tavernarakis, N. 2013. Oxidative stress and mitochondrial protein quality control in aging. *Journal of Proteomics*. 92: 181–194.

Lipshultz, S. E., Alvarez, J. A., & Scully, R. E. 2008. Anthracycline associated cardiotoxicity in survivors of childhood cancer. *Hear*. 94(4): 525–533.

Liu, B., Bai, Q.-X., Chen, X.-Q., Gao, G.-X., & Gu, H.-T. 2007. Effect of curcumin on expression of survivin, Bcl-2 and Bax in human multiple myeloma cell line. *Journal of Experimental Hematology / Chinese Association of Pathophysiology*. 15(4): 762–766.

Stellenbosch University https://scholar.sun.ac.za

Liu, J., Mao, W., Ding, B., & Liang, C. 2008. ERKs/p53 signal transduction pathway is involved in doxorubicin-induced apoptosis in H9c2 cells and cardiomyocytes. *American Journal of Physiology. Heart and Circulatory Physiology*. 295(5): H1956–H1965.

Livnat-Levanon, N., & Glickman, M. H. 2011. Ubiquitin-proteasome system and mitochondria - reciprocity. *Biochimica et Biophysica Acta*. 1809(2): 80–87.

Lokireddy, S., Wijesoma, I. W., Teng, S., Bonala, S., Gluckman, P. D., McFarlane, C., Sharma, M., & Kambadur, R. 2012. The ubiquitin ligase Mul1 induces mitophagy in skeletal muscle in response to muscle-wasting stimuli. *Cell Metabolism*. 16(5): 613–624.

Loos, B., Lochner, A., & Engelbrecht, A.-M. 2011. Autophagy in heart disease: a strong hypothesis for an untouched metabolic reserve. *Medical Hypotheses*. 77(1): 52–7.

Lu, L., Wu, W., Yan, J., Li, X., Yu, H., & Yu, X. 2009. Adriamycin-induced autophagic cardiomyocyte death plays a pathogenic role in a rat model of heart failure. *International Journal of Cardiology*. 134(1): 82–90.

Luo, X., Reichetzer, B., Trines, J., Benson, L. N., & Lehotay, D. C. 1999. L-carnitine attenuates doxorubicin-induced lipid peroxidation in rats. *Free Radical Biology and Medicine*. 26(9-10): 1158–1165.

Malhi, H., & Kaufman, R. J. 2011. Endoplasmic reticulum stress in liver disease. *Journal of Hepatology*. 54(4): 795–809.

Malhotra, J. D., & Kaufman, R. J. 2007. Endoplasmic reticulum stress and oxidative stress: a vicious cycle or a double-edged sword? *Antioxidants & Redox Signaling*. 9(12): 2277–2793.

Marchi, S., Patergnani, S., & Pinton, P. 2014. The endoplasmic reticulum-mitochondria connection: one touch, multiple functions. *Biochimica et Biophysica Acta*. 1837(4): 461–469.

Marechal, X., Montaigne, D., Marciniak, C., Marchetti, P., Hassoun, S. M., Beauvillain, J. C., Lancel, S., & Neviere, R. 2011. Doxorubicin-induced cardiac dysfunction is attenuated

Stellenbosch University https://scholar.sun.ac.za

by cyclosporin treatment in mice through improvements in mitochondrial bioenergetics. *Clinical Science.* 121(9): 405–413.

Margariti. A.. Li. H.. Chen. T.. Martin. D.. Vizcay-Barrena. G.. Alam. S. Karamariti, E., Xiao, Q., Zampetaki, A., Zhang, Z., Wang, W., Jiang, Z., Gao, C., Ma, B., Chen, Y. G., Cockerill, G., Hu, H., Xu, Q., & Zeng. L. 2013. XBP1 mRNA splicing triggers an autophagic response in endothelial cells through BECLIN-1 transcriptional activation. *The Journal of Biological Chemistry*. 288(2): 859–782.

Marín-García, J., Akhmedov, A., & Moe, G. 2013. Mitochondria in heart failure: the emerging role of mitochondrial dynamics. *Heart Failure Reviews*. 18(4): 439–456.

Marques, A. R., Palanimurugan, A. M., Pauls, C. R., & Dohmen R. J. 2009. Catalytic mechanisms and assembly of the proteasome. *Chemical Reviews.* 109: 1509-1536.

Martínez, R., Navarro, R., Lacort, M., Ruiz-Sanz, J. I., & Ruiz-Larrea, M. B. 2009. Doxorubicin induces ceramide and diacylglycerol accumulation in rat hepatocytes through independent routes. *Toxicology Letters.* 190(1): 86-90.

McBride, H. M., Neuspiel, M., & Wasiak, S. 2006. Mitochondrial: more than just a powerhouse. *Current Biology.* 16(14): R551-R560.

Mimnaugh, E. G., Siddik, Z. H., Drew, R., Sikic, B. I., & Gram, T. E. 1979. The effects of alpha-tocopherol on the toxicity, disposition, and metabolism of adriamycin in mice. *Toxicology and Applied Pharmacology*. 49(1): 119–126.

Minamino, T., & Kitakaze, M. 2010. ER stress in cardiovascular disease. *Journal of Molecular and Cellular Cardiology*. 48(6): 1105–1110.

Minamino, T., Komuro, I., & Kitakaze, M. 2010. Endoplasmic reticulum stress as a therapeutic target in cardiovascular disease. *Circulation Research*. 107(9): 1071–82.

Minners, J., Lacerda, L., McCarthy, J., Meiring, J. J., Yellon, D. M., & Sack, M. N. 2001. Ischemic and pharmacological preconditioning in girardi cells and C2C12 myotubes induce mitochondrial uncoupling. *Circulation Research*. 89(9): 787–792.

Stellenbosch University https://scholar.sun.ac.za

Minotti, G., Cairo, G., & Monti, E. 1999. Role of iron in anthracycline cardiotoxicity: new tunes for an old song? *FASEB Journal : Official Publication of the Federation of American Societies for Experimental Biology*. 13(2): 199–212.

Minotti, G., Menna, P., Salvatorelli, E., Cairo, G., & Gianni, L. 2004. Anthracyclines: molecular advances and pharmacologic developments in antitumor activity and cardiotoxicity. *Pharmacological Reviews*. 56(2): 185–229.

Momparler, R. L., Karon, M., Siegel, S. E., & Avila, F. 1976. Effect of Adriamycin on DNA, RNA, and Protein Synthesis in Cell-free Systems and Intact Cells. *Cancer Research.* 36(8): 2891–2895.

Montagaine, D., Hurt, C., & Neviere, R. 2012. Mitochondrial death/survival signaling pathways in cardiotoxicity induced by anthracyclines and anticancer-targeted therapies. *Biochemistry Research International.* 2012: 1-12.

Morán, M., Delmiro, A., Blázquez, A., Ugalde, C., Arenas, J., & Martín, M. A. 2014. Bulk autophagy, but not mitophagy, is increased in cellular model of mitochondrial disease. *Biochimica et Biophysica Acta*. 1842(7): 1059–70.

Mozdy, A. D., McCaffery, J. M., & Shaw, J. M. 2000. Dnm1p GTPase-mediated mitochondrial fission is a multi-step process requiring the novel integral membrane component Fis1p. *The Journal of Cell Biology*. 151(2): 367–380.

Mross, K., Massing, U., & Kratz, F. 2006. DNA-intercalators — the anthracyclines. In H. Pinedo & C. Smorenburg (Ed.): *Drugs Affecting Growth of Tumours SE ,* Birkhäuser Basel. *2* (pp. 19–81).

Muller, C., Salvayre, R., Nègre-Salvayre, A., & Vindis, C. 2011. Oxidized LDLs trigger endoplasmic reticulum stress and autophagy: prevention by HDLs. *Autophagy*. 7(5): 541–543.

Myers, C. 1998. The role of iron in doxorubicin-induced cardiomyopathy. *Seminars in Oncology*. *25*(4 Suppl 10): 10–14.

Stellenbosch University https://scholar.sun.ac.za

Nagashima, S., Tokuyama, T., Yonashiro, R., Inatome, R., & Yanagi, S. 2014. Roles of mitochondrial ubiquitin ligase MITOL/MARCH5 in mitochondrial dynamics and diseases. *Journal of Biochemistry*. 155(5): 273-279.

Nagata, S. 1997. Apoptosis by Death Factor. *Cell*. 88(3): 355–365.

Nakagawa, T., & Yuan, J. 2000. Cross-talk between two cysteine protease families. Activation of caspase-12 by calpain in apoptosis. *The Journal of Cell Biology*. 150(4): 887–894.

Nakamura, K., Kimura, Y., Tokuda, M., Honda, S., & Hirose, S. 2006. MARCH-V is a novel mitofusin 2- and Drp1-binding protein able to change mitochondrial morphology. *EMBO Reports*. 7(10): 1019-1022.

Neutzner, A., Li, S., Xu, S., & Karbowski, M. 2012. The ubiquitin/proteasome system-dependent control of mitochondrial steps in apoptosis. *Seminars in Cell and Development Biology*. 23(5): 499-508.

Nitiss, J. L. 2009. Targeting DNA topoisomerase II in cancer chemotherapy. *Nature Reviews. Cancer*. 9(5): 338–350.

Nitobe. J.. Yamaguchi. S.. Okuyama. M.. Nozaki. N.. Sata. M.. Miyamoto. T. Takeishi, Y., Kubota, T., & Tomoike. H. 2003. Reactive oxygen species regulate FLICE inhibitory protein (FLIP) and susceptibility to Fas-mediated apoptosis in cardiac myocytes. *Cardiovascular Research*. 57(1): 119–128.

Nowak, D., Pierscinski, G., & Drzewoski, J. 1995. Ambroxol inhibits doxorubicin-induced lipid peroxidation in heart of mice. *Free Radical Biology & Medicine*. 19(5): 659-663.

Octavia, Y., Tocchetti, C. G., Gabrielson, K. L., Janssens, S., Crijns, H. J., & Moens, A. L. 2012. Doxorubicin-induced cardiomyopathy: from molecular mechanisms to therapeutic strategies. *Journal of Molecular and Cellular Cardiology*. 52(6): 1213–25.

Ogata, M., Hino, S., Saito, A., Morikawa, K., Kondo, S., Kanemoto, S., Murakami, T., Taniguchi, M., Tanii, I., Yoshinaga, K., Shiosake, S., Hammarback, J. A., Urano, F., &

Stellenbosch University https://scholar.sun.ac.za

Imaizumi, K. 2006. Autophagy is activated for cell survival after endoplasmic reticulum stress. *Molecular and Cellular Biology*. 26(24): 9220–9231.

Okada, K., Minamino, T., Tsukamoto, Y., Liao, Y., Tsukamoto, O., Takashima, S., Hirata, A., Fujita, M., Nagamachi, Y., Nakatani, T., Yutani, C., Ozawa, K., Tomoike, H., Hori, M., & Kitakaze, M. 2004. Prolonged endoplasmic reticulum stress in hypertrophic and failing heart after aortic constriction: possible contribution of endoplasmic reticulum stress to cardiac myocyte apoptosis. *Circulation*. 110(6): 705–712.

Olson, H. M., Young, D. M., Prieur, D. J., LeRoy, A. F., & Reagan, R. L. 1974. Electrolyte and morphologic alterations of myocardium in adriamycin-treated rabbits. *The American Journal of Pathology*. 77(3): 439–454.

Ondrias, K., Borgatta, L., Kim, D. H., & Ehrlich, B. E. 1990. Biphasic effects of doxorubicin on the calcium release channel from sarcoplasmic reticulum of cardiac muscle. *Circulation Research*. 67(5): 1167–1174.

Ong, S., & Hausenloy, D. J. 2010. Mitochondrial morphology and cardiovascular disease. *Cardiovascular Research.* 88(1): 16-29.

Ong, S.-B., Subrayan, S., Lim, S. Y., Yellon, D. M., Davidson, S. M., & Hausenloy, D. J. 2010. Inhibiting mitochondrial fission protects the heart against ischemia/reperfusion injury. *Circulation*. 121(18): 2012–2022.

Otera, H., & Mihara, K. 2012. Mitochondrial Dynamics: Functional link with Apoptosis. *International Journal of Cell Biology.* 2012(2012): 1-10.

Ou, B., Hampsch-Woodill, M., & Prior, R. L. 2001. Development and Validation of an Improved Oxygen Radical Absorbance Capacity Assay Using Fluorescein as the Fluorescent Probe. *Journal of Agricultural and Food Chemistry*. 49(10): 4619–4626.

Palikaras, K., & Tavernarakis, N. 2014. Mitochondrial homeostasis: the interplay between mitophagy and mitochondrial biogenesis. *Experimental Gerontology*. 56: 182–188.

Pang, B., Qiao, X., Janssen, L., Velds, A., Groothuis, T., Kerkhoven, R., Nieuwland, M., Ovaa, H., Rottenberg, S., van Tellingen, O., Janssen, J., Huijgens, P., Zwart, W., &

Stellenbosch University https://scholar.sun.ac.za

Neefjes, J. 2013. Drug-induced histone eviction from open chromatin contributes to the chemotherapeutic effects of doxorubicin. *Nature Communications*. 4: 1908.

Papadopoulou, L. C., Theophilidis, G., Thomopoulos, G. N., & Tsiftsoglou, A. S. 1999. Structural and functional impairment of mitochondria in adriamycin-induced cardiomyopathy in mice: suppression of cytochrome c oxidase II gene expression. *Biochemical Pharmacology*. 57(5): 481–489.

Papanicolaou, K. N., Ngoh, G. A., Dabkowski, E. R., O'Connell, K. A., Ribeiro, R. F., Stanley, W. C., & Walsh, K. 2012. Cardiomyocyte deletion of mitofusin-1 leads to mitochondrial fragmentation and improves tolerance to ROS-induced mitochondrial dysfunction and cell death. *American Journal of Physiology. Heart and Circulatory Physiology*. 302(1): H167–H179.

Paradies, G., Petrosillo, G., Paradies, V., & Ruggiero, F. M. 2009. Role of cardiolipin peroxidation and Ca2+ in mitochondrial dysfunction and disease. *Cell Calcium*. 45(6): 643–50.

Park, D., Lee, M. N., Jeong, H., Koh, A., Yang, Y. R., Suh, P.-G., & Ryu, S. H. 2014a. Parkin ubiquitinates mTOR to regulate mTORC1 activity under mitochondrial stress. *Cellular Signaling*. 26(10): 2122–2130.

Park, Y.-Y., Lee, S., Karbowski, M., Neutzner, A., Youle, R. J., & Cho, H. 2010. Loss of MARCH5 mitochondrial E3 ubiquitin ligase induces cellular senescence through dynamin-related protein 1 and mitofusin 1. *Journal of Cell Science*. 123(4): 619–626.

Park, Y.-Y., Nguyen, O. T. K., Kang, H., & Cho, H. 2014b. MARCH5-mediated quality control on acetylated Mfn1 facilitates mitochondrial homeostasis and cell survival. *Cell Death & Disease*. 5: e1172.

Parra, V., Eisner, V., Chiong, M., Criollo, A., Moraga, F., Garcia, A., Härtel, S., Jaimovich, E., Zorzano, A., Hidalgo, C., & Lavandero, S. 2008. Changes in mitochondrial dynamics during ceramide-induced cardiomyocyte early apoptosis. *Cardiovascular Research*. 77(2): 387–397.

Stellenbosch University https://scholar.sun.ac.za

Patten, I. S., & Arany, Z. 2012. PGC-1 coactivators in the cardiovascular system. *Trends in Endocrinology & Metabolism.* 23(2): 90-97.

Pessah, I. N., Durie, E. L., Schiedt, M. J., & Zimanvi, I. 1990. Anthraquinone-sensitized Ca^{2+} release channel from rat cardiac sarcoplasmic reticulum: possible receptor-mediated mechanism of doxorubicin cardiomyopathy. *Molecular Pharmacology.* 37(4): 503-514.

Petrosillo, G., Ruggiero, F. M., & Paradies, G. 2003. Role of reactive oxygen species and cardiolipin in the release of cytochrome c from mitochondria. *FASEB Journal : Official Publication of the Federation of American Societies for Experimental Biology*. 17(15): 2202–2208.

Pizzo, P., & Pozzan, T. 2007. Mitochondria-endoplasmic reticulum choreography: structure and signaling dynamics. *Trends in Cell Biology*. 17(10): 511–517.

Pletjushkina, O. Y., Lyamzaev, K. G., Popova, E. N., Nepryakhina, O. K., Domnina, L. V., Chernyak, B. V., & Skulachev, V. P. 2006. Effect of oxidative stress on dynamics of mitochondrial reticulum. *Biochimica et Biophysica Acta.* 1757(5-6): 518-524.

Pommier, Y., Leo, E., Zhang, H., & Marchand, C. 2010. DNA topoisomerases and their poisoning by anticancer and antibacterial drugs. *Chemistry & Biology*. 17(5): 421–433.

Pope, S., Land, J. M., & Heales, S. J. R. 2008. Oxidative stress and mitochondrial dysfunction in neurodegeneration; cardiolipin a critical target? *Biochimica et Biophysica Acta*. 1777(7-8): 794–799.

Powell, S. R. 2006. The ubiquitin-proteasome system in cardiac physiology and pathology. *American Journal of Physiology. Heart and Circulatory Physiology*. 291(1): H1–H19.

Powers, S. K., Wiggs, M. P., Duarte, J. A., Zergeroglu, A. M., & Demirel, H. A. 2012. Mitochondrial signaling contributes to disuse muscle atrophy. *American Journal of Physiology. Endocrinology and Metabolism*. 303(1): E31–9.

Puigserver, P., Wu, Z., Park, C. W., Graves, R., Wright, M., & Spiegelman, B. M. 1998. A cold-inducible coactivator of nuclear receptors linked to adaptive thermogenesis. *Cell*. 92(6): 829–839.

Stellenbosch University https://scholar.sun.ac.za

Ranek, M. J., & Wang, X. 2009. Activation of the ubiquitin-proteasome system in doxorubicin cardiomyopathy. *Current Hypertension Reports*. 11(6): 389–395.

Ren, D., Zhu, Q., Li, J., Ha, T., Wang, X., & Li, Y. 2012. Overexpression of angiopoietin-1 reduces doxorubicin-induced apoptosis in cardiomyocytes. *Journal of Biomedical Research*. 26(6): 432–438.

Rolland, S. G. 2014. How to analyze mitochondrial morphology in healthy cells and apoptotic cells in caenorhabditis elegans. *Methods in Enzymology*. 544: 75–98.

Ron, D., & Walter, P. 2007. Signal integration in the endoplasmic reticulum unfolded protein response. *Nature Reviews. Molecular Cell Biology*. 8(7): 519–529.

Rossini, L., Monti, E., Cova, D., & Piccinini, F. 1986. Determination of doxorubicin and doxorubicin-3-ol in rat heart. *Archives of Toxicology. Supplement*. 9: 474–478.

Saeki, K., Obi, I., Ogiku, N., Shigekawa, M., Imagawa, T., & Matsumoto, T. 2002. Doxorubicin directly binds to the cardiac-type ryanodine receptor. *Life Sciences*. 70(20): 2377–2389.

Saleem, M. T. S., Chetty, M. C., & Kavimani, S. 2014. Antioxidants and tumor necrosis factor alpha-inhibiting activity of sesame oil against doxorubicin-induced cardiotoxicity. *Therapeutic Advances in Cardiovascular Disease*. 8(1): 4–11.

Sano, R., & Reed, J. C. 2013. ER stress-induced cell death mechanisms. *Biochemica et Biophsica acta.* 1833(12): 3460-3470.

Sardão, V., Oliveira, P., Holy, J., Oliveira, C., & Wallace, K. 2009. Doxorubicin-induced mitochondrial dysfunction is secondary to nuclear p53 activation in H9c2 cardiomyoblasts. *Cancer Chemotherapy and Pharmacology*. 64(4): 811–827.

Sasikala, W. D., & Mukherjee, A. 2013. Intercalation and de-intercalation pathway of proflavine through the minor and major grooves of DNA: roles of water and entropy. *Physical Chemistry Chemical Physics : PCCP*. 15(17): 6446–6455.

Sawyer, D. B., Zuppinger, C., Miller, T. A., Eppenberger, H. M., & Suter, T. M. 2002. Modulation of anthracycline-induced myofibrillar disarray in rat ventricular myocytes

Stellenbosch University https://scholar.sun.ac.za

by neuregulin-1beta and anti-erbB2: potential mechanism for trastuzumab-induced cardiotoxicity. *Circulation*. 105(13): 1551–1514.

Schlame, M., & Hostetler, K. Y. 1992. Phospholipid Biosynthesis. *Methods in Enzymology*. 209: 330–337.

Schlame, M., Rua, D., & Greenberg, M. L. 2000. The biosynthesis and functional role of cardiolipin. *Progress in Lipid Research*. 39(3): 257–288.

Schulz, R. A., & Yutzey, K. E. 2004. Calcineurin signaling and NFAT activation in cardiovascular and skeletal muscle development. *Developmental Biology*. 266(1): 1–16.

Schönthal, A. H. 2012. Endoplasmic reticulum stress: its role in disease and novel prospects for therapy. *Scientifica.* 2012: 26 pages.

Sebastiani, M., Giordano, C., Nediani, C., Travaglini, C., Borchi, E., Zani, M., Feccia, M., Mancicni, M., Petrozza, V., Cossarizza, A., Gallo, P., Taylor, R. W., & d'Amati, G. 2007. Induction of mitochondrial biogenesis is a maladaptive mechanism in mitochondrial cardiomyopathies. *Journal of the American College of Cardiology*. 50(14): 1362–9.

Senchenkov, A., Litvak, D., & Cabot, M. 2001. Targeting ceramide metabolism--a strategy for overcoming drug resistance. *Journal of the National Cancer Institute*. 93(5): 347–537.

Seo, A. Y., Joseph, A.-M., Dutta, D., Hwang, J. C. Y., Aris, J. P., & Leeuwenburgh, C. 2010. New insights into the role of mitochondria in aging: mitochondrial dynamics and more. *Journal of Cell Science*. 123(15): 2533–2542.

Sereno, M., Brunello, A., Chiappori, A., Barriuso, J., Casado, E., Belda, C., de Castro, J., Feliu, J., & González-Barón, M. 2008. Cardiac toxicity: old and new issues in anti-cancer drugs. *Clinical & Translational Oncology*. 10(1): 35–46.

Shamu, C. E., & Walter, P. 1996. Oligomerization and phosphorylation of the Ire1p kinase during intracellular signaling from the endoplasmic reticulum to the nucleus. *The EMBO Journal*. 15(12): 3028–3039.

Stellenbosch University https://scholar.sun.ac.za

Shimpo, K., Nagatsu, T., Yamada, K., Sato, T., Niimi, H., Shamoto, M., Takuchi, T., Umezawa, H., & Fujita, K. 1991. Ascorbic acid and adriamycin. *The American Journal of Clinical Nutrition*. 54(6): 1298S-1301S.

Sihag, S., Cresci, S., Li, A. Y., Sucharov, C. C., & Lehman, J. J. 2009. PGC-1alpha and ERRalpha target gene downregulation is a signature of the failing human heart. *Journal of Molecular and Cellular Cardiology*. 46(2): 201–212.

Simůnek, T., Stérba, M., Popelová, O., Adamcová, M., Hrdina, R., & Gersl, V. 2009. Anthracycline-induced cardiotoxicity: overview of studies examining the roles of oxidative stress and free cellular iron. *Pharmacological Reports.* 61(1): 154–171.

Singal, P. K., Iliskovic, N., Li, T., & Kumar, D. 1997. Adriamycin cardiomyopathy: pathophysiology and prevention. *FASEB Journal : Official Publication of the Federation of American Societies for Experimental Biology*. 11(12): 931–936.

Singal, P. K., Li, T., Kumar, D., Danelisen, I., & Iliskovic, N. 2000. Adriamycin-induced heart failure: mechanism and modulation . *Molecular and Cellular Biochemistry.* 207(1-2): 77-86

Sishi, B. J. N., Loos, B., van Rooyen, J., & Engelbrecht, A.-M. 2013a. Autophagy upregulation promotes survival and attenuates doxorubicin-induced cardiotoxicity. *Biochemical Pharmacology*. 85(1): 124–134.

Sishi, B. J. N., Loos, B., van Rooyen, J., & Engelbrecht, A.-M. 2013b. Doxorubicin induces protein ubiquitination and inhibits proteasome activity during cardiotoxicity. *Toxicology*. 5: 23-29.

Smirnova, E., Griparic, L., Shurland, D. L., & van der Bliek, A. M. 2001. Dynamin-related protein Drp1 is required for mitochondrial division in mammalian cells. *Molecular Biology of the Cell*. 12(8): 2245–2256.

Smuder, A. J., Kavazis, A. N., Min, K., & Powers, S. K. 2013. Doxorubicin-induced markers of myocardial autophagic signaling in sedentary and exercise trained animals. *Journal of Applied Physiology.* 115(2): 176–85.

Stellenbosch University https://scholar.sun.ac.za

Solem, L. E., Heller, L. J., & Wallace, K. B. 1996. Dose-dependent increase in sensitivity to calcium-induced mitochondrial dysfunction and cardiomyocyte cell injury by doxorubicin. *Journal of Molecular and Cellular Cardiology*. *28*(5): 1023–1032.

Solem, L. E., Henry, T. R., & Wallace, K. B. 1994. Disruption of mitochondrial calcium homeostasis following chronic doxorubicin administration. *Toxicology and Applied Pharmacology*. 129(2): 214–222.

Sørensen, B. S., Sinding, J., Andersen, A. H., Alsner, J., Jensen, P. B., & Westergaard, O. 1992. Mode of action of topoisomerase II-targeting agents at a specific DNA sequence. *Journal of Molecular Biology*. 228(3): 778–786.

Speyer, J. L., Green, M. D., Kramer, E., Rey, M., Sanger, J., Ward, C., Dubin, N., Ferrans, V., Stecy, P., & Zeleniuch-Jacquotte, A. 1988. Protective effect of the bispiperazinedione ICRF-187 against doxorubicin induced cardiac toxicity in women with advanced breast cancer. *New England Journal of Medicine.* 319(12): 745-752.

Speyer, J. L., Green, M. D., Zeleniuch-Jacquotte, A., Wernz, J. C., Rey, M., Sanger, J., Kramer, E., Ferrans, V., Hochster, H., & Meyers, M. 1992. ICRF-187 permits longer treatment with doxorubicin in women with breast cancer. *Journal of Clinical Oncology.* 10(1): 117–27.

Steinbrecher, U. P., Gómez-Muñoz, A., & Duronio, V. 2004. Acid sphingomyelinase in macrophage apoptosis. *Current Opinion in Lipidology*. 15(5): 531–537.

Stutzmann, G. E., & Mattson, M. P. 2011. Endoplasmic reticulum Ca(2+) handling in excitable cells in health and disease. *Pharmacological Reviews*. 63(3): 700–727.

Suda, T., Takahashi, T., Golstein, P., & Nagata, S. 2993. Molecular cloning and expression of the Fas ligand, a novel member of the tumor necrosis factor family. *Cell.* 75(6): 1169-1178.

Sugamura, K., & Keaney, J. F. 2011. Reactive oxygen species in cardiovascular disease. *Free Radical Biology & Medicine*. 51(5): 978–992.

Stellenbosch University https://scholar.sun.ac.za

Sugiura, A., Yonashiro, R., Fukuda, T., Matsushita, N., Nagashima, S., Inatome, R., & Yanagi, S. 2011. A mitochondrial ubiquitin ligase MITOL controls cell toxicity of polyglutamine-expanded protein. *Mitochondrion*. 11(1): 139–146.

Suliman, H. B., Carraway, M. S., Ali, A. S., Reynolds, C. M., Welty-Wolf, K. E., & Piantadosi, C. A. 2007. The CO/HO system reverses inhibition of mitochondrial biogenesis and prevents murine doxorubicin cardiomyopathy. *The Journal of Clinical Investigation*. 117(12): 3730–3741.

Svenning, S., & Johansen, T. 2013. Selective autophagy. *Essays in Biochemistry*. 55: 79–92.

Swain, S. M., Whaley, F. S., & Ewer, M. S. 2003. Congestive heart failure in patients treated with doxorubicin: a retrospective analysis of three trials. *Cancer*. 97(11): 2869–2879.

Swain, S. M., Whaley, F. S., Gerber, M. C., Weisberg, S., York, M., Spicer, D., Jones, S. E., Walder, S., Desai, A., Vogel, C., Speyer, J., Mittelman, A., Reddy, S., Pendergrass, K., Velez-Gardcoa, E., Ewer, M. S., Biachine, J. R., & Gams, R. A. 1997. Cardioprotection with dexrazoxane for doxorubicin-containing therapy in advanced breast cancer. *Journal of Clinical Oncology*. 15(4): 1318–1332.

Swift, L. P., Rephaeli, A., Nudelman, A., Phillips, D. R., & Cutts, S. M. 2006. Doxorubicin-DNA adducts induce a non-topoisomerase II-mediated form of cell death. *Cancer Research*. *66*(9): 4863–71.

Szegezdi, E., Macdonald, D. C., Ní Chonghaile, T., Gupta, S., & Samali, A. 2009. Bcl-2 family on guard at the ER. *American Journal of Physiology. Cell Physiology*. 296(5): C941–C953.

Takemura, G., & Fujiwara, H. 2007. Doxorubicin-induced cardiomyopathy from the cardiotoxic mechanisms to management. *Progress in Cardiovascular Diseases*. 49(5): 330-352.

Tanaka, A., Cleland, M. M., Xu, S., Narendra, D. P., Suen, D.-F., Karbowski, M., & Youle, R. J. 2010. Proteasome and p97 mediate mitophagy and degradation of mitofusins induced by Parkin. *The Journal of Cell Biology*. 191(7): 1367–1380.

Stellenbosch University https://scholar.sun.ac.za

Tavares, D. C., Cecchi, A. O., Antunes, L. M., & Takahashi, C. S. 1998. Protective effects of the amino acid glutamine and of ascorbic acid against chromosomal damage induced by doxorubicin in mammalian cells. *Teratogenesis, Carcinogenesis, and Mutagenesis*. *18*(4): 153–161.

Tetef, M. L., Synold, T. W., Chow, W., Leong, L., Margolin, R., Morgan, R., Raschko, J., Shibata, S., Somlo, G., Yen, Y., Groshen, S., Johnson, K., Lenz, H. J., Gandara, D., & Doroshow, J. H. 2001. Phase I trial of 960hour continuous infusion of dexrazoxane in patients with advanced malignancies. *Clinical Cancer Research.* 7(6): 1569-1576.

Tidball, J. G., & Wehling-Henricks, M. 2007. Macrophages promote muscle membrane repair and muscle fiber growth and regeneration during modified muscle loading in mice in vivo. *The Journal of Physiology*. 578(Pt 1): 327–336.

Tokarska-Schlattner, M., Dolder, M., Gerber, I., Speer, O., Wallimann, T., & Schlattner, U. 2007. Reduced creatine-stimulated respiration in doxorubicin challenged mitochondria: particular sensitivity of the heart. *Biochimica et Biophysica Acta*. 1767(11): 1276–1284.

Tolkovsky, A. M. 2009. Mitophagy. *Biochimica et Biophysica Acta*. 1793(9): 1508–1515.

Trenker, M., Malli, R., Fertschai, I., Levak-Frank, S., & Graier, W. F. 2007. Uncoupling proteins 2 and 3 are fundamental for mitochondrial Ca2+ uniport. *Nature Cell Biology*. 9(4): 445–452.

Twig, G., Elorza, A., Molina, A. J. A., Mohamed, H., Wikstrom, J. D., Walzer, G., Stiles, L., Haigh, S. E., Katz, S., Las, G., Alroy, J., Wu, M., Py, B. F., Yuan, J., Deeney, J. T., Corkey, B. E., & Shirihai, O. S. 2008. Fission and selective fusion govern mitochondrial segregation and elimination by autophagy. *The EMBO Journal*. 27(2): 433–446.

Twig, G., & Shirihai, O. S. 2011. The interplay between mitochondrial dynamics and mitophagy. *Antioxidants & Redox Signaling*. 14(10): 1939–1951.

Ueno, M., Kakinuma, Y., Yuhki, K., Murakoshi, N., Iemitsu, M., Miyauchi, T., & Yamaguchi, I. 2006. Doxorubicin induces apoptosis by activation of caspase-3 in cultured cardiomyocytes in vitro and rat cardiac ventricles in vivo. *Journal of Pharmacological Sciences*. 101(2): 151–158.

Stellenbosch University https://scholar.sun.ac.za

Vadlamudi, R. K., Joung, I., Strominger, J. L., & Shin, J. 1996. P62, a phosphotyrosine independent ligands of the SH2 domain of p56lck, belongs to a new class of ubiquitin-binding proteins. *Journal of Biological Chemistry.* 271: 20235-20237.

Valko, M., Leibfritz, D., Moncol, J., Cronin, M. T. D., Mazur, M., & Telser, J. 2007. Free radicals and antioxidants in normal physiological functions and human disease. *The International Journal of Biochemistry & Cell Biology*. 39(1): 44–84.

Van Acker, S. A., Boven, E., Kuiper, K., van den Berg, D. J., Grimbergen, J. A., Kramer, K., Bast, A., & van der Vijgh, W. J. 1997. Monohydroxyethylrutoside, a dose-dependent cardioprotective agent, does not affect the antitumor activity of doxorubicin. *Clinical Cancer Research*. 3(10): 1747–1754.

Van Acker, S. A., Kramer, K., Grimbergen, J. A., van den Berg, D. J., van der Vijgh, W. J., & Bast, A. 1995. Monohydroxyethylrutoside as protector against chronic doxorubicin-induced cardiotoxicity. *British Journal of Pharmacology*. 115(7): 1260–1264.

Van Vleet, J. F., Ferrans, V. J., & Weirich, W. E. 1980. Cardiac disease induced by chronic adriamycin administration in dogs and an evaluation of vitamin E and selenium as cardioprotectants. *The American Journal of Pathology*. 99(1): 13–42.

Ventura-Clapier, R., Garnier, A., & Veksler, V. 2008. Transcriptional control of mitochondrial biogenesis: the central role of PGC-1α. *Cardiovascular Research*.

Verfaillie, T., Abnishek, D. G., & Patrizia, A. 2013. Targeting ER stress induced apoptosis and inflammation in cancer. *Cancer Letters.* 2: 249-264

Vives-Bauza, C., Zhou, C., Cui, M., de Vries, R. L. A., Kim, J., Tocilescu, M. A., Ko, H. S., Margrańe, J., Moore, D. J., Dawson, V. L., Grailhe, R., Dawson, T. M., Tieu, K., & Przedborski, S. 2010. PINK1-dependent recruitment of Parkin to mitochondria in mitophagy. *Proceedings of the National Academy of Sciences of the United States of America.* 107(1): 378-383

Von Hoff, D. D., Layard, M. W., Basa, P., Davis, H. L., Von Hoff, A. L., Rozencweig, M., & Muggia, F. M. 1979. Risk factors for doxorubicin-induced congestive heart failure. *Annals of Internal Medicine*. 91(5): 710–717.

Stellenbosch University https://scholar.sun.ac.za

Vejpongsa, P., & Yeh, E. T. H. 2014. Topoisomerase 2β: a promising molecular target for primary prevention of anthracycline-induced cardiotoxicity. *Clinical Pharmacology and Therapeutics*. 95(2): 45-52.

Wang, C., & Wang, X. 2014. The interplay between autophagy and the ubiquitin-proteasome system in cardiac proteotoxicity. *Biochimica et Biophysica Acta*.

Wang, H., Song, P., Du, L., Tian, W., Yue, W., Liu, M., Wang, B., Zhu, Y., Cao, C., Zhou, J., & Chen, Q. 2011. Parkin ubiquitinates Drp1 for proteasome-dependent degradation: implication of dysregulated mitochondrial dynamics in Parkinson disease. *The Journal of Biological Chemistry*. 286(13): 11649–58.

Wang, J., Pareja, K. A., Kaiser, C. A., & Sevier, C. S. 2014. Redox signaling via the molecular chaperone BiP protects cells against endoplasmic reticulum-derived oxidative stress. *eLife*. 3: e03496.

Wang, L., Ma, W., Markovich, R., Chen, J. W., & Wang, P. H. 1998. Regulation of cardiomyocyte apoptotic signaling by insulin-like growth factor I. *Circulation Research*. 83(5): 516–522.

Wang, M., & Kaufman, R. J. 2014. The impact of the endoplasmic reticulum protein-folding environment on cancer development. *Nature Reviews Cancer*. 14(9): 581–597.

Wang, S., Konorev, E. A., Kotamraju, S., Joseph, J., Kalivendi, S., & Kalyanaraman, B. 2004. Doxorubicin induces apoptosis in normal and tumor cells via distinctly different mechanisms intermediacy of H(2)O(2)- and p53-dependent pathways. *The Journal of Biological Chemistry*. 279(24): 25535–25543.

Wang, S., Kotamraju, S., Konorev, E., Kalivendi, S., Joseph, J., & Kalyanaraman, B. 2002. Activation of nuclear factor-kappaB during doxorubicin-induced apoptosis in endothelial cells and myocytes is pro-apoptotic: the role of hydrogen peroxide. *The Biochemical Journal*. 367(Pt 3): 729–740.

Welihinda, A. A., Tirasophon, W., & Kaufman, R. J. 1999. The cellular response to protein misfolding in the endoplasmic reticulum. *Gene Expression*. *7*(4-6): 293–300.

Stellenbosch University https://scholar.sun.ac.za

Wergeland, A., Bester, D. J., Sishi, B. J. N., Engelbrecht, A. M., Jonassen, A. K., & Van Rooyen, J. 2011. Dietary red palm oil protects the heart against the cytotoxic effects of anthracycline. *Cell Biochemistry and Function*. 29(5): 356–364.

Westermann, B. 2010. Mitochondrial fusion and fission in cell life and death. *Nature Reviews: Molecular Cell Biology*. 11(12): 872-884.

Wilkinson, K. D. 1999. Ubiquitin-dependent signaling: the role of ubiquitination in the response of cells to their environment. *The Journal of Nutrition.* 129: 1933-1936.

Williams, G. S. B., Boyman, L., Chikando, A. C., Khairallah, R. J., & Lederer, W. J. 2013. Mitochondrial calcium uptake. *Proceedings of the National Academy of Sciences of the United States of America*. 110(26): 10479–10486.

Witt, H., Schubert, C., Jaekel, J., Fliegner, D., Penkalla, A., Tiemann, K., Stypmann, J., Roepcke, S., Brokat, S., Mahmoodzadeh, S., Brozova, E., Davidson, M. M., Noppinger, P. R., Grohé, C., & Regitz-Zagrosek, V. 2008. Sex-specific pathways in early cardiac response to pressure overload in mice. *Journal of Molecular Medicine.* 86(9): 1013–1024.

Wu, C., Li, T., & Chan, N. 2011. Structural basis of type II topoisomerase inhibition by the anticancer drug etoposide. *Science.* 333(6041): 459–462.

Xiong, Y., Liu, X., Lee, C.-P., Chua, B. H. L., & Ho, Y.-S. 2006. Attenuation of doxorubicin-induced contractile and mitochondrial dysfunction in mouse heart by cellular glutathione peroxidase. *Free Radical Biology & Medicine*. 41(1): 46–55.

Xu, C., Bailly-Maitre, B., & Reed, J. C. 2005. Endoplasmic reticulum stress: cell life and death decisions. *The Journal of Clinical Investigation*. 115(10): 2656–6264.

Xu, M. F., Tang, P. L., Qian, Z. M., & Ashraf, M. 2001. Effects by doxorubicin on the myocardium are mediated by oxygen free radicals. *Life Sciences*. 68(8): 889–901.

Xu, X., Chen, K., Kobayashi, S., Timm, D., & Liang, Q. 2012. Resveratrol attenuates doxorubicin-induced cardiomyocyte death via inhibition of p70 S6 kinase 1-mediated

Stellenbosch University https://scholar.sun.ac.za

autophagy. *The Journal of Pharmacology and Experimental Therapeutics*. 341(1): 183–195.

Xu, X., Hua, Y., Nair, S., Sreejayan, N., Zhang, Y., & Ren, J. 2013. Akt2 knockout preserves cardiac function in high-fat diet-induced obesity by rescuing cardiac autophagosome maturation. *Journal of Molecular Cell Biology*. *5*(1): 61–63.

Yagmurca, M. 2003. Erdosteine prevents doxorubicin-induced cardiotoxicity in rats. *Pharmacological Research*. 48(4): 377–382.

Yamamoto, Y., Hoshino, Y., Ito, T., Nariai, T., Mohri, T., Obana, M., & Azuma, J. 2008. Atrogin-1 ubiquitin ligase is upregulated by doxorubicin via p38-MAP kinase in cardiac myocytes. *Cardiovascular Research*. 79(1): 89–96.

Yamaoka, M., Yamaguchi, S., Suzuki, T., Okuyama, M., Nitobe, J., Nakamura, N., Nakamura, N., Mitsui, Y., & Tomoike, H. 2000. Apoptosis in rat cardiac myocytes induced by Fas ligand: priming for Fas-mediated apoptosis with doxorubicin. *Journal of Molecular and Cellular Cardiology*. 32(6): 881–889.

Yan, Z., Lira, V. A., & Greene, N. P. 2012. Exercise training-induced regulation of mitochondrial quality control . *Exercise Sport Sciences Review*. 40(3): 159-164.

Yang, F., Teves, S. S., Kemp, C. J., & Henikoff, S. 2014. Doxorubicin, DNA torsion, and chromatin dynamics. *Biochimica et Biophysica Acta*. 1845(1): 84–89.

Yeh, E. T. H., & Bickford, C. L. 2009. Cardiovascular complications of cancer therapy: incidence, pathogenesis, diagnosis, and management. *Journal of the American College of Cardiology*. 53(24): 2231–47.

Yonehara, S. 1989. A cell-killing monoclonal antibody (anti-Fas) to a cell surface antigen co-downregulated with the receptor of tumor necrosis factor. *Journal of Experimental Medicine*. 169(5): 1747–1756.

Yonashiro, R., Ishido, S., Kyo, S., Fukuda, T., Goto, E., Ohmura-Hoshino, M., Sada, K., Yamamura, H., Inatome, R., & Yanagi, S. 2006. A novel mitochondrial ubiquitin ligase plays a critical role in mitochondrial dynamics. *The EMBO Journal*. 25(1): 3618-3626.

Stellenbosch University https://scholar.sun.ac.za

Yoon, Y., Krueger, E. W., Oswald, B. J., & McNiven, M. A. 2003. The mitochondrial protein hFis1 regulates mitochondrial fission in mammalian cells through an interaction with the dynamin-like protein DLP1. *Molecular and Cellular Biology*. 23(15): 5409–5420.

Yoshida, H., Okada, T., Haze, K., Yanagi, H., Yura, T., Negishi, M., & Mori, K. 2000. ATF6 activated by proteolysis binds in the presence of NF-Y (CBF) directly to the cis-acting element responsible for the mammalian unfolded protein response. *Molecular and Cellular Biology*. 20(18): 6755–6767.

Youle, R. J., & Narendra, D. P. 2011. Mechanisms of mitophagy. *Nature Reviews. Molecular Cell Biology*. 12(1): 9–14.

Youle, R. J., & van der Bliek, A. M. 2012. Mitochondrial fission, fusion, and stress. *Science.* 337(6098): 1062–105.

Youn, H.-J., Kim, H.-S., Jeon, M.-H., Lee, J.-H., Seo, Y.-J., Lee, Y.-J., & Lee, J.-H. 2005. Induction of caspase-independent apoptosis in H9c2 cardiomyocytes by adriamycin. *Molecular and Cellular Biochemistry.* 270(1-2): 13-19.

Yu, T., Robotham, J. L., & Yoon, Y. 2006. Increased production of reactive oxygen species in hyperglycemic conditions requires dynamic change of mitochondrial morphology. *Proceedings of the National Academy of Sciences of the United States of America.* 103(8): 2653-2658.

Zhang, P., & Mende, U. 2011. Regulators of G-protein signaling in the heart and their potential as therapeutic targets. *Circulation Research*. 109(3): 320–333.

Zhang, S., Liu, X., Bawa-Khalfe, T., Lu, L.-S., Lyu, Y. L., Liu, L. F., & Yeh, E. T. H. 2012. Identification of the molecular basis of doxorubicin-induced cardiotoxicity. *Nature Medicine*. 18(11): 1639–1642.

Zheng, Q., Su, H., Ranek, M. J., & Wang, X. 2011. Autophagy and p62 in cardiac proteinopathy. *Circulation Research.* 109(3): 296-308.

Stellenbosch University https://scholar.sun.ac.za

Zhong, H., Lu, J., Xia, L., Zhu, M., & Yin, H. 2014. Formation of electrophilic oxidation products from mitochondrial cardiolipin in vitro and in vivo in the context of apoptosis and atherosclerosis. *Redox Biology*. 2: 878–883.

Zhu, J. H., Gusdon, A. M., Cimen, H., Van Houten, B., Koc, E., & Chu, C. T. 2012. Impaired mitochondrial biogenesis contributes to depletion of functional mitochondrial in chronic MPP toxicity: dual roles for ERK1/2. *Cell Death Disease.* 3(5): e312.

Zitka, O., Skalickova, S., Gumulec, J., Masarik, M., Adam, V., Hubalek, J., Trinkova, L., Kruseova, J., Eckschlager, T., & Kizek, R. 2012. Redox status expressed as GSH:GSSG ratio as a marker for oxidative stress in paediatric tumour patients. *Oncology Letters*. 4(6): 1247–1253.

Zungu, M., Schisler, J., & Willis, M. S. 2011. All the little pieces. -Regulation of mitochondrial fusion and fission by ubiquitin and small ubiquitin-like modifier and their potential relevance in the heart.-. *Circulation Journal.* 75(11): 2513–2521.

Stellenbosch University https://scholar.sun.ac.za

APPENDIX A – Supplementary Data

The following results were obtained from experiments conducted on the second, *in vitro* cardiac cell line; the human-derived Girardi heart cells.

The Effect of Chronic DOX Treatment Regimes on Mitochondrial Dynamics

Evaluation of Mitochondrial Fission

In order to establish the effect of chronic DOX treatment regimes on mitochondrial fission in human-derived Girardi heart cells, western blotting assessed the expression Drp1 and hFis1. No significant increase in Drp1 expression was observed following treatment with the lowest concentration of DOX after 96 hours. However treatment with the highest dose of DOX induced a significant increase in Drp1 expression [181.30 ± 10.51%, ($p < 0.01$)] when compared to the control (100%) (Figure 5.1). Following 120 hours of exposure, DOX induced an even greater incremental increase in Drp1 at both the 0.2 μM [171.40 ± 12.21%, ($p < 0.05$)] and 1.0 μM [246.70 ± 14,17%, ($p < 0.01$)]. No significant change in hFis1 expression was observed in the Girardi cells following treatment (Figure 5.2). These results demonstrate that chronic DOX treatment increases Drp1-mediated mitochondrial fission in a time- and dose-dependent manner.

Evaluation of Mitochondrial Fusion

In contrast to results obtained in the H9C2 cardiomyoblasts, a significant increase in Mfn 1 expression occurred following 120 hours treatment in the Girardi cells [0.2 μM: 173.00 ± 1.99%, ($p < 0.01$) and 1.0 μM: 135.80 ± 7.89%, ($p < 0.05$) compared to the control group (100%) (Figure 5.3). Further analysis of Mfn 1 expression within concentration groups demonstrated that protein levels substantially increased over time, suggesting that cumulative DOX treatment elevates Mfn 1 expression. However, Mfn 2 expression was significantly reduced in both a time- and dose- dependent manner (Figure 5.4). These results demonstrate that the Girardi cells are still able to try maintain mitochondrial dynamics in the presence of chronic DOX treatment via the upregulation of Mfn 1, but mitochondrial fusion requires the assembling activities of both Mfn 1 and Mfn 2 (Papanicolaou *et al*., 2012). Therefore similar

Stellenbosch University https://scholar.sun.ac.za

to the H9C2 cardiomyoblasts, these results together with the significant increase in Drp1 expression suggest chronic DOX treatment in Girardi cells also disrupts mitochondrial dynamics.

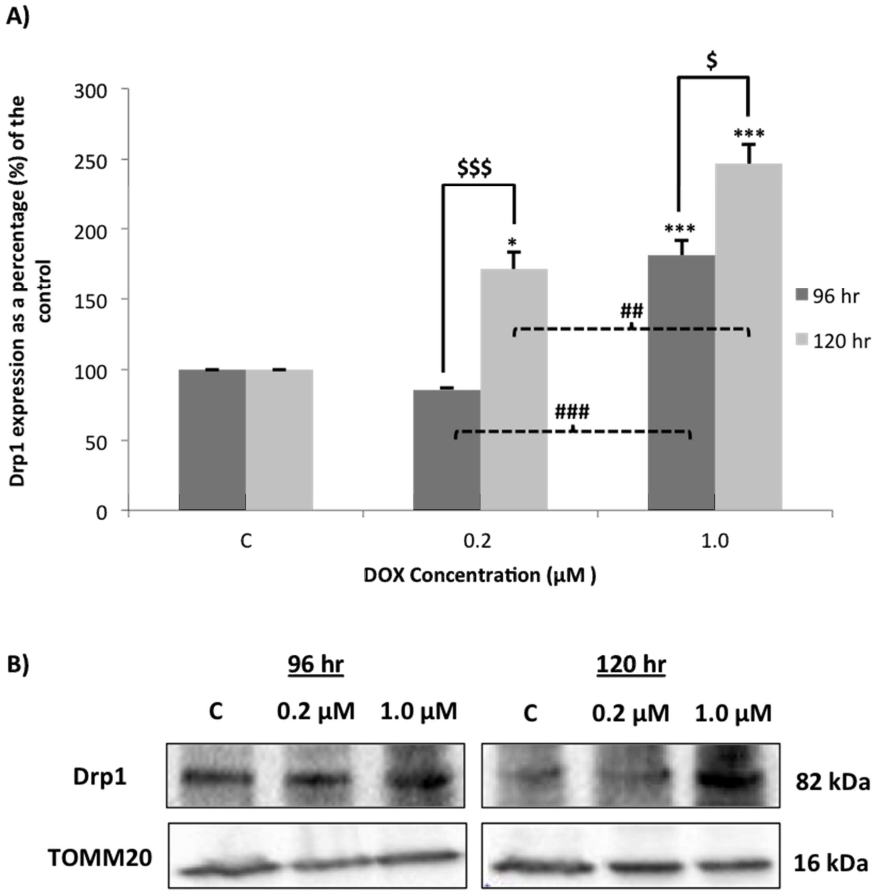

Figure 5.1: The effect of chronic doxorubicin treatment regimes on Drp1 expression in human-derived Girardi heart cells. (A) Lane profile analysis of Drp1. (B) Representative immunoblot of Drp1. TOMM20 served as the loading control. Girardi cells were treated daily with 0.2 and 1.0 µM DOX for 96 and 120 hours. Results are presented as mean ± SEM (n=3). *P < 0.05 and ***P< 0.001 vs. Control. $^{\$}$P < 0.05 and $^{\$\$\$}$P < 0.001 96 hr vs. 120 hr. $^{\#\#}$P < 0.01 and $^{\#\#\#}$P < 0.001 0.2 µM vs. 1.0 µM. Abbreviations – C: control, DOX: doxorubicin, Drp1: dynamin-related protein 1, hr: hour, vs: versus.

Stellenbosch University https://scholar.sun.ac.za

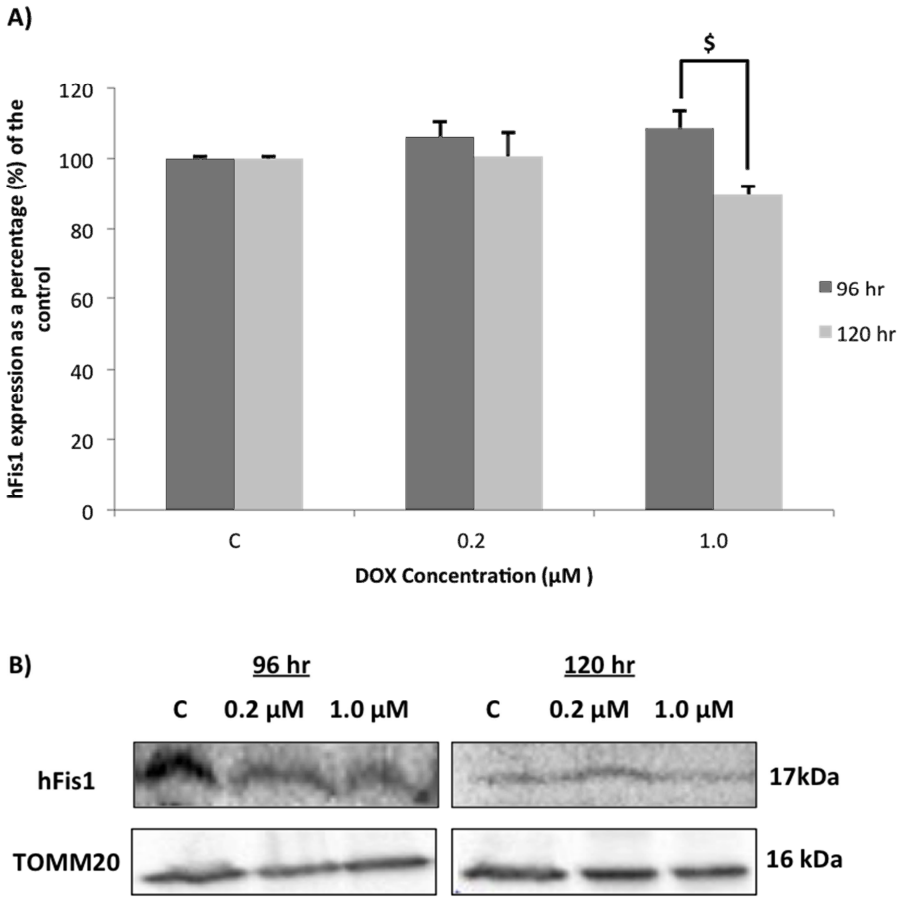

Figure 5.2: The effect of chronic doxorubicin treatment regimes on hFis1 expression in human-derived Girardi heart cells. (A) Lane profile analysis of hFis1. (B) Representative immunoblot of hFis1. TOMM20 served as the loading control. Girardi cells were treated daily with 0.2 and 1.0 µM DOX for 96 and 120 hours. Results are presented as mean ± SEM (n=3). $^{\$}P < 0.51$ 96 hr vs. 120 hr. Abbreviations – C: control, DOX: doxorubicin, hFis1: mitochondrial fission factor 1, hr: hour, vs: versus

Stellenbosch University https://scholar.sun.ac.za

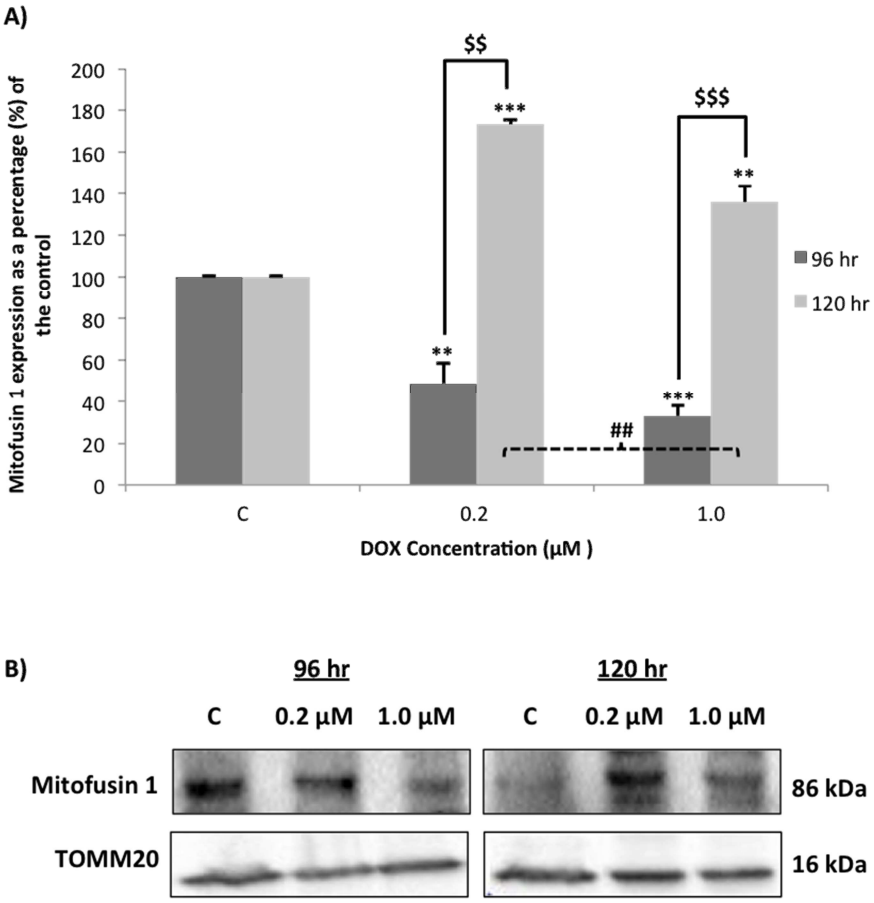

Figure 5.3: The effect of chronic doxorubicin treatment regimes on Mitofusin 1 expression in human-derived Girardi heart cells. (A) Lane profile analysis of Mitofusin 1. (B) Representative immunoblot of Mitofusin 1 TOMM20 served as the loading control. Girardi cells were treated daily with 0.2 and 1.0 µM DOX for 96 and 120 hours. Results are presented as mean ± SEM (n=3). **P < 0.01 and ***P< 0.001 vs. Control. $^{\$\$}$P < 0.01 and $^{\$\$\$}$P < 0.001 96 hr vs. 120 hr. $^{\#\#}$P < 0.01 0.2 µM vs. 1.0 µM. Abbreviations – C: control, DOX: doxorubicin, hr: hour, vs: versus.

Stellenbosch University https://scholar.sun.ac.za

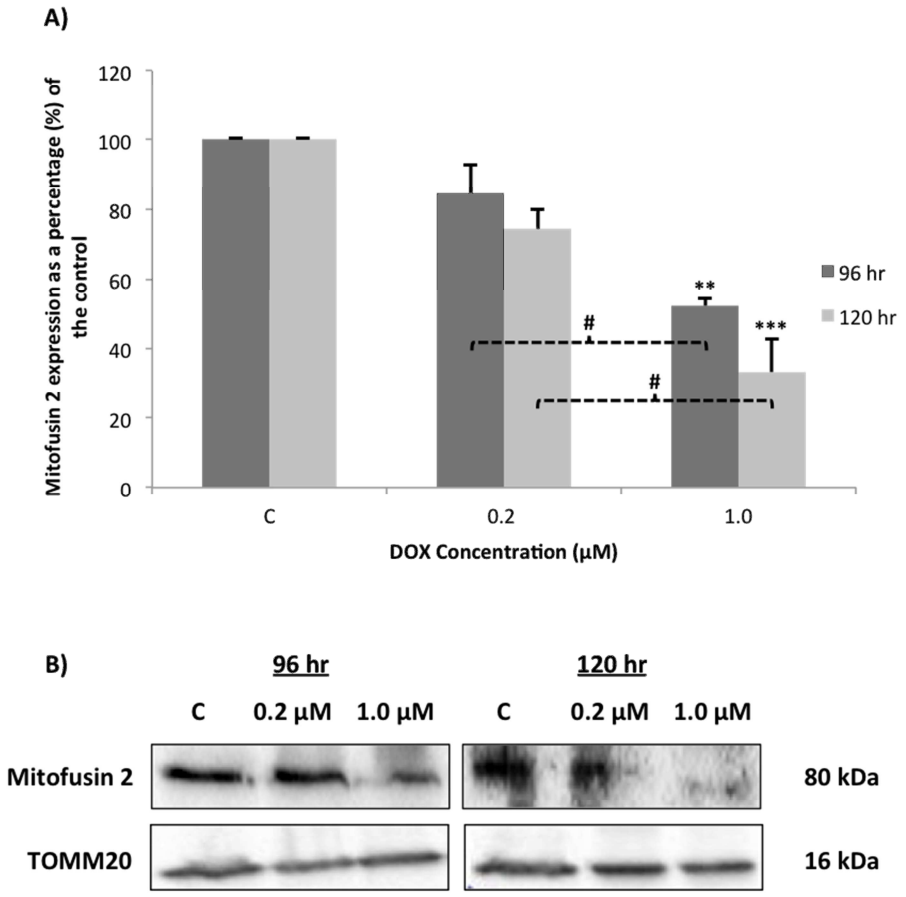

Figure 5.4: The effect of chronic doxorubicin treatment regimes on Mitofusin 2 expression in human-derived Girardi heart cells. (A) Lane profile analysis of Mitofusin 2. (B) Representative immunoblot of Mitofusin 2. TOMM20 served as the loading control. Girardi cells were treated daily with 0.2 µM and 1.0 µM DOX for 96 and 120 hours. Results are presented as mean ± SEM (n=3). *P < 0.05 and ***P< 0.001 vs. Control. $^{\#}$P < 0.05 0.2 µM vs 1.0 µM. Abbreviations – C: control, DOX: doxorubicin, hr: hour, vs: versus.

Evaluation of Mitochondrial Morphology

In order to establish whether chronic DOX treatment induced any changes in mitochondrial morphology, cells where stained as previously described with MitoTracker green and visualized with fluorescence microscopy. However, since the Girardi cells were extremely sensitive to DOX with a high rate of cell death, not enough cells could be visualized on the small area of the 8-well chamber slide. Furthermore, those cells that were either in the control

Stellenbosch University https://scholar.sun.ac.za

group and/or did survive, did not provide adequate images where mitochondrial morphology could be assessed. Therefore colocalization of DOX with the mitochondria could not be performed on the Girardi cells. Mitochondrial load was rather used to determine the number of mitochondria present following chronic DOX treatment (Figure 5.5). Cells were again stained with MitoTracker green and analyzed by flow cytometry. Following 1.0 µM DOX treatment significant increased in fluorescence at the 96 hour [117.40 ± 10.05%, ($p < 0.05$)] and 120 hour [291.70 ± 31.24%, ($p < 0.01$)] time points in comparison to the control (100%). As the mitochondria become more fragmented, mitochondrial load increases. Therefore these results suggest that mitochondrial fission increases following DOX treatment, in a time- and dose- dependent manner.

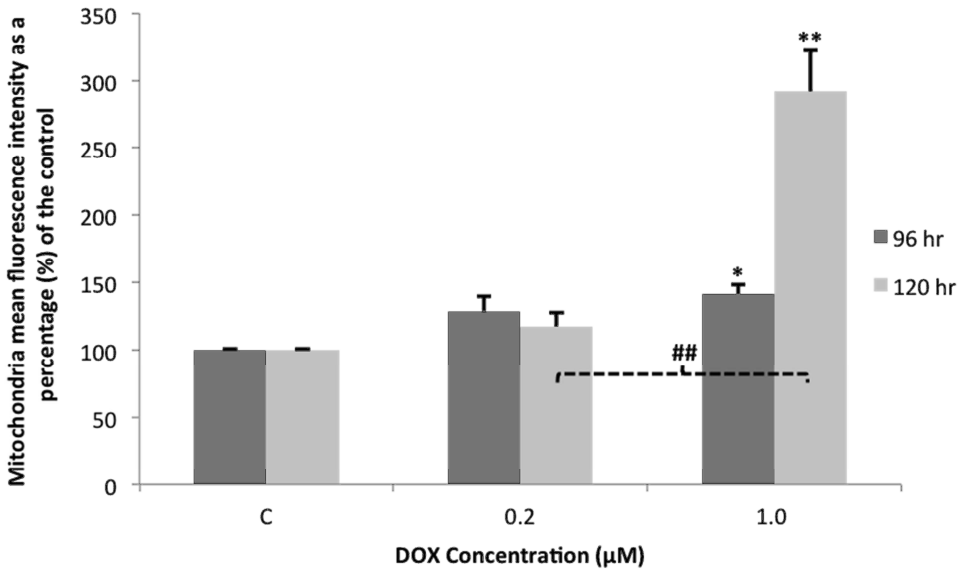

Figure 5.5: The effect of chronic doxorubicin treatment regimes on mitochondrial load in human-derived Girardi heart cells. Girardi cells were treated daily with 0.2 and 1.0 µM DOX for 96 and 120 hours, followed by staining with MitoTracker Green and assessed using flow cytometry (n=3). *P < 0.05 and **P< 0.01 vs. Control. $^{\#\#}$P < 0.01 0.2 µM vs. 1.0 µM. Abbreviations – C: control, DOX: doxorubicin, hr: hour., vs: versus.

Stellenbosch University https://scholar.sun.ac.za

The Effect of Chronic DOX Treatment Regimes on the Ubiquitin Proteasome Pathway

Evaluation of E3 ligase expression

Evaluation of the E3 ligase, MARCH5 expression in Girardi cells was assessed with western blotting. MARCH5 expression was demonstrated to be significantly elevated following chronic DOX treatment. Although no significance was obtained in the low concentration group following 96 hours [140.80 ± 14.37%], treatment with the highest concentration of DOX significantly increased MARCH5 expression [211.60 ± 8.63%, ($p < 0.01$)] at the same time point compared to the control (100%) (Figure 5.6). Similarly, further analysis showed that following 120 hours of treatment, MARCH5 was significantly elevated as the concentration DOX increased [0.2 μM: 173.50 ± 2.92%, ($p < 0.01$) and 1.0 μM: 220.00 ± 9.01%, ($p < 0.01$)].

Since mitochondrial fission activates mitophagy, mitophagic activity following chronic DOX treatment was also assessed. The expression of the E3 ubiquitin ligase, Parkin was used as a marker for mitophagy and evaluated with western blotting (Figure 5.7). Although Parkin expression was initially statistically upregulated following 96 hours treatment with the lowest dose of DOX [146.30 ± 7.92%, ($p < 0.01$)] versus the control group (100%), additional analysis between groups demonstrated that Parkin expression was significantly downregulated as the concentration of DOX increased [0.2 μM: 146.30 ± 7.92% and 1.0 μM: 77.94 ± 6.02%, ($p < 0.001$ 0.2 μM vs. 1.0 μM)]. Conversely, following 120 hours of treatment, Parkin expression remained elevated at the low [112.90 ± 3.92%, ($p < 0.05$)] and high [128.50 ± 0.99%, ($p < 0.001$)] concentration group compared to the control, and was significantly upregulated in a dose-dependent manner ($p < 0.05$). These results suggest that mitophagic activity is dependent on the cumulative, concentration of DOX rather that treatment time. Mitophagy activity was extremely sporadic in the Girardi cell model, compared to results obtained in the H9C2 cardiomyoblasts.

Stellenbosch University https://scholar.sun.ac.za

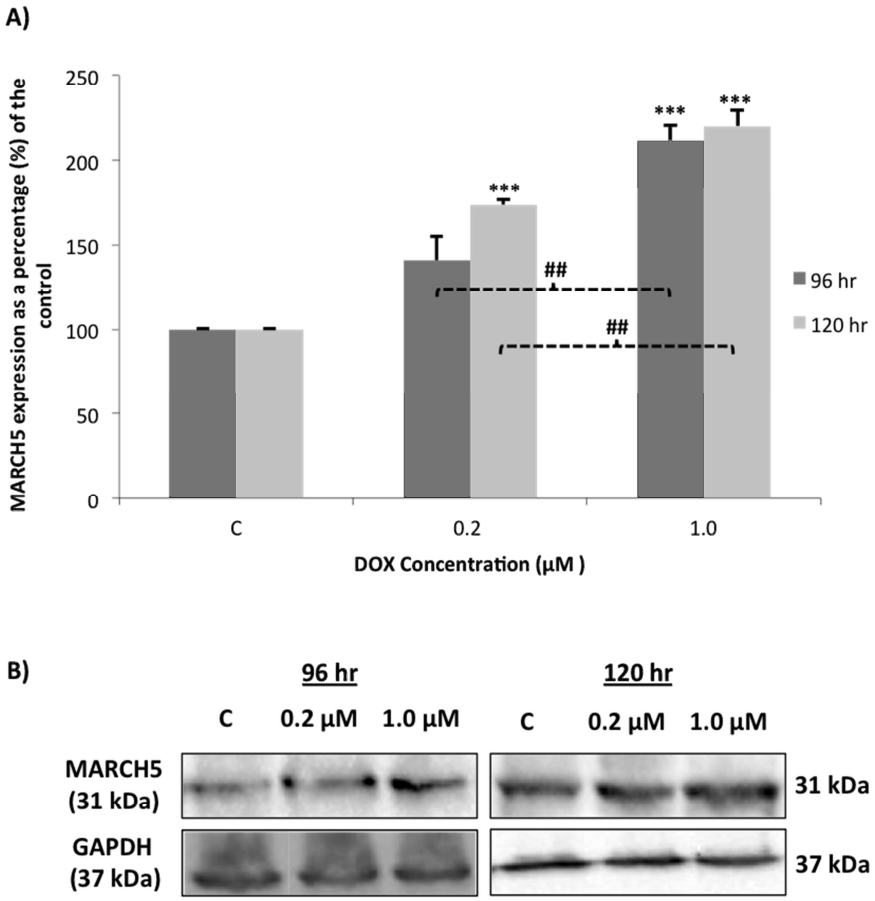

Figure 5.6: The effect of chronic doxorubicin treatment regimes on MARCH5 expression in human-derived Girardi heart cells. (A) Lane profile analysis of MARCH5. (B) Representative immunoblot of MARCH5. GAPDH served as the loading control. Girardi cells were treated daily with 0.2 µM and 1.0 µM DOX for 96 and 120 hours. Results are presented as mean ± SEM (n=3). ***P< 0.001 vs Control. $^{\#\#}$P < 0.01 0.2 µM vs 1.0 µM. Abbreviations – C: control, DOX: Doxorubicin, hr: hour, MARCH5: membrane-associated RING finger 5, vs: versus.

Stellenbosch University https://scholar.sun.ac.za

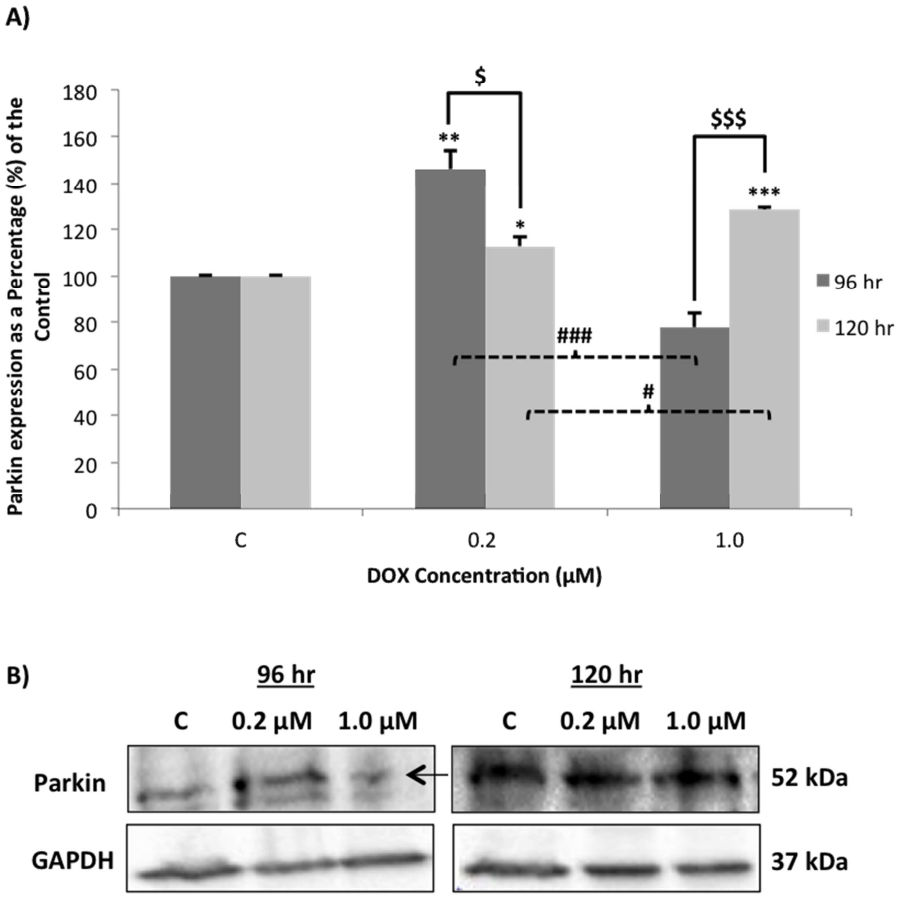

Figure 5.7: The effect of chronic doxorubicin treatment regimes on Parkin expression in human-derived Girardi heart cells. (A) Lane profile analysis of Parkin. (B) Representative immunoblot of Parkin. GAPDH served as the loading control. Girardi cells were treated daily with 0.2 µM and 1.0 µM DOX for 96 and 120 hours. Results are presented as mean ± SEM (n=3). *P < 0.05, **P < 0.01 and ***P< 0.001 vs Control. $^{\$}$P < 0.05 and $^{\$\$\$}$P < 0.001 96 hr vs 120 hr. $^{\#}$P < 0.05 and $^{\#\#\#}$P < 0.001 0.2 µM vs 1.0 µM. Abbreviations – C: control, DOX: Doxorubicin, hr: hour, vs: versus.

Evaluation of K48 Protein Ubiquitination

The K48 ubiquitin antibody detects proteins with have been tagged with polyubiquitin chains, and targeted for proteasomal degradation. K48 ubiquitination was significantly increased at the 0.2 µM [130.30 ± 2.26%, ($p < 0.01$)] and 1.0 µM [172.80 ± 7.25%, ($p < 0.001$)] concentration groups following 96 hours of treatment compared to the control group (100%) (Figure 5.8a). However after 120 hours of treatment, elevated ubiquitination was only

Stellenbosch University https://scholar.sun.ac.za

observed in the 1.0 µM group [127.30 ± 1.45%, ($p < 0.001$)] versus the control. Analysis within concentration groups demonstrated that over time, K48 ubiquitination was significantly reduced ($p < 0.001$), which is opposite to the augmented ubiquitination observed over time in the H9C2 model (Figure 3.14, pg. 62). Additionally, as seen in the representative immunoblot image (Figure 5.8b), a difference in protein tagging was observed across the two concentration groups. Low concentrations of DOX resulted tagging of proteins with the molecular weight of ±63 kDa and 130 – 245 kDa. Whereas treatment with the higher concentrations of DOX resulted in reduced ubiquitination over time of proteins with a relatively higher molecular weight range, which is suggestive of myofibrillar protein targeting.

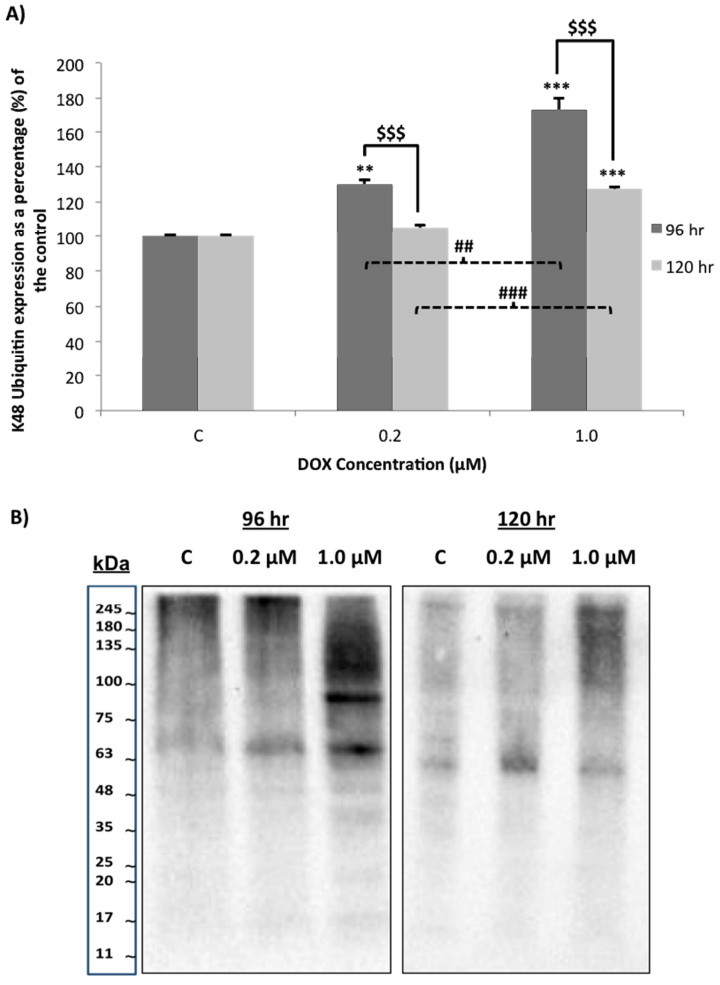

Figure 3.8: The effect of chronic doxorubicin treatment regimes on K48 ubiquitination in human-derived Girardi heart cells. (A) Lane profile analysis of K48 Ubiquitin. (B) Representative immunoblot of K48 ubiquitination. GAPDH served as the loading control. Girardi cells were treated daily with 0.2 µM and 1.0 µM DOX for 96 and 120 hours. Results are presented as mean ± SEM (n=3). **P < 0.01 and ***P< 0.001 vs Control. $^{\$\$\$}$P < 0.001 96

Stellenbosch University https://scholar.sun.ac.za

hr vs 120 hr. ##P < 0.01 and ###P < 0.001 0.2 µM vs 1.0 µM Abbreviations – C: control, DOX: doxorubicin, hr: hour, vs: versus.

Evaluation of the 26S Proteasome

Chronic DOX treatment significantly reduced the activity of all three catalytic sites over time as the concentration of DOX increased relative to the controls (100%). However, the activity of both the chymotrypsin-like site (Figure 5.9), and the trypsin-like site (Figure 3.10) significantly increased after 120 hours at the 0.2 µM concentration compared to their respective activity following 96 hours of treatment with the same concentration ($p < 0.01$) and ($p < 0.05$). Caspase-like activity was initially elevated [125.60 ± 8.40%, ($p < 0.05$)] following treatment with the lower dose of DOX for 96 hours compared to the control, and significantly reduced following 120 hours [90.93 ± 3.66%, ($p < 0.001$ 0.2 µM vs. 1.0 µM)] (Figure 5.11). Although proteasome activity was also inhibited in the H9C2 cells after treatment, inhibition was more pronounced in the Girardi heart cells. These results further demonstrate the heightened Girardi cell sensitivity to DOX treatment.

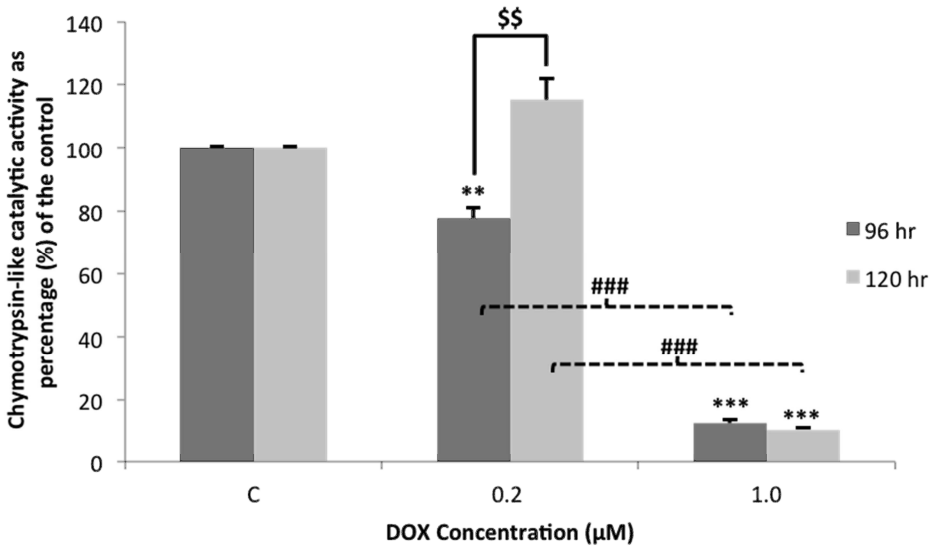

Figure 5.9: The effect of chronic doxorubicin treatment regimes on chymotrypsin-like catalytic activity in human-derived Girardi heart cells. Girardi cells were treated daily with 0.2 µM and 1.0 µM DOX for 96 and 120 hours. Results are presented as mean ± SEM

Stellenbosch University https://scholar.sun.ac.za

(n=3). **P < 0.01 and ***P< 0.001 vs Control. $^{\$\$}$P < 0.01 96 hr vs 120 hr. $^{\#\#\#}$P < 0.001 0.2 µM vs 1.0 µM. Abbreviations – C: control, DOX: doxorubicin, hr: hour, vs: versus.

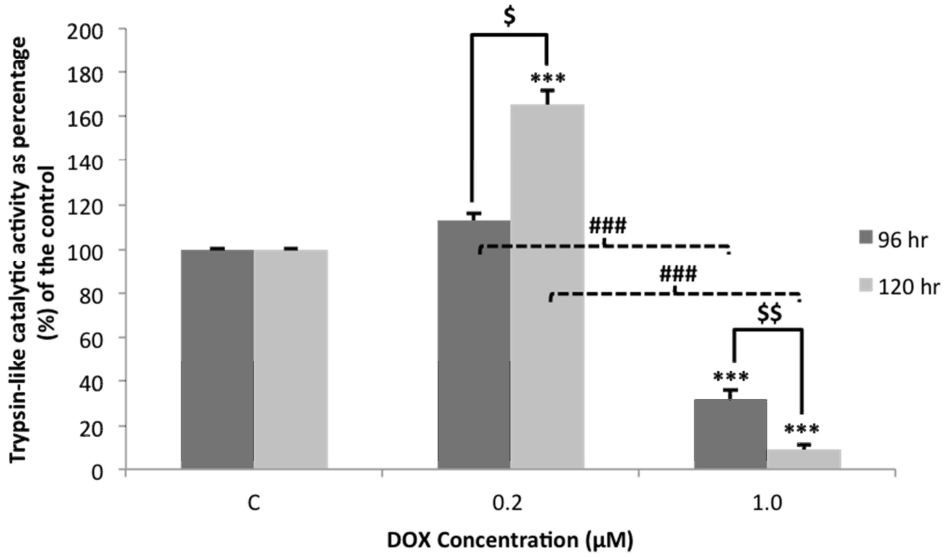

Figure 5.10: The effect of chronic doxorubicin treatment regimes on trypsin-like catalytic activity in human-derived Girardi heart cells. Girardi cells were treated daily with 0.2 µM and 1.0 µM DOX for 96 and 120 hours. Results are presented as mean ± SEM (n=3). ***P< 0.001 vs Control. $^{\$}$P < 0.05 and $^{\$\$}$P < 0.01 96 hr vs 120 hr. $^{\#\#\#}$P < 0.001 0.2 µM vs 1.0 µM. Abbreviations: C: control, DOX: doxorubicin, hr: hour., vs.: versus.

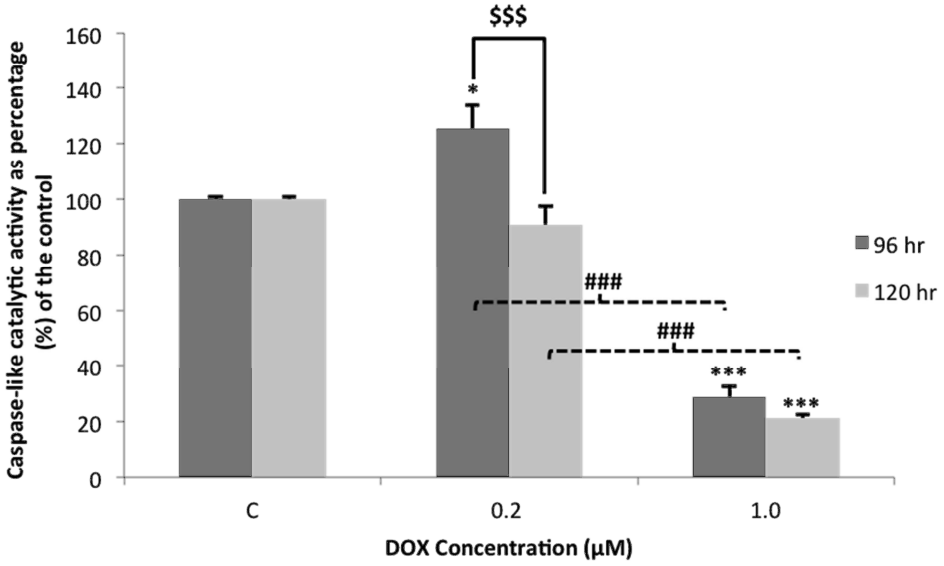

Figure 5.11: The effect of chronic doxorubicin treatment regimes on caspase-like catalytic activity in human-derived Girardi heart cells. Girardi cells were treated daily

Stellenbosch University https://scholar.sun.ac.za

with 0.2 µM and 1.0 µM DOX for 96 and 120 hours. Results are presented as mean ± SEM (n=3). ***P < 0.001 vs Control. $^{\$\$\$}$P < 0.001 96 hr vs 120 hr. $^{\#\#\#}$P < 0.001 0.2 µM vs 1.0 µM. Abbreviations – C: control, DOX: doxorubicin, hr: hour, vs: versus.

The Effect of Chronic DOX Treatment Regimes on Autophagy

Following chronic DOX treatment, the expression of the two biomarkers for the autophagic, LC-3 (Figure 5.12) and p62 (Figure 5.13), were assessed by western blotting. As mentioned earlier, there are many accepted methods in which LC3 expression can be interpreted and this study chose to analyze the LC3-II/LC3-I ratio (Figure 5.12). LC3 lipidation was significantly reduced over time following treatment with 0.2 µM DOX [45.42 ± 2.16%, ($p < 0.01$ 96 hr vs. 120 hr)]. However following treatment with 1.0 µM DOX, LC3 lipidation was significantly elevated after 96 hours [113.30 ± 6.23%, ($p < 0.05$)] and 120 hours [120.20 ± 3.55%, ($p < 0.05$)] of treatment in comparison to the control (100%). These results demonstrated that flux through the autophagic pathway is dependent on both the concentration of DOX administrated and the treatment duration. Low, chronic DOX administration significantly reduced LC3 lipidation, while high, chronic DOX treatment augmented autophagy. These results are different to those observed in the H9C2 cardiomyoblasts, where LC3 lipidation incrementally increased in a time- and dose- dependent manner. P62 promotes the formation of protein aggregates, and directs them to the autophagosome through its interactions with LC3.

Thereafter p62, along with the targeted and defective cargo are engulfed and subsequently degraded by the autophagolysosome (Ichimura *et al.*, 2008). Since LC3 lipidation was previously shown to be inhibited with low, chronic administration of DOX, it is not surprising that p62 significantly accumulated over time following treatment with 0.2 µM [96 hrs.: 75.00 ± 0.93% and 120 hrs.: 116.70 ± 5.77%, ($p < 0.01$ 96 hr vs. 120 hr)]. However following high, chronic DOX administration p62 continued to accumulate, and a significant increase in protein expression was observed following 120 hours [112.30 ± 2.39%, ($p < 0.01$ vs. Control)]. It is important to note that even though p62 accumulated over time, p62 expression was initially downregulated after 96 hours of treatment [0.2 µM: 75.00 ± 0.93%, ($p < 0.01$) and 1.0 µM: 38.92 ± 5.78%, ($p < 0.001$)] compared to the control.

Stellenbosch University https://scholar.sun.ac.za

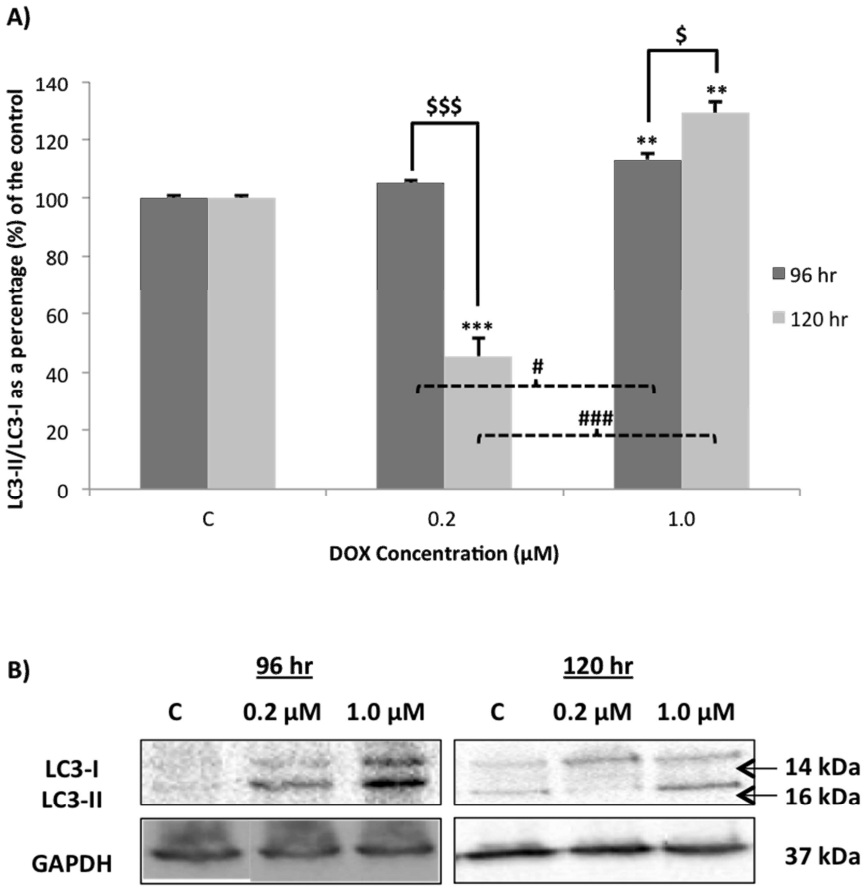

Figure 5.12: The effect of chronic doxorubicin treatment regimes on LC3 expression in human-derived Girardi heart cells. (A) Lane profile analysis of LC3-II/LC3-Ratio. (B) Representative immunoblot of LC3-I and LC3-II. GAPDH served as the loading control. Girardi cells were treated daily with 0.2 µM and 1.0 µM DOX for 96 and 120 hours. Results are presented as mean ± SEM (n=3). **P < 0.05 and ***P < 0.01 vs Control. $^{\$}$P < 0.05 and $^{\$\$\$}$P < 0.001 96 hr vs 120 hr. $^{\#}$P < 0.05 and $^{\#\#\#}$P < 0.001 0.2 µM vs 1.0 µM. Abbreviations – C: control, DOX: doxorubicin, hr: hour, LC3: microtubule –associated protein light chain 3, vs.: versus.

Stellenbosch University https://scholar.sun.ac.za

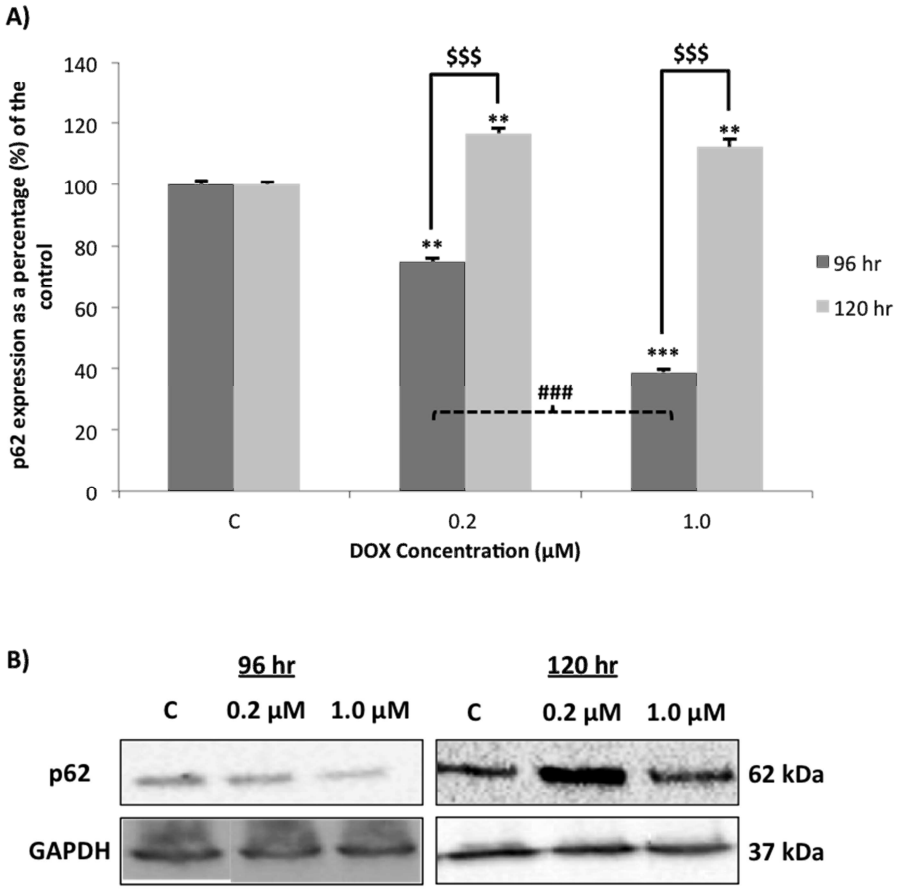

Figure 5.13: The effect of chronic doxorubicin treatment regimes on p62 expression in human-derived Girardi heart cells. (A) Lane profile analysis of p62. (B) Representative immunoblot of p62. GAPDH served as the loading control. Girardi cells were treated daily with 0.2 µM and 1.0 µM DOX for 96 and 120 hours. Results are presented as mean ± SEM (n=3). **P < 0.01 and ***P < 0.001 vs Control. $^{\$\$\$}$P < 0.001 96 hr vs 120 hr. $^{\#\#\#}$ P < 0.001 0.2 µM vs 1.0 µM. Abbreviations – C: control, DOX: doxorubicin, hr: hour, vs.: versus.

The Effect of Chronic DOX Treatment Regimes on Mitochondrial Biogenesis

Western blotting was used to assess the transcription factor, PGC-1α (peroxisome proliferator-activated receptor gammer co-activator 1-alpha), an important protein involved in regulating mitochondrial biogenesis. PGC-1α controls the synthesis of new mitochondrial by coordinating the transcription of both the mitochondrial and nuclear genomes (Baker *et al.*, 2007; Puigserver *et al.*, 1998). Compared to the control group (100%), PGC-1α expression was significantly downregulated following 96 hours of with 0.2 µM DOX [31.61

Stellenbosch University https://scholar.sun.ac.za

± 3.02%, ($p < 0.001$)]. However no significant difference was observed at the 1.0 µM group at the same time point [80.12 ± 4.46%]. Following 120 hours of treatment results obtained demonstrated that PGC-1α levels were significantly downregulated at both the low [41.69 ± 6.67%, ($p < 0.001$)] and high [48.40 ± 3.24%, ($p < 0.001$)] concentration groups (Figure 5.14).

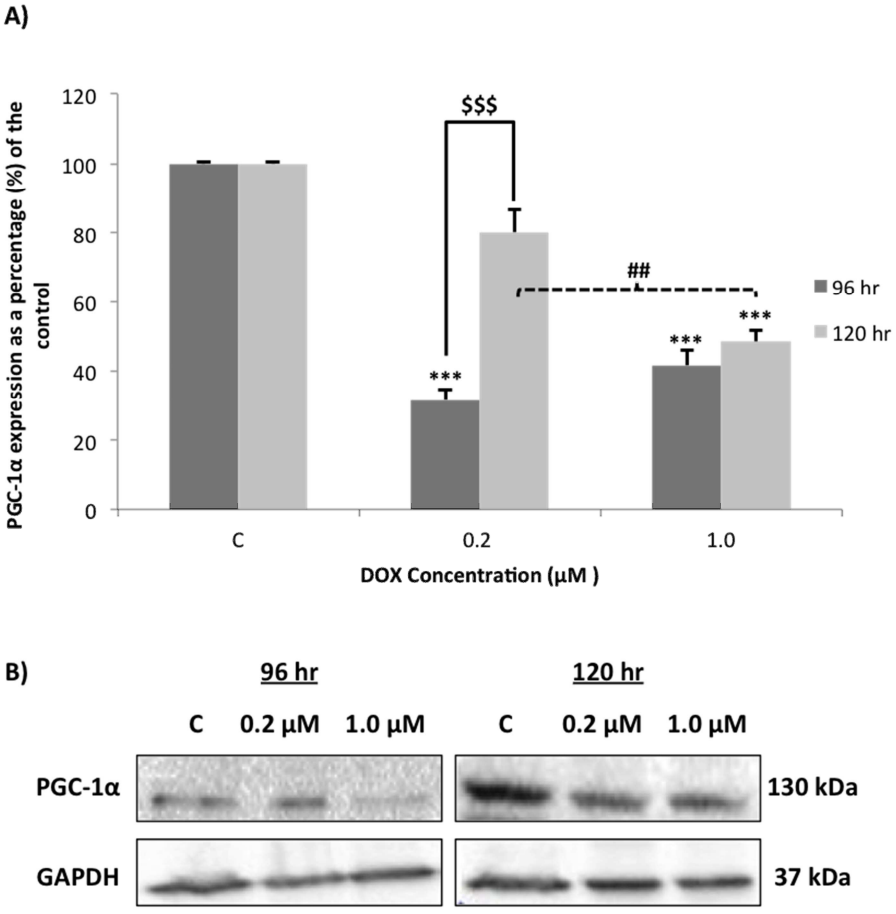

Figure 5.14: The effect of chronic doxorubicin treatment regimes on PGC-1α expression in human-derived Girardi heart cells. (A) Lane profile analysis of PGC-1α. (B) Representative immunoblot of PGC-1α. GAPDH served as the loading control. Girardi cells were treated daily with 0.2 µM and 1.0 µM DOX for 96 and 120 hours. Results are presented as mean ± SEM (n=3). ***P < 0.001 vs Control. $^{\$\$\$}$P < 0.001 96 hr vs 120 hr. $^{\#\#}$P < 0.01 0.2 µM vs 1.0 µM. Abbreviations – C: control, DOX: Doxorubicin, hr: hour, PGC-1α: peroxisome proliferator-activated receptor gamma co-activator 1-alpha, vs: versus.

Stellenbosch University https://scholar.sun.ac.za

The Effect of Chronic DOX Treatment Regimes on Apoptosis

In order to further validate the results obtained from the Caspase-Glo 3/7 Assay, the expression of cleaved-caspase 3 was analyzed with immunoblotting (Figure 5.15). As seen in the results from the Caspase-Glo assay, caspase 3 cleavage was elevated in the 0.2 µM group following both 96 hours [102.00 ± 1.76%] and 120 hours [122.30 ± 3.36%] of treatment, although no significance was observed when compared to the control (100%). However, as the treatment duration increased, a significant reduction in caspase cleavage was observed at both the low [86.28 ± 5.76%, ($p < 0.01$ 96 hr vs. 120 hr.] and high [91.73 ± 4.50%, ($p < 0.01$ 96 hr vs. 120 hr], which further corresponds to the results obtained from the Caspase-Glo assay. These results suggest that apoptosis decreases over time as the concentration of DOX increases.

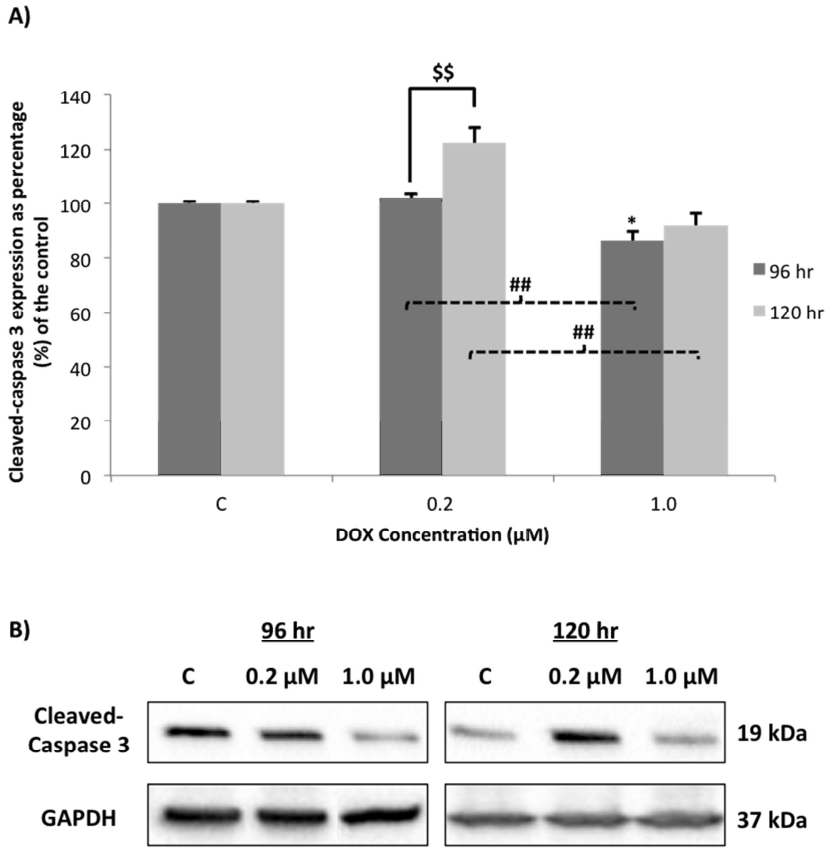

Figure 5.15: The effect of chronic doxorubicin treatment regimes on apoptosis in human-derived Girardi heart cells. Girardi cells were treated daily with 0.2 µM and 1.0 µM DOX for 96 and 120 hours. Results are presented as mean ± SEM (n=3). $^{\Diamond}P< 0.001$. Abbreviations: C = control, DOX = doxorubicin, hr = hour.

Stellenbosch University https://scholar.sun.ac.za

The Effect of Chronic DOX Treatment Regimes on Oxidative Stress

Evaluation of Antioxidant Capacity (ORAC assay)

Results from the ORAC assay indicated that the antioxidant capacity was significantly increased following 0.2 µM DOX treatment for 96 hours [488.90 ± 2.07 µmol TE/L, ($p < 0.001$)] and 120 hours [456.40 ± 1.30 µmol TE/L, ($p < 0.001$)] compared to the control [260.50 ± 18.65 µmol TE/L] respectively (Figure 5.16). However, following 120 hours of treatment antioxidant capacity was significantly reduced compared to the same concentration group after 96 hours of exposure [0.2 µM: 267.70 ± 6.97 µmol TE/L and 1.0 µM: 218.00 ± 7.29 µmol TE/L, ($p < 0.001$ 96 hr vs. 120 hr)]. These results indicate that although cells initially try to survive under these harsh environmental conditions, as the concentration of DOX increases over time the antioxidant capacity is severely diminished. This suggests that cumulative and chronic doses of DOX impair the cells ability to cope under conditions of oxidative stress.

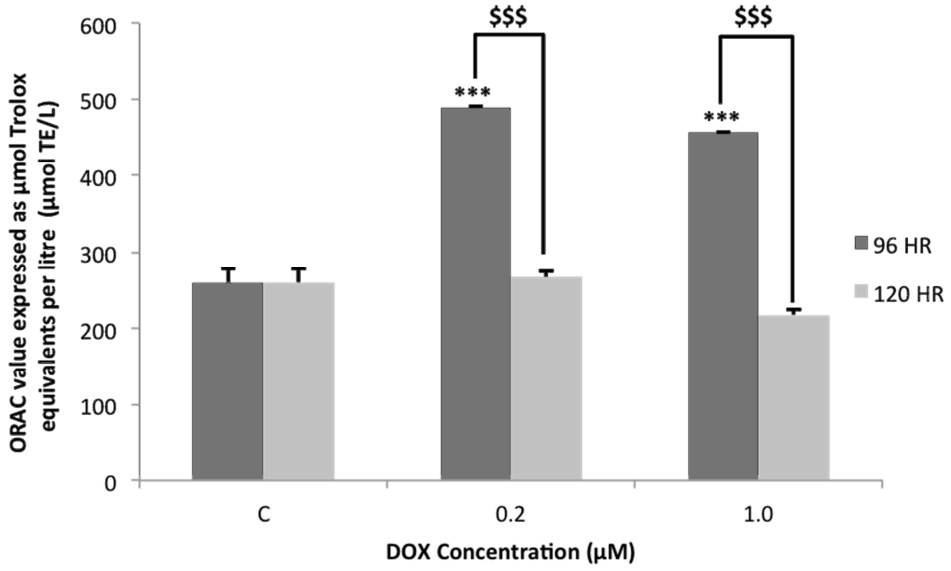

Figure 5.16: The effect of chronic doxorubicin treatment regimes on antioxidant capacity in H9C2 cardiomyoblasts. Cells were treated daily with 0.2 µM and 1.0 µM DOX for 96 and 120 hours. Following treatment the oxygen radical absorbance capacity (ORAC) of each treatment group was determined with a fluorometric assay (n=3). ***P < 0.001 vs

Stellenbosch University https://scholar.sun.ac.za

Control. $^{\$\$\$}$P < 0.001 96 hr vs 120 hr. Abbreviations – C: control, DOX: doxorubicin, hr: hour, TE/L: Trolox equivalent per litre, vs: versus.

Evaluation of Oxidative Damage (TBARS assay)

MDH is a natural by-product of lipid peroxidation, and is used as an indicator for oxidative damage. Lipid peroxidation was significantly reduced following treatment with 0.2 µM DOX for 96 hours [0.71 ± 0.05 µmol/L, ($p < 0.01$)] in comparison to the untreated control [1.33 ± 0.09 µmol/L] (Figure 5.17). No significance difference was however observed following 1.0 µM at the same time point [1.30 ± 0.16 µmol/L]. Treatment with the high DOX also induced no lipid peroxidation, and significance was only observed following 120 hours [0.61 ± 0.07 µmol/L, ($p < 0.001$)] compared to the control group. These results suggest DOX induces no lipid peroxidation or oxidative damage within the Girardi heart cells.

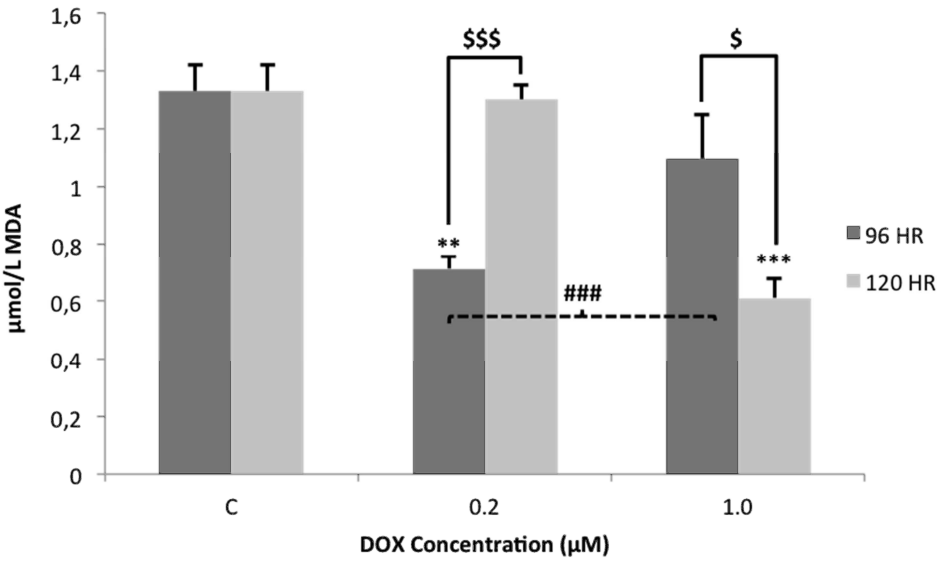

Figure 5.17: The effect of chronic doxorubicin treatment regimes on lipid peroxidation in human-derived Girardi heart cells. Girardi cells were treated daily with 0.2 µM and 1.0 µM DOX for 96 and 120 hours. Following treatment the concentration of thiobarbituric acid reacting substance (TBARS) per sample was determined (n=3). **P < 0.01 and ***P < 0.001 vs Control. $^{\$}$P < 0.05 and $^{\$\$\$}$P < 0.001 96 hr vs 120 hr. $^{\#\#\#}$P < 0.001 0.2 µM vs 1.0 µM Abbreviations – C: control, DOX: doxorubicin, hr: hour, MDA: Malondialdehyde, vs.: versus.

Stellenbosch University https://scholar.sun.ac.za

Evaluation of Oxidative Status (GSH assay)

Determination of reduced glutathione (GSH) to oxidized glutathione (GSSG) was assessed using the GSH:GSSG ratio. This assay could not be performed successfully in the Girardi heart cells. For reasons unknown the results from the assay yielded negative results, which could not be statistically analyzed.

The Effect of Chronic DOX Treatment Regimes on the Endoplasmic Reticulum

Evaluation of BiP Expression

BiP is an ER-associated E3 ubiquitin ligase, which is activated under conditions of ER Stress and regulates UPR signaling (Minamino *et al*., 2010). The effect of chronic DOX treatment on BiP expression was evaluated with western blotting (Figure 5.18). Following 96 hours of treatment with 0.2 μM DOX [] and 1.0 μM DOX [] BiP expression progressively decreased compared to the untreated control (100%). However, after 120 hours BiP expression moderately elevated at both concentration groups ($p < 0.001$ 96 hr vs. 120 hr), with significance observed only in the 0.2 μM DOX group [119.00 ± 6.08%, ($p < 0.05$)] in comparison to the control. Since BiP is not activated after 96 hours treatment suggests that no ER stress has been induced by DOX. Yet following the most chronic treatment with DOX, BiP expression is significantly upregulated thereby suggesting ER stress is produced under conditions of chronic-DOX induced cardiotoxicity.

Stellenbosch University https://scholar.sun.ac.za

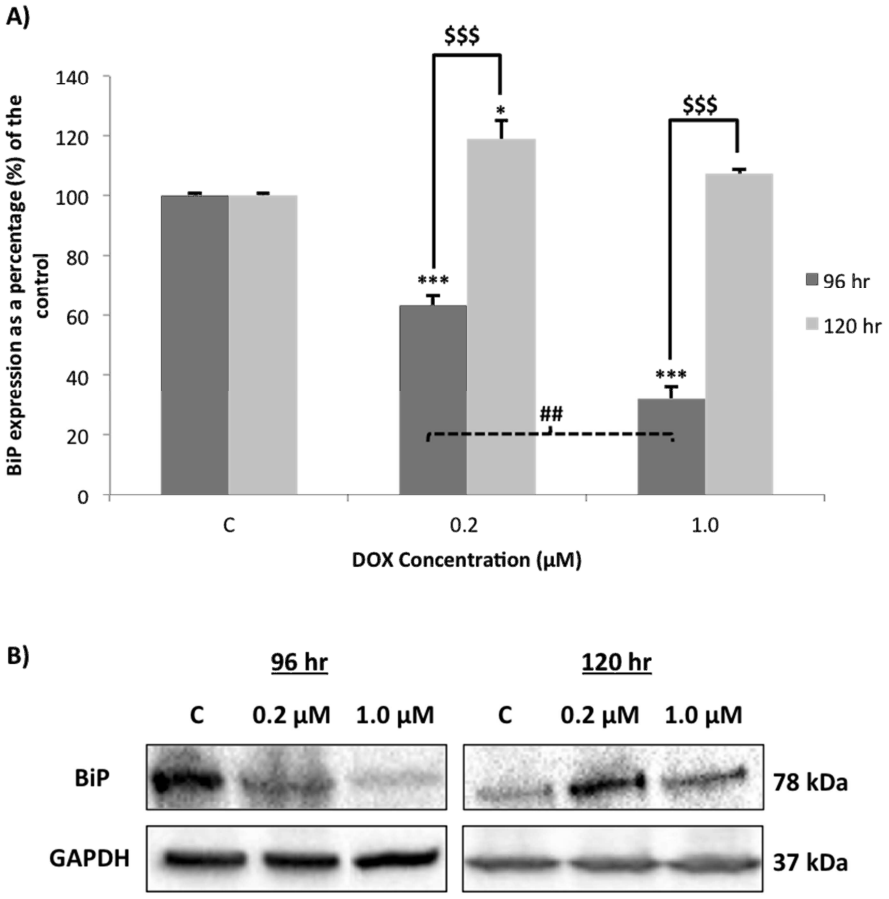

Figure 5.18: The effect of chronic doxorubicin treatment regimes on BiP expression in human-derived Girardi heart cells. (A) Lane profile analysis of BiP. (B) Representative immunoblot of BiP. GAPDH served as the loading control. Girardi cells were treated daily with 0.2 µM and 1.0 µM DOX for 96 and 120 hours (n=3). *P < 0.05, **P < 0.01 and ***P < 0.001 vs Control. $^{\$\$\$}$P < 0.001 96 hr vs 120 hr. $^{\#\#\#}$P < 0.001 0.2 µM vs 1.0 µM. Abbreviations – BiP: binding immunoglobulin protein, C: control, DOX: doxorubicin, hr: hour, vs: versus.

Evaluation of ATF4 Expression

ATF4 downstream UPR protein activated via the PERK-elF2α-ATF4 axis of the UPR pathway. To examine whether chronic DOX-induced cardiotoxicity influenced ATF4 expression by ER stress, western blotting analysis was performed (Figure 5.19). Compared to the control (100%), relatively no change in ATF expression was observed following

Stellenbosch University https://scholar.sun.ac.za

treatment. Except for treatment with the most cumulative, chronic concentration of DOX, which significantly reduced ATF4 expression in comparison to the control [62.10 ± 5.23%, ($p < 0.001$)]. In addition, the evaluation of ATF4 expression between groups demonstrated that after 120 hours of treatment, ATF4 was significantly reduced as the concentration of DOX increased ($p < 0.01$). These results are similar to those observed in the H9C2 cardiomyocytes and suggest that chronic DOX treatment may inhibit downstream UPR signaling.

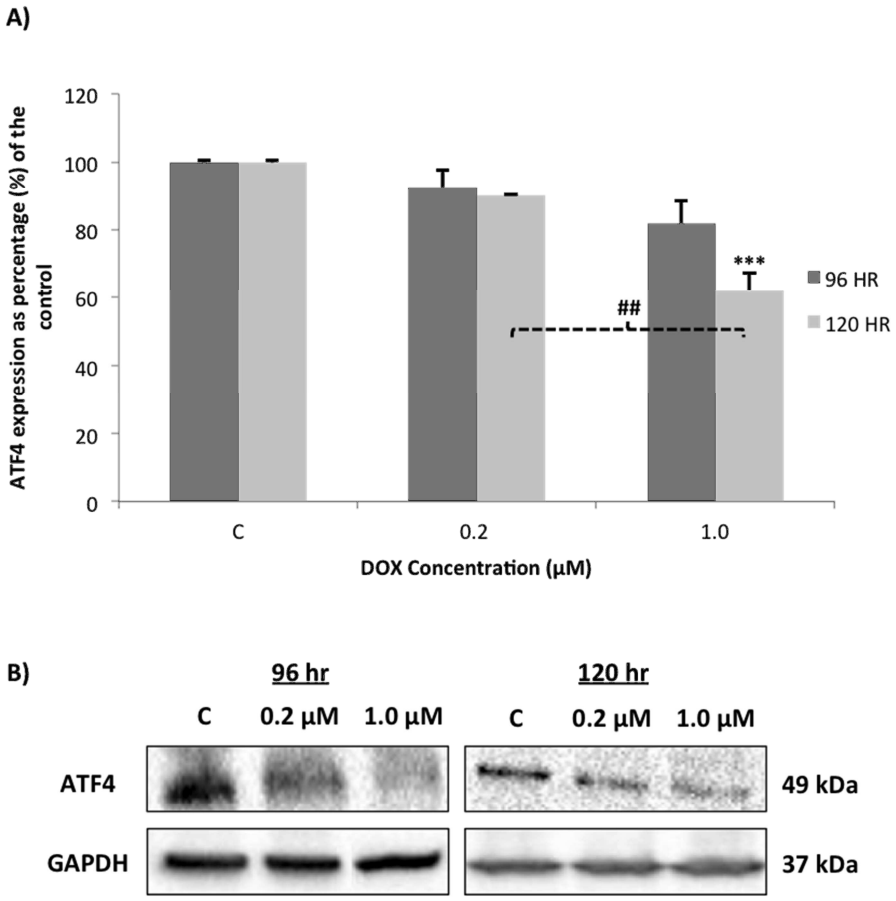

Figure 5.19: The effect of chronic doxorubicin treatment regimes on ATF4 expression in human-derived Girardi heart cells. (A) Lane profile analysis of ATF4. (B) Representative immunoblot of ATF4. GAPDH served as the loading control. Girardi cells were treated daily with 0.2 µM and 1.0 µM DOX for 96 and 120 hours (n=3). ***P < 0.001 vs Control. $^{##}$P < 0.01 0.2 µM vs 1.0 µM. Abbreviations – ATF4: activating transcription factor 4, C: control, DOX: doxorubicin, hr: hour, vs: versus.

Stellenbosch University https://scholar.sun.ac.za

Evaluation of ER Load

As previously discussed, ER load, an indicator for ER expansion, was used as an additional marker to evaluate ER stress. Results from flow cytometry analysis demonstrate that ER load was significantly increased after 96 hours of treatment with both the 0.2 µM DOX [162.40 ± 9.43%, ($p < 0.05$)] and 1.0 µM DOX [172.70 ± 9.11%, ($p < 0.01$)] when compared to the control (100%), (Figure 5.20). Whereas after 120 hours, ER load was significantly increased following treatment with only the highest concentration of DOX [258.30 ± 14.89%, ($p < 0.01$ vs. Control)]. Treatment with the highest concentration of DOX induced ER stress at both time points, which correlates to the increase in BiP observed after 120 hours. Together with results discussed above, this study showed that only chronic DOX treatment induces ER stress activation of the UPR in Girardi heart cells.

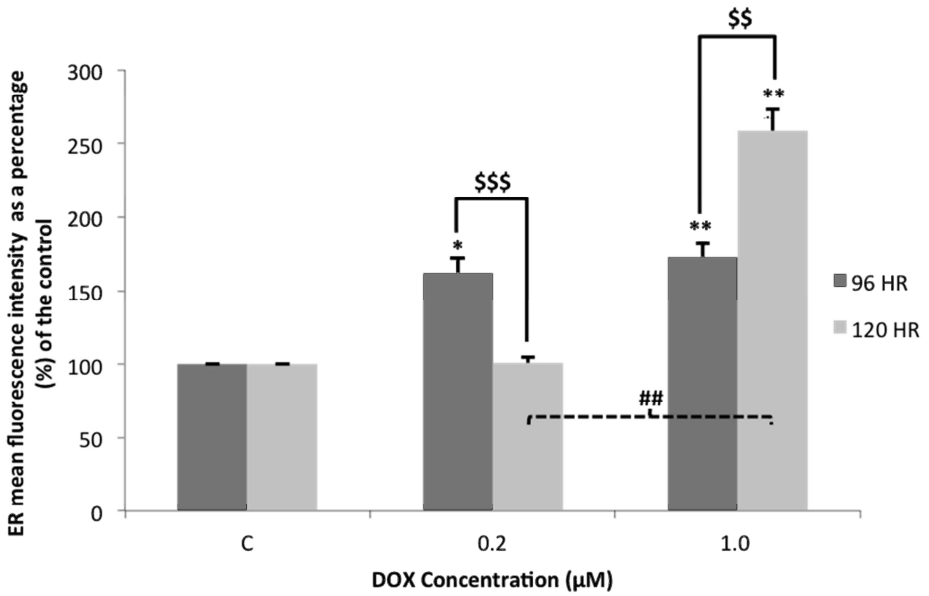

Figure 5.20: The effect of chronic doxorubicin treatment regimes on ER load in human-derived Girardi heart cells. Girardi cells were treated daily with 0.2 µM and 1.0 µM DOX for 96 and 120 hours. Following treatment cell were stained with ER-tracker and mean fluorescence intensity was measured by flow cytometry (n=3). *P < 0.05 and **P < 0.01 vs Control. $^{\$\$}$P < 0.01 and $^{\$\$\$}$P < 0.001 96 hr vs 120 hr. $^{\#\#}$P < 0.01 0.2 µM vs 1.0 µM. Abbreviations – C: control, DOX: doxorubicin, ER: endoplasmic reticulum, hr: hour, vs: versus.

Stellenbosch University https://scholar.sun.ac.za

The Effect of Chronic DOX Treatment Regimes on Intracellular and Mitochondrial Calcium Levels

Calcium is an essential component of the excitation-contraction coupling process, and a disruption of intracellular calcium levels has previously been associated with contractile dysfunction and the pathogenesis of heart failure (Rossini *et al*., 1986). Given the role ER stress, oxidative stress and mitochondrial dysfunction play in disrupting calcium homeostasis this study chose to investigate the effects of chronic DOX cardiotoxicity on calcium activity within the cells. Due to financial constraints this study could not investigate the effects of chronic DOX treatment on mitochondrial calcium levels.

Following chronic DOX administration the intracellular calcium levels were determined using flow cytometry (Figure 5.21). Results demonstrated that intracellular calcium levels were significantly increased over time following treatment with 0.2 μM DOX ($p < 0.05$ 96 hr vs. 120 hr), however no significance was observed when compared to the control group (100%). Following treatment with 1.0 μM DOX significantly and progressively increased cytosolic calcium levels following 96 hours [319.40 ± 8.34%, ($p < 0.001$)] and 120 hours [581.00 ± 10.50%, ($p < 0.001$)] of administration compared to the control. Overall these results indicate that elevated cytosolic calcium is not only highly dependent on duration of DOX treatment, but also on the concentration of DOX administrated, which is comparable to results obtained from the H9C2 cell line.

Stellenbosch University https://scholar.sun.ac.za

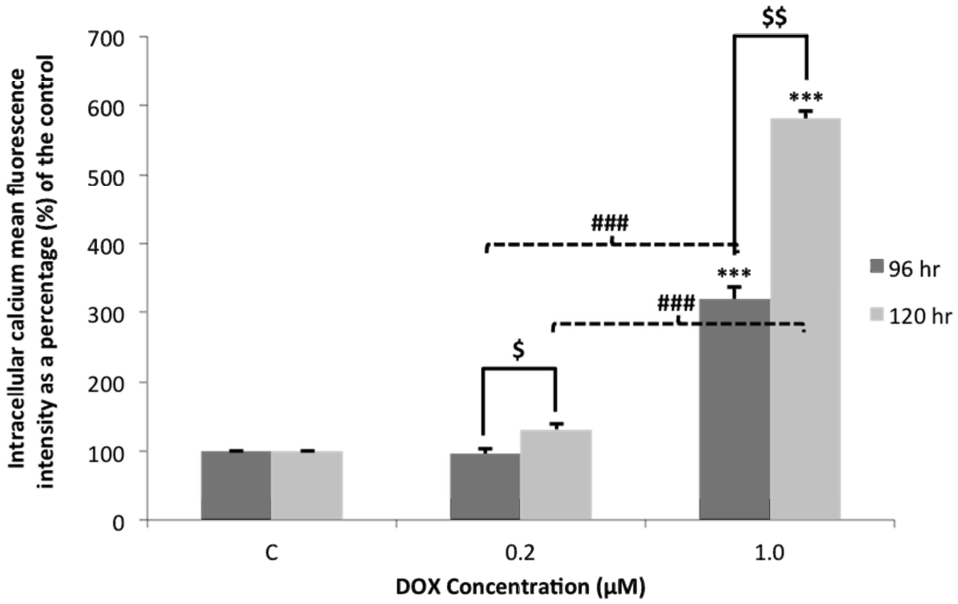

Figure 5.21: The effect of chronic doxorubicin treatment regimes on intracellular calcium in human-derived Girardi heart cells. Girardi cells were treated daily with 0.2 µM and 1.0 µM DOX for 96 and 120 hours. Following treatment H9C2 cardiomyoblasts were stained with the specific intracellular calcium dye, Calcium Green and mean fluorescence intensity was measured using flow cytometry (n=3). ***P < 0.001 vs Control. $^{\$}$P < 0.05 and $^{\$\$}$P < 0.01 96 hr vs 120 hr. $^{\#\#\#}$P < 0.001 0.2 µM vs 1.0 µM. Abbreviations – C: control, DOX: doxorubicin, hr: hour.

Stellenbosch University https://scholar.sun.ac.za

APPENDIX B – Protocols

Protocol 1: Cell Culture

Before any work or experiments were carried out under the hoods, hands were washed and sterile gloves were put on. Hands with gloves were washed again and sprayed with 70% ethanol before laminar hoods were cleaned. Hoods were sprayed and wiped down with 70% ethanol, and hands were sprayed again each time before placing them under the hood in order to maintain a sterile environment

- Growth medium pre-heated to 37˚C in bead bath
- Remove cryovile (freezing tube) containing H9C2 cardiomyoblasts/Girardi's from liquid nitrogen freezing chamber
- Cryovile containing 1ml of FBS/DMSO with 1 x 10^6 cells thawed at room temperature
- 8 ml of growth medium (see Appendix C) added to 1 x 75cm^2 flask
- Thawed cells added to 75cm^2 flask
- Gently swirl flask to ensure the equal distribution of cells
- Cells incubated at 37˚C in a 5% CO_2 atmosphere
- Following day, check to ensure cells have plated. Pre-heat growth medium and PBS (see Appendix C).
- Refresh growth medium; Growth medium discarded and cell monolayer rinsed with 8 ml warm PBS. 8 ml of new, warm and sterile growth medium added to falcon tube.
- Cells placed back into incubator
- Growth medium refreshed every 2 days hereafter, until desired confluency established.

Subcultering (seeding for experiments)

- Growth medium, PBS and Trypsin pre-heated to 37˚C in bead bath
- Remove growth medium from 75cm^2 flask containing cells (75 – 80 % confluent)
- Rinse cell monolayer with warm, sterile PBS
- Discard PBS
- Add 4 ml with Trypsin
- Incubate cells at 37˚C for ± 5 minutes in cell shaker.

Stellenbosch University https://scholar.sun.ac.za

- Using microscope monitor flask intermittently, to check if cells have lifted.
- Add 8 ml growth medium to 75cm^2 flask in order to neutralize trypsin
- Decant into 50 ml falcon
- Count cells using haemocytometer (see protocol 2)
- Pipette desired density of cells into flasks/plates required for experiments:

Flask/plate	Cell Density
6-well plate	200 – 250 000
12-well plate	250 – 300 000
96-well plate	30 000
25cm^2 flask	350 – 450 000

- New culture flask/plate with appropriate amount of growth medium incubated at 37˚C in a 5% CO_2 atmosphere. Cell growth was monitored until desired confluency was established and experimental protocols were carried out.

Stellenbosch University https://scholar.sun.ac.za

Protocol 2: Cell counting with haemocytometer

- Clean haemocytometer with ethanol before use
- Breath on the coverslip and place on haemocytometer (breathing enables the coverslip to stick to the surface of the plate)
- A sample *(10-15ul)* of resuspended cell solution added to each chamber, until both counting grids are covered.
- Check for bubbles – if bubbles form, redo above 3 steps
- Total number of cells are counted under the microscope
    a. Count cells in each block of A first (record number)
    b. Then count cells in each of block B (record number)
- Average number of cells calculated. This average was then multiplied by 1×10^4 in order to calculate the number of cells per milliliter of the original cell suspension

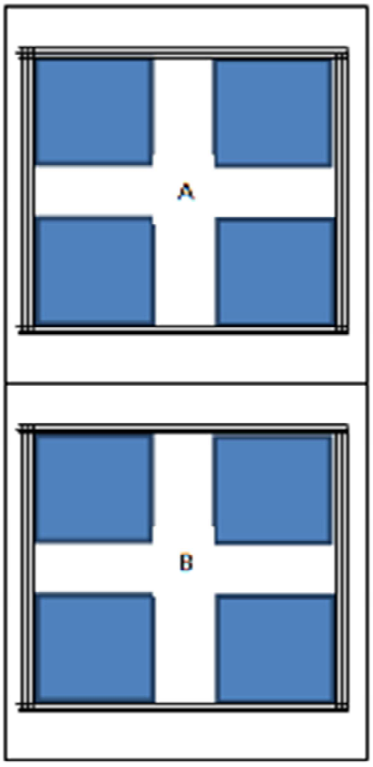

Stellenbosch University https://scholar.sun.ac.za

Protocol 3: Doxorubicin dose-response treatment protocol

- Cells were cultured in 24-well plates as previously described
- Once desired confluency was established cells were treated with increasing concentration of DOX (as indicated in the figure below) for 72, 96 and 120 hours (1 x 24 well plate = 1 time point).

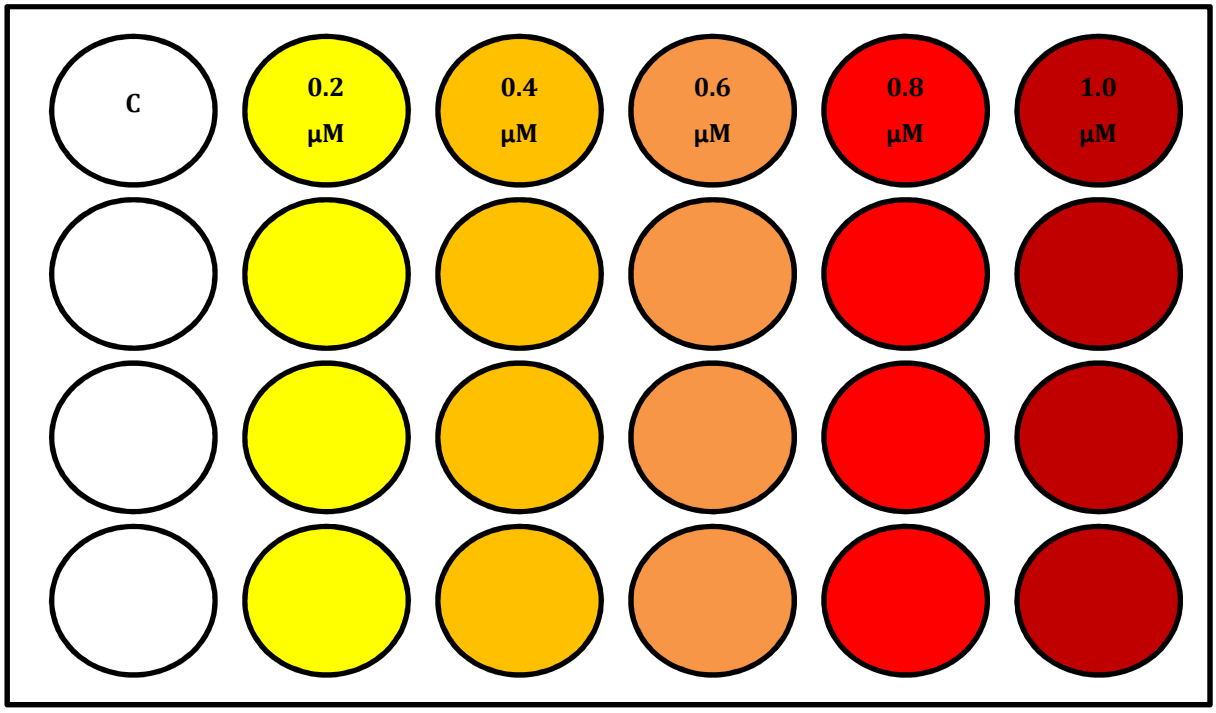

- Treatment was made up fresh each day throughout treatment protocol.
- Following last day of treatment, specific experiments were carried out

Stellenbosch University https://scholar.sun.ac.za

Protocol 4: MTT Assay

- Prepare the following MTT solutions (see appendix C);
  - 1% Isopropanol
  - 0.1% Triton
  - Isopropanol/Triton solution in 50/1 ratio
  - 1% MTT (0.01g/1ml PBS) – *this solution must be made fresh before use, and covered in foil to protect from light.*
- Cells were cultured and treated as previously described in protocol 3
- Following last day of treatment, cell growth medium was discarded.
- DO NOT rinse cell monolayer with PBS *(this will prevent cells from lifting/loosening)*
- Turn off hood light *(remember MTT is light sensitive)*
- 1% MTT added to each well
- Cover plates in foil and place in humidified incubator (37˚C) for two hours
- After two hours:
  - <u>If some cells have loosened:</u>
    - Contents of wells transferred to corresponding, labeled eppendorf tubes
    - Epi's are placed in centrifuge and spun down for 2 min at 1000 rpm
    - Supernatant discarded
    - 2ml isopropanol:triton solution added to each epi
    - Cells resuspended
    - Contents of epi's added back into corresponding wells
    - Plates covered in foil and placed on belly dancer for 5 min
  - <u>If no cells have loosened:</u>
    - Contents of cell discarded
    - 2ml isopropanol:triton solution added to each well
    - plates covered in foil and placed on belly dancer for 5 min
- Absorbency read at 540 nm on spectrophotometer, using isopropanol:triton solution as blank. If any absorbency values are greater than one, the supernatant must be diluted.

Stellenbosch University https://scholar.sun.ac.za

Protocol 5: Caspase-Glo® 3/7 Assay

- Allow the Caspase-Glo® Reagent to thaw to room temperature ± 45 minutes before beginning assay
- Cells cultured and treated as previously described in protocol 2
- Remove culture plate from incubator, and allow for 10 minutes to equilibrate to room temperature
- Transfer 100 µl of cell growth media to the corresponding well of the white-walled 96-well plate (supplied by Promega)
- Add 100 µl of Caspase-Glo® reagents to each well of white-walled 96-well plates
- Place plate on belly dancer at 300-500 rpm for ± 30 seconds, in order to mix well contents
- Incubate plates in the dark for 1 hour at a constant temperature
- Using luminometer plate reader, measure the caspase luminescence

Protocol 6: Doxorubicin main experimental treatment protocol

Following MTT and Caspase-Glo® 3/7 assay's the following time points and DOX concentrations were selected to continue with for the remainder of the study;

  - 96 and 120 hour treatment times
  - 0.2 µM and 1.0 µM DOX concentrations
- Cells were cultured as previously described in protocol 1
- Once desired confluency was established, cells were treated daily with 0.2 µM and 1.0 µM DOX for 96 and 120 hours
- Fresh treatment was made up daily
- Following last day of treatment, specific experiments were carried out accordingly

Stellenbosch University https://scholar.sun.ac.za

Protocol 7: Assessment of Mitochondrial and ER Load with Flow Cytometry

- For this technique cells were cultured in 25 cm^2 flasks and treated as previously described in protocol 5. The mitochondrial specific dye, MitoTracker® Green FM and the ER specific dye, ER-Tracker™ Blue-White were used to measure mitochondrial and ER load respectively

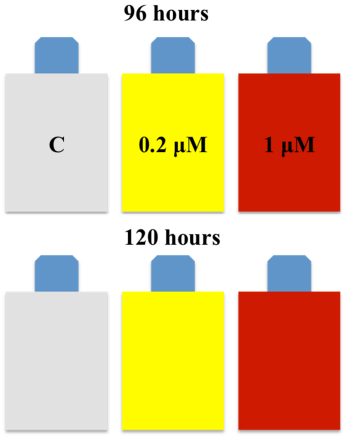

- PBS, Trypsin and Growth medium were pre-heated to 37˚C in bead bath
- Growth medium was discarded and cells were rinsed with warm, sterile PBS
- 2 ml trypsin was incubated with cells for 2-3 minutes, until cells detached from the flask surface
- 4 ml culture medium was added to cell suspension to neutralize trypsin. Cell suspension transferred to corresponding 15 ml falcon tube and centrifuged for 3 minutes at 1500 rpm

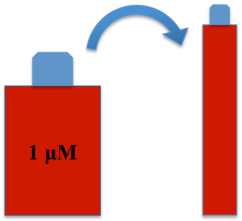

- Decant supernatant
- Cells resuspended in 500 µL PBS
- Prepare 1-5 mM DMSO stock solution of Mitotracker (see Appendix C)
- MitoTracker® and ER-Tracker™ were directly added into the cell suspension at final concentration of 0.5 µM and 1.0 µM respectively and incubated for 15 minutes at room temperature (see appendix C for dye preparation)

Stellenbosch University https://scholar.sun.ac.za

- Analysis followed on the flow cytometer (BD FASCAria I) immediately after incubation. Cells resuspended/vortexed again in order to prevent clumping and blocking of the stream.
- A minimum of 10 000 cells were collected using the 470 nm and 490 nm laser and the 430-640 nm emission filters. Fluorescence intensity signal was measured using the geometric mean on the intensity histogram.
-

Protocol 8: Assessment of Intracellular Calcium with Flow cytometry

For this technique cells were cultured in 25 cm^2 flasks and treated as previously described in protocol 5. The dye, Calcium Green™ -5N AM was used specifically to measure intracellular calcium following

- PBS, Trypsin and Growth medium were pre-heated to 37˚C in bead bath
- Growth medium was discarded and cells were rinsed with warm, sterile PBS
- 2 ml trypsin was incubated with cells for 2-3 minutes, until cells detached from the flask surface
- 4 ml culture medium was added to cell suspension to neutralize trypsin. Cell suspension transferred to corresponding 15 ml falcon tube and centrifuged for 3 minutes at 1500 rpm
- Decant supernatant
- Cells resuspended in 500 µL PBS
- Prepare 1-5 mM DMSO stock solution of Calcium Green™ (see Appendix C)
- 5 µM Calcium Green™ was directly added to cell suspension and left to incubate for 20 minutes at room temperature (see appendix C for dye preparation)
- Analysis followed on the flow cytometer (BD FASCAria I) immediately after incubation. Cells resuspended/vortexed again in order to prevent clumping and blocking of the stream.
- A minimum of 10 000 cells were collected using the 488 nm laser and 530/30 nm emission filters. Fluorescence intensity signal was measured using the geometric mean on the intensity histogram.

Stellenbosch University https://scholar.sun.ac.za

Protocol 9: Visualization of mitochondria and ER morphology with fluorescence microscopy

For this technique cells were cultured in 8-chamber slides and treated as previously described in protocol 5. The mitochondrial specific dye, MitoTracker® Green FM and the ER specific dye, ER-Tracker™ Blue-White were used to measure mitochondrial and ER load respectively.

- PBS, Trypsin and Growth medium were pre-heated to 37˚C in bead bath
- Growth medium was discarded and cells were rinsed with warm, sterile PBS
- Prepare 1-5 mM DMSO stock solution of Mitotracker (see Appendix C)
- MitoTracker® and ER-Tracker™ were directly added to the adherent cells at final concentration of 0.5 µM and 1.0 µM respectively and incubated for 20 minutes at room temperature (see appendix C for dye preparation)
- Cells were visualized with the fluorescence microscope at 60 X magnification with the FITC and DAPI excitation filters respectively. Z-stack images were acquired.

Protocol 10: Visualization of intracellular calcium

For this technique cells were cultured in 8-chamber slides and treated as previously described in protocol 5. The dye, Calcium Green™ -5N AM was used specifically to measure intracellular calcium following treatment.

- PBS, Trypsin and Growth medium were pre-heated to 37˚C in bead bath
- Growth medium was discarded and cells were rinsed with warm, sterile PBS
- Prepare 1-5 mM DMSO stock solution of Mitotracker (see Appendix C)
- 5 µM Calcium Green™ was directly added to cell suspension and left to incubate for 20 minutes at room temperature (see appendix C for dye preparation)
- Cells were visualized with the confocal fluorescence microscope at 60 X magnification with the 488 nm laser and 534-569 excitation filter.

Stellenbosch University https://scholar.sun.ac.za

Protocol 11: Visualization of mitochondrial calcium

For this technique cells were cultured in 8-chamber slides and treated as previously described in protocol 5. The dyes, MitoTracker® Green FM and Rhod-2 AM cell permeant were used specifically to colocalize and measure mitochondrial calcium following treatment.

- PBS, Trypsin and Growth medium were pre-heated to 37˚C in bead bath
- Growth medium was discarded and cells were rinsed with warm, sterile PBS
- Prepare 1-5 mM DMSO stock solution of MitoTracker® Green and Rhod-2 (see Appendix C)
- 0.5 μM MitoTracker® Green and 4 μM Rhod-2 was directly added to adherent cells and left to incubate for 20 minutes at room temperature (see appendix C for dye preparation)
- Cells were visualized with the confocal fluorescence microscope at 60 X magnification with the 488 nm and 561 nm lasers and 575-635 and 534-569 excitation filters. Colocalization of PE-Texas Red and FITC specific excitation filters were used to determine specific mitochondrial calcium.

Stellenbosch University https://scholar.sun.ac.za

Protocol 12: ORAC Assay

This experiment was performed at the Oxidative Stress Research Center at the Cape Peninsular University of Technology. The following protocol was provided by CPUT.

Cells were cultured in 6-well plates and treated as previously described in protocol 5. This assay runs at 37 °C. Do not use the first two columns and the last column of plate as the machine will provide an inaccurate read. Switch on the plate reader and Fluoroskan 30 minutes before beginning experiment.

Sample Preparation:

- Following treatment, cells were washed with PBS.
- 75 µL PBS added to each well (Please note: 2 wells combined = 1 sample. Therefore total PBS/sample in Epi = 150 µL)
- Cells scraped using cell scraper (no RIPA or TRYPSIN should be used)
- Cells added to their corresponding, iced epi's
- Sonicate cells
- Centrifuge cells at 1500 rpm for 3 minutes
- Aliquot and store supernatant at -80°C until required for assay.

Procedure:

- ORAC assay performed in black 96-well plate
- Prepare the following reagents (see appendix C)
    - PBS (75 mM, pH 7.4)
    - Fluorescein Stock (Sigma #F6377)
    - Fluorescein working solution
    - Peroxyl radical (Sigma #440914) / AAPH
    - Trolox (standard) 250 µM stock (Sigma #238831)
- Prepare Antioxidant standard curve:

Stellenbosch University https://scholar.sun.ac.za

Epi	Concentration (µM)	Trolox stock (µL)	Phosphate buffer (uL)	Well
A	0	0	750	A1-3
B	83	125	625	A4-6
C	167	250	500	A7-9
D	250	375	375	A10-12
E	333	500	250	B1-3
F	417	625	125	B4-6

- Spin down samples – they must not be turbid
- Add 6 mL phosphate buffer to the AAPH weighed earlier, mix well. Put solution in water bath at 37 °C until needed.
- Add 12 µL standards to each well
- Add 12 µL of controls per well
- Add 12 µL of samples per well in triplicate
- Add 138 µL of fluorescein working solution to each well using a multichannel pipette
- Add 50 µL of the AAPH solution to each well using a multichannel (add this solution AT the plate reader)
- Put the plate into the plate reader
- Read for 2 hours (excitation = 485 nm and emission = 530 nm)

Stellenbosch University https://scholar.sun.ac.za

Protocol 13: TBARS assay

This experiment was performed at the Oxidative Stress Research Center at the Cape Peninsular University of Technology. The following protocol was provided by CPUT.

Cells were cultured in 6-well plates and treated as previously described in protocol 5.

Sample Preparation:

- Following treatment, cells were washed with PBS.
- 75 µL PBS added to each well (Please note: 2 wells combined = 1 sample. Therefore total PBS/sample in Epi = 150 µL)
- Cells scraped using cell scraper (no RIPA or TRYPSIN should be used)
- Cells added to their corresponding, iced epi's
- Sonicate cells
- Centrifuge cells at 1500 rpm for 3 minutes
- Aliquot and store supernatant at -80°C until required for assay.

Procedure:

- Set waterbath to 100°C
- Prepare TBARs reagents (see appendix C)
  - 4 mM BHT
  - 0.2 M ortho-phosphoric acid
  - 0.1 M NaOH
  - TBA Reagent
  - Saturated NaCl
- Use 2 ml epi's for remainder of experiment, and punch holes in their lids.
- Let 50 µL water/PBS be the blank
- Transfer 50 µL of sampler into corresponding epi (with hole in the lid)
- Add 6.25 µL BHT to each sample
- Add 50 µL ortho-phosphoric acid to each sample
- Vortex epi's
- Add 6,25 µL TBA reagent to each sample
- Add 30 µL of n-butanol and 50 µL saturated NaCl

Stellenbosch University https://scholar.sun.ac.za

- Vortex epi's
- Heat samples in 100°C waterbath for 45 minutes (be strict with time and degrees for each repeat)
- Transfer 75 µL of separated butanol phase into white 96-well plate
- Read absorbency at 532-573 nm

Protocol 14: Glutathione Assay

This experiment was performed at the Oxidative Stress Research Center at the Cape Peninsular University of Technology. The following protocol was provided by CPUT.

Cells were cultured in 6-well plates and treated as previously described in protocol 5.

Sample Preparation:

- Following treatment, cells were washed with PBS.
- 75 µL PBS added to each well (Please note: 2 wells combined = 1 sample. Therefore total PBS/sample in Epi = 150 µL)
- Cells scraped using cell scraper (no RIPA or TRYPSIN should be used)
- Cells added to their corresponding, iced epi's
- Sonicate cells
- Centrifuge cells at 1500 rpm for 3 minutes
- Aliquot and store supernatant at -80°C until required for assay.

Procedure:

- The following reagents where prepared prior to experiment by staff at CPUT:
  - Buffer A (500 nM $NaPO_4$, 1mM EDTA, pH 7.4)
  - 1 mM NADPH in 12 mL Buffer A
  - M2VP (30 mM in 0.1 M HCl)
  - DTNB (0.3 mM in Buffer A)
  - Standard solution prepared in Buffer A
    - GSH = 2 µM
    - GSSG = 1.5 µM
  - 1 mL Glutathione reductase (16 µL in 984 µl Buffer A)
- Prepare GSH standards as follows:

Stellenbosch University https://scholar.sun.ac.za

	Blank	1	2	3	4	5
GSH (µL)	0	167	333	500	667	833
Buffer A (µL)	1000	833	667	500	333	167

- Prepare GSSG standard as follows:

	Blank	1	2	3	4	5
GSSG (µL)	0	167	333	500	667	833
Buffer A (µL)	1000	833	667	500	333	167

Apply the following procedure for both the GSH and GSSG 96-well plates:

- Add 50 µL standards/samples to the wells of a 96-well plate
- Add 50 µL of the DTNB using a multichannel
- Add 50 µL of the glutathione reductase using a multichannel
- Mix briefly and incubate for 5 minutes at 25 °C in a preheated BioTek plate reader
- Add 50 µL NADPH to each well as quickly as possible (30 seconds max)
- Measure absorbance at 412 nm every 30 seconds for 3 minutes
- Use linear slope of the standards to calculate concentration of samples

Stellenbosch University https://scholar.sun.ac.za

Protocol 15: Proteasome-Glo™ assay

For this technique cells were cultured in clear-bottomed, sterile 96-well plates and treated as previously described in protocol 5. Three different catalytic activities were assessed in this assay; chymotrypsin-like, casapse-like and trypsin-like catalytic activities, therefore 1 x 96-well plate represented 1 catalytic site.

Preparation of Proteasome-Glo™ reagent:

Protocol according to manufacturers instructions

- Thaw the Proteasome-Glo Buffer
- Allow the buffer and the Luciferin Detection Reagent to set to room temperature
- Add appropriate volume of the buffer to the detection reagent (in amber bottle)
- Thaw appropriate substrate (chymotrypsin-like, trypsin-like or caspase-like) and let it equilibrate to the room temperature. Vortex briefly before use
- Prepare the Proteasome-Glo Reagent by adding the substrate (chymotrypsin-like, trypsin-like or caspase-like) to the Luciferin Detection Reagent. Remember to label reagent bottle so you know which substrate was used.

Proteasome-Glo Assay	Substrate	Volume of substrate added	Substrate concentration in reagent
Chymotrypsin-Like Assay	Suc-LLVY-Glo	50ul	40uM
Trypsin-Like Assay	Z-LRR-Glo	100ul	30uM
Caspase-Like Assay	Z-nLPnLD-Glo	50ul	40uM

- Allow the Proteasome-Glo Reagent to sit at room temperature for 1 hour before use.

Stellenbosch University https://scholar.sun.ac.za

Procedure:

Protocol according to manufacturers instructions

- Following treatment, remove growth medium.
- Add 50 µl growth medium to each 96-well using multichannel pipette
- Use multichannel pipette to add 50ul of Proteasome-Glo Reagent to each 96-well. Be careful not to cross contaminate.
- Gently mix the well contents using plate shaker at 300-500rmp for 30seconds
- Incubate at room temperature for 20-30minutes. Temperature fluctuations will affect the luminescent readings, so constant-temperature incubator may be required if room temperature constantly changes
- Record luminescence with plate-reading luminator

Stellenbosch University https://scholar.sun.ac.za

Protocol 16: Western Blotting

For this technique cells were cultured in 6-well plates and treated as previously described in protocol 5.

Cell harvesting and preparation of lysates:

- Work on ice at all times
- Following last day of treatment, old growth medium is discarded
- Monolayer of cells is quickly washed 3 x with ice cold PBS (to ensure all FBS is removed from cells)
- PBS discarded
- 50 µL of RIPA buffer is added to the monolayer of cells
- Plates/flasks are swirled around to ensure entire base is covered with RIPA buffer and left for 3 -5 minutes
- Cells are scraped from the surface of the plate/flasks using a sterile cell scraper
- Scraped cells are pipetted into their corresponding, chilled epi's
- Epi's can be stored in the -80˚C until further experiments are carried out

Bradford protein quantification:

- Work on ice at all times to prevent the proteins from denaturing
- Cell samples are thawed (if frozen) and placed on ice
- Cell samples are sonnicated in order to rupture cell walls and release proteins
- After sonication, samples are centrifuged at 8000rpm for 10minutes
- Using Bradford working solution, make up the standard curve in 7 different eppendorf (epi) tubes as follows:

Epi	Distilled Water	BSA	Bradford Reagent
1	0ul	100ul	900ul
2	20ul	80ul	900ul
3	40ul	60ul	900ul
4	60ul	40ul	900ul
5	80ul	20ul	900ul
6	90ul	10ul	900ul
7	100ul	0ul	900ul

Stellenbosch University https://scholar.sun.ac.za

(BLANK)			

- Vortex solutions thoroughly
- Leave solutions to stand on ice for a few minutes
- Samples from previous protocol are used to prepare for protein determination
    - Pipette 5 µl from each centrifuged sample into a new epi
    - Add 95 µl distilled water to the epi
    - Add 900 µl Bradford reagent to the epi
    - Vortex solutions
- Read absorbance values at 595 nm
    - Use epi #7 to zero the spectrophotometer
    - Read and record values for standard curve first
    - Read and record values for samples second
- Using excel, plot standard curve (x-axis = protein concentration, y-axis = the mean OD). Add in the absorbance values for the samples and determine final calculation for protein concentration in µl/ug
- Once the concentration of each sample has been determined, pipette desired amount into a new eppendorf tube and add required amount of sample buffer
- Freeze and store protein samples in -80˚C freezer until needed

Preparation and loading of polyacrylamide gels:

- Prepare the following solutions (see appendix C)
    - 1.5 M Tris-HCl (ph. 8.8)
    - 0.5 M Tris-HCl (ph. 6.8)
    - 10% Sodium dodecyle sulfate (SDS)
    - 10% Ammonium persufate (APS)
    - 1 X Running buffer
    - 10 X Running buffer
    - 1 x TBS
    - 10 X TBS-T
    - 5% Milk blocking solution
- Clean glass plates with 70% alcohol

Stellenbosch University https://scholar.sun.ac.za

- Assemble glass places and place onto plastic apparatus with rubber and firmly clip it into place
- Check for leaks using distilled water. If leaks, reassemble glass plates and apparatus. If there is no leak, shake out water and absorb any remaining water with a paper towel.
- Make up desired separating gel (see appendix C). Ensure that temed is added last.
- Using squeeze pipette, add separating gel into the assembly. Avoid making bubbles
- Add iso-butanol using squeeze pipette. Iso-butanol ensure that the gel sets in a straight line and prevent the oxidation of the gel
- Allow gel to set for 30-40 minutes
- Rinse of iso-butanol with dH_{2O}
- Make up stacking gel
- Using squeeze pipette, add stacking gel on top of separating gel.
- Immediately add 10/15 well combs into stacking gel at an angle (prevent formation of bubbles). Do not push too deep or push combs in too fast
- Allow gel to set. While gel is setting prepare 10 x running buffer and thaw samples
- Denature samples by boiling at 95˚C for 5 minutes.
- Centrifuge samples for 1 minute at 5000 rpm
- Remove combs from gel gently and rinse with dH_2O. Use blotting paper to drain water that remains in each well
- Take glass off assembly and place onto U-shaped Core-latch and then click to secure. Fill with 10 x running buffer and check for leaks.
- Place apparatus into the tank and add 10 x running buffer into the middle compartment until it overflows into the wells

Loading the protein samples:

- Place yellow guide on top of the apparatus (over the middle compartment)
- Using 20 µl pipette, add 6 µl pre-stained marker into the first well on the left
- Add samples into the next wells, using a new pipette head for each sample
- Once all the samples have been loaded, remove well guide and add running buffer to the outer compartments (1/2 = 2 gels, full = 4 gels)
- Place green lid on apparatus (red to red, black to black)
- Connect electrodes to electrophoresis machine
- Allow samples to run for 10minutes at 400mA and 100V

Stellenbosch University https://scholar.sun.ac.za

- After 10minutes, run samples for 50minutes at 400mA and 200V

Protein transfer with Bio-Rad Trans-Blot Turbo System

- After gels have run for 60 minutes, take Bio-Rad midi transfer pack out of the fridge
- Open transfer pack
- Take out trans-blot turbo system cassettes. Open the cassettes and wipe dry
- Place blotting paper and transfer membrane down inside the cassette
- Roll out bubbles with roller
- Place gel on top of transfer membrane, carefully so as not to break the gel
- Place 'top' blotting paper from transfer pack on top of the gel
- Roll out bubbles with roller
- Soak up excess transfer buffer with paper towel
- Close cassette, and place back into trans-blot turbo system
- Set system: 12 minutes, 12 V and 12 A
- Wait to transfer to complete. During this time make up 5% milk blocking solution
- Once transfer is complete, rinse membrane 3 x 5 minutes with TBS-T
- Place membrane in blocking solution for 2 hours

Specific binding of protein:

- Wash membrane 3 x for 5minutes each with TBS-T
- Make primary antibody in a 50ml falcon tube (keep cold) (see appendix C)
- After washing, place membrane in primary antibody tube. Place falcon tube on rotating machine for minimum of 8 hours, or overnight in walk in fridge (4˚C).
- Wash membrane 3 x for 5 minutes each with TBS-T
- Make up secondary antibody in 50ml falcon tube (see appendix C)
- After washing, place membrane in secondary antibody for 1hour on rotating belly dancer

Exposure with Bio-Rad ChemiDocTM XRS+ System:

- Prepare ECL cocktail (see appendix C)
- Discard secondary antibody, and rinse membrane 3 x 5 minutes with TBS-T
- Drain excess TBS-T off membrane using paper towel
- Add 500 µL ECL cocktail to membrane, and leave on for 1 minute
- Lift membrane, and drain excess ECL
- Open bottom draw of ChemiDoc, and place membrane inside
- Open Image Lab™ Software

Stellenbosch University https://scholar.sun.ac.za

- Select single channel analysis → Chemi → blots
- Set pictures to be taken every 5 seconds, for 300 seconds (total for 30 pictures)
- Align the membrane and Select ‘run protocol’
- Collect images

Stripping membranes

- After developing rinse ECL off membrane with distilled water 3 x 3 minutes
- Rinse membrane in NaOH for a few minutes
- Rinse membrane with distilled water 3 x 3 minutes
- Place membrane in blocking solution for 2 hours
- Rinse membrane with TBS-T 3 x for 5minutes each
- Place membrane in primary antibody overnight

Stellenbosch University https://scholar.sun.ac.za

APPENDIX C - Reagent and Solution Preparation

Preparation of cell culture solutions

Growth Medium

- 500 ml high glucose DMEM
- 1 % (5.5 ml) Antibiotic Antimyocotic (AA) (100X)
- 10% (50 ml) fetal bovine serum (FBS)
- Aliquot into 50 ml falcon tubes and store at -4°C until needed

1X Phosphate buffered saline solution (PBS)

- Dissolve the following in 1L distilled water (dH_2O): 16 g NaCl (sodium chloride), 0.4 g KCl (potassium chloride), 2.88 g Na_2HPO_4 (di sodium hydrogen phosphate) and 0.48 g KH_2PO_4 (potassium dihydrogen phosphate)
- Adjust pH to 7.4
- Add 1L dH_2O
- Autoclave solution
- Aliquot into 50 ml falcon tubes and store at -4°C until needed

Preparation of Doxorubicin Stock Solution [3.4 mM]

Doxorubicin Hydrochloride (DOX) is light sensitive and the following method should therefore be performed in appropriate lighting conditions

- Under sterile conditions dissolve 10 mg of DOX in 5071 µL growth medium
- Vortex solution and ensure all powder is completely dissolved
- Aliquot into 0.5 ml eppendorf tubes and store at -20°C until needed
- In order to avoid freeze-thaw cycles, 60 µL aliquots were made
- Protect epi's from light, and cover in foil.

Preparation of 95% Ethanol (1L)

- Dilute 950 ml 100% ethanol with 50 ml dH_2O

Stellenbosch University https://scholar.sun.ac.za

Preparation of 70% Ethanol (1L)

- Dilute 700 ml 100% ethanol with 300 ml dH_2O

Preparation of MTT solutions

1% Isopropanol

- 1 ml concentrated HCl + 99 ml Isopropanol

20..... **% Triton**

- 0.1 ml of Triton-X-100 + 99.9 ml dH_2O

Isopropanol/Triton solution (50/1)

- 50 ml isopropanol + 1 ml 0.5% Triton

1% MTT:

- 0.01g MTT in 1 ml PBS. Cover in foil, as solution is light sensitive. *NOTE: 0.01g MTT enough for 2 x wells in 6-well plate*

Preparation of 1mM MitoTracker® Green FM stock solution

- MitoTracker® Green FM MW = 671.88
- Add 74.41 µL DMSO to 50 µg (packaged by supplier) MitoTracker® Green FM stock powder
- Vortex until dissolved
- Aliquot to prevent freeze-thaw cycles, protect from light and store at -20°C

Preparation of 0.5 µM MitoTracker® Green FM working solution

- Dissolve 0.25 µL of MitoTracker® Green FM stock solution (1mM) in 500 µl PBS

Preparation of 1.0 µM ER-Tracker™ Blue-White working solution

- 50 µL of ER-Tracker™ Blue-White supplied as 1 mM stock solution by Molecular Probes

Stellenbosch University https://scholar.sun.ac.za

- Dissolve 0.5 µL of ER-Tracker™ Blue-White in 500 µL PBS

Preparation of 5 mM Calcium Green™ -5N AM stock solution

- Calcium Green™ -5N AM MW = 1290.98
- Add 77.40 µL of DMSO to 500 µg , Calcium Green™ -5N AM stock powder
- Vortex until dissolved
- Aliquot to prevent freeze-thaw cycles, protect from light and store at -20°C

Preparation of 5 µM Calcium Green™ -5N working solution

- Dissolve 0.5 µL Calcium Green™ -5N in 500 µL PBS

Preparation of 1 mM Rhod-2 AM, cell permeant stock solution

- Rhod-2 AM MW = 1123.96
- Add 889.7 µl DMSO to 1 mg of Rhod-2 AM stock powder
- Vortex until dissolved
- Aliquot to prevent freeze-thaw cycles, protect from light and store at -20°C

Preparation of 4 µM Rhod-2 AM, cell permeant working solution

- Dissolve 2 µL of Rhod-2 AM in 500 µL PBS

Preparation of ORAC assay reagents

Phosphate buffer 75 mM, pH 7.4:

- Weigh 1.035g sodium di-hydrogen orthophosphate-1-hydrate in 100 mL ddH_2O and mix until dissolved.
- Weigh 1.335g di-sodium hydrogen orthophosphate dehydrate (Merck #5822880EM) in 100 mL ddH_2O and mix until dissolved.
- Mix 18 mL of 1st solution with 82 mL 2nd solution
- Check pH – adjust with phosphate buffer

Stellenbosch University https://scholar.sun.ac.za

- Store at 4 °C

Fluorescein Stock: Sigma #F6377

- Dissolve 0.0225g in 50 mL phosphate buffer (above)
- Store at 4 °C in a brown bottle (reused for 1 year)

Fluorescein Working Solution:

- Take 10 µL of the stock and add it to 2 mL phosphate buffer (epi)
- Then take 240 µL of this and dilute in 15 mL phosphate buffer (15 mL falcon)

Peroxyl radical: Sigma #440914 25 mg/mL

- Weigh 150 mg of AAPH into a 15 mL falcon tube
- Only add solute later on

Trolox (standard): 250 µM stock Sigma # 238831

- Weigh 0.00312 g and add 50 mL phosphate buffer
- Mix until dissolved
- Should give an absorbance of 0.670 at 289nm

Preparation of TBARS reagents

BHT

- Dissolve BHT in 100% ethanol to a final concentration of 4 mM

Ortho-phosphoric acid (0.2 M)

- CPUT supplies 14.6M stock solution
- Add 684.93 µL of stock solution to 50 mL dH_2O

NaOH (0.1 M)

- Dissolve 0.792 g of NaOH in 50 µL ortho-phosphoric acid

TBA Reagent

- Concentration of 0.11 M TBA in 0.1 M NaOH

Saturated NaCl

- Add 10g of NaCl to 25 ml of dH_2

Stellenbosch University https://scholar.sun.ac.za

Preparation of western blot reagents

RIPA

- Prepare 50 mM Tris-HCl: add 790 mg Tris to 75 mL dH_2O. Add 900 mg NaCl and stir. Adjust pH to 7.4 using HCl. Pour the prepared Tris-HCl into a 100 mL beaker.
- Add the following in the same order that they appear:

	Volume	Final Concentration
NP-40	10 mL	1%
Na-deoxycholate	2.5 mL	0.25%
EDTA	1 mL	1 mM
Phenylmethylsulponyl Fluoride (PMSF)	1 mL	1 mM
Leupeptin	1 µL	1 µg/mL
SBTI-1	80 µL	4 µg/mL
Benzamidine	100 µL	1 mM
Na_3VO_4	1 mL	1 mM
NaF	500 µL	1 mM

- Add 1000 µL Triton-X-1000 to the solution and fill up to the mL mark with dH_2O
- Mix thoroughly.
- Aliquot the RIPA into 1 mL epi's tubes

Bradford working solution

- Dissolve 200 mg Comassie Brilliant Blue G250 in 100 mL 95% Ethanol
- Mix on stirrer
- Add 200 mL 85% ortho-phosphoric acid
    - 85% ortho-phosphoric acid: 120 mL O-P in 30 ml dH_2O)
- transfer solution into brown/light protected bottle
- Add 1.7 L dH_2O
- Mix on stirrer
- Filter solution until brown (± 7 times)

Laemmli's sample buffer stock solution

- Mix the following together in a beaker:

Stellenbosch University https://scholar.sun.ac.za

- 3.8 mL distilled water
- 1 mL 0.5M Tris-HCl (pH 6.8)
- 0.8 mL glycerol
- 1.6 mL 10% (w/v) SDS
- 0.4 mL 0.05% (w/v) Bromophenol blue

- Note: For use in western blotting, make a working solution by adding 150 µL β-mercaptoethanol to 850 µL Laemmli's stock solution

21..... **M Tris-HCl (ph. 8.8)**

- Weigh out 68.1 g Tris (1.124 M) and 1.5 g SDS (0.3%) into a glass beaker
- Add 400 ml dH_2O
- Adjust pH to 8.8
- Add 100 ml dH_2O to make up final volume
- Store at room temperature

0.5 M Tris-HCl (pH 6.8)

- Weigh out 30.3 g Tris (0.5M) and 2 g SDS (0.4%) into glass beaker
- Add 80 ml dH_2O
- Adjust pH to 6.8
- Add 20 ml dH_2O to make up final volume
- Store at room temperature

10% Sodium dodecyle sulfate (SDS)

- Dissolve 50 g SDS in 500 ml dH_2O
- Store at room temperature

10% Ammonium persulfate (APS)

- Dissolve 0.1 g APS in 100 µL dH_2O
- Store in fridge at -4°C

Stellenbosch University https://scholar.sun.ac.za

1 x Running buffer

- Weigh out 60.6 g Tris and 288 g glycine
- Add to 1.5L dH_2O
- Add 20 g SDS
- Adjust the pH to 8.6
- Fill up to the 2L mark dH_2O.

10 x Running buffer

- Dissolve 100 ml 1 x Running buffer in 900 ml dH_2O

1 X TBS

- Weigh out 48.4 g TRIS (trizma base) and 32 g NaCl into a glass beaker
- Add 1L dH_2O
- Stir until dissolved, and adjust pH 7.6
- Add 1L dH_2O
- Store at room temperature

1 x TBS-T

- Dissolve 200ml 1 X TBS in 1900 ml dH_2O
- Add 2 ml Tween
- Mix thoroughly
- Can be stored at room temperature (± 1 week)

5% Milk blocking solution

- Weigh out 5g non-fat, dry instant milk powder into glass beaker
- Add 100 ml TBS-T and mix well
- 100 ml blocking solution per membrane

Stripping buffer

- Dissolve 4 g NaOH pellets in 500 ml dH_2O
- Store at room temperature

Stellenbosch University https://scholar.sun.ac.za

Preparation of acrylamide separating gel:

	10% acrylamide (separating) gel	15% acrylamide (separating) gel
dH_2O	3.85 ml	1.1 ml
1.5M Tris-HCL (ph. 8.8)	2.5ml	2.5 ml
10% SDS	100 µl	100 µl
40% Acrylamide	2.5 ml	2.5 ml
10% APS	50 µl	50 µl
Temed	5 µl	2 µl

Preparation of 4% acrylamide stacking gel (enough for 4 gels)

	Stacking Gel
dH_2O	6.1 ml
0.5M Tris-HCL (ph. 6.8)	2.5 ml
10% SDS	100 µl
40% Acrylamide	1 ml
10% APS	100 µl
Temed	20 µl

Preparation of primary and secondary antibodies

All antibodies diluted in TBS-T. Primary antibodies can be reused 5-6 times, but must be stored at -4°C. Secondary antibodies cannot be reused.

Stellenbosch University https://scholar.sun.ac.za

Primary Antibody	Primary Antibody Dilution	Secondary Antibody	Secondary Antibody Dilution	Molecular Weight (kDa)
ATF-4	1/1000	Anti-Rb IgG	1/10 000	49
BiP	1/1000	Anti-Rb IgG	1/10 000	78
Cleaved Caspase 3	1/1000	Anti-Rb IgG	1/10 000	17, 19
Drp1	1/1000	Goat anti-Ms IgG	1/2000	82
GAPDH	1/1000	Anti-Rb IgG	1/10 000	37
K48 ubiquitin	1/1000	Anti-Rb IgG	1/ 10 000	Whole lane
LC3	1/1000	Anti-Rb IgG	1/10 000	14, 16
MARCH5	1/1000	Anti-Rb IgG	1/10 000	31
Mitofusion 1	1/10 000	Goat anti-Rb HRP	1/1000	86
Mitofusion 2	1/ 1000	Anti-Rb IgG	1/2000	80
p-62	1/1000	Anti-Rb IgG	1/10 000	62
Parkin	1/1000	Anti-Rb IgG	1/10 000	52
PGC-1α	1/1000	Anti-Rb IgG	1/10 000	130
hFis1	1/ 10 000	Goat anti-Rb HRP	1/1000	Spec: 17 Nonspec: 25
Tomm20	1/1000	Anti-Rb IgG	1/3000	Spec: 16 Nonspec : 25

Stellenbosch University https://scholar.sun.ac.za

Appendix D - List of Reagents and Materials

Reagents	Catalogue Number	Company
AAPH (2,2'-azobis(2-amidino-propane) dihydrochloride)	44091	Sigma-Aldrich
Antibiotic-Antimyocotic (AA) 100x	15240-062	Invitrogen-Gibco
Acrylamide	A3699	Sigma
Ammonium Persulphate (APS)	A3678	Sigma
BHT (2, 6-di-tert-butyl-4-methyphenol)	B1378	Sigma-Aldrich
BLUeye pre-stained protein ladder	PM007-0500	GeneDirex
Bovine Serum Albumin (BSA)	A4503	Sigma
Calcium-Green™ -5N, AM, cell permeant	C-3739	Molecular Probes
Caspase-Glo® 3/7 Assay	G8091	Promega
Clarity™ Western ECL Substrate	170-5061	Bio-Rad
Dulbecco's Modified Eagles Medium (DMEM), high Glucose	41965-039	Invitrogen-Gibco
DTNB (5 5'-dithiobis(2-nitrobenzoic acid))	D8130	Sigma-Aldrich
Doxorubicin (DOX)	D1515	Sigma
ER-Tracker™ Blue-White DPX	E-12353	Molecular Probes
Fetal Bovine Serum (FBS)	BC/S0615-HI	Biochrom
Fluorescein	F6377	Sigma-Aldrich

Glutathione Reductase	G3664	Sigma-Aldrich
Hydrochloric Acid (HCl)	UN1789	Merck
M2VP (1—methyl-2-vinylpyridinium)	69701	Sigma-Aldrich
Mitotracker® Green FM	M-7514	Molecular Probes
MTT (Thiazolyl Blue Tetrazolium Bromide)	M2003	Sigma-Aldrich
NADPH (β-nicotinamide adenine dinucleotide)	N7505	Sigma-Aldrich
Ortho-phosphoric acid	100563	Merck
Penicillin-Streptomycin (PenStrep)	10378-016	Invitrogen-Gibco
Ponceau S Solution	P5447	Sigma
Proteasome-Glo™ Assay	G8531	Promega
Rhod-2, AM, cell permeant	R-1244	Molecular Probes
Sodium Dodecyle Sulphate (SDS)	L3771	Sigma
TBA (2-thiobarbituric acid)	T5500	Sigma-Aldrich
Temed	T9281	Sigma
Trizma-base	93304	Fluka
Trolox	238813	Sigma-Aldrich
Trypsin-EDTA (0.25%)	25200072	Invitrogen-Gibco
Tween 20	T6146	Sigma

Primary Antibodies	Catalogue Number	Company
ATF-4	11815	Cell Signaling
BiP	3177	Cell Signaling

Stellenbosch University https://scholar.sun.ac.za

Cleaved Caspase 3	9661	Cell Signaling
Drp1	Ab56788	Abcam
GAPDH	2118	Cell Signaling
K48 ubiquitin	4289	Cell Signaling
LC3	2775	Cell Signaling
MARCH5	Ab77585	Abcam
Mitofusion 1	Ab129154	Abcam
Mitofusion 2	Ab124773	Abcam
p-62	5114	Cell Signaling
Parkin	2132	Cell Signaling
PGC-1α	2178	Cell Signaling
hFis1	Ab71498	Abcam
Tomm20	Ab56783	Abcam

Secondary Antibodies	**Catalogue Number**	**Company**
Anti-rabbit IgC, AP-linked antibody	7054	Cell Signaling
Goat anti-Mouse IgG H&L (HRP)	Ab97040	Abcam
Goat anti-Rabbit IgG H&L (HRP)	Ab97069	Abcam

Western Blotting	**Catalogue Number**	**Company**
Trans-Blot Turbo™ Mini PDVF Transfer Pack	170-4156	Biorad

Stellenbosch University https://scholar.sun.ac.za

Materials	Catalogue Number	Company
25 cm^2 sterile tissue culture flask (vent cap)	707003	Nest Biotechnology
75 cm^2 sterile tissue culture flask (vent cap)	708003	Nest Biotechnology
5 ml Serological Pipette	500052	White Sci
10 ml Serological Pipette	500053	White Sci
25 ml Serological Pipette	500055	White Sci
BD Falcon conical centrifuge tubes (15 ml)	352099	Corning
BD Falcon conical centrifuge tubes (50 ml)	352070	Corning
Cell Scrapers	710011	Nest Biotechnology
Nunc® Lab-Tek® 8-well Chamber Slide™	C7182	Sigma-Aldrich
Reagent Reservoirs	95128085	Thermo Scientific
Sterile, 6-well culture plate (flat bottomed)	703001	
Sterile, 96-well culture plate (Flat bottomed)	701001	Nest Biotechnology
Sterile, black 96-well clear bottomed culture plate	CL S3603 -48EA	Nest Biotechnology